

Thèse de doctorat de l'Université des Sciences et technologies de Lille
Ecole Doctorale Sciences de la Matière, du Rayonnement et de l'Environnement

Présentée par

Julien BAILLEUL



DYNAMIQUE SEDIMENTAIRE ET STRUCTURALE DES BASSINS PERCHES SUR LES PRISMES DE SUBDUCTION

L'EXEMPLE DU PRISME HIKURANGI, NOUVELLE-ZELANDE

En vue de l'obtention du titre de

**DOCTEUR DE L'UNIVERSITE EN DYNAMIQUE
ET ENVIRONNEMENTS SEDIMENTAIRES**

Soutenue le 17 juin 2005, devant la commission d'examen:

Rapporteurs : Nadine Ellouz
Michel Lopez
Examineurs : Frank Chanier
Jacky Ferrière
François Guillocheau (président)
Siegfried Lallemand
Invitée : Cécile Robin



AVANT-PROPOS ET REMERCIEMENTS

Cette page, bien que la première de ce manuscrit, marque pourtant la fin d'une aventure scientifique débutée en septembre 2001. Ce travail de thèse a été effectué au laboratoire Processus et Bilan des Domaines Sédimentaires (UMR 8110) de l'Université de Lille 1. Six mois de terrain en Nouvelle-Zélande (et oui ... il y a pire !!!) ont été également nécessaires à l'acquisition des données sédimentologiques, stratigraphiques et structurales présentées dans ce mémoire.

Je tiens tout d'abord à remercier (que les mots sont faibles) Frank Chanier et Jacky Ferrière pour la confiance qu'ils m'ont témoigné non seulement en me permettant de travailler sur ce sujet mais également tout au long de ma thèse. Leurs qualités scientifiques et humaines, leur patience ainsi que leur pédagogie m'ont appris énormément sur ce que doit être un directeur de thèse et plus encore, un enseignant-chercheur. Jacky, je ne te remercierais jamais assez de nous avoir autorisé à manger parfois avant 16h00 lors de notre première mission. Frank, merci pour les oranges et pour ta passion (communicative) du terrain.

J'associe bien entendu à ce mémoire les personnes avec lesquelles j'ai eu la chance de travailler. En premier lieu, celles qui m'ont accompagné et formé sur le terrain : Cécile Robin (grâce à toi j'ai enfin une petite idée de ce à quoi peut ressembler une turbidite), Geoffroy Mahieux (notre cobra du Gamma-Ray), Christophe Buret (we are french), et Isabelle Coutand (merci encore de m'avoir sauvé la vie suite à l'attaque à l'arme blanche de cet avocat surnois). Mais également, celles qui m'ont apporté énormément lors des travaux en laboratoire et/ou des phases d'interprétation : François Guillocheau, Christian Gorini (la NZ c'est comme le golfe du Lyon ... sauf que la marge est active), et Jean-Christophe Embry (merci pour les deux semaines de goulag ...).

Je remercie également vivement nos collaborateurs néo-zélandais : Brad Field pour son aide et sa disponibilité lors de mes séjours à Wellington, ainsi que les paléontologues, Hugh Morgans et Alan Beu, pour les datations qu'ils ont effectué en vue de ce travail.

Ce travail n'aurait pas été possible sans les concours financiers apportés par mon laboratoire d'accueil, l'UMR 8110 (qui a su en particulier reconnaître l'importance des travaux de terrain et en supporter le coût), par le programme BQR mobilité des doctorants de l'université de Lille1, par le GDR marge, par le projet ECLIPSE, par le projet RELEFS et par le ministère des affaires étrangères en Nouvelle-Zélande.

Merci aux membres du Jury d'avoir accepté de prendre de leur temps pour lire et juger ce travail, ainsi que d'avoir permis de l'améliorer par leur expertise scientifique et leurs conseils sur le manuscrit.

Au cours de mes missions sur le terrain, j'ai eu la chance d'être accueilli par la famille Wardle. Leur soutien et leur amitié m'ont été très précieux, particulièrement lorsque j'étais seul sur le terrain. J'adresse donc toute ma reconnaissance à Pauline et George, ainsi qu'aux autres éleveurs du Wairarapa qui m'ont chaleureusement donné accès à leurs Terres.

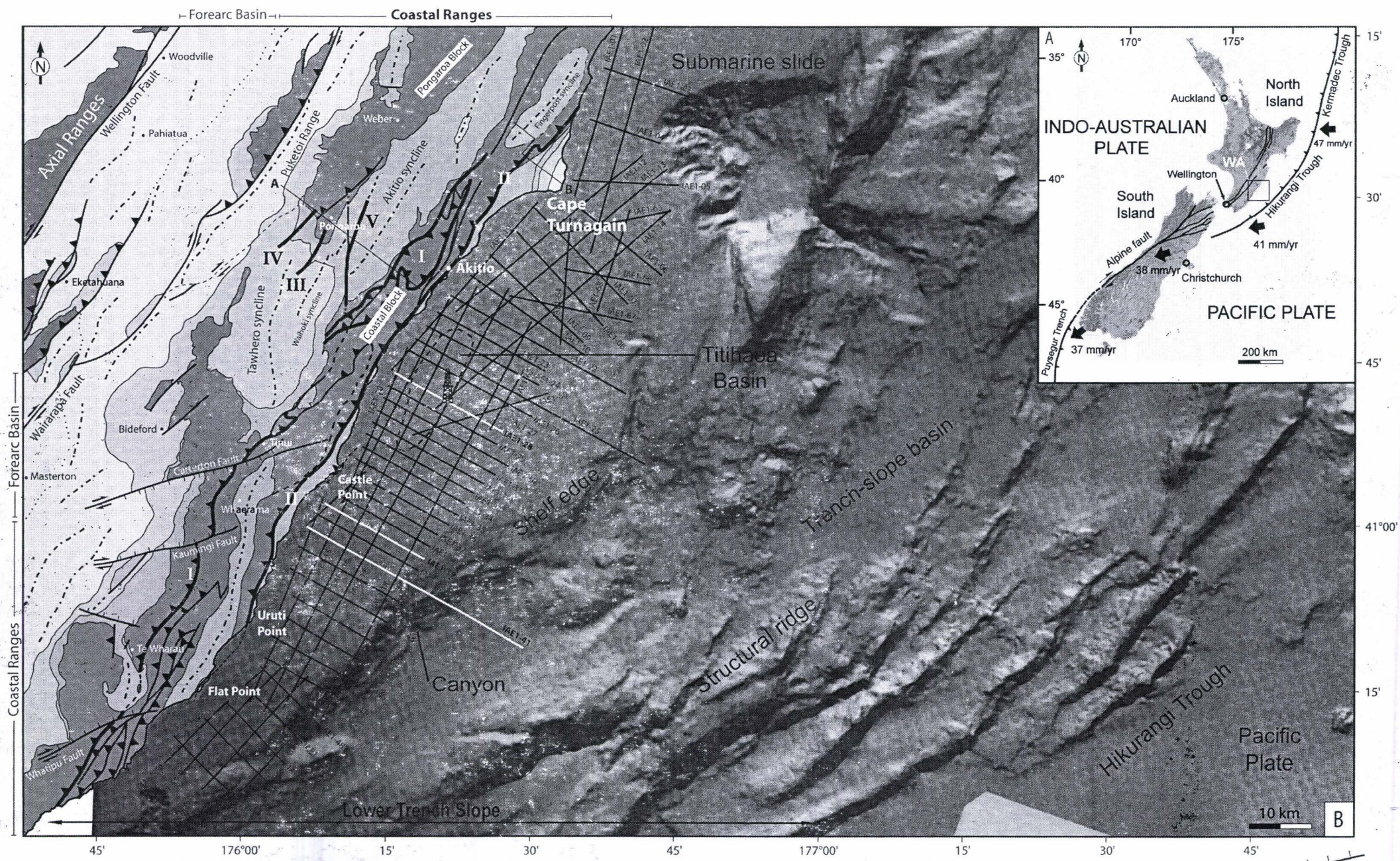
Merci aux thésards, ATER et étudiants de DEA qui se sont succédés au cours de ces quatre années et m'ont permis de passer de si bons moments au laboratoire et en dehors. Je pense particulièrement à Yvanous, Lucia, Sabrina (sacré bassin de Norfolk ... !!!), les Sophie's, Dimi3, Pierre Bachelet et Florence Arthaud, Nidal, Roberto, El Thonio, Lhoulou et Lud, Laurent Ri(u)quiet, Aurélie Blanchet, Manu Gandoin, le Shrunck, Mylène, Lies Loncke, Toto, la Patin, Lucie et autres lucipilliens, Cathy (pour avoir été une étudiante *modèle*), Nico et ses approvisionnements de maroilles. Ma reconnaissance va également à tous les membres du laboratoire : techniciens, secrétaires, enseignants chercheurs ainsi qu'à tous ceux que j'ai malheureusement oublié de citer ici.

Je m'excuse d'autre part auprès de ceux, amis et famille, que j'ai malheureusement négligé ces derniers temps. Qu'ils sachent qu'il y a forcément un peu de chacun d'entre eux dans ce manuscrit : la sœurlette, ses trois héritiers ainsi que le beauf, Francis et Arlette, Patou et sa fratrie, Sandra, JuM, Doud (Gwenn bientôt à Wechter !!!), Nanard, les raclettes-girls (Elodie, Christelle et Geneviève), Sandro, Jean-Mich, Céline, Juliette ...

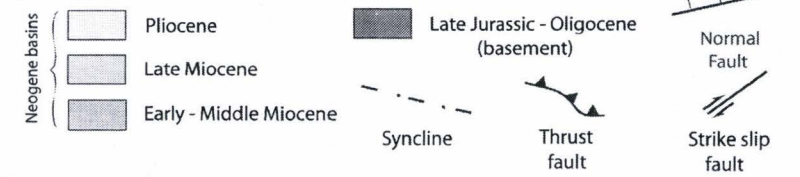
Je n'oublie évidemment pas mes parents qui m'ont soutenu et guidé tout en me laissant faire mes choix (et donc mes erreurs ...) tout au long de mon cursus. Si cette thèse a été possible, c'est en grande partie grâce à eux.

Finalement, un grand merci, et non le moindre, à Yolaine pour son espantante patiente (ce n'est pas donné à tout le monde de rousiguer son freing sans rouméguer), ainsi que pour les bulles d'oxygène qu'elle a su m'apporter pendant que je m'escagassais sur ce manuscrit.

Je dédie ce mémoire à mes grand-pères, l'un, mineur, m'a peut-être communiqué le virus du cailloux, et l'autre, positivement curieux, celui de la recherche ...



A - Plate tectonic setting of New Zealand, black arrows show present-day relative plate motion between Pacific and Australian plates (WA - Wairarapa Area). **B** - Bathymetric map (Lewis *et al.*, 1999) and onshore structural map (modified from Lee and Begg, 2002) of the Wairarapa area. The offshore Wairarapa area includes location of the Amoco IAE1 seismic survey and well Titihaoa-1. I - Tinui Fault Complex, II - Whakataki Fault, III - Waihoki Fault, IV - Mangatiti Fault, V - Breakdown Fault, A-B location of cross-section shown figure VI-7.



Time in Ma	STANDARD CHRONOSTRATIGRAPHY (International Units)			NZ UNITS		
	SYSTEM	SERIES	STAGES	EPOCHS	STAGES	
0	QUATER-NARY	^{HOLOCENE} PLEISTOCENE	IONIAN	WANGANUI	Haweran 0.34 (Wq)	
		PLIOCENE	U		0.95 CALABRIAN	Castlecliffian (Wc)
	L				1.77 GELASIAN	Nukumaruan 1.71 (Wn)
			PIACENZIAN		2.60	Mangapanian 2.40 (Wm)
					ZANCLEAN	3.58
5	CENOZOIC TERTIARY		MIOCENE		5.32 MESSINIAN	TARANAKI
		UPPER		7.12 TORTONIAN	Kapitean (Tk) 6.50	
10			NEOGENE	MIDDLE	SOUTHLAND	Tongaporutuan (Tt) 11.00
		11.20 SERRAVALLIAN				Waiauian (Sw) 13.20
15		LOWER		PAREORA	Lillburnian (Sl) 15.10	
					14.8 LANGHIAN	Clifdenian (Sc) 16.00
20		PALEOGENE	OLIGOCENE	UPPER	LANDON	Altonian (Pl) 19.00
						BURDIGALIAN
25			CHATTIAN	L	23.80	Waitakian (Lw) 25.20
		28.50			Duntroonian (Ld) 27.30	

Echelle chronostratigraphique utilisée en Nouvelle-Zélande, et équivalences internationales, du Néogène à l'actuel. Etages néo-zélandais d'après Cooper *et al.* (2004).

TABLE DES MATIERES

Résumé	p. 1
Abstract	p. 3
Introduction générale	p. 5
Question scientifique	p. 5
Organisation du mémoire	p. 6

CHAPITRE I

Les bassins de pente associés aux prismes de subduction (p. 11)

I) Les bassins perchés : structure et morphologie	p. 13
II) Les bassins perchés : faciès et systèmes de dépôt	p. 21

CHAPITRE II

Cadre géodynamique et bassins de la marge Hikurangi (p. 25)

I) Cadre géodynamique de la marge active Hikurangi	p. 27
A) La Nouvelle-Zélande dans le Sud-Ouest Pacifique	p. 27
1) La limite de plaques Pacifique-Australie	p. 27
2) Les rides et bassins de la plaque Australie	p. 30
B) Ile Nord de Nouvelle-Zélande : une subduction active	p. 35
1) Contexte géodynamique actuel	p. 35
2) Les grands traits de l'évolution géologique	p. 39
3) Stratigraphie régionale	p. 45

II) Les bassins de pente du prisme de subduction Hikurangi	p. 49
A) En mer	p. 49
B) A terre	p. 53
1) Le bassin de Makara	p. 53
2) Les bassins de la zone d'étude	p. 55

CHAPITRE III

Les systèmes turbiditiques du domaine avant-arc interne de la marge convergente Hikurangi (Nouvelle-Zélande): de nouvelles contraintes sur le développement des bassins perchés sur le prisme de subduction (p. 61)

Résumé	p. 63
I) Introduction	p. 65
II) Caractéristiques structurales et géométrie des bassins perchés	p. 67
III) Faciès et systèmes de dépôt des bassins perchés	p. 67
IV) Contexte structural	p. 69
A) La marge Hikurangi	p. 69
B) Le bassin d'Akitio	p. 73
V) Stratigraphie régionale et sédimentologie	p. 74
VI) Localisation et méthodologie	p. 75
VII) Analyse de faciès	p. 76
VIII) Evolution stratigraphique du bassin d'Akitio	p. 83
A) Lithostratigraphie du bassin d'Akitio	p. 83
1) Colonne lithostratigraphique de Pongaroa	p. 83
2) Colonne lithostratigraphique de Branscombe	p. 84
B) Biostratigraphie du bassin d'Akitio	p. 85

IX) Corrélations et évolution géométrique du bassin d'Akitio	p. 87
A) U1 : Progradation vers le Sud-Est d'un système mixte plate-forme externe/rampe (c. 25 – c. 17.5 Ma)	p. 87
B) U2 : Progradation vers l'Ouest d'un système turbiditique (c. 17.5 – c. 16.5 Ma)	p. 89
C) U3 : Partitionnement des systèmes sédimentaires ; plate-forme externe à l'Ouest et progradation vers l'Ouest d'un système turbiditique à l'Est (c. 16.5 – c. 15 Ma)	p. 89
D) U4 : Partitionnement des systèmes sédimentaires ; système silteux aggradant à l'Ouest et poursuite de la progradation vers l'Ouest du système turbiditique à l'Est (c. 15 – c. 13.2 Ma)	p. 90
E) U5 : Turbidites distales de type plaine sous-marine (c.13.2 – c. 12 Ma)	p. 91
X) Discussion	p. 91
A) Systèmes turbiditiques et modèle de faciès des bassins perchés	p. 91
B) Contrôle tectonique sur les systèmes turbiditiques	p. 95
C) Evolution structurale et stratigraphique du bassin d'Akitio : implications pour l'histoire structurale régionale	p. 96
Remerciements	p. 100

CHAPITRE IV

Structure et stratigraphie sismique d'un bassin perché immergé, comparaison avec un analogue de terrain (marge de subduction Hikurangi, Nouvelle-Zélande) (p. 101)

Résumé	p. 103
I) Introduction	p. 105
II) Morphologie et déformation des bassins perchés	p. 107
III) Modèles de dépôt pour les bassins perchés	p. 109
IV) Le prisme de subduction Hikurangi	p. 111
V) Localisation, données et méthodologie	p. 115
A) Localisation	p. 115
B) Données et méthodologie	p. 117
1) Analyse des lignes de sismique marine (campagne sismique IAE1)	p. 117
2) Analyse des données diagraphiques (forage Titihaoa-1)	p. 117
VI) Stratigraphie du secteur de Titihaoa	p. 119
A) Stratigraphie sismique	p. 119
1) Unité sismique désorganisée (SI)	p. 119
2) Unité sismique irrégulière et discontinue (SII)	p. 119
3) Unité sismique organisée et continue (SIII)	p. 123
B) Lithostratigraphie	p. 125
C) Biostratigraphie	p. 128
VII) Age et caractéristiques sédimentologiques des unités sismiques	p. 129
A) SI - socle acoustique (anté - 14.2 Ma)	p. 131
B) SII - Unité sédimentaire confinée (c. 14.2-6.2 Ma)	p. 131
C) SIII - Unité sédimentaire latéralement continue (c. 6.2-0 Ma)	p. 132

VIII) Discussion	p. 134
A) Processus de déformation et évolution stratigraphique du secteur de Titihaoa ...	p. 134
1) Le bassin perché miocène de Titihaoa (bassin « a »)	p. 134
2) Développement des bassins perchés miocènes situés plus à l'Est (bassins « b », « c » et « d »)	p. 135
3) Le bassin de pente plio-quaternaire de Turnagain	p. 136
B) Comparaison du bassin de Titihaoa (situé en mer) avec un analogue plus ancien connu à l'affleurement, le bassin perché d'Akitio	p. 137
1) Le bassin perché d'Akitio (étude à terre)	p. 137
2) Comparaison avec le bassin de Titihaoa, situé en mer	p. 141
a) Limites inférieures et supérieures du remplissage sédimentaire des bassins perchés	p. 141
b) Architecture stratigraphique et déformation des bassins perchés ..	p. 144
c) Analyse de faciès	p. 145
IX) Conclusions	p. 146
Remerciements	p. 148

CHAPITRE V

Déformation discontinue d'un prisme de subduction : Evolution de la marge Hikurangi (Nouvelle-Zélande) au cours des derniers 25 Ma (p. 149)

Résumé.....	p. 151
I) Introduction	p. 153
II) Contexte géologique	p. 155
III) Evolution tectonique de la région Nord-Est Wairarapa	p. 157
IV) Le prisme de subduction immergé	p. 161
A) Les bassins perchés situés à proximité du front de subduction	p. 161
B) Etude du domaine interne immergé du prisme de subduction	p. 163
1) Structure de la plate-forme du Wairarapa sur la transversale d'Akitio	p. 163
a) Le soubassement acoustique (SI)	p. 165
b) Les bassins perchés miocènes moyens à supérieur (SII)	p. 165
c) Le bassin de pente Plio-Quaternaire de Turnagain (SIII)	p. 166
2) Structure de la plate-forme du Wairarapa sur la transversale de Castlepoint	p. 169
V) Le prisme de subduction émergé	p. 173
A) Analyse structurale	p. 173
B) Analyse de bassin	p. 176
1) Les flysch du miocène basal : la sédimentation syn-nappes	p. 179
2) Le bassin perché confiné d'Akitio (Miocène inférieur à moyen)	p. 180
3) Le bassin de pente de Tawhero (Miocène supérieur)	p. 185
4) La plate-forme Pliocène	p. 189

VI) Evolution du prisme de subduction Hikurangi sur la transversale d'Akitio	p. 191
A) Miocène basal : la phase d'emplacement de nappes	p. 191
B) Altonien supérieur – Lillburnien : déformation compressive N-S (c. 17.5-15 Ma)	p. 192
C) Waiauan – Tongaporutuan : subsidence et extension (c. 15-6.5 Ma)	p. 193
D) Kapitean – Actuel : raccourcissement et surrection de la marge (c. 6.5-0 Ma) ...	p. 195
VII) Conclusions	p. 197

CHAPITRE VI

Synthèse et Conclusions (p. 199)

I) Les bassins perchés confinés	p. 202
A) Faciès et systèmes de dépôt	p. 202
1) Faciès	p. 205
2) Les systèmes gravitaires	p. 209
B) Architecture stratigraphique et déformation	p. 211
1) Les méga-séquences de comblement	p. 211
2) Les discontinuités d'origine tectonique	p. 213
3) Les séquences de quatrième ordre	p. 215
II) Les phases de déformation du prisme Hikurangi et l'évolution des bassins de pente et de leurs bordures (hauts structuraux)	p. 217
A) Evolution structurale du prisme de subduction Hikurangi	p. 217
B) Evolution de la subsidence des bassins perchés	p. 223
1) Méthode	p. 223
2) Résultats	p. 225

C) Les domaines morpho-structuraux du prisme de subduction Hikurangi	p. 231
III) Conclusions et perspectives	p. 233

BIBLIOGRAPHIE (p. 235)

TABLE DES FIGURES (p. 249)

ANNEXES (p. 265)

Annexe 1 : Colonnes lithostratigraphiques	p. 265
Annexe 2 : Datations et données paléobathymétriques (foraminifères)	p. 277
Annexe 3 : Calage sur les courbes eustatiques des discontinuités identifiées à terre et en mer sur la transversale d'Akitio	p. 287

RESUME

L'étude stratigraphique et structurale d'un transect complet de la marge active Hikurangi (côté Est de l'île Nord de Nouvelle-Zélande), basée sur des données marines et terrestres, permet d'identifier trois domaines morpho-structuraux depuis la fosse jusqu'au bassin avant-arc : le prisme d'accrétion sensu-stricto, la plate-forme du Wairarapa, et la plus haute ride du prisme Hikurangi qui émerge au niveau de la Chaîne côtière. Les différences entre ces domaines sont liées à la fois à leurs différences d'âge et à leur position relative au sein du prisme de subduction au cours du temps. Ces domaines morphostructuraux sont séparés par des zones de chevauchements majeurs qui forment les actuelles limites géographiques : la ligne de côte de la région du Wairarapa et la bordure de plate-forme. Ces zones de failles majeures ont contrôlé la croissance de rides structurales qui ont bordé des bassins de pente matures mio-pliocènes : les bassins très confinés (5 à 10 km de large) d'Akitio (à terre) et de Titihaoa (en mer), et les larges (30 à 40 km) bassins de pente de Tawhero (à terre) et de Turnagain (en mer).

L'analyse détaillée des bassins perchés confinés montre que trois principaux systèmes gravitaires, caractérisés par des granulométries très fines, peuvent se développer à des stades différents de l'évolution du bassin. Il s'agit, de bas en haut, de larges glissements sous-marins (dépôts d'olistostromes), de cônes sous-marins de type riche en sable fin et de rampes sous-marines à faible gradient de pente (dépôts de drappages turbiditiques). L'étude du remplissage sédimentaire des bassins confinés souligne également l'importante contribution des processus de pente à leur budget sédimentaire. Ceci s'explique par la croissance syn-sédimentaire des rides structurales adjacentes. En effet, les pulsations tectoniques aux bordures des bassins sont à l'origine du basculement vers la terre ou vers la mer des surfaces de dépôt. Ces surfaces sont alors caractérisées par de rapides variations de faciès et d'importants changements paleoenvironnementaux qui traduisent des créations ou des modifications de pente. Tant que les rides se développent, les pentes sont régulièrement rajeunies ce qui favorise, en plus des forts flux terrigènes, la progradation des systèmes sédimentaires. La sédimentation au sein des bassins perchés matures est donc dominée par les processus de remplissage qui conduisent au développement de méga-séquences de comblement similaires à celles identifiées dans les bassins d'avant-pays. Dans les bassins perchés, ces méga-séquences peuvent-être subdivisées en unités sédimentaires, d'une durée de 1 à 2 Ma, séparées par les surfaces de discontinuité associées au développement des rides structurales.

Notre étude montre également que l'évolution du prisme de subduction Hikurangi est discontinue et a été contrôlée par des épisodes tectoniques successifs identifiés le long de la transversale d'Akitio : **1**) Une phase de mise en place de nappes au Miocène basal (c. 25 – 18 Ma), **2**) Un épisode de raccourcissement E-W au Miocène inférieur à moyen (c. 17.5 – 15 Ma). Cet épisode est à l'origine du développement de hauts structuraux et du confinement des bassins perchés, **3**) Un épisode de subsidence majeure associé à des déformations en extension (c. 15 – 6.5 Ma) et probablement contrôlée par des processus d'érosion tectonique, et **4**) Une période Miocène terminal à Quaternaire (c. 6.5 – 0 Ma) dominée par des épisodes de raccourcissement rapide (c. 1 Ma) de direction E-W à NW-SE. Cette dernière période tectonique se traduit par la surrection de l'ensemble de la marge qui aboutit à l'émergence de la partie interne du prisme de subduction au cours du Quaternaire. Les changements de régime tectonique peuvent correspondre à des modifications de l'alimentation de la fosse Hikurangi en matériel terrigène ou à d'autres modifications des caractéristiques de la subduction, comme par exemple des variations de l'épaisseur et de la rugosité du panneau plongeant.

Nous avons démontré que la complexité stratigraphique et structurale du prisme de subduction Hikurangi ne résulte pas seulement de cette histoire tectonique polyphasée, mais aussi de variations transversales dans le style et l'amplitude de la déformation au cours du même épisode tectonique. Nous montrons notamment que de l'accrétion frontale peut se développer près du front de subduction alors que la partie supérieure du prisme subit de l'extension et une phase de subsidence au cours d'une période dominée par de l'érosion tectonique.

ABSTRACT

The stratigraphic and structural analysis of a complete transect of the Hikurangi subduction margin (eastern North Island, New Zealand), based on both offshore and onshore data, led to identify three main morpho-structural domains from the trench to the forearc basin: the accretionary prism *sensu-stricto*, the Wairarapa shelf and the present-day emerged trench-slope break of the Hikurangi margin (Coastal Ranges). The differences between these domains are related to both their difference in age and their relative position in the subduction wedge through time. The boundaries between the present-day morpho-structural domains correspond to subduction-related major thrust faults, which coincide with present-day geographic boundaries: the Wairarapa coast-line and the Wairarapa shelf edge. These faults controlled the growth of structural ridges bounding Mio-Pliocene mature slope basins: the highly confined Akitio (onshore) and Titihaoa (offshore) trench-slope basins (5-10 km wide), and the large Tawhero (onshore) and Turnagain (offshore) slope basins (30-40 km wide).

The detailed analysis of the confined trench-slope basins, shows that three main fine grained gravitary systems may develop during various stages of basin development. These are, from base to top, large submarine slides (olistostromes deposits), fine grained sand-rich submarine fans and low gradient submarine ramps (sheet like turbidites). The study of the confined basins sedimentary record also outlines the important contribution of slope processes to the basin sediment budget in such a depositional setting. This is explained by the syn-depositional growth of adjacent structural highs. Indeed, tectonic pulses at basin borders are responsible for landward or seaward tilting of depositional surfaces that are also characterized by rapid shifts of facies and important paleoenvironmental changes traducing slope creations or modifications. As long as the structural ridges develop, slopes are regularly rejuvenated favouring progradation of gravitary systems in association with high sedimentary flux. The very fine grained sedimentation within mature trench-slope basins is therefore dominated by filling processes leading to the development of filling-up mega-sequences similar to those identified in foreland basins. Such mega-sequence comprises sedimentary units, 1 to 2 Myr in duration, delimited by major discontinuities related to the development of the bounding structural ridges.

Our study also shows that the evolution of the Hikurangi subduction wedge is discontinuous and was controlled by successive tectonic periods identified across the Akitio transect: **1)** A basal Miocene phase of nappes emplacement (*c.* 25 – 18 Ma), **2)** An early-middle Miocene E-W compressional episode responsible for the development of structural highs and trench-slope basins (*c.* 17.5 – 15 Ma), **3)** A major subsidence episode associated with extensional deformation (*c.* 15 – 6.5 Ma) and probably related to tectonic erosion, and **4)** A latest Miocene-Quaternary period (*c.* 6.5 – 0 Ma) dominated by short-term (*c.* 1 Ma) episodes of E-W to NW-SE shortening. That last tectonic period is accompanied by overall uplift of the margin leading to the emersion of the inner subduction wedge during the Quaternary. Changes in the tectonic regime may have been induced by modifications of the terrigenous flux within the Hikurangi Trough or by other subduction related processes such as variations in thickness and coupling of the downgoing slab.

We demonstrate that the complex structural and stratigraphic pattern of the Hikurangi subduction wedge results not only from this polyphased tectonic history, but also from transverse variations in style and amplitude of the deformation during a single tectonic episode. We show notably that some frontal accretion can occur close to the subduction front while extensional deformation and subsidence develops upslope during the period dominated by tectonic erosion.

INTRODUCTION GENERALE

QUESTION SCIENTIFIQUE

Les marges actives, caractérisées par les processus de subduction océanique, portent des bassins sédimentaires aux caractéristiques structurales et aux modes de développement variables selon leur localisation au sein du complexe de subduction. Environ 50% des zones de subduction océanique montrent le développement d'un prisme d'accrétion. On distingue alors quatre types de bassins sédimentaires, depuis le front de subduction jusqu'au domaine arrière-arc: la fosse de subduction, les bassins de pente perchés sur le prisme d'accrétion, le bassin avant-arc et le bassin arrière-arc. Ces domaines de sédimentation sont généralement parallèles à la frontière de plaque et leur développement est fondamentalement contrôlé par les processus de subduction. Les bassins perchés (*trench-slope basins* ; Moore et Karig, 1976) sont des dépressions structurales étroites (1 à 10 km) et allongées (20 à 100 km) qui se situent sur la pente du prisme d'accrétion (*lower trench slope* ; Underwood et Moore, 1995), entre la fosse et la plus haute ride du prisme (*trench slope break* ; Underwood et Moore, 1995).

La structure du prisme d'accrétion, et par conséquent la morphologie de sa pente vers la fosse, est contrôlée par les paramètres de la subduction (mouvements du panneau plongeant, nature du décollement basal, épaisseur des sédiments accrétés, ...) . La dynamique de convergence exerce ainsi un contrôle prépondérant sur la géométrie et la subsidence des bassins perchés sur le prisme. En sus des variations climatiques et eustatiques, le remplissage sédimentaire de ces bassins peut donc avoir enregistré les variations du régime tectonique au cours du processus apparemment continu de subduction.

L'objectif de cette étude est de caractériser les interactions entre l'activité tectonique, liée à la dynamique de subduction, et l'architecture stratigraphique qui se développe sur la pente d'un prisme d'accrétion. Il s'agit en particulier de contraindre le développement structural des bassins de pente à partir d'une étude stratigraphique haute résolution de leur remplissage sédimentaire.

L'objet choisi pour cette approche est le complexe de subduction Hikurangi. Celui-ci résulte de la subduction, depuis 25 Ma, de la plaque Pacifique sous l'Ile Nord de Nouvelle-Zélande (plaque Australie). Au cours de cette période orogénique (orogénèse Kaikoura, 25 – 0 Ma), la structuration de la marge s'est notamment caractérisée par le développement d'un prisme d'accrétion actif: le prisme Hikurangi. Au cours de l'épisode compressif récent qui se poursuit actuellement, le domaine interne de ce prisme a pu être émergé. Cette particularité

permet une étude intégrée terre-mer des épaisses séries sédimentaires constituant le remplissage des bassins perchés, depuis le bassin avant-arc jusqu'à la fosse de subduction.

ORGANISATION DU MEMOIRE

Le manuscrit, construit à partir de publications soumises, s'articule en 6 parties :

Un **premier chapitre** présente un état des connaissances publiées sur les bassins de pentes associés aux marges actives, permettant ainsi de préciser les questions scientifiques qui se posent quant au développement et à l'organisation sédimentaire de ces bassins. Le chapitre suivant (**Chapitre II**) expose le cadre géodynamique de la zone d'étude : la marge orientale de Nouvelle-Zélande. Il présente tout d'abord le microcontinent néo-zélandais dans le cadre général des subductions du Sud-Ouest Pacifique. Ensuite, le chantier sur lequel repose essentiellement cette étude est précisé. Il s'agit de la marge Hikurangi, située sur la côte orientale de l'Ile du Nord de Nouvelle-Zélande, et des bassins qui lui sont associés.

Les 3 chapitres suivants sont consacrés à l'étude stratigraphique des épaisses séries sédimentaires miocènes, essentiellement détritiques, et à une analyse de la déformation sur la pente du prisme d'accrétion Hikurangi. Il s'agit de trois publications soumises dans le cadre de ce travail de thèse :

Le premier papier (**Chapitre III**), accepté au *Journal of Sedimentary Research* en mai 2005, porte sur l'analyse stratigraphique d'un bassin perché, miocène inférieur à miocène moyen, situé à terre : le bassin d'Akitio. Ce travail est tout d'abord basé sur une analyse de faciès effectuée sur le terrain pour l'ensemble de la zone d'étude. Nos observations et interprétations en termes de milieu de dépôt et de système sédimentaire ont été synthétisées sous forme d'un nouveau modèle de faciès, nécessaire du fait d'une sédimentation dominée par les faibles granulométries. Nous présentons une synthèse du remplissage sédimentaire de ce bassin à partir de deux levés stratigraphiques représentatifs et localisés sur une même transversale du bassin. L'interprétation et les corrélations de ces deux sections permettent de caractériser qualitativement, géométriquement et temporellement l'architecture stratigraphique d'un tel bassin. Couplées à cette analyse, l'identification et l'interprétation des discontinuités sédimentaires au sein du remplissage permettent de reconstituer l'évolution tectono-sédimentaire du bassin, d'évaluer l'importance des processus tectoniques sur la

localisation et l'évolution des environnements de dépôts et d'intégrer ces résultats à l'échelle de l'histoire tectonique de la marge Hikurangi.

Le deuxième papier (**Chapitre IV**), soumis à *Basin Research* en mai 2005, est consacré à l'étude du bassin de Titihaoa, situé en mer et daté du Miocène moyen au Miocène supérieur. L'architecture stratigraphique du bassin a pu être décrite à partir d'une analyse de stratigraphie sismique couplée à des données de forage. Les discontinuités sismiques renseignent particulièrement sur la déformation du bassin et de ses bordures. L'interprétation des données diagraphiques (Gamma Ray et Sonic) a permis de caractériser plus précisément les séquences identifiées en sismique. L'évolution sédimentaire et structurale de ce bassin est ensuite comparée au bassin émergé d'Akitio. L'intégration des données aux différentes échelles d'observation (de celle de la sismique à celle du faciès) permet, tenant compte des différences et des similarités entre les deux bassins, d'appréhender de manière plus globale leur développement et les processus tectono-sédimentaires qui y président.

Le troisième papier (**Chapitre V**), dont la soumission est prévue à *Tectonophysics* pour juin 2005, présente une synthèse de la répartition spatio-temporelle de la déformation et du développement des bassins perchés à l'échelle de l'ensemble de la marge. Ce travail se base non seulement sur l'étude des bassins à terre et en mer (dont deux exemples ont été traités en détail dans les deux premiers papiers) mais aussi sur une analyse structurale détaillée (cartographie des bassins et des rides structurales, analyse macro- et micro-tectonique). Nous nous sommes particulièrement intéressés aux hauts structuraux qui constituent les bordures des bassins perchés : répartition géographique ainsi que succession de phases de croissance ou d'enneigement des hauts topographiques ou bathymétriques. Ceci a pu être effectué sur une transversale donnée, depuis le domaine du bassin avant-arc jusqu'à la fosse de subduction. Cette approche a permis de mieux caractériser les processus tectoniques et la déformation de la marge au cours d'un épisode de déformation donné, mais a également conduit à une détermination plus précise de l'évolution géologique de la marge active Hikurangi.

En guise de synthèse et de conclusion, le **chapitre VII**, en français, reprend les éléments clefs développés dans les différentes publications tout en développant certains aspects n'ayant pas été intégrés dans les papiers. Il s'agit par exemple de présenter les résultats obtenus concernant l'évolution des mouvements verticaux à partir de courbes de subsidence.

Les publications intégrées au manuscrit sont présentées toutes les trois en anglais. La plupart des figures ont été agrandies afin d'en améliorer la lisibilité. Les références bibliographiques ont été regroupées en une liste unique située en fin de manuscrit. Il est également à noter que, par souci de précision quant aux datations, les étages utilisés dans ce manuscrit sont les étages néo-zélandais (Cooper *et al.*, 2004). La correspondance avec les étages internationaux pour le Néogène est présentée figure I-1. Les méthodologies employées au cours de ma thèse n'ont délibérément pas fait l'objet d'un chapitre particulier au sein de ce mémoire car chacune d'entre elles est explicitée lorsqu'elles sont utilisées pour les besoins des publications.

Time in Ma	STANDARD CHRONOSTRATIGRAPHY (International Units)			NZ UNITS		
	SYSTEM	SERIES	STAGES	EPOCHS	STAGES	
0	QUATERNARY	^{HOLOCENE} PLEISTOCENE	IONIAN	WANGANUI	Haweran 0.34 (Wq)	
		PLIOCENE	U		0.95 CALABRIAN	Castlecliffian (Wc)
	L				1.77 GELASIAN	Nukumaruan 1.71 (Wn)
			PIACENZIAN		2.60	Mangapanian 2.40 (Wm)
					3.58	Waipipian 3.03 (Wp)
			ZANCLEAN		3.60	Opoitian (Wo)
5	NEOGENE		UPPER		5.32 MESSINIAN	TARANAKI
		TORTONIAN		7.12	Tongaporutuan (Tt)	
10				MIDDLE	11.20 SERRAVALLIAN	SOUTHLAND
		LANGHIAN	14.8		13.20 Lillburnian (Sl)	
15			LOWER		16.40 BURDIGALIAN	
		AQUITANIAN		16.00	16.00 Altonian (Pl)	
20		PALEOGENE	UPPER	20.52	PAREORA	19.00 Otaian (Po)
				23.80 CHATTIAN		21.70 Waitakian (Lw)
25					28.50	LANDON
					27.30	

Fig.I-1. Echelle chronostratigraphique utilisée en Nouvelle-Zélande, et équivalences internationales, du Néogène à l'actuel. Etages néo-zélandais d'après Cooper *et al.* (2004).

Chapitre I

Les bassins de pente associés aux prismes de subduction

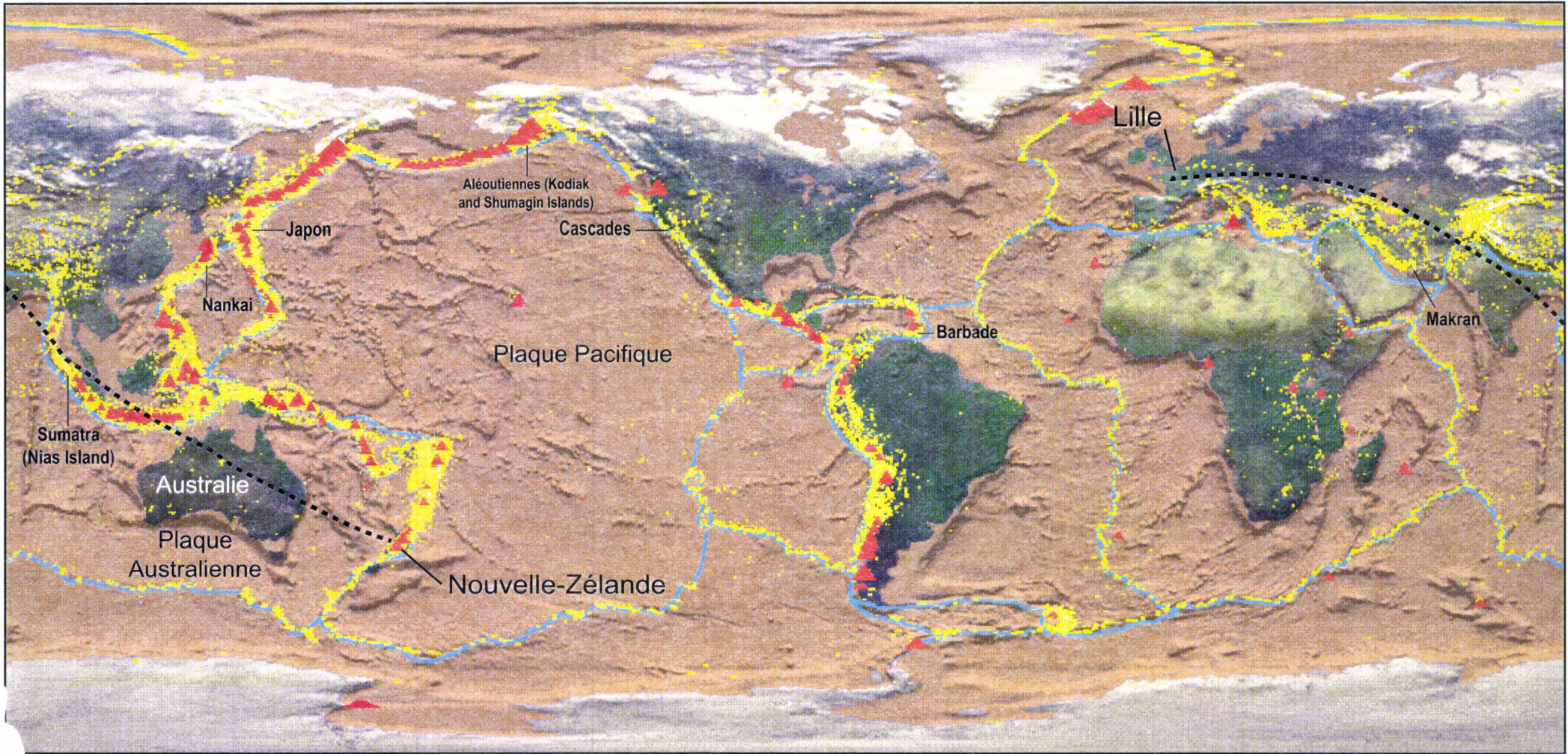


Fig.I-2. Carte bathymétrique et du relief mondial, localisation de la sismicité et du volcanisme aux limites de plaques (<http://www.solarviews.com>). Localisation des marges actives dont les bassins perchés ont fait l'objet d'études antérieures. Position géographique de la région du Sud-Ouest Pacifique, incluant la Nouvelle-Zélande.

Chapitre I

Les bassins de pente associés aux prismes de subduction

Ce premier chapitre présente l'état des connaissances sur la géométrie et l'évolution des bassins perchés sur les prismes d'accrétion et permet d'introduire les processus tectoniques et sédimentaires mis en jeu lors de leur développement.

Les bassins de pente perchés sur les prismes d'accrétion se rencontrent généralement en domaine marin. La plupart des connaissances actuelles concernant leur développement, leur géométrie et les processus tectono-sédimentaires impliqués résulte d'études de sismique marine et de forages. Ces études de géologie marine ont essentiellement porté sur des bassins récents associés aux systèmes en accrétion des Aléoutiennes (Moore et Karig, 1976; Underwood et Norville, 1986; Lewis *et al.*, 1988; Underwood et Moore, 1995), de la Barbade (Masclé *et al.*, 1990; Underwood et Moore, 1995; Huyghe *et al.*, 1996), des Cascades (Davis et Hyndman, 1989; Underwood et Moore, 1995; McAdoo *et al.*, 1997), de Nouvelle-Zélande (Lewis, 1980; Davey *et al.*, 1986), du Makran (White et Loudon, 1982), de Nankai et du Japon (Moore et Karig, 1976; Von Huene et Arthur, 1982; Okada, 1989; Underwood et Moore, 1995; Underwood *et al.*, 2003) et de Sumatra (Moore et Karig, 1976; Karig *et al.*, 1979, 1980; Stevens et Moore, 1985; Underwood et Moore, 1995) (Fig. I-2).

I) LES BASSINS PERCHES : STRUCTURE ET MORPHOLOGIE

En contexte de convergence, la pente du prisme d'accrétion est caractérisée par le développement de rides sous-marines linéaires sub-parallèles au front de subduction (Fig. I-3 et I-4). Au cours de la structuration du prisme d'accrétion, le développement de ces rides est contrôlé par la mise en place de chevauchements (Fig. I-3 et I-5) et/ou par la croissance de plis anticlinaux (Moore et Karig, 1976; Lewis, 1980; Stevens et Moore, 1985; Davey *et al.*, 1986; Lewis *et al.*, 1988; Okada, 1989; Huyghe *et al.*, 1996). Ce grain structural contrôle la géométrie de ces bassins étroits et allongés (Fig. I-3, I-5, et I-6) : les bassins de pente ou bassins perchés (*trench-slope basins*; Moore et Karig, 1976; Stevens et Moore, 1985; Underwood et Moore, 1995). Ces bassins sont donc portés par le prisme d'accrétion et se situent ainsi dans une zone géographique comprise entre la fosse et la plus haute ride du prisme (Fig. I-7). Dans ce mémoire, afin d'éviter toute analogie avec les bassins de pente présents dans d'autres contextes géodynamiques (*e.g.* marge passive, avant-pays de chaîne de montagnes), nous privilégierons le terme **bassin perché**.

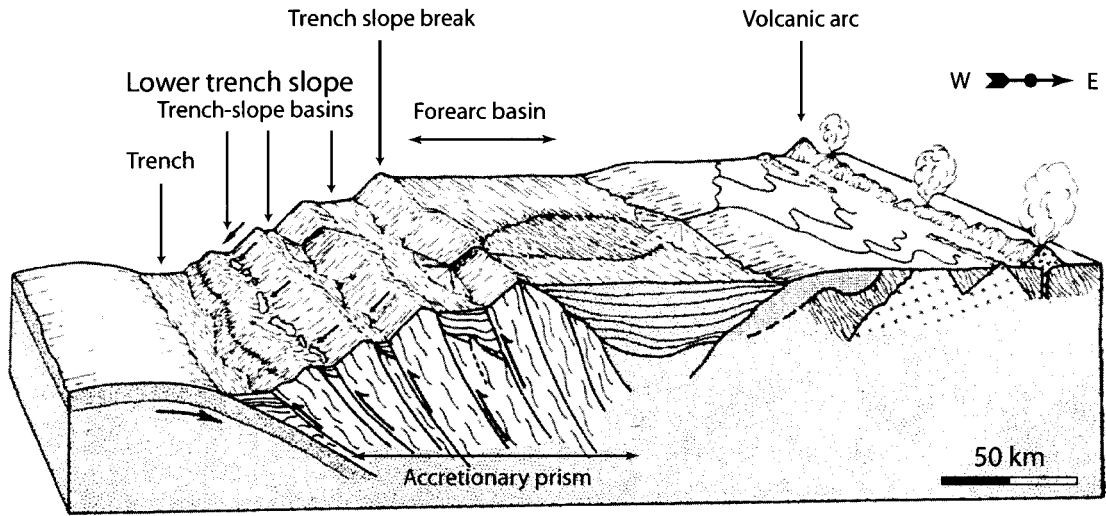


Fig.I-3. Bloc diagramme synthétique du complexe de subduction de Sumatra (Indonésie). Localisation des bassins perchés (*trench-slope basins*) et des rides structurales sur le prisme d'accrétion. Cette succession de hauts bathymétriques rectilignes et de dépressions structurales étroites caractérise le grain structural de la pente vers la fosse (*lower trench slope*). Cette structuration s'effectue parallèlement à la limite de plaque. D'après Moore *et al.* (1980).

Fig.I-4. Schéma structural du prisme d'accrétion de Sumatra (Indonésie) au niveau de la transversale de Nias Island. Notons la bonne corrélation entre les rides structurales, les chevauchements inclinés vers le Nord-Est (vers l'arc) et les bassins perchés. Toutes ces structures sont sub-parallèles à la fosse de Sunda. Stevens et Moore (1985).

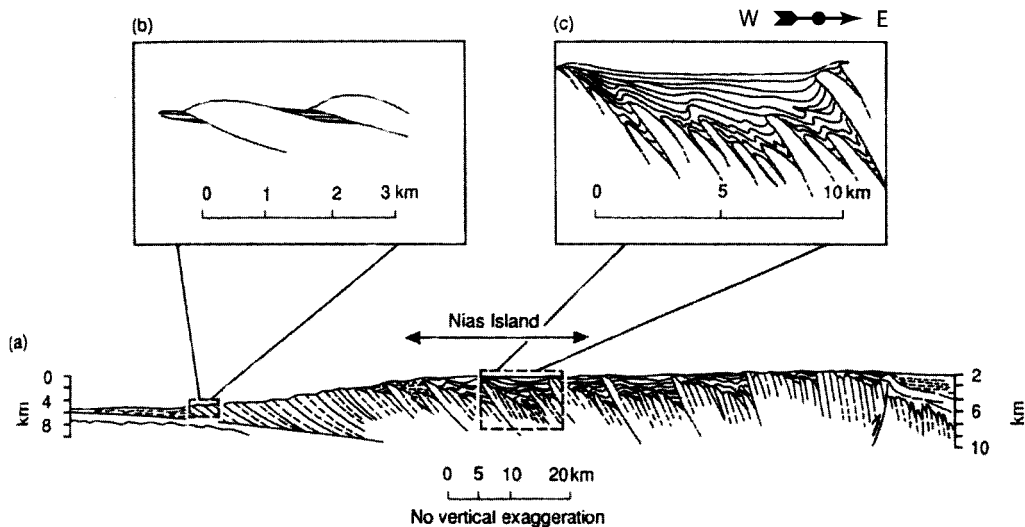
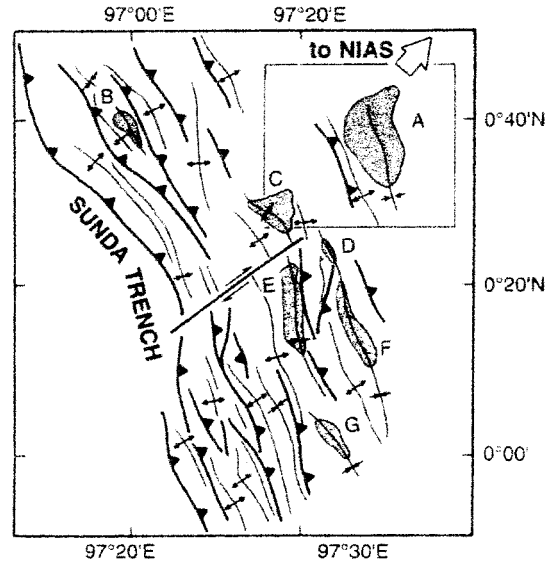


Fig.I-5. Coupe schématique du prisme d'accrétion de Sumatra (Indonésie) montrant la répartition, la géométrie et la structure des bassins perchés. Cette coupe interprétative est issue de données de sismique marine. D'après Moore et Karig (1976), Karig *et al.* (1978)

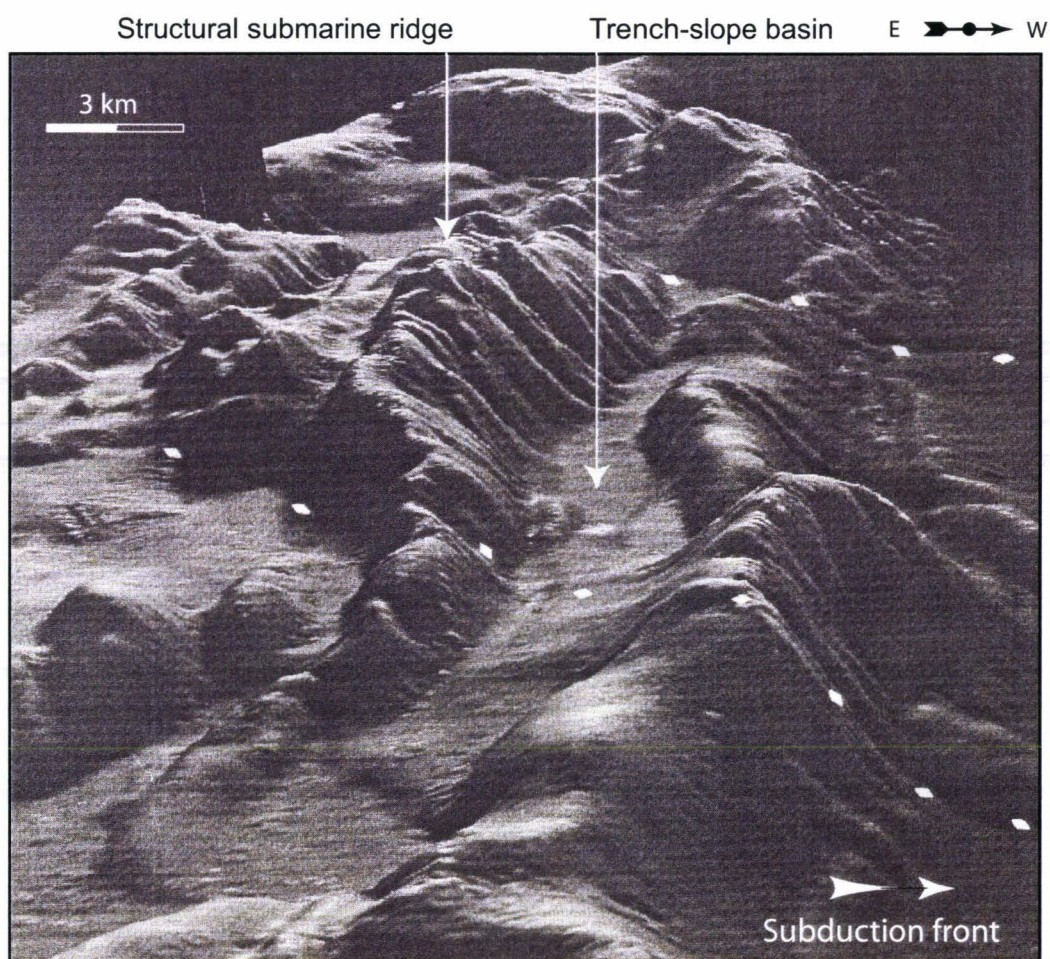


Fig.I-6. Vue 3D de la pente du prisme d'accrétion des Cascades (Amérique du Nord). Les rides structurales constituent les bordures de bassins perchés étroits et allongés parallèlement à la fosse. L'espacement de la grille est de 135 m et l'exagération verticale d'environ 5 x. McAdoo (1997).

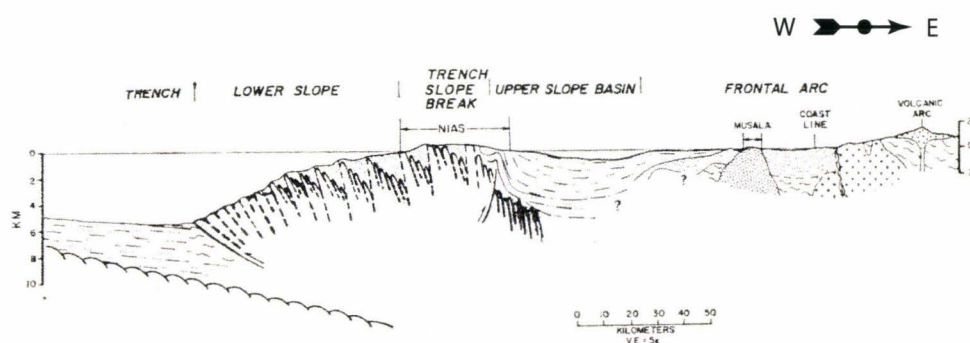


Fig.I-7. Coupe schématique du complexe de subduction de Sumatra (Indonésie) dans la région de Nias Island. Cette île correspond à l'émergence de la plus haute ride du prisme d'accrétion (trench slope break) et présente à l'affleurement les séries sédimentaires de bassins perchés néogènes. Ces bassins se développent sur la pente du prisme d'accrétion, depuis la fosse jusqu'au trench slope break. Karig *et al.* (1979).

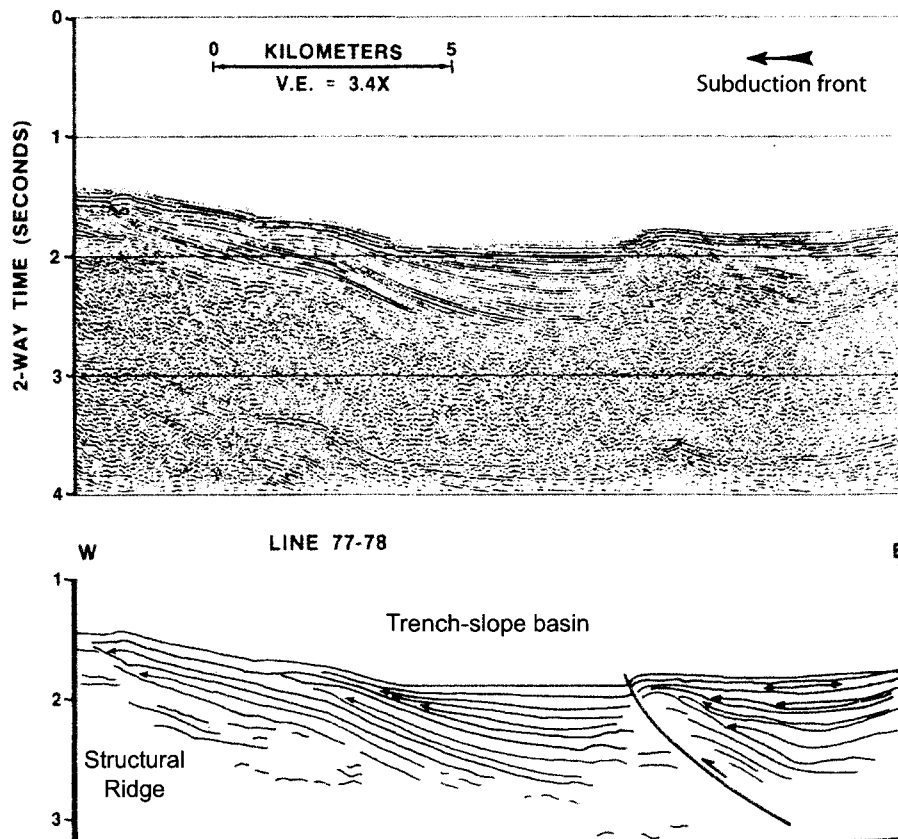


Fig.I-8. Profil de sismique réflexion et interprétation d'un bassin perché récent situé à proximité du front de subduction de Sumatra (Indonésie). Stevens et Moore (1995). Noter l'asymétrie du bassin et le chevauchement qui contrôle la surrection d'une bordure.

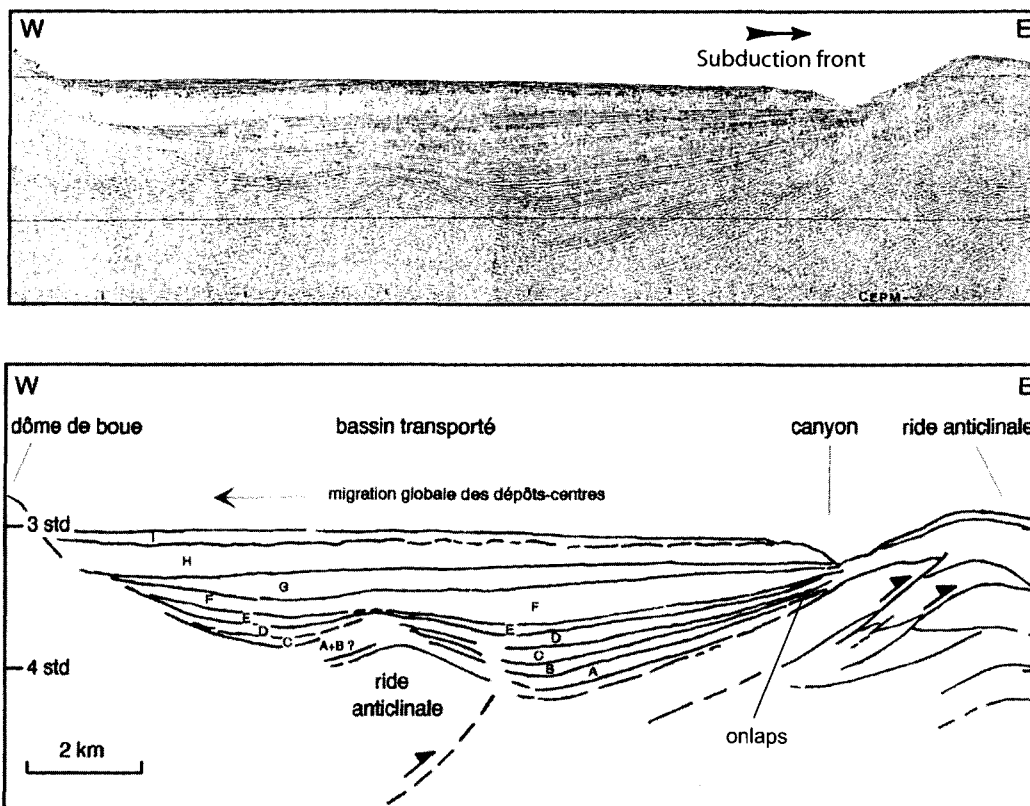
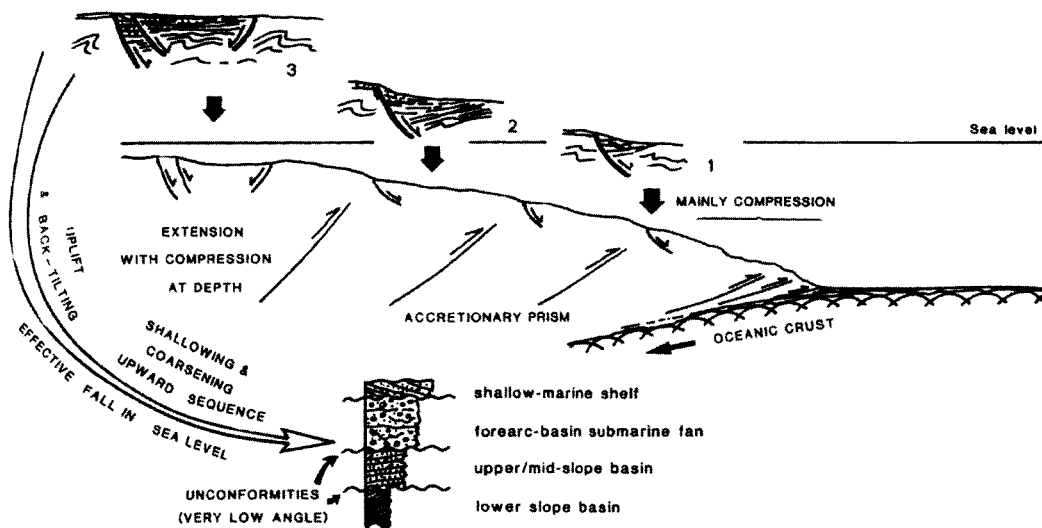


Fig.I-9. Profil de sismique réflexion et interprétation d'un bassin perché récent situé à proximité du front de subduction de la Barbade (Caraïbes). Huyghe *et al.* (1996). Noter le développement de rides anticlinales constituant les bordures du bassin, la migration rétrograde des dépôts-centres et les onlaps sur la bordure externe.

Cette terminologie reste cependant moins précise que son équivalent anglo-saxon "*trench-slope basin*" car elle ne permet pas de préciser clairement le cadre géodynamique où se rencontrent ces bassins. Par le terme de « bassin perché », nous sous-entendons donc « perché sur le prisme d'accrétion ».

Les rides structurales correspondent généralement à des plissements anticlinaux au-dessus de grands chevauchements inclinés vers l'arc (Fig. I-8 et I-9). Ces plis, et donc les rides structurales qu'ils engendrent, chevauchent vers la fosse et sont de ce fait très asymétriques (Moore et Karig, 1976; Lewis, 1980; Davey *et al.*, 1986; Okada, 1989) : un flanc long et de pente faible vers l'arc (sur le flanc interne de la ride, côté continent), un flanc court et de pente plus forte vers la fosse (sur le flanc externe de la ride, côté océanique). Les bassins perchés sont confinés entre ces rides et présentent par conséquent une géométrie dissymétrique qui se caractérise par une bordure côté fosse (bord océanique) à faible gradient de pente, et une bordure côté arc (bord continental) à fort gradient de pente (Fig. I-8). Les bassins perchés ont une largeur pouvant aller de 5 à 30 km et leur remplissage sédimentaire peut atteindre de 200 à 3000 m d'épaisseur (Lewis, 1980; Stevens et Moore, 1985, Davey *et al.*, 1986, Okada, 1989; Mascle *et al.*, 1990). La largeur des bassins dépend de l'espacement entre les hauts bathymétriques (rides structurales).

Les études de sismique marine ont montré que les séries sédimentaires des bassins perchés reposent en discordance sur le soubassement (substratum) du prisme d'accrétion (Fig. I-5). Cette discordance est mise en évidence par un onlap des séries sédimentaires sur la bordure externe (vers l'océan) des bassins (Fig. I-8 et I-9 ; Moore et Karig, 1976; Lewis, 1980; Stevens et Moore, 1985). À proximité de leur bordure interne (vers le continent), la succession sédimentaire est fortement déformée ce qui suggère la présence d'un contact par faille, avec chevauchement des séries du soubassement sur celles du bassin (Fig. I-8 ; Moore et Karig, 1980; Stevens et Moore, 1985). Le substratum des bassins perchés est généralement composé de turbidites et de sédiments marins profonds qui ont été accrétés de la fosse (Moore et Allwardt, 1980). Au cours de l'accrétion, ces séries ont été intensément déformées (Fig. I-5). Il s'agit d'ailleurs d'un critère majeur permettant de distinguer les séries du substratum de celles qui constituent le remplissage des bassins. En effet, ces sédiments peuvent présenter des faciès très similaires et ne se différencient parfois que sur des critères d'âge et d'intensité de la déformation. Contrairement au soubassement très structuré, on observe peu de déformation au sein des bassins perchés, pourtant contemporains de la subduction active (Fig. I-9 ; Stevens et Moore, 1985; Okada, 1989).



A GENERAL MODEL FOR THE EVOLUTION OF A COARSENING-UPWARD STRATIGRAPHY IN FOREARC SLOPE BASINS

- ± Progradation of clastic system at any stage
- ± Fluctuating eustatic sea level
- ± Change in nature of source sediments

Fig.I-10. Modèle synthétique d'évolution stratigraphique et structurale de bassins perchés sur un prisme d'accrétion. La surrection progressive des bassins et leur éloignement du front de subduction au cours du temps (*i.e.* rapprochement des zones d'alimentation) conduisent à la formation de séquences strato- et grano-croissantes caractéristiques de leur remplissage. Pickering *et al.* (1989). Noter que, contrairement à ce modèle, le développement de ce type de séquences au sein des bassins perchés peut s'effectuer en relation avec la surrection de hauts structuraux contrôlés par des chevauchements, sans intervention des phénomènes d'extension ici invoqués.

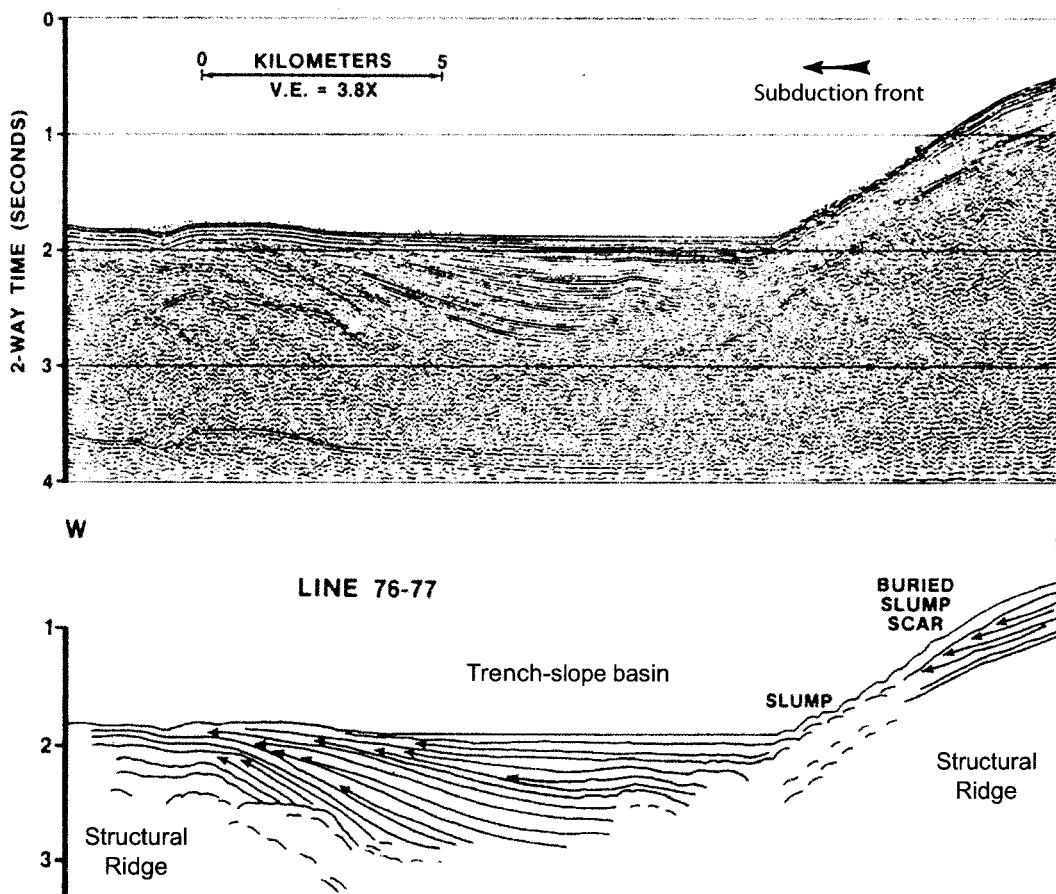


Fig.I-11. Profil de sismique réflexion et interprétation d'un bassin perché récent situé à proximité du front de subduction de Sumatra (Indonésie), Stevens et Moore (1995). Noter l'asymétrie du bassin, les onlaps sur sa bordure externe, les discontinuités à l'Est et la présence d'importantes instabilités gravitaires affectant la bordure Est du bassin.

Ainsi, le remplissage sédimentaire de ces bassins est nécessairement plus récent que les processus d'accrétion tectonique (Lewis *et al.*, 1988) et leurs séries doivent naturellement être beaucoup moins déformées que les sédiments accrétés qui constituent leur soubassement (Smith *et al.*, 1979; Moore et Karig, 1980; Moore et Allwardt, 1980; Stevens et Moore, 1985; Okada, 1989).

Dans la plupart des études sur le développement structural des bassins perchés, le soubassement est considéré comme résultant de processus d'accrétion *sensu stricto* (e.g. Moore et Karig, 1976; Moore et Karig, 1980; Davey *et al.*, 1986; Okada, 1989). Comme nous le verrons au cours de cette étude, ceci peut être admis dans le cas de bassins récents localisés à proximité du front de subduction (prisme d'accrétion externe). Dans ce contexte d'accrétion pure, les bassins perchés s'initient à proximité de la limite de plaques suite à la mise en place de chevauchements qui affectent le mur interne de la fosse de subduction (Fig. I-10). Ces chevauchements incorporent des sédiments de la fosse et de la plaque plongeante. Ensuite, les bassins sont progressivement soulevés au cours de la croissance du prisme d'accrétion (Moore et Karig, 1976; Lewis *et al.*, 1988). Au cours de cette surrection, les bassins s'éloignent du front de déformation sur le dos des unités soulevées, à la manière de bassins de type « piggy-back », au moins tant que les chevauchements développés à la base des bassins restent actifs (Fig. I-10). Le développement des bordures structurales des bassins est à l'origine d'un basculement progressif des unités sédimentaires vers le continent (Fig. I-5, I-8, I-9 et I-11 ; Moore et Karig, 1976; Moore et Karig, 1980; Lewis, 1980; Stevens et Moore, 1985; Davey *et al.*, 1986, Lewis *et al.*, 1988; Underwood et Moore, 1995; Huyghe *et al.*, 1996). Plus haut sur la pente du prisme d'accrétion, les chevauchements peuvent devenir inactifs (la déformation compressive restant préférentiellement localisée à proximité de la fosse), et les rides structurales sont alors scellées par les séries sédimentaires (Moore et Karig, 1976; Karig *et al.*, 1980; Lewis, 1980). Ce modèle d'évolution structurale implique une augmentation de la largeur des bassins, de l'épaisseur de leur remplissage sédimentaire et de leur âge lorsqu'on s'éloigne de la fosse (Fig. I-3, I-5, et I-10 ; Moore et Karig, 1976; Karig *et al.*, 1980; Stevens et Moore, 1985).

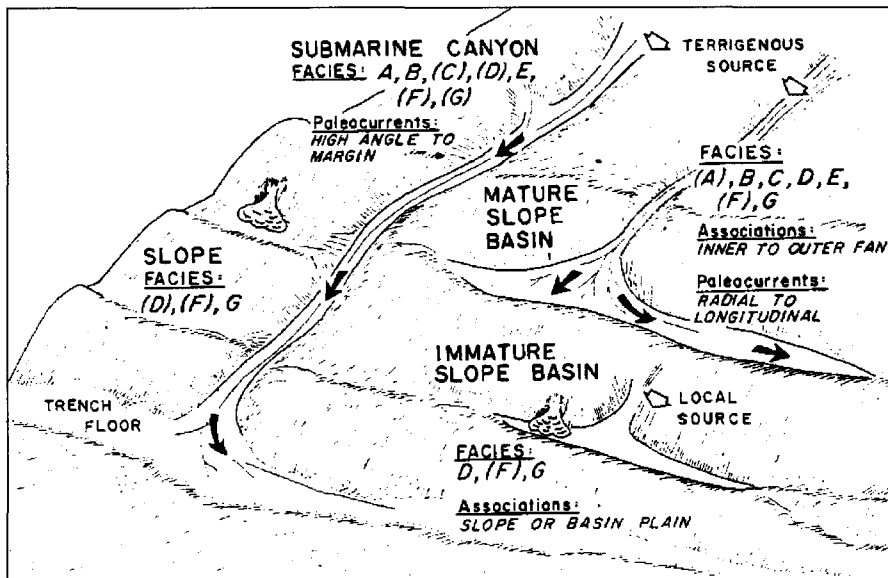


Fig.I-12. Modèle synthétique montrant une localisation prédictive des faciès marins profonds, dont les turbidites, et leurs relations sur la pente du prisme d'accrétion. Le code de lithofaciès (lettres) réfère au modèle de faciès marins profonds de Mutti et Ricci Lucchi (1978). D'après Underwood et Bachman (1982).

Facies A	<i>Description:</i>	coarse sandstone and conglomerate irregular cut-and-fill structures size grading and shale rip-up clasts
Facies B	<i>Interpretation:</i> <i>Description:</i>	grain flows and high-concentration turbidity currents thick sandstone, coarse to medium-fine lenticular beds parallel or broadly undulating current laminae dewatering features
Facies C	<i>Interpretation:</i> <i>Description:</i>	grain flows and high-concentration turbidity currents thick-bedded, medium to fine sandstone; minor shale good lateral continuity, low-relief channels sandstone: shale ratio > 1 rip-up clasts, complete Bouma sequences
Facies D	<i>Interpretation:</i> <i>Description:</i>	classical turbidity currents thin-bedded, fine-grained sandstone; shale interbeds marked lateral continuity sandstone: shale ratio < 1 base-missing Bouma sequences
Facies E	<i>Interpretation:</i> <i>Description:</i>	dilute, low-density turbidity currents thin sandstone and shale interbeds discontinuous beds with wedging and lensing ripple marks, cross-laminae, sharp tops and bases sandstone: shale ratio > 1
Facies F	<i>Interpretation:</i> <i>Description:</i>	overbank deposition on levees, interchannel chaotic deformation, soft-sediment folds blocks in fine-grained matrix
Facies G	<i>Interpretation:</i> <i>Description:</i> <i>Interpretation:</i>	submarine slides, mudflows, debris flows mudstone, shale, marl indistinct to even, parallel bedding hemipelagic and pelagic deposition

Fig.I-13. Modèle de faciès de Mutti et Ricci Lucchi (1978) - Caractéristiques et interprétations des lithofaciès correspondant aux turbidites et aux dépôts marins profonds qui leur sont associés. Underwood et Moore (1995).

II) LES BASSINS PERCHES : FACIES ET SYSTEMES DE DEPOT

Underwood et Bachman (1982) ont proposé un modèle de dépôt synthétique basé sur des études géophysiques et des forages de bassins perchés récents ainsi que sur des analogues anciens à l’affleurement (Fig. I-12). Ce modèle propose une localisation prédictive des faciès marins profonds sur la pente du prisme d’accrétion basée sur le modèle de lithofaciès de Mutti et Ricci Lucchi (1978) (Fig. I-13). La pente régionale de la marge, vers l’océan, est entaillée par d’importants canyons sous-marins et par des chenaux qui canalisent l’apport sédimentaire vers la fosse et les bassins perchés (Fig. I-12 et I-14). Du fait du développement des hauts structuraux, nombre de ces canyons sont bloqués sur la pente et n’atteignent pas la fosse (Karig *et al.*, 1979; Underwood et Karig, 1980; Underwood et Bachman, 1982). Les faciès turbiditiques et autres dépôts gravitaires sont donc majoritairement piégés dans les bassins perchés localisés sur la partie haute du prisme d’accrétion, à proximité de la plus haute ride du prisme (Fig. I-15). De plus, ces bassins, qualifiés de matures (Underwood et Bachman, 1982), piègent préférentiellement les sédiments grossiers (Moore *et al.*, 1980; Underwood et Bachman, 1982; Stevens et Moore, 1985). Plus bas sur la pente, les bassins perchés peuvent être déconnectés des zones d’alimentation et sont alors dominés par une sédimentation hémipélagique (Fig. I-12 et I-15). Ces bassins sont alors qualifiés d’immatures (Underwood et Bachman, 1982). L’augmentation du bas vers le haut de la pente des apports terrigènes est à l’origine du dépôt de méga-séquences turbiditiques strato- et grano-croissantes au sein des bassins (Fig. I-16 ; Moore *et al.*, 1980 ; Underwood et Moore, 1995). Ceci reflète la surrection progressive des domaines de sédimentation depuis la fosse de subduction (Fig. I-10 ; Moore *et al.*, 1980; Underwood et Bachman, 1982). Cependant ce modèle stratigraphique général contraste avec les résultats obtenus récemment lors de forages sur le prisme d’accrétion de Nankai (Underwood *et al.*, 2003). Cette étude met en évidence l’existence de séquences strato- et grano-décroissantes au sein de bassins perchés (Fig. I-17). La formation de telles séquences peut être attribuée soit à un blocage d’un système d’alimentation antérieur (développement de hauts structuraux en amont du système suite à la mise en place de chevauchements hors-séquences, déformation de la marge en réponse au passage en subduction d’aspérités, ...), soit à une déconnection du réseau de canyons de la ligne de côte (augmentation du niveau marin relatif ou subsidence). En ce qui concerne les bassins perchés matures (Fig. I-12), les directions d’alimentation sont généralement parallèles à la marge (c’est-à-dire perpendiculaires à la ligne de plus grande pente) ce qui reflète une canalisation des apports sédimentaires le long de l’axe des bassins (Underwood et Bachman, 1982).

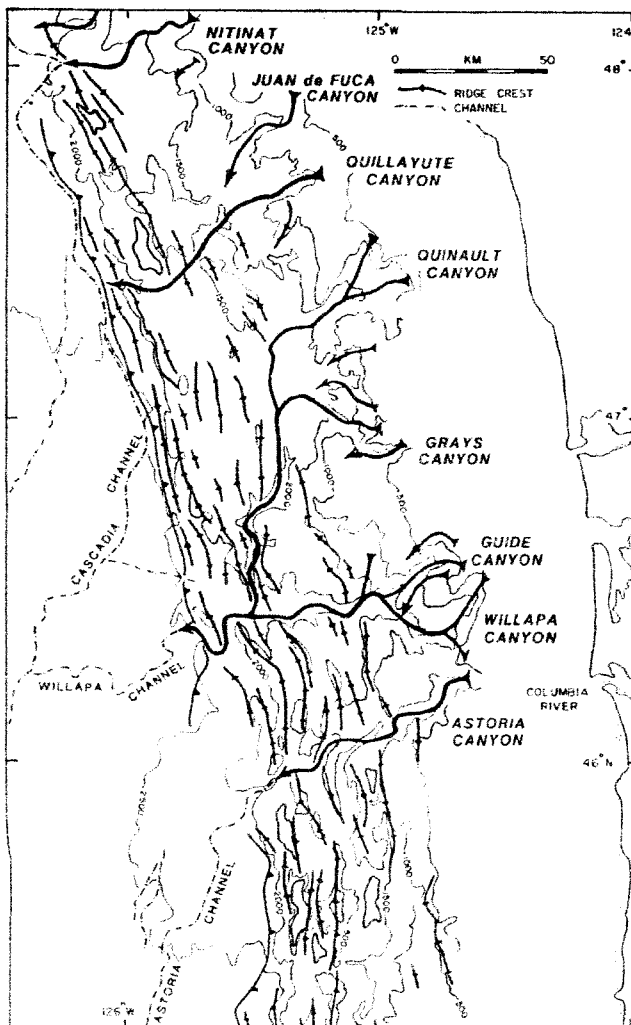
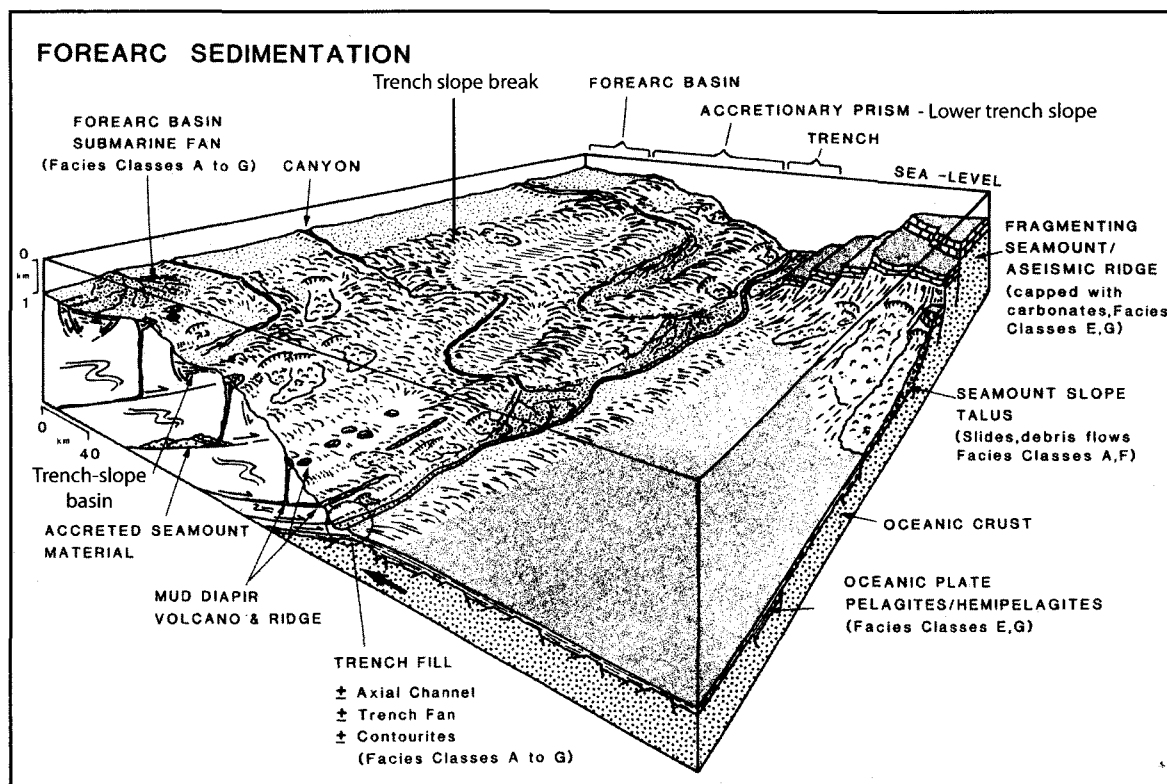


Fig.I-14. Carte bathymétrique simplifiée et structure du prisme d'accrétion des Cascades (Amérique du Nord). La pente du prisme est entaillée de nombreux canyons sous-marins (marqués par des flèches) qui alimentent la fosse et les bassins perchés (marqués en traits gras sub-parallèles à la fosse). Underwood et Moore (1995), d'après l'équipe scientifique EEZ SCAN 84 (1986).

Fig.I-15. Modèle sédimentaire et morphostructural d'une zone de subduction. Pickering *et al.* (1989).



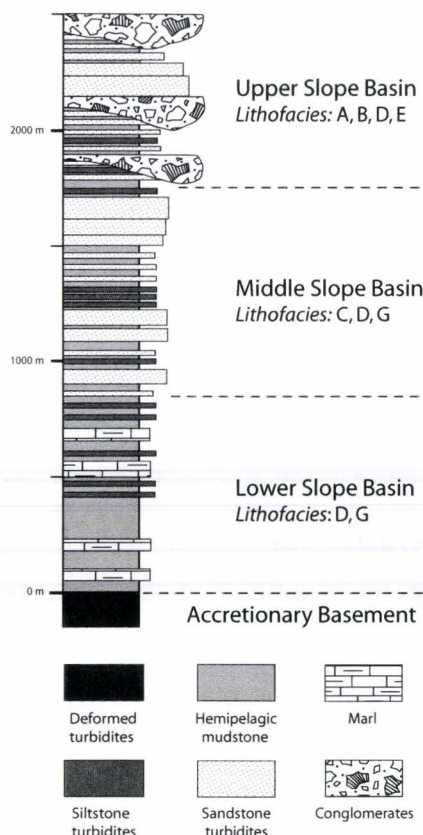


Fig.I-16. Modèle conceptuel d'évolution stratigraphique d'un bassin perché. La séquence strato- et grano-croissante reflète ici la surrection progressive du bassin qui est associée à une augmentation des apports terrigènes. Log sédimentologique d'après Underwood and Moore (1995), et Underwood *et al.* (2003). Synthèse basée sur les observations de Moore *et al.* (1980), Nias Island (Indonesia).

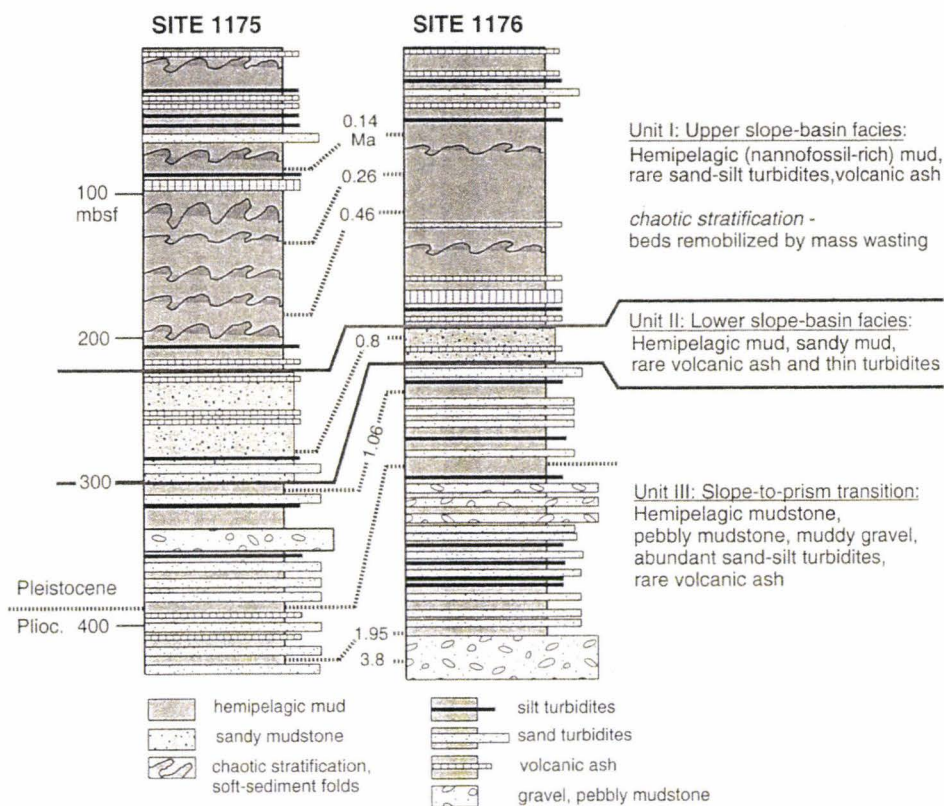


Fig.I-17. Alternative au modèle précédent (Fig.I-Q) - Lithostratigraphie des sites ODP 1175 et 1176 montrant l'existence de séquences strato- et grano-décroissantes au sein des bassins perchés du prisme d'accrétion de Nankai (Japon). Ces séquences peuvent résulter soit d'un blocage des systèmes d'alimentation (déformation du prisme), soit d'une déconnection des systèmes par rapport aux sources (*i.e.* augmentation du niveau eustatique). Underwood *et al.* (2003).

Au débouché des canyons, les alimentations peuvent cependant être perpendiculaires à sub-perpendiculaires à la marge (Fig. I-12). Bien que les canyons sous-marins jouent un rôle prépondérant dans la distribution et la répartition des sédiments sur la pente du prisme d'accrétion (Fig. I-14), d'autres processus contribuent également de manière importante au budget sédimentaire des bassins perchés. Ainsi, d'importantes variations du mode détritique le long de la pente de la partie Est du prisme d'accrétion des Aléoutiennes (DSDP Leg 18, Site 181) suggèrent un dépôt par des courants turbiditiques non-confinés ayant pour origine des sources sédimentaires multiples (Underwood et Norville, 1986). De plus, les instabilités de pente qui affectent les bordures des bassins, suite à une activité tectonique et/ou à des fluctuations du niveau eustatique, sont à l'origine d'importants remaniements sous-marins (Fig. I-11, I-12, et I-15). Ce dernier processus est responsable de la création de sources sédimentaires locales, identifiées notamment dans la partie Ouest du complexe de subduction de Sumatra (Stevens et Moore, 1985).

Les bassins de pente, qui font l'objet de notre étude, sont liés au développement du complexe de subduction Hikurangi, sur la marge orientale de l'île Nord de Nouvelle-Zélande. Le Chapitre suivant présente d'une part le contexte géodynamique de la Nouvelle-Zélande, puis plus précisément l'état des connaissances antérieures sur le remplissage et la dynamique de ces bassins perchés sur la marge Hikurangi.

Chapitre II

Cadre Géodynamique et bassins de la marge Hikurangi

Papouasie Nouvelle-Guinée

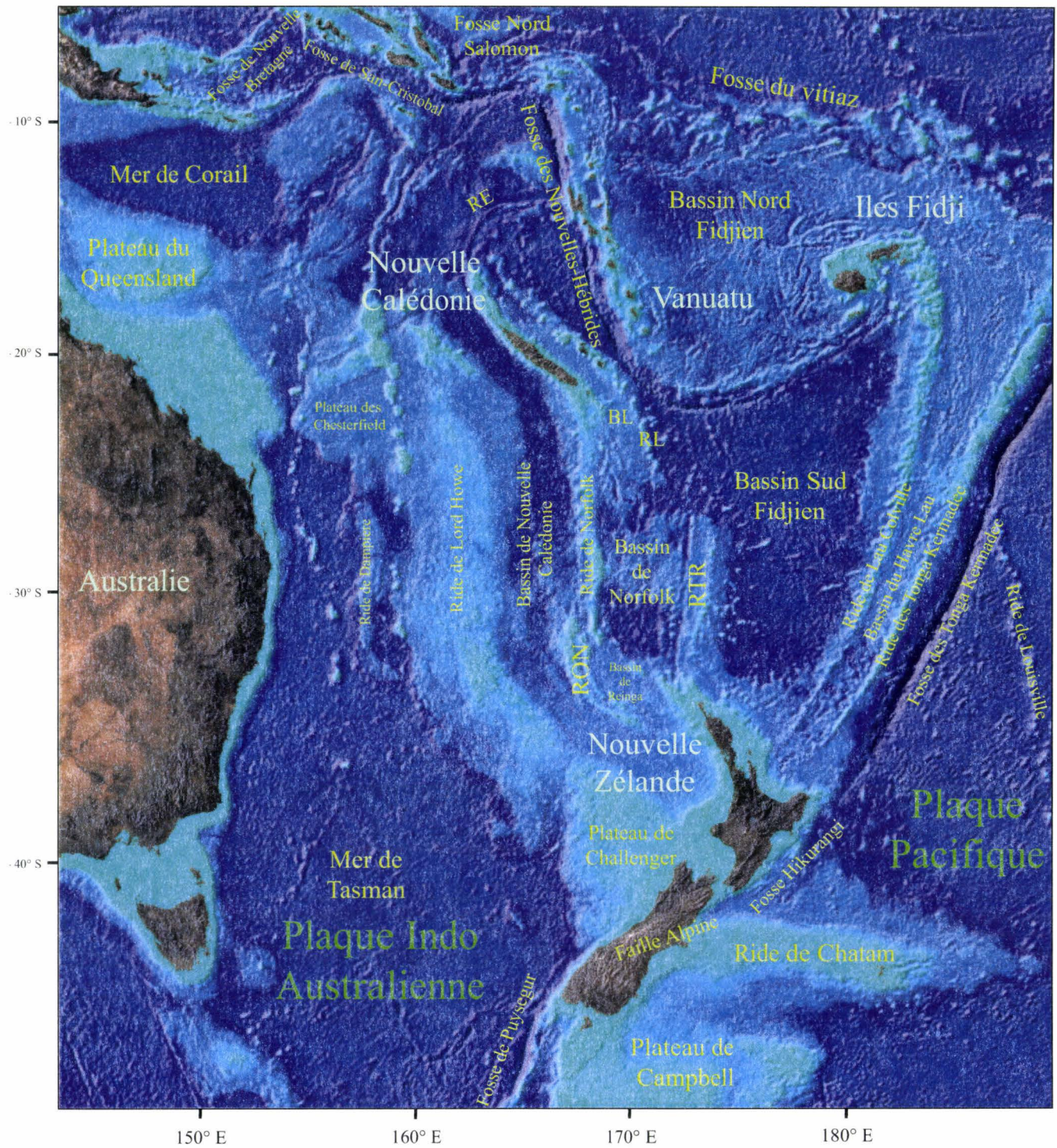


Fig.II-1. Carte bathymétrique du Sud-Ouest Pacifique et localisation des structures majeures (la bathymétrie est issue du site internet du groupe de géodésie de l'université de Curtin, Australie; <http://www.cage.curtin.edu.au/~geogrp/links.html>). BL - Bassin des Loyauté, RL - Ride des Loyauté, RE - Ride d'entrecasteaux, RTR - Ride des Trois-Rois, RON - Ride Ouest-Norfolk.

Chapitre II

Cadre Géodynamique et bassins de la marge Hikurangi

Ce chapitre présente tout d'abord le microcontinent de Nouvelle-Zélande, dans son environnement géodynamique du Sud-Ouest Pacifique. Il expose ensuite les principales caractéristiques morphologiques, structurales et sédimentaires associées à la zone de subduction Hikurangi. Nous précisons également, plus particulièrement, les résultats des études antérieures à propos des bassins perchés signalés sur la marge néo-zélandaise.

I) CADRE GEODYNAMIQUE DE LA MARGE ACTIVE HIKURANGI

A) La Nouvelle-Zélande dans le Sud-Ouest Pacifique

La Nouvelle-Zélande est située aux antipodes, dans la région du Sud-Ouest Pacifique (Fig. I-2). Cette zone d'affrontement majeur des plaques Pacifique à l'Est et Australie à l'Ouest, présente une forme triangulaire définie par la Papouasie-Nouvelle-Guinée, les îles Tonga-Fidji et la Nouvelle-Zélande (Fig. II-1). Cette région du globe correspond à une zone complexe, marquée par des processus orogéniques majeurs (subduction, obduction, et plus rarement collision), distincts dans le temps et dans l'espace. Actuellement, les processus géodynamiques dominants sont ceux qui sont associés aux limites de plaques actives, principalement des zones de subduction.

1) La limite de plaques Pacifique-Australie

Il s'agit du trait structural dominant dans le domaine du Sud-Ouest Pacifique. Cette limite de plaques s'étend du Sud vers le Nord depuis la Nouvelle-Zélande, jusqu'en Nouvelle-Bretagne, à proximité de la Papouasie-Nouvelle-Guinée (Fig. II-1 et II-2).

→ Au niveau de la Nouvelle-Zélande, la limite de plaques Pacifique- Australie présente deux subductions à vergences opposées : au Sud, celle de la fosse de Puysegur à vergence Est et au Nord, celle de la fosse Hikurangi à vergence Ouest (Fig. II-2). Ces deux subductions sont reliées par une grande faille transformante intracontinentale : la Faille Alpine qui montre un décalage dextre total de 440 à 470 km selon les marqueurs géologiques utilisés (Sutherland, 1999a).

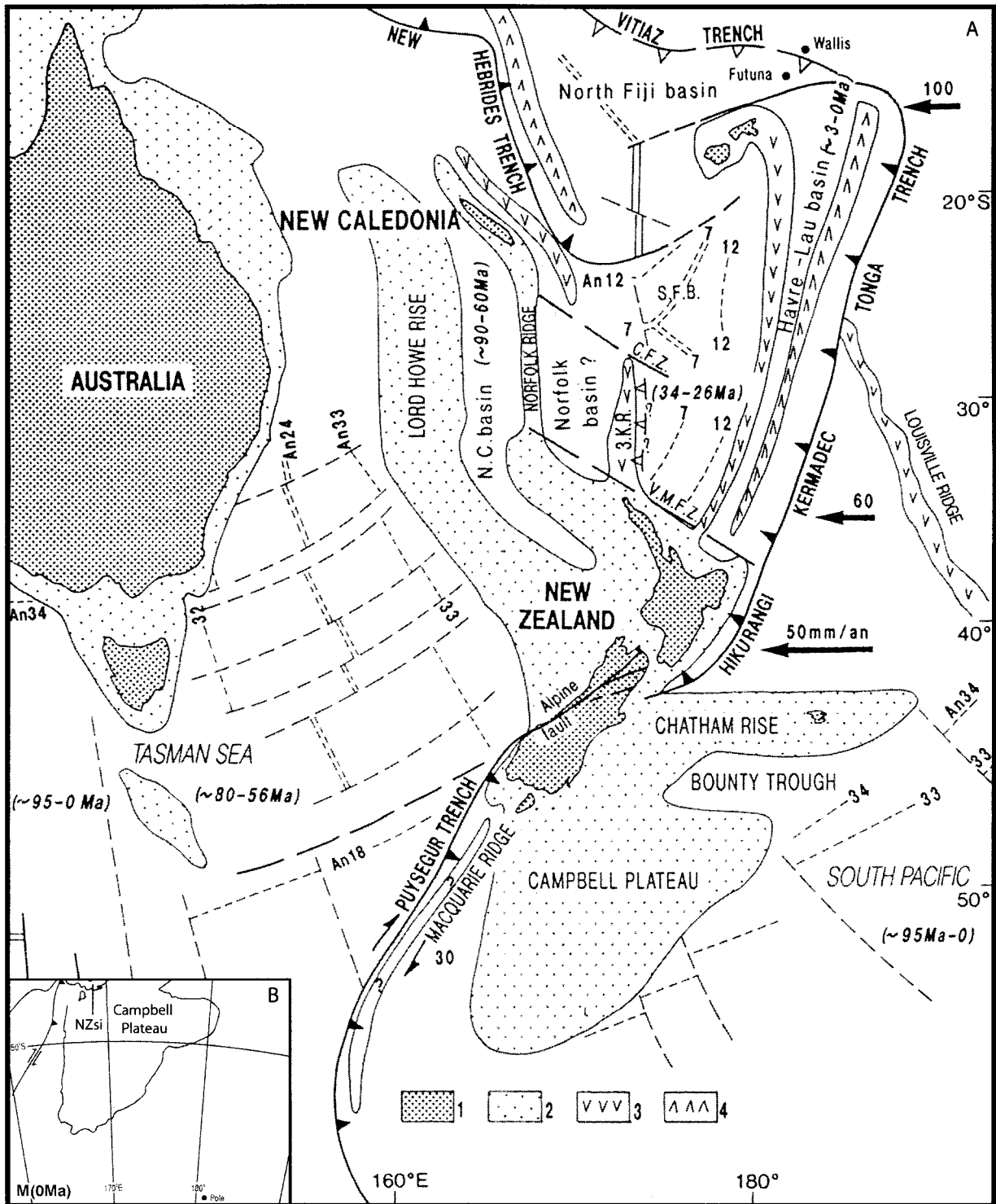


Fig.II-2. A - La Nouvelle-Zélande dans son cadre géodynamique. 1 - zones émergées ; 2- croûte continentale immergée; 3 - arcs volcaniques inactifs probables; 4 - arcs volcaniques actifs. An - anomalies magnétiques. L'âge des différents bassins océaniques est indiqué entre parenthèses; 3 K.R. - ride des Trois-Rois; N.C. - bassin de Nouvelle-Calédonie; S.F.B. - bassin Sud-Fidjien; V.M.F.Z. - zone de fracture de Vening-Meinesz; C.F.Z. - zone de fracture de Cook (Ferrière et Chanier, 1993). **B** - Localisation du pôle de rotation Pacifique/Australie au Sud-Est du plateau de Campbell. NZsi - Ile Sud de Nouvelle-Zélande. King, 2000.

Le mouvement le long de la Faille Alpine a fortement varié au cours du Cénozoïque ; après une période probablement extensive entre 45 et 25 Ma, il est devenu nettement décrochant dextre à partir de 25 Ma (Sutherland *et al.*, 2000). C'est seulement à partir de 6 Ma (Walcott, 1998) que le mouvement entre les deux blocs continentaux devient clairement transpressif et cette convergence oblique conduit ainsi à la surrection des Alpes du Sud (« *Southern Alps* »).

→ Le long de la fosse des Tonga-Kermadec, zone de subduction à vergence Ouest, la vitesse de convergence augmente progressivement vers le Nord, de 60 à 100 mm/an (Fig. II-2 ; Pelletier *et al.*, 1998). Le passage en subduction de la ride de Louisville (Fig. II-1) marque la limite entre la fosse des Kermadec au Sud et celle des Tonga au Nord (Dupont, 1982 ; Pelletier et Dupont, 1990). L'ensemble de cette zone de subduction est dominé par des processus d'érosion tectonique (Von Huene et Scholl, 1991).

→ La fosse des Nouvelles-Hébrides, subduction à vergence Est, a pris le relais d'une subduction fossile à vergence opposée dont la fosse du Vitiaz, située plus au Nord, est le témoin (Fig. II-2). L'abandon de cette paléo-subduction au profit de la subduction actuelle des Nouvelles-Hébrides est accompagné par l'ouverture entre les deux fosses du bassin océanique Nord-Fidjien (Auzende *et al.*, 1995).

→ Les zones de subduction actives de Cristobal, à vergence Nord, et Nord-Salomon, à vergence Sud, se prolongent vers l'Ouest par la fosse de Nouvelle-Bretagne, à vergence Sud. Cette dernière rejoint la Papouasie-Nouvelle-Guinée où la plate-forme australienne entre en collision avec les marges du Sud-Est asiatique (Fig. II-1).

Les vitesses de convergence entre les plaques Pacifique et Australie augmentent globalement vers le Nord (Fig. II-2). Cependant, des diminutions locales de ces vitesses sont enregistrées au niveau des zones où l'entrée en subduction de rides sous-marines majeures est observée (ride de Louisville/Tonga-Kermadec, ride d'Entrecasteaux et ride des Loyauté/Nouvelles-Hébrides ; Pelletier *et al.*, 1998). Du point de vue cinématique, l'accélération de la convergence vers le Nord s'explique par la position du pôle de rotation Pacifique-Australie (Fig. II-2B) situé actuellement au Sud-Est du plateau de Campbell (Walcott, 1978 ; DeMets *et al.*, 1994). Cette position rend compte également de l'obliquité du vecteur vitesse Pacifique-Australie au Sud de la subduction Hikurangi.

Notons également qu'aux zones de subduction du Sud-Ouest Pacifique sont naturellement associés des arcs volcaniques actifs comme la zone volcanique de Taupo (Nouvelle-Zélande), les arcs des Tonga Kermadec, des Vanuatu, des Nouvelles-Hébrides ...

2) Les rides et bassins de la plaque Australie

Le Sud-Ouest Pacifique montre une morphologie complexe comprenant une succession de rides et de bassins allongés qui convergent presque tous vers le microcontinent néo-zélandais (Fig. II-1 et II-2). Ces éléments, dont l'âge et/ou la nature crustale ne sont pas toujours bien connus, sont de l'Ouest vers l'Est:

→ La mer de Tasman : il s'agit d'un bassin océanique en accretion de *c.* 80 Ma (An.33) à *c.* 56 Ma (An.24) (Hayes et Ringis, 1973 ; Weissel et Hayes, 1977 ; Leitch, 1984).

→ La ride de Lord Howe : cette ride sous-marine d'affinité continentale est apparentée à la croûte du continent australien dont elle s'est détachée au cours de l'ouverture de la mer de Tasman au Crétacé supérieur (Woodward et Hunt, 1971 ; Shor *et al.*, 1971).

→ Le bassin de Nouvelle-Calédonie : bien qu'aucune anomalie magnétique n'y ait été identifiée, ce bassin à couverture sédimentaire épaisse (734 m ; Van der Lingen *et al.*, 1973) serait de nature océanique (Shor *et al.*, 1971 ; Sutherland, 1999b). Son ouverture serait d'âge Crétacé supérieur, contemporain de l'anomalie magnétique 33 (79-83 Ma) (Sutherland, 1999b).

→ Les rides de Norfolk et Ouest-Norfolk : il s'agit de lanières continentales à croûte amincie, épaisse de 21 à 30 km (Woodward et Hunt, 1971 ; Shor *et al.*, 1971, Zhu et Symonds, 1994 ; Herzer *et al.*, 1997), séparées du Gondwana lors d'une phase de rifting créacé (Willcox *et al.*, 1980 ; Kroenke, 1984). L'histoire tertiaire de la ride de Norfolk est plus controversée. D'une part, il pourrait s'agir d'un système complexe d'arc résultant d'une subduction à vergence Est située à l'Ouest de la ride (Dubois *et al.*, 1974 ; Kroenke et Eade, 1982). D'autre part, la ride pourrait être liée à une subduction à vergence opposée (Ouest) qui s'intègre dans une évolution du secteur caractérisée par la migration vers l'Est de la limite de plaque et le développement de bassins marginaux (Karig, 1971 ; Packham et Falvey, 1971). La ride sous-marine de Norfolk émerge en grande partie au niveau de la Nouvelle-Calédonie. La ride Ouest-Norfolk se prolonge jusqu'en Nouvelle-Zélande où elle émerge au niveau du Northland. L'émersion de ces rides montre la présence d'un socle Permien à Jurassique (Paris et Lillie, 1977 ; Suggate *et al.*, 1978 ; Paris, 1981 ; Spörli et Kear, 1989) ainsi que la mise en place d'ophiolites à l'Eocène supérieur en Nouvelle-Calédonie (Paris *et al.*, 1979 ; Paris, 1981 ; Collot *et al.*, 1987 ; Cluzel *et al.*, 1994), puis au Miocène basal en Nouvelle-Zélande (Ballance et Spörli, 1979 ; Cassidy et Locke, 1987 ; Spörli et Kear, 1989 ; Malpas *et al.*, 1992). Les rides de Norfolk et Ouest Norfolk pourraient correspondre à une ride unique décalée ultérieurement par le jeu dextre de la zone de fracture de Vening-Meinesz (Fig. II-2).

→ Les bassins des Loyauté, Nord et Sud Norfolk et de Reinga : Ces sous-bassins constituaient un bassin océanique unique au Crétacé supérieur (Collot *et al.*, 1982 ; Launay *et al.*, 1982 ; Eade, 1988 ; Van de Beuque, 1999). Le bassin de Norfolk a ensuite subi une seconde phase d'ouverture de l'Oligocène terminal au Miocène inférieur (c. 25-15 Ma ; Bailleul, 2001). L'origine de cette ouverture tardive est encore discutée, mais il semble que le bassin de Norfolk constituait alors le domaine arrière-arc d'une subduction à vergence Ouest localisée à l'Est de la ride des Trois-Rois (Herzer *et al.*, 1997 ; Mortimer *et al.*, 1998 ; Bailleul, 2001).

→ Les rides des Loyauté et des Trois-Rois : ces rides sous-marines, décalées par le jeu senestre de la zone de fracture de Cook (Bailleul, 2001), correspondent à d'anciens arcs volcaniques d'âge oligocène supérieur à miocène inférieur (Maillet *et al.*, 1982 ; Mortimer *et al.*, 1998). Pour certains auteurs, le volcanisme de la ride des Loyauté serait plutôt daté du Miocène supérieur (Kroenke, 1984). La ride des Loyauté pourrait également s'être formée lors d'un épisode extensif par magmatisme anorogénique de l'Oligocène au Miocène supérieur (Rigolot, 1989 ; Monzier, 1993). Quoiqu'il en soit, Cluzel *et al.* (1994) montrent qu'un volcanisme anorogénique plus récent vient se superposer à la première phase. La ride des Trois-Rois est vraisemblablement associée à la subduction à vergence Ouest de la bordure Ouest du bassin Sud-Fidjien, subduction à l'origine de la seconde phase d'ouverture du bassin de Norfolk (Karig, 1970 ; Weissel et Watts, 1975 ; Watts *et al.*, 1977 ; Kroenke et Dupont, 1982 ; Kroenke et Eade, 1982 ; Lapouille, 1982 ; Herzer et Mascle, 1996 ; Herzer *et al.*, 1997 ; Mortimer *et al.*, 1998 ; Bailleul, 2001).

→ Les bassins Nord et Sud-Fidjien : ces bassins océaniques (Shor *et al.*, 1971) s'ouvrent respectivement entre c. 33 Ma (An.13) et c. 25 Ma (An.7) pour le bassin Sud-fidjien (Davey, 1982 ; Malahoff *et al.*, 1982 ; Sdrolias, 2000) et du miocène à l'actuel pour le bassin Nord-Fidjien. Le bassin Sud-Fidjien résulte du fonctionnement d'un système complexe de dorsales organisées autour de deux points triples (Sdrolias, 2000).

→ La ride de Lau-Colville : cette ride sous-marine est un arc volcanique rémanent séparé de l'arc des Tonga-Kermadec par l'ouverture du bassin du Havre-Lau (Karig, 1970 ; Weissel, 1977 ; Malahoff *et al.*, 1982). Le volcanisme actif est daté de 28 à 23 Ma (Kroenke, 1984 ; Yan et Kroenke, 1993 ; Ballance *et al.*, 1999).

→ Le bassin du Havre-Lau : il s'agit d'un bassin arrière-arc récent associé à la subduction des Tonga-Kermadec. L'ouverture s'effectue depuis le Pliocène (Malahoff *et al.*, 1982) et est plus ancienne (c. 5.5 Ma) dans la partie Nord du bassin que plus au Sud (c. 2 Ma) (Hawkins et Parson, 1994 ; Clift *et al.*, 1994).

→ La ride des Tonga-Kermadec : c'est un arc volcanique actif associé à la subduction des Tonga-Kermadec.

La formation de cet ensemble de bassins marginaux, de domaines continentaux immergés et d'arcs volcaniques anciens résulte de quatre phases tectoniques majeures, marquées par une migration vers l'Est de la limite de plaques Pacifique/ Australie :

1) La première phase, anté- fin Crétacé inférieur (anté- 110 - 100 Ma), est caractérisée par la subduction de la plaque Pacifique ou Phoenix sous la marge orientale du Gondwana (Bradshaw, 1989 ; Luyendyk, 1995).

2) La seconde phase, fin Crétacé inférieur - Crétacé supérieur (c. 100 Ma à c. 80 Ma), est marquée par la fragmentation de cette marge et l'ouverture des bassins de Nouvelle-Calédonie, de Reinga et des Loyauté (Kroenke, 1984; Uruski et Wood, 1991; Herzer *et al.*, 1997; Auzende *et al.*, 2000). L'ouverture océanique s'est prolongée dans la mer de Tasman, jusqu'au Paléocène inférieur (Hayes et Ringis, 1973 ; Weissel et Hayes, 1977) ce qui a imposé une trame sigmoïde aux bassins marginaux et rides initialement rectilignes.

3) La troisième phase, Paléocène-Oligocène, correspond à la migration vers le Nord de la plaque Australie (Willcox et Stagg, 1990) associée à des processus de déformation compressive intra-plaque (Eade, 1988 ; Van de Beuque *et al.*, 1998). Cette phase est caractérisée par des processus d'obduction avec notamment la mise en place des ophiolites de Nouvelle-Calédonie à l'Eocène supérieur (Paris *et al.*, 1979 ; Paris, 1981 ; Collot *et al.*, 1987 ; Cluzel *et al.*, 1994), et un écaillage de la croûte océanique crétacée du bassin des Loyauté (Auzende *et al.*, 2000).

4) La quatrième et dernière phase, Oligocène à l'actuel, est marquée par des épisodes de compression et d'extension associés aux processus de subduction entre plaques Australienne et Pacifique. Le bassin marginal Sud-Fidjien s'ouvre à l'Oligocène en réponse à l'initiation de la subduction le long de la fosse du Vitiaz et des Tonga-Kermadec (Davey, 1982). L'ensemble des arcs volcaniques associés comprend le proto-arc des Nouvelles-Hébrides, les îles Fidji et la ride de Lau-Colville. Au Miocène inférieur, des ophiolites d'âge Crétacé se mettent en place par obduction sur la partie Nord de la Nouvelle-Zélande (Ballance et Spörli, 1979 ; Cassidy et Locke, 1987 ; Spörli et Kear, 1989 ; Malpas *et al.*, 1992) Ces ophiolites, essentiellement des basaltes, proviendraient soit du bassin de Norfolk (*e.g.* Malpas *et al.*, 1992), soit du Pacifique (*e.g.* Rait *et al.*, 1991). Cette période est également marquée par l'ouverture du bassin Nord-Fidjien au sein de l'arc « Nouvelles Hébrides-Fidji-Lau-Tonga », au détriment du bassin Sud-Fidjien (Auzende *et al.*, 1995). Cette réorganisation des

subductions et bassins océaniques peut être liée à l'arrivée dans la fosse de subduction "Pacifique-Australie" du Plateau d'Otong-Java. Ce phénomène de collision du Plateau d'Otong-Java est aussi considéré comme responsable de l'arrêt de la subduction dans la fosse du Vitiaz (Kroenke, 1984). Au Pliocène supérieur, la ride des Loyauté entre en collision avec l'arc des Nouvelles - Hébrides (Monzier *et al.*, 1990). La migration vers l'Est de la limite entre la plaque Pacifique et la plaque Australie reprend avec l'ouverture des bassins du Havre et de Lau et la formation de la ride des Tonga Kermadec (Taylor *et al.*, 1996).

En résumé, la morphologie actuelle du Sud-Ouest Pacifique résulte d'une évolution géodynamique très complexe et comprend schématiquement : **1)** à l'Ouest, un ensemble de lanières continentales qui résultent de la phase de rifting de la marge orientale du Gondwana (c. 110-80 Ma), et **2)** à l'Est, un ensemble de bassins marginaux et d'arcs volcaniques plus récents (c. 35-0 Ma) et associés à l'activité des zones de subduction (Fig. II-1 et II-2). Vers le Sud, l'ensemble de ces lanières continentales, arcs volcaniques actifs ou rémanents, et bassins, convergent vers la Nouvelle-Zélande.

Fig.II-3. Bloc diagramme montrant le plongement de la plaque Pacifique sous l'île Nord de Nouvelle-Zélande (dont la projection en surface des lignes d'isoprofondeurs 20 km et 60 km) et la localisation en coupe de la sismicité superficielle sur la transversale de Wellington. Ansell et Bannister (1996).

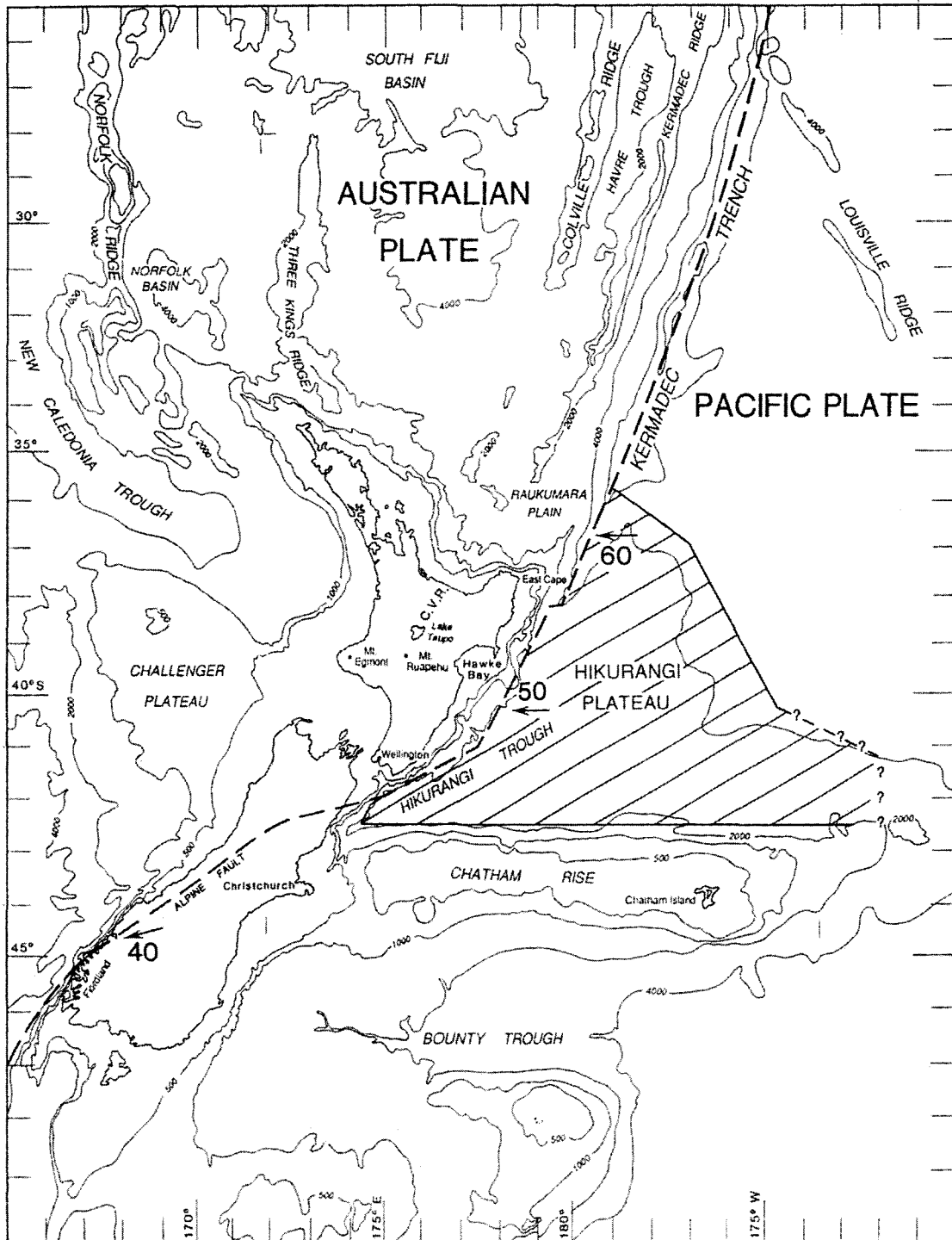
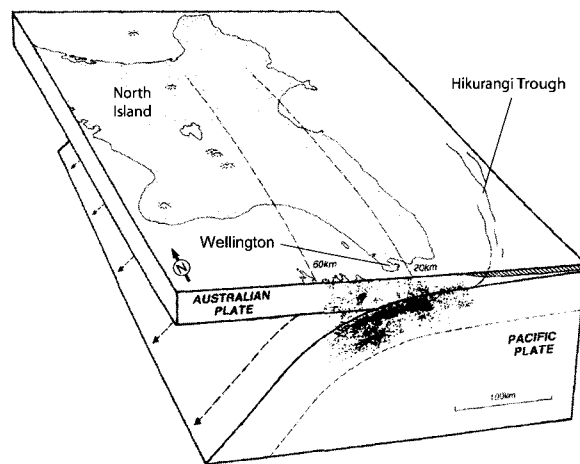


Fig.II-4. Le plateau Hikurangi dans son cadre géodynamique. Porté par la plaque Pacifique, il correspond à une croûte océanique épaissie (10 à 15 km d'épaisseur) qui passe en subduction sous l'île Nord de Nouvelle-Zélande au niveau de la fosse Hikurangi. Wood et Davy (1994).

B) Ile Nord de Nouvelle-Zélande : une subduction active

La Nouvelle-Zélande se situe dans la région du Sud-Ouest Pacifique, entre 35° et 50° de latitude Sud et entre 160° et 180° de longitude Est (Fig. I-2 et II-1). Elle constitue la partie émergée de domaines continentaux sous-marins actuellement en affrontement au niveau de la faille Alpine (Fig. II-2). Ces domaines incluent : **1)** les rides de Lord Howe et de Norfolk ainsi que le plateau de Challenger portés par la plaque Australie et séparés du continent australien au cours du Crétacé ; **2)** le plateau de Campbell et la ride de Chatham, séparés du bloc Antarctique au Crétacé (Weissel *et al.*, 1977), portés par la plaque Pacifique. L'Ile Nord de Nouvelle-Zélande appartient entièrement à la plaque Australie. Elle est longée à l'Est par la limite entre les plaques Pacifique et Australie (fosse Hikurangi) qui correspond à la terminaison méridionale du système de subduction des Tonga-Kermadec (Fig. II-2).

1) Contexte géodynamique actuel

Au niveau de l'Ile Nord de Nouvelle-Zélande, les plaques Pacifique et Australie convergent avec une vitesse relative décroissante et une obliquité croissante du Nord vers le Sud. La limite de plaques apparaît au niveau de la fosse Hikurangi, qui marque la subduction vers l'Ouest de la lithosphère du Pacifique (Fig. II-3). Dans ce domaine, la lithosphère plongeante porte une croûte particulière qui caractérise le Plateau Hikurangi. Ce plateau de forme triangulaire (Fig. II-4) apparaît entre la Ride de Chatham (continentale) au Sud, la plaine abyssale du Pacifique (océanique) au Nord-Est, et la marge orientale de l'Ile Nord de Nouvelle-Zélande (continentale) à l'Ouest. Ce Plateau Hikurangi correspond à une croûte, de 10 à 15 km d'épaisseur, de nature océanique et épaissie par des épanchements basaltiques mésozoïques (Davy et Wood, 1994 ; Wood et Davy, 1994 ; Collot *et al.*, 1996 ; Mortimer et Parkinson, 1996).

La morphologie de l'Ile Nord est ainsi fortement contrôlée par les processus géodynamiques associés à la zone de subduction Hikurangi (Spörli, 1980). Les éléments morpho-structuraux majeurs de cette marge active (complexe de subduction Hikurangi ; Van der Lingen, 1982 ; Chanier, 1991) sont d'Est en Ouest (Fig. II-5) :

1) La fosse Hikurangi, de 2.5 à 3.5 km de profondeur, elle est alimentée par des flux sédimentaires issus essentiellement de l'érosion des chaînes Alpines et Kaikoura qui se situent dans l'Ile Sud (Lewis et Barnes, 1999 ; Lewis et Pantin, 2002). Le transit des sédiments vers la fosse s'effectue principalement par le canyon de Kaikoura puis le flux sédimentaire est transporté axialement le long du chenal Hikurangi (Fig. II-6).

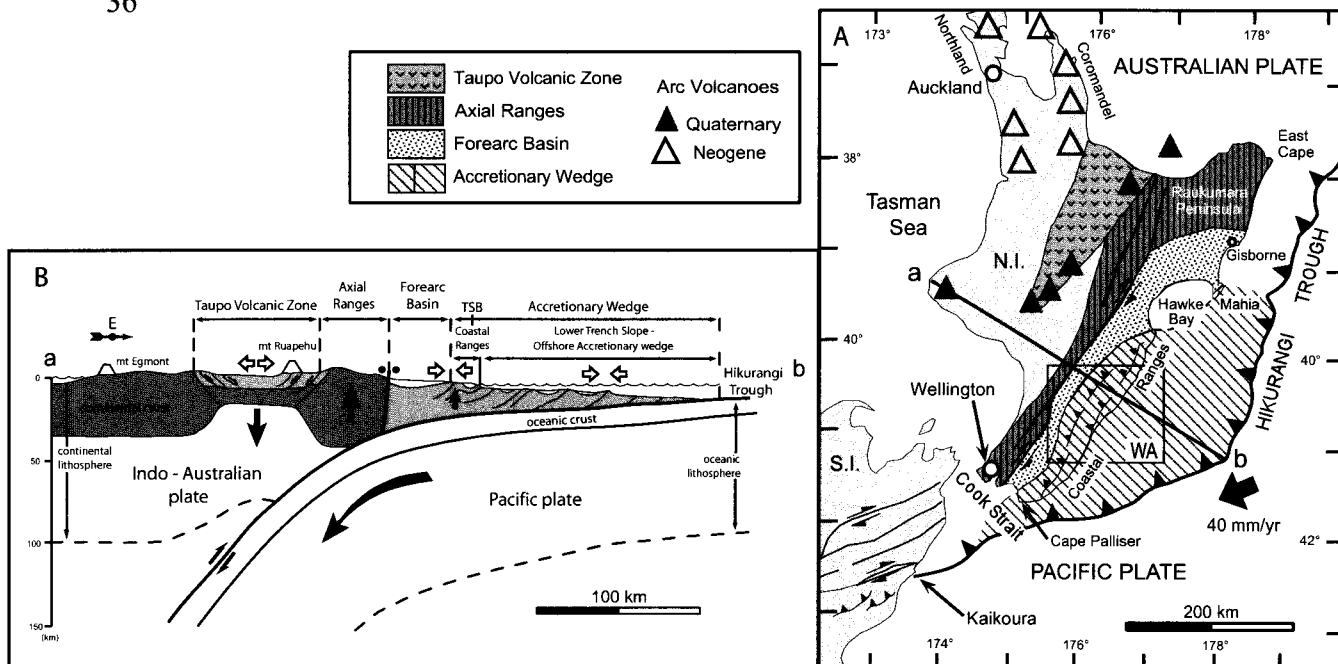


Fig.II-5. Carte (A) et coupe (B) des grands éléments morphostructuraux constituant le complexe de subduction Hikurangi, Ile Nord de Nouvelle-Zélande. N.I. - North Island, S.I. - South Island, WA - Wairarapa Area, TSB - Trench Slope Break. Modifié d'après Chanier *et al.* (1999).

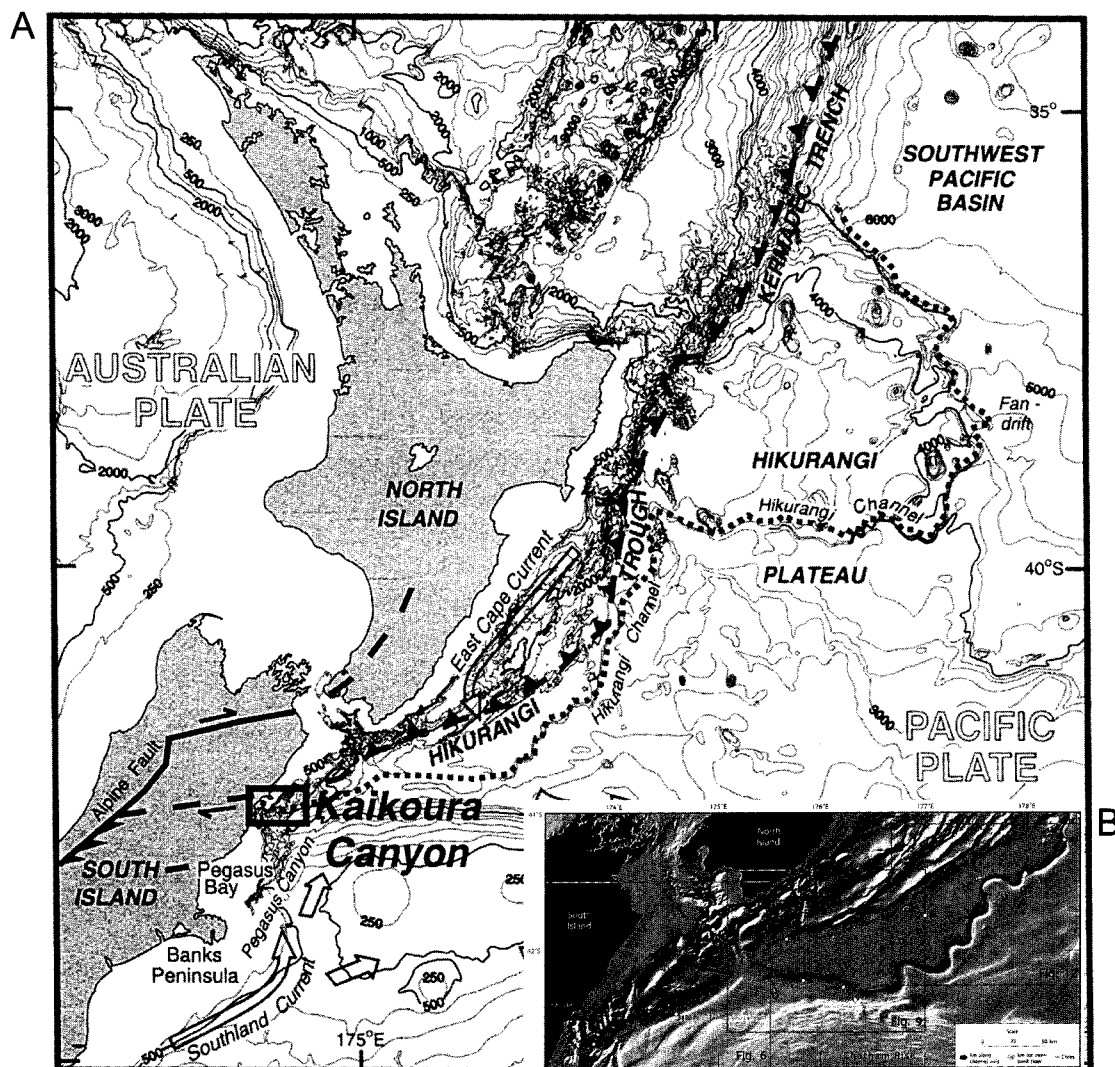


Fig.II-6. A - Localisation du chenal Hikurangi et du canyon de Kaikoura. La fosse Hikurangi est essentiellement alimentée par un flux sédimentaire issu de l'érosion de la Chaîne Alpine dans L'Ile Sud de Nouvelle-Zélande. Les sédiments transitent par le canyon de Kaikoura. Lewis et Barnes (1999). **B** - morphologie du système d'alimentation canyon de Kaikoura/chenal Hikurangi. Lewis et Pantin (2002).

2) Le prisme d'accrétion Hikurangi (*s.l.*) qui porte d'étroits bassins de pente (Fig. II-5B), allongés parallèlement à l'axe de la fosse (Lewis, 1980 ; Davey *et al.*, 1986). En mer, le prisme Hikurangi est actif et le processus d'accrétion se caractérise par le développement de chevauchements actifs imbriqués (Fig. II-5B) incorporant des sédiments de la fosse et de la plaque plongeante (Lewis, 1980; Davey *et al.*, 1986; Lewis et Pettinga, 1993). À terre, les plus hautes rides et bassins de ce prisme d'accrétion forment la Chaîne Côtière (Lewis et Pettinga, 1993) qui culmine à presque 1000 m. La Chaîne côtière, nommée également *East Coast Deformed Belt* (Spörli, 1980), s'étend de Cape Palliser à Hawke Bay (Fig. II-5A). Elle représente une lanière déformée qui s'étire du Nord-Est au Sud-Ouest sur 260 km pour 30 km de large. Au Sud de Hawke Bay, la Chaîne Côtière est donc considérée comme la plus haute ride du prisme d'accrétion Hikurangi (*trench slope break*) et est dominée par des structures compressives sub-parallèles à la fosse (Pettinga, 1982; Lewis et Pettinga, 1993). Ces déformations compressives sont encore actives actuellement (Wellman, 1971 ; Sing, 1971 ; Ghani, 1978 ; Nicol *et al.*, 2002) et s'expriment par la présence de failles à l'origine d'une activité sismique marquée, la formation de plis, et le fonctionnement de volcans de boue en relation avec l'activité tectonique (Chanier et Ferrière, 1990). Les taux de surrection, moyennés sur les derniers 125 000 ans, sont de l'ordre de 1 à 2 mm/an (Ghani, 1978 ; Pillans, 1986 ; Chanier *et al.*, 1994). Ces taux ont pu notamment être calculés à partir de l'étude du soulèvement des terrasses marines dont certaines, datées de 125 000 ans, coiffent actuellement des falaises de la Chaîne Côtière à 200 – 220 m d'altitude.

3) Le bassin avant-arc (Plaine du Wairarapa) qui se développe au dos du prisme d'accrétion (Cape *et al.*, 1990 ; Chanier *et al.*, 1994 ; Buret, 1996 ; Buret *et al.*, 1997). Ce bassin, large d'environ 10 km, forme une dépression longitudinale bien marquée entre les reliefs de la Chaîne Côtière et de la Chaîne Axiale (Fig. II-5).

4) La Chaîne axiale (Tararua Range) qui correspond à une lanière décrochante dextre qui montre de forts taux de soulèvement (2 à 4 mm/an, Pillans, 1986). Les décrochements majeurs sont parallèles à la fosse et présentent des jeux dextres (Kingma, 1967 ; Lensen, 1969 ; Walcott, 1978, 1987 ; Spörli, 1980 ; Cashman *et al.*, 1992).

5) Les volcans actifs associés à la subduction Hikurangi forment l'arc magmatique de Taupo (Fig. II-5). Le magmatisme d'arc de la zone volcanique de Taupo est essentiellement d'âge Quaternaire (Cole, 1979, 1986). Au Néogène, le volcanisme d'arc se concentrait au niveau des arcs de Coromandel et du Northland aujourd'hui inactifs (Ballance, 1976, 1993). Cet arc de Coromandel-Northland a valeur d'arc rémanent, devenu inactif du fait de l'ouverture depuis 2 Ma d'un bassin arrière-arc juvénile, intracontinental, derrière l'arc actif de Taupo (Fig. II-5A).

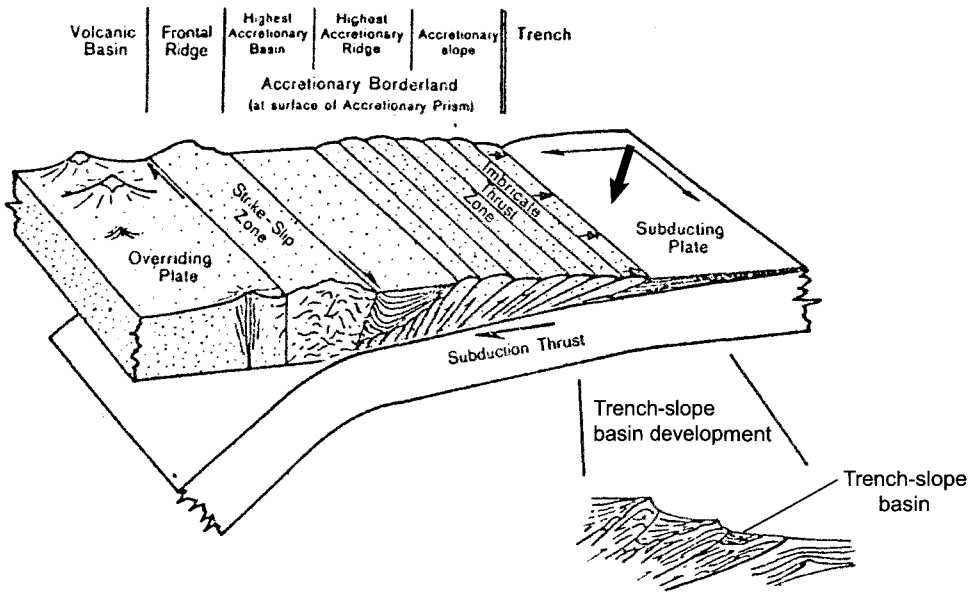


Fig.II-7. Bloc diagramme d'une marge active en convergence oblique. Appliqué à la subduction Hikurangi (Nouvelle-Zélande): *trench* - fosse Hikurangi, *accretionary slope* (lower trench slope) - pente du prisme d'accrétion Hikurangi, *highest accretionary ridge* (trench slope break) - Chaîne Côtière, *highest accretionary basin* - bassin avant-arc, *frontal ridge* - Chaîne Axiale (Tararua Range), *Volcanic basin* - zone volcanique de Taupo. Lewis (1980), adapté de Walcott (1978), Karig et Sharman (1975).

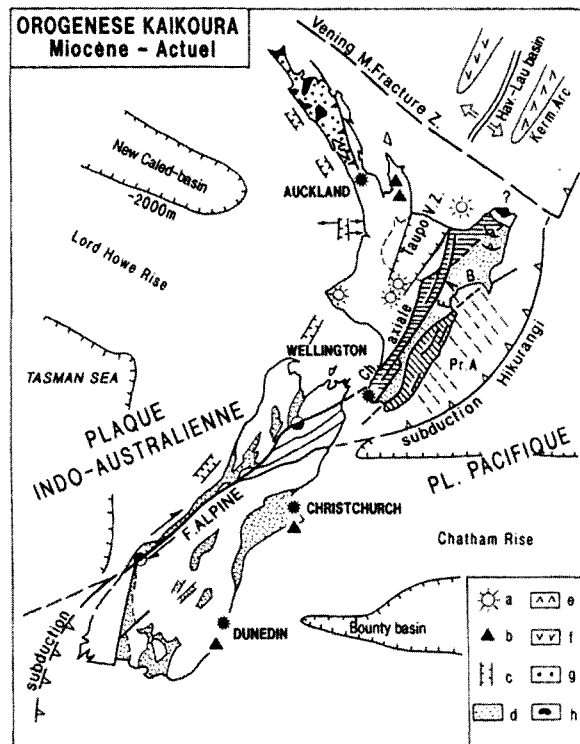
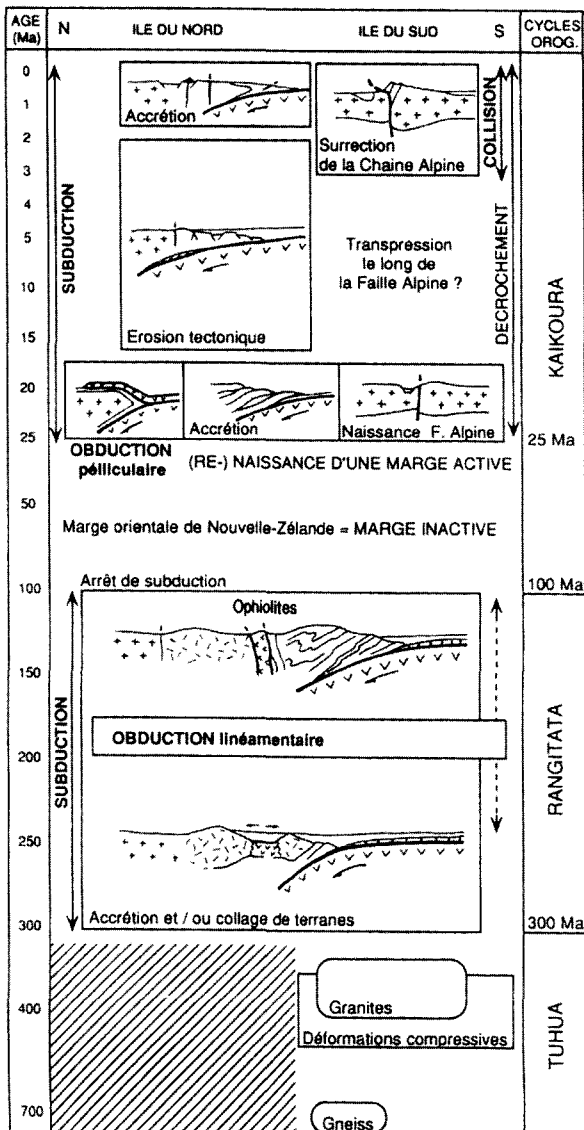


Fig.II-9. Orogenèse Kaikoura (25-0 Ma). a- volcans actifs, b- volcans néogènes éteints, c- fossés récents, d- bassins cénozoïques, e- arc volcanique actif des Kermadec, f- arc volcanique inactif (ride de Colville), g et h- sédiments et ophiolites de l'allochtone du Northland (obduction du Miocène basal), F.A.B.- bassin avant-arc, Pr.A- prisme d'accrétion Hikurangi, Taupo V.Z.- Taupo Volcanic Zone. Ferrière et Chanier (1993).

Fig.II-8. Synthèse de l'histoire géodynamique de la Nouvelle-Zélande depuis 700 Ma. Ferrière et Chanier (1993).

Les principales particularités du dispositif de subduction néo-zélandais sont donc, d'une part, l'épaisseur relativement importante du panneau plongeant (Plateau Hikurangi), et, d'autre part, l'obliquité croissante vers le Sud de la convergence entre pacifique et Australie (Fig. II-4 et II-5A). La présence du Plateau Hikurangi engagé dans la subduction est probablement responsable de la surélévation de l'ensemble du complexe de subduction (fosse peu profonde, partie interne du prisme et bassin avant-arc émergés). L'obliquité de la convergence (Fig. II-7) est à l'origine d'un partitionnement important de la déformation entre une ceinture nettement décrochante à l'Ouest et une ceinture principalement compressive à l'Est (Cashman *et al.*, 1992; Kelsey *et al.*, 1995; Barnes *et al.*, 1998). En effet, la composante normale (compressive) de la convergence se localise préférentiellement à proximité du front de subduction (prisme d'accrétion actif) puis s'atténue progressivement vers l'Ouest où des structures compressives actives, parallèles à la fosse, sont cependant encore observées au sein de la Chaîne Côtière et même du bassin avant-arc (Ghani, 1978; Walcott, 1978, 1984 ; Spörli, 1980; Lamb et Vella, 1987; Wells, 1989; Cape *et al.*, 1990; Chanier, 1991; Beanland *et al.*, 1998 ; Nicol *et al.*, 2002). La composante décrochante de la convergence se traduit par le développement de grands décrochements d'échelle régionale (*e.g.* Faille de Wairarapa, Faille de Wellington) qui affectent la Chaîne axiale ou sa bordure avec le bassin avant-arc (Kingma, 1967 ; Lensen, 1969 ; Walcott, 1978, 1987 ; Spörli, 1980 ; Cashman *et al.*, 1992 ; Kelsey *et al.*, 1995).

2) Les grands traits de l'évolution géologique

Depuis 700 Ma, la Nouvelle-Zélande a subi 3 cycles orogéniques majeurs (Fig. II-8 ; Suggate *et al.*, 1978) :

→ Le cycle paléozoïque Tuhua (anté-300 Ma), mal connu, correspond à des déformations compressives majeures au cours du Siluro-dévonien et à la mise en place d'importants corps granitiques au Dévono-Carbonifère (Suggate *et al.*, 1978 ; Cooper, 1979 ; Crook et Feary, 1982 ; Bishop *et al.*, 1985 ; Spörli, 1987 ; Bradshaw, 1989).

→ Le cycle Rangitata, de *c.* 300 à 100 Ma, est attribué à des processus de subduction à l'origine de l'accrétion d'un prisme sédimentaire qui incorpore les sédiments Permien à Crétacé inférieur d'un vaste cône détritique sous-marin : la formation de grès et d'arkoses du Torlesse (Spörli, 1978 ; Bradshaw *et al.*, 1980 ; Howell, 1980 ; MacKinnon, 1983 ; MacKinnon et Howell, 1985 ; Ferrière, 1987 ; Ferrière et Chanier, 1993). Suite à l'arrêt de cette marge active à la fin du Crétacé inférieur (Bradshaw, 1989), débute le cycle orogénique Kaikoura (Fig. II-9 ; Brothers, 1974).


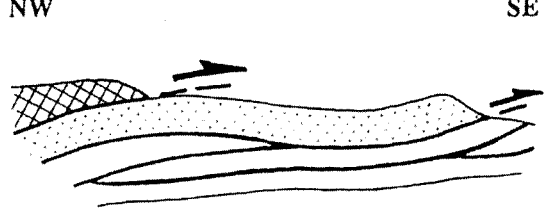
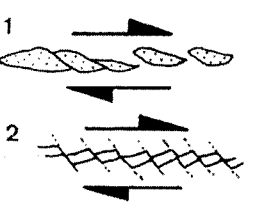

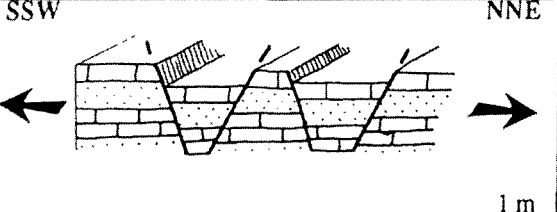
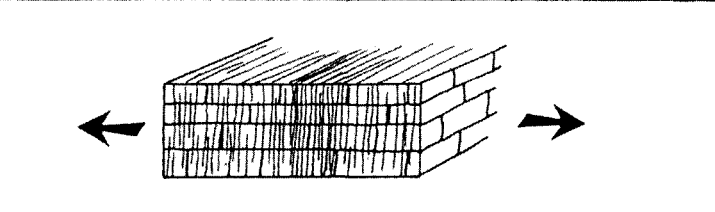

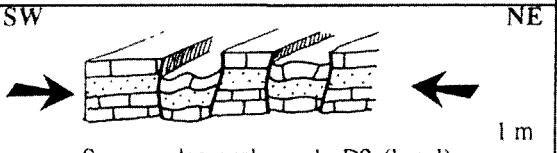

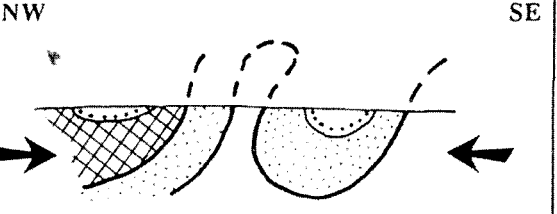
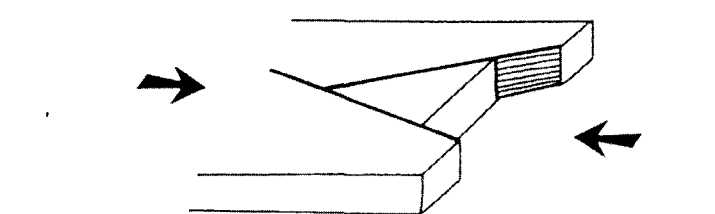
Episodes de déformation	Direction de contrainte moyenne	Nature des déformations	
		Structures majeures	Structures associées
Compression D1 (25 - 18 Ma)	σ_1 : N130°E ($\pm 40^\circ$) 	NW SE  Nappes à vergence Sud-Est 1 km ----	 1 2 Mélanges tectoniques (1) Débit de cisaillement normal (2)
Extension D2 (10 - 4 Ma) (18 - 2 Ma ?)	σ_3 variable ~ N030°E ($\pm 80^\circ$) 	SSW NNE  Failles normales 1 m ----	 Joints de tension serrés
Compression D3'	σ_1 : N045°E 	SW NE  Serrage des grabens de D2 (local) 1 m ----	
Compression D3 (1,5 - 0 Ma)	σ_1 : N115°E ($\pm 20^\circ$) 	NW SE  Plissement des séries post-nappes 1 km ----	 décrochements anté-, syn-, et post-plis

Fig.II-10. Episodes de déformation enregistrés dans la Chaîne Cotière (marge Hikurangi - côte Est de l'île Nord de Nouvelle-Zélande) depuis le démarrage de la subduction il y a 25 Ma. Chanier (1991).

→ Le cycle Kaikoura peut-être divisé en deux phases majeures (Fig. II-8) : **1**) de 100 à 25 Ma, la marge orientale de Nouvelle-Zélande est considérée comme une marge passive (marge *inactive* ; Chanier, 1991 ; Chanier et Ferrière, 1991 ; Ferrière et Chanier, 1993), et **2**) à partir de 25 Ma, la mise en place de déformations compressives majeures sub-contemporaines du développement d'un volcanisme d'arc (arcs de Coromandel et du Northland), ainsi que l'augmentation brutale des apports terrigènes sur la marge (notamment de volumes importants de mélanges de type olistostromes), suggèrent un retour à un contexte géodynamique actif de type subduction (Van der Lingen, 1982 ; Chanier et Ferrière, 1991 ; Ferrière et Chanier, 1993 ; Rait *et al.*, 1991, King, 2000).

L'évolution structurale de la Chaîne Côtière (Fig. II-5) depuis 25 Ma a tout d'abord été considérée comme résultant de déformations compressives continues au cours de la croissance du prisme d'accrétion Hikurangi (Van der Lingen et Pettinga, 1980 ; Pettinga, 1982 ; Lewis et Pettinga, 1993). Plus récemment, des études structurales détaillées suggèrent une succession de trois épisodes tectoniques majeurs (Fig. II-10) plutôt qu'une déformation continue et homogène depuis le démarrage de la subduction (Chanier, 1991).

Le premier régime tectonique est en relation avec l'initiation de la subduction. Cette phase est marquée par la mise en place de nappes qui chevauchent vers le front de subduction (Fig. II-11), de nombreuses failles inverses et d'un plissement des séries sédimentaires le long de l'ensemble de la marge (Chanier et Ferrière, 1989, 1991 ; Rait *et al.*, 1991). Un autre modèle tectonique pour cette période évoque en outre de grands décrochements dextres (Fig. II-12) qui montrent un jeu de l'ordre de 300 kilomètres et succèdent à la phase de nappe du miocène basal (Delteil *et al.*, 1996). Quoi qu'il en soit, cet épisode précoce (*c.* 25-19 Ma) de développement du prisme d'accrétion dans la Chaîne Côtière (Fig. II-10 et II-13) semble suivi par une période significative de calme relatif du point de vue tectonique, bien que la subduction perdure. On observe cependant pendant cette période le développement d'une tectonique en extension marquée par des failles normales et par des déformations syn-sédimentaires locales de type roll-over (Fig. II-14 et II-15). Cet épisode étant contemporain d'une subsidence généralisée de la marge, Chanier *et al.* (1999) envisagent des processus d'érosion tectonique à la base de la marge active, approximativement entre 15 et 5 Ma (Fig. II-13).

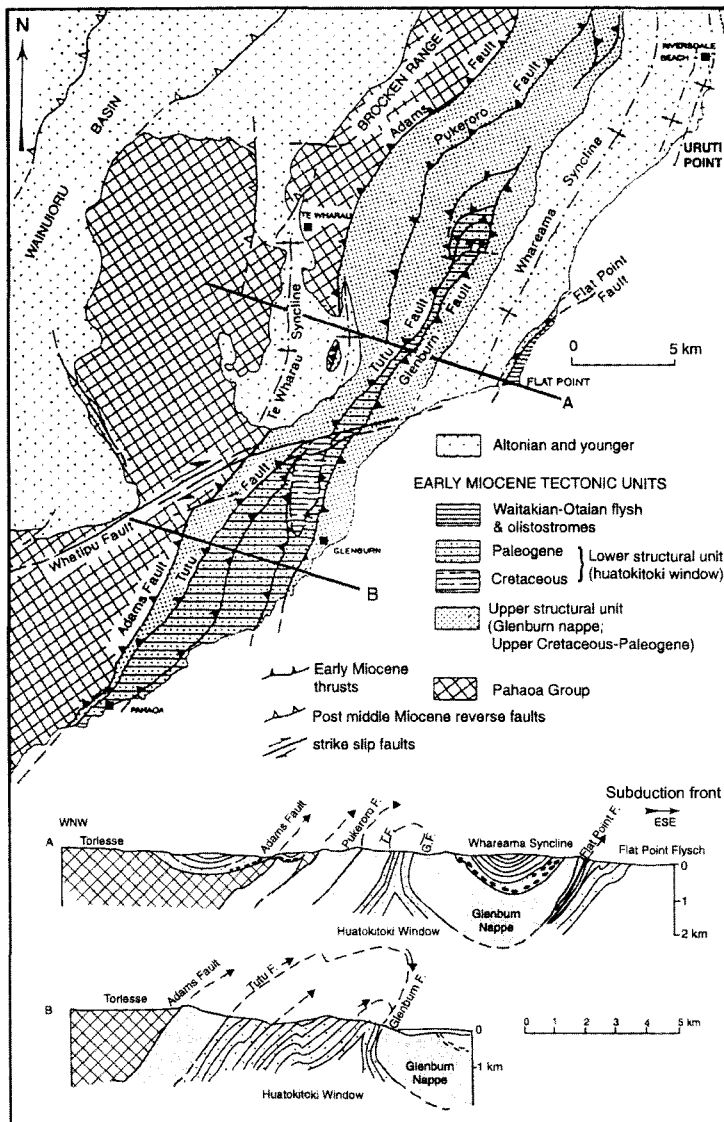


Fig.II-11. Schéma structural et coupes au sein du domaine Sud-Wairarapa (marge Hikurangi - côte Est de l'île Nord de Nouvelle-Zélande). Mise en évidence d'une tectonique de nappe au Miocène inférieur (cf. carte et coupe A). Les nappes ont ensuite été plissées au cours d'épisodes de déformation plus récents. Chanier (1991); dans Field, Uruski *et al.* (1997).

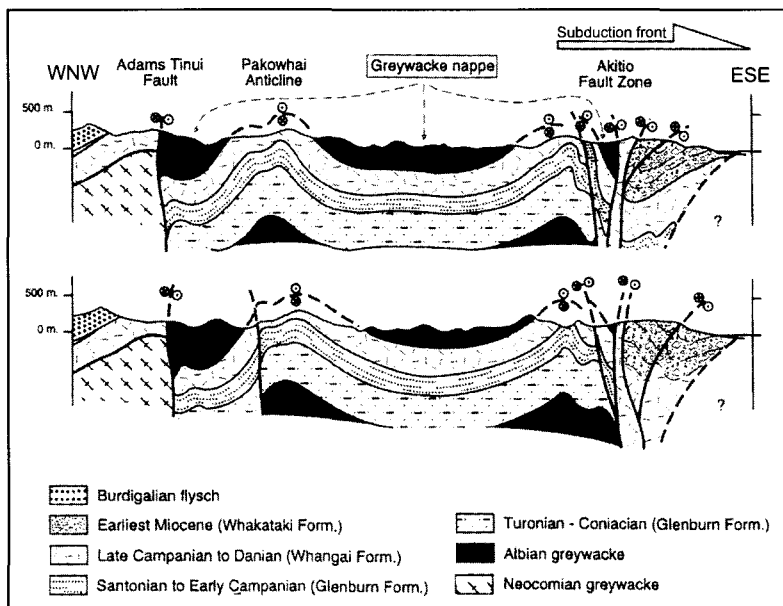


Fig.II-12. Coupes au sein du domaine Nord-Wairarapa (marge Hikurangi - côte Est de l'île Nord de Nouvelle-Zélande). Hypothèse d'une tectonique dominée par du décrochement au Miocène inférieur. Delteil *et al.* (1996); dans Field, Uruski *et al.* (1997).

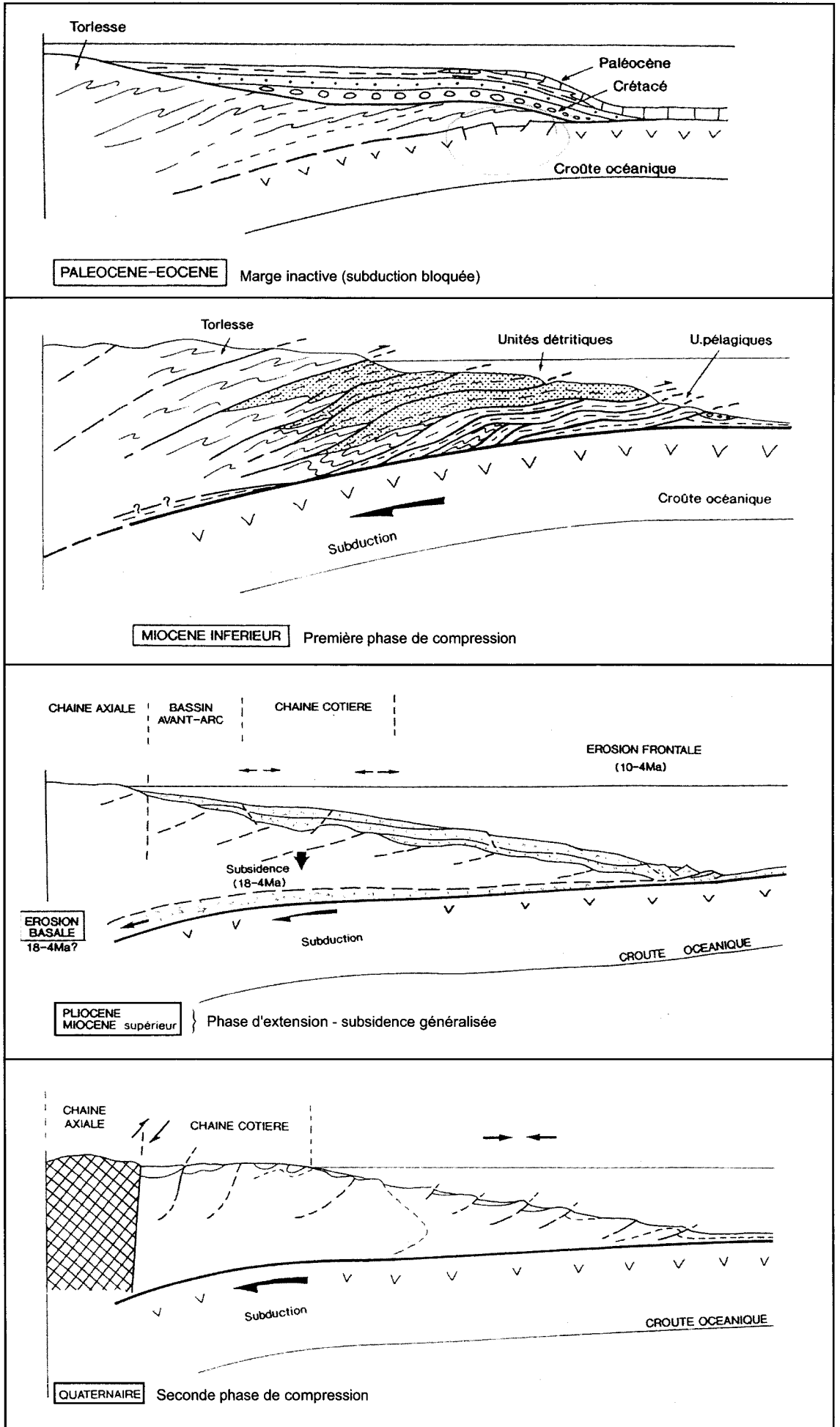


Fig.II-13. Coupes schématiques montrant l'évolution du prisme d'accrétion Hikurangi du Miocène basal à l'actuel. Echelles approximatives: cf. croûte océanique (6 à 8 km). Chanier (1991).

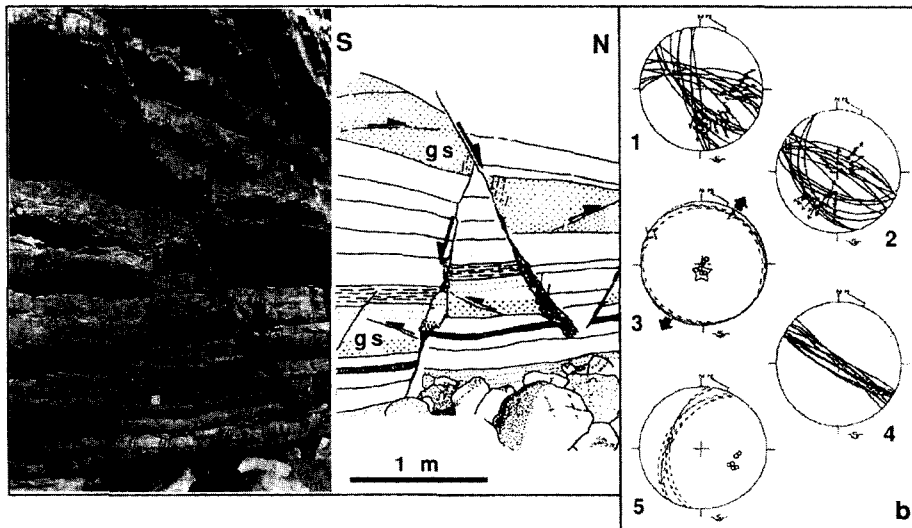


Fig.II-14. a - Failles normales conjuguées, antérieures à la compression la plus récente (c. 5-0 Ma), affectant des calcaires paléocènes dans la région du Wairarapa (marge Hikurangi - côte Est de l'île Nord de Nouvelle-Zélande). Ces failles décalent de plus des plans inverses d'angle faible (compression du Miocène basal). **b** - analyse stéréographique associée. Chanier *et al.* (1999).

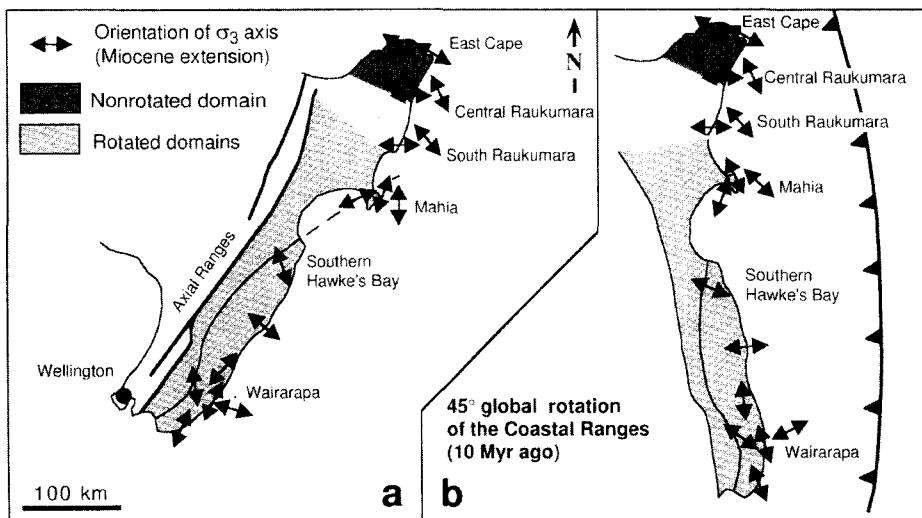


Fig.II-15. Résumé des déformations en extension miocènes le long de la marge Est de l'île Nord de Nouvelle-Zélande. **a** - Axes d'extension majeurs déduits des calculs de paléocontraintes. **b** - Orientation des axes d'extension il y a 10 Ma en considérant une rotation générale de 45° de l'ensemble de la marge. Chanier *et al.* (1999).

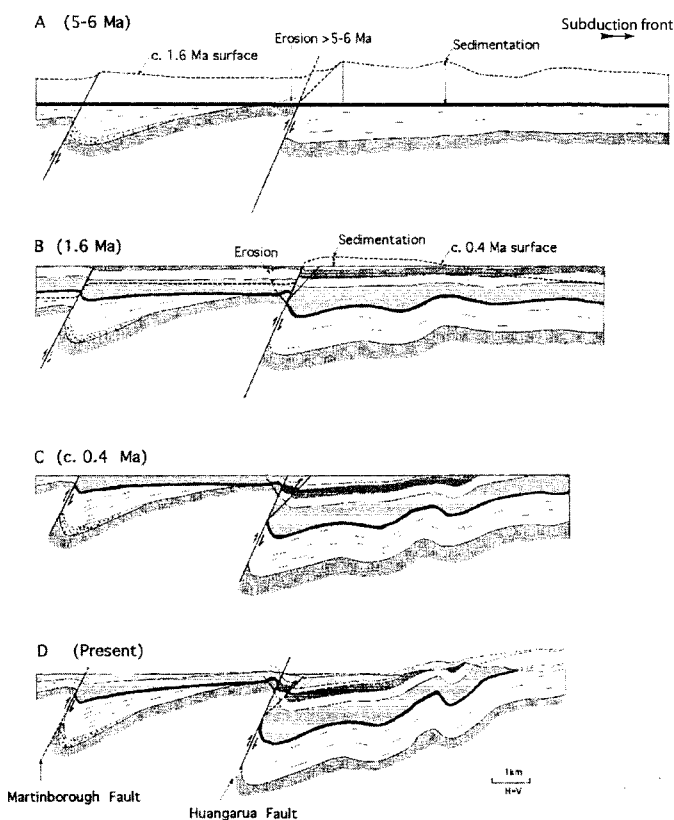


Fig.II-16. Raccourcissement enregistré au Sud de la chaîne Côtière (marge Hikurangi - côte Est de l'île Nord de Nouvelle-Zélande) au cours de l'essive récente. Nicol *et al.*

Le troisième épisode de déformation, Plio-Quaternaire, est caractérisé par un retour à une tectonique compressive dominante (Walcott, 1984; Lamb et Vella, 1987; Wells, 1989; Cape *et al.*, 1990; Chanier, 1991; Beanland *et al.*, 1998; Nicol *et al.*, 2002). Cette phase de plissement et de mise en place de failles inverses (Fig. II-10 et II-16) s'enregistre sur l'ensemble de la marge et conduit à la surrection puis à l'émergence très récente (vraisemblablement au cours des derniers 300 000 ans ; Ghani, 1978) de la Chaîne Côtière (Fig. II-13). Il est possible que ce soit l'entrée en subduction du plateau Hikurangi (Fig. II-4), il y a 5 à 6 millions d'années, qui soit responsable de cette phase compressive récente.

3) Stratigraphie régionale

Du fait de complexités structurales et surtout d'importantes et rapides variations latérales de faciès, la lithostratigraphie de la région du Wairarapa (Chaîne Côtière – Côte Est de l'Île Nord de Nouvelle-Zélande) est complexe (Fig. II-17A). Un grand nombre de noms de groupes, de formations et de membres a été défini par le passé (*e.g.* Vella et Briggs, 1971; Johnston, 1975, 1980; Crundwell, 1987, 1997; Neef, 1992a, 1992b, 1995, 1997a, 1997b). Cette nomenclature lithostratigraphique d'approche anglo-saxonne est non seulement difficilement utilisable mais est de plus, comme signalé par Buret (1996), source d'erreur. En effet, des unités sédimentaires d'âge identique peuvent bénéficier de noms différents tandis que d'autres, d'âges différents, peuvent être regroupées sous le même nom. À ceci il faut ajouter les nombreux changements de noms ainsi que les re-définitions ou sub-divisions fréquentes de ces unités au fil des nouvelles publications.

Des travaux récents consacrés à la synthèse géologique de la Côte Est de l'Île Nord (Field, Uruski *et al.*, 1997) et à la carte géologique de la région du Wairarapa (Lee et Begg, 2002) ont permis de clarifier la stratigraphie régionale (Fig. II-17A,B). Les séries sédimentaires du Miocène sont dans leur ensemble désormais incluses au sein d'une unité stratigraphique unique : le *Palliser Group* (modifié d'après Vella et Briggs, 1971). Ce groupe inclus à sa base les séries du Miocène basal de la *Whakataki Formation* (Johnston, 1975, 1980). Cette formation comprend principalement des flyschs et des olistostromes qui marquent un contraste de sédimentation fort avec les sédiments pélagiques (silts carbonatés et calcaires pélagiques) sous-jacents datés de l'Eocène-Oligocène. Ce changement de faciès brutal, observé sur l'ensemble de la Chaîne Côtière, est corrélé au démarrage de la subduction sous l'Île du Nord (Chanier et Ferrière, 1991). Cependant, le contact entre les séries détritiques du Miocène basal (*Whakataki Formation*) et le soubassement Crétacé-Oligocène est généralement concordant, contrairement au Miocène inférieur qui est discordant.

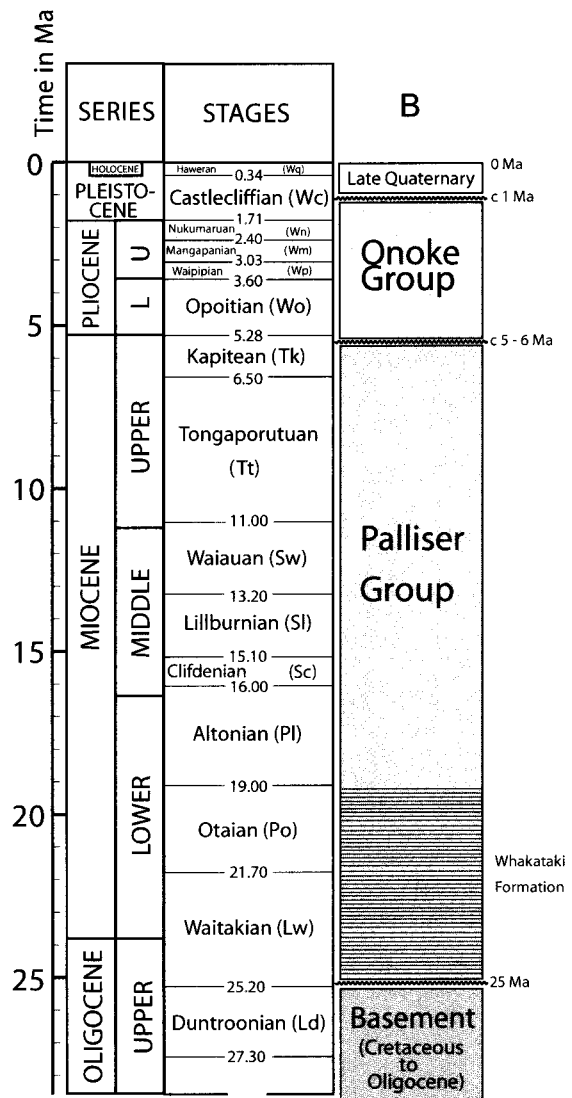
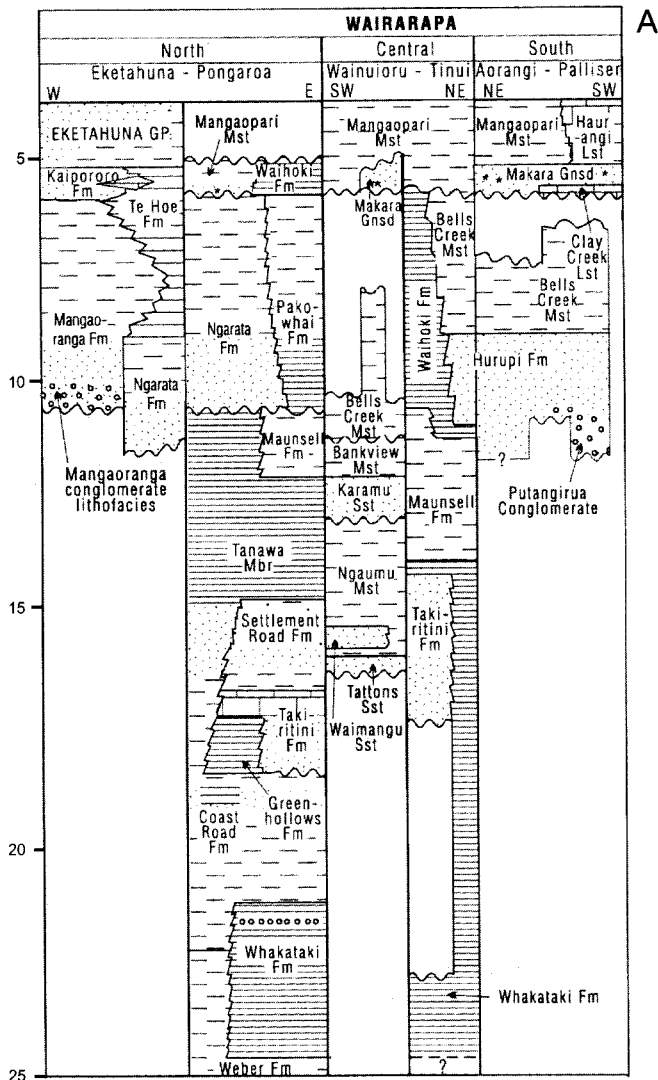


Fig.II-17. A - Lithostratigraphie détaillée de la région du Wairarapa (marge Hikurangi - côte Est de l'île Nord de Nouvelle-Zélande). Field, Uruski *et al.* (1997); et **B** - Principales unités stratigraphiques de la Chaîne Côtière. Lee et begg (2002).

La suite du *Palliser Group* comprend des sédiments du Miocène moyen et supérieur qui montrent des discontinuités successives associées à un ennoisement progressif du soubassement. Vella et Briggs (1971) considèrent cette séquence comme le résultat d'une transgression marine majeure au cours d'une période de subsidence généralisée de la marge. Les unités du Miocène moyen-supérieur sont principalement constituées de turbidites, de silts et/ou argiles bathyales et de grès néritiques. Des changements de faciès au sein de cette séquence transgressive sont par ailleurs attribués à des variations du niveau marin relatif et/ou à des activités tectoniques locales (*e.g.* Neef, 1997a). Discordant sur le *Palliser Group* (Fig. II-17B), l'*Onoke Group* (Vella et Briggs, 1971 ; Lee et Begg, 2002) est composé de sédiments marins datés du Miocène supérieur terminal au Quaternaire inférieur (*c.* 6.5-1.5 Ma). Ils témoignent d'une régression marine régionale qui peut-être attribuée à l'épisode de surrection plio-quaternaire (Walcott, 1984; Lamb et Vella, 1987; Wells, 1989; Cape *et al.*, 1990; Beanland *et al.*, 1998; Nicol *et al.*, 2002).

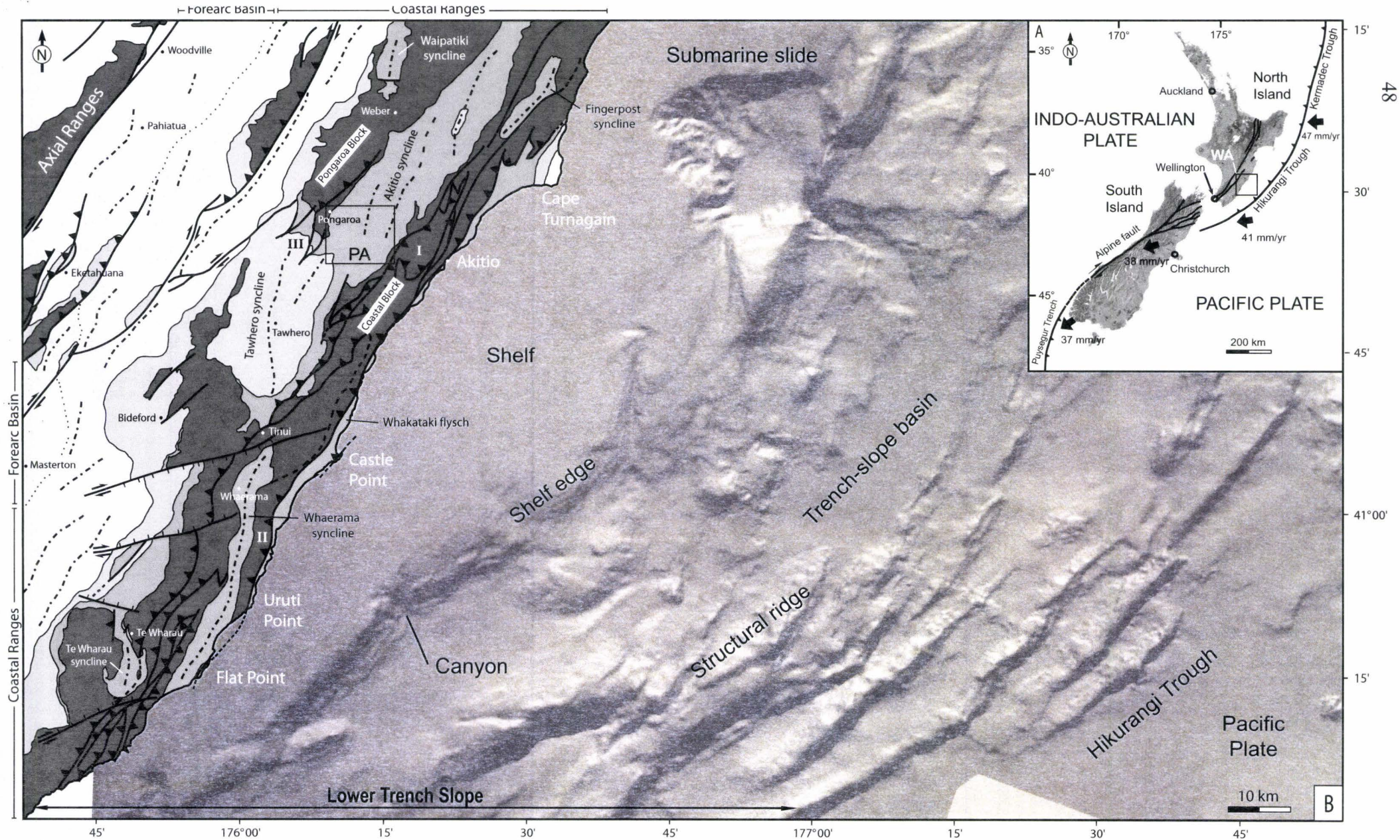


Fig.II-18. A - Cadre géodynamique de la Nouvelle-Zélande, les flèches noires indiquent les taux de convergence actuels entre les plaques Pacifique et Australienne (WA - Wairarapa Area). **B** - Carte bathymétrique (Lewis *et al.*, 1999) et schéma structural (d'après Lee et Begg, 2002) du secteur du Wairarapa. En mer, localisation des bassins perchés récents et des rides structurales majeures de la marge Hikurangi. A terre, localisation des synclinaux où affleurent les épaisses séries turbiditiques constituant le remplissage de bassins perchés néogènes. PA - Pongaroa Area, I - Tinui Fault Complex, II - Whakataki fault, III - Waihoki Fault Complex.

II) LES BASSINS DE PENTE DU PRISME DE SUBDUCTION HIKURANGI

Le long de la côte Est de l'île Nord de Nouvelle-Zélande (*Wairarapa Coast*, Fig. II-5 et II-18), des bassins perchés sont connus à l'affleurement (Van der Lingen et Pettinga, 1980; Pettinga, 1982 ; Van der Lingen, 1982, 1988; Neef, 1992a; Turnbull, 1988; Lewis et Pettinga, 1993; Reid, 1998) et en mer (Lewis, 1980; Davey *et al.*, 1986; Lewis et Pettinga, 1993).

A) En mer

A proximité du front de subduction, le prisme d'accrétion immergé correspond à des sédiments récents accrétés de la fosse. Ce domaine situé à proximité du front de subduction correspond donc à un prisme d'accrétion *sensu stricto* (Seely *et al.*, 1974 ; Karig et Sharman, 1975 ; Moore et Karig, 1976 ; Scholl *et al.*, 1977 ; Seely, 1979). Il est caractérisé par des chevauchements actifs et par le développement de bassins perchés quaternaires (Lewis, 1980 ; Davey *et al.*, 1986 ; Lewis et Pettinga, 1993). Lewis (1980) a décrit, d'après des données de sismique réflexion, les principales caractéristiques de ces bassins sub-parallèles à la fosse et particulièrement développés entre les latitudes de Hawke Bay et d'Uruti Point (Fig. II-19). Ces dépressions sous-marines font 5 à 30 km de large pour 10 à 60 km de long (Fig. II-18) et présentent un remplissage de 200 à 2000 m d'épaisseur. Les séries sédimentaires sont peu déformées et basculées vers le pôle continental (Fig. II-19). Ce basculement augmente progressivement vers le fond du bassin. Les bordures correspondent à des rides anticlinales sur le flanc Ouest (interne) desquelles les séries sédimentaires reposent en onlap (Lewis et Pettinga, 1993). Les hauts structuraux sont associés à des chevauchements inclinés vers le continent. Le remplissage de ces bassins de pente, alimentés par des canyons incisant la pente du prisme (Fig. II-18) comprend principalement des turbidites, des argiles hémipélagiques et des niveaux de cendres volcaniques. D'importants phénomènes de slumps sur les pentes sont également à l'origine du dépôt de formations sédimentaires chaotiques pouvant atteindre 10 km d'extension latérale dans le bassin pour une épaisseur de quelques mètres. La sédimentation au sommet des rides structurales est dominée par des dépôts biogéniques comprenant des mollusques, des foraminifères et des débris de coraux (Lewis, 1980). Lewis (1980) différencie les bassins les plus proches du front de subduction, qui présentent des taux de sédimentation de l'ordre de 0.1 m/1000 ans, de ceux qui sont situés plus haut sur le prisme d'accrétion, qui montrent des taux de sédimentation plus élevés, de l'ordre de 0.3m/1000 ans. Il évalue de plus la différence entre les taux de surrection des crêtes anticlinales et les taux de subsidence au niveau de l'axe des bassins à environ 3 m/1000 ans (3mm/an).

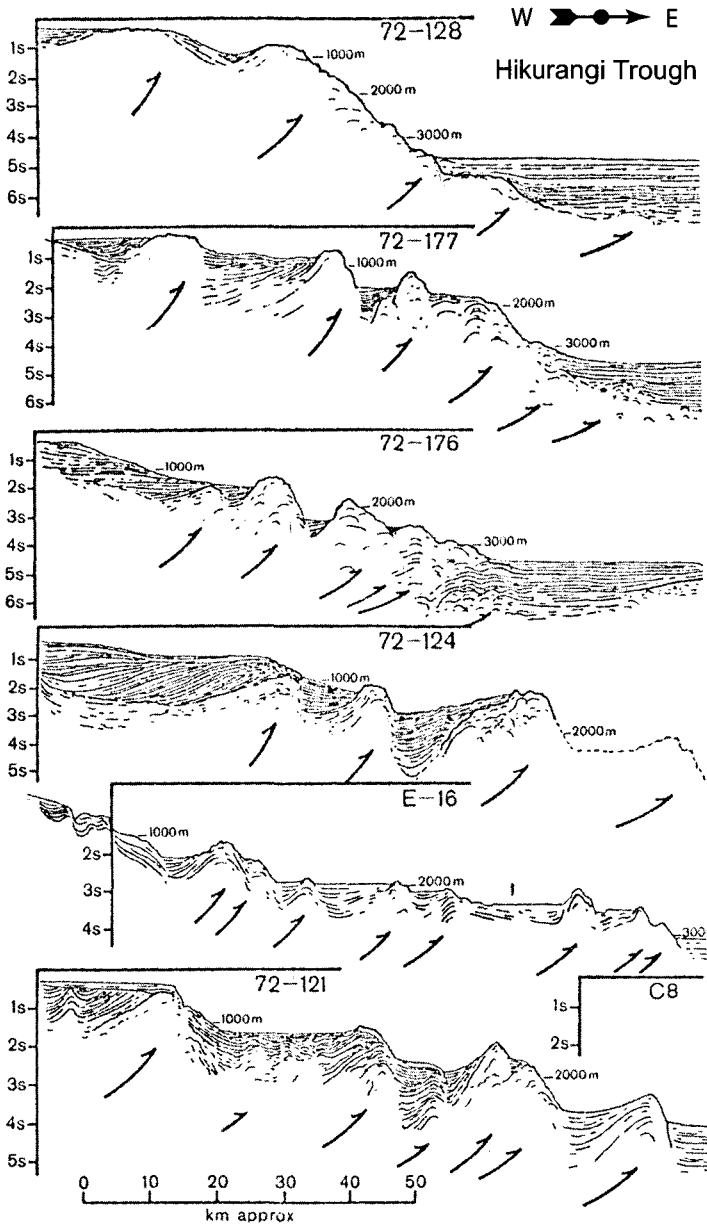


Fig.II-19. Coupes séries au travers du prisme d'accrétion Hikurangi (Nouvelle-Zélande). Géométrie, structure et localisation de bassins perchés quaternaires. Lewis (1980).

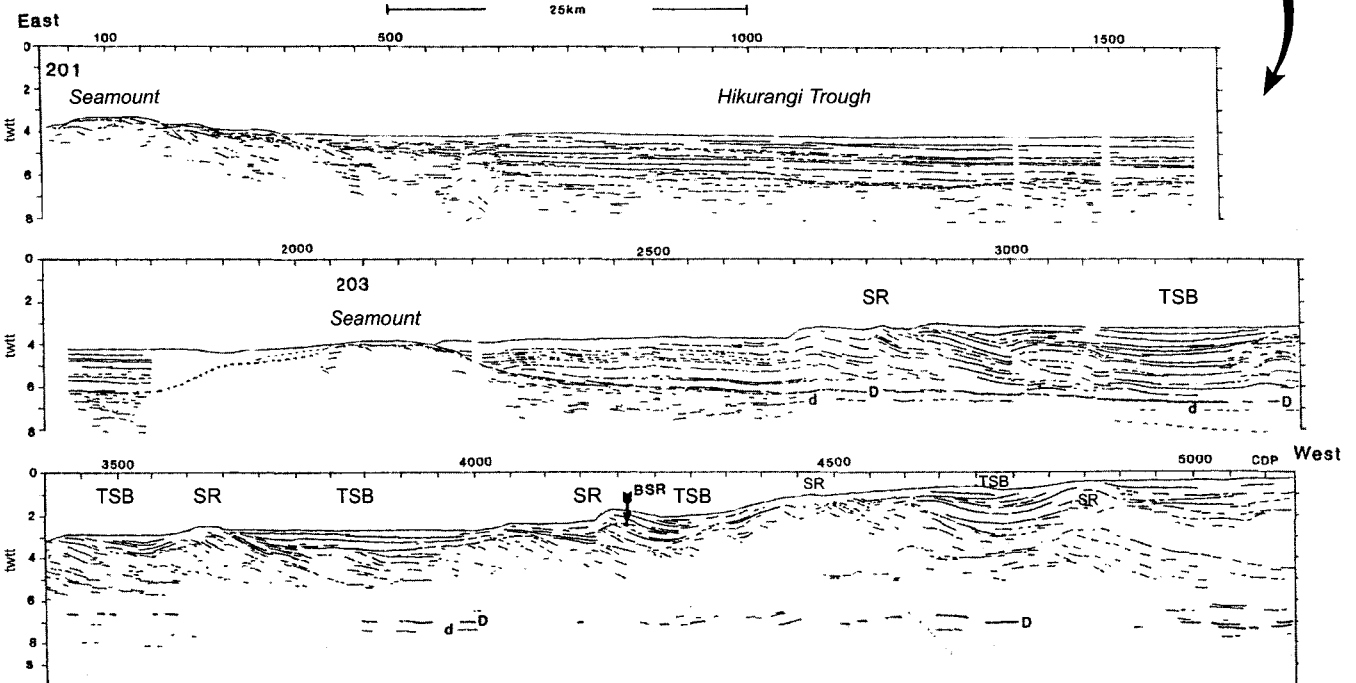


Fig.II-20. Coupe au travers de la fosse (ligne sismique 201) et du prisme d'accrétion (ligne sismique 203) Hikurangi (Nouvelle-Zélande). Géométrie, structure et localisation des bassins perchés. TSB - bassins perchés (*Trench Slope Basins*), SR - rides structurales associées à des chevauchements inclinés vers l'arc (*Structural Ridges*), D - niveau de décollement. Davey et al. (1986).

Ces bassins ont également été décrits par Davey *et al.* (1986) qui bénéficiaient de nouvelles données de sismique réflexion (Fig. II-20 ; profils DSIR-USGS 201 et 203). Leur analyse montre que les chevauchements qui contrôlent la croissance des hauts structuraux se connectent en profondeur sur un niveau de décollement majeur à la base du prisme d'accrétion (Fig. II-20, D). Ils mettent également en évidence la séparation de certains bassins en plusieurs sous-bassins par la mise en place de chevauchements qui affectent les séries sédimentaires d'un bassin initialement plus large. L'amalgamation (*i.e.* comblement du bassin suite à l'arrêt de la croissance des hauts structuraux) ou la séparation de certains bassins suggèrent qu'avec leur surrection progressive, il est de plus en plus difficile de différencier en sismique les sédiments accrétés de la fosse de ceux qui constituent le remplissage des bassins perchés (Davey *et al.*, 1986 ; Lewis et Pettinga, 1993). Sur les forages, cette distinction reste perceptible entre les sédiments turbiditiques grossiers de la fosse et ceux plus fins (turbidites distales) des bassins perchés (Davey *et al.*, 1986).

Plus haut sur la pente du prisme d'accrétion, dans un domaine incluant l'étroite plateforme actuelle (Fig. II-18), les données sismiques montrent une complexité stratigraphique et structurale importante (Lewis et Pettinga, 1993 ; Field, Uruski *et al.*, 1997). À ce niveau, des bassins perchés miocènes sont scellés par les sédiments fins d'un bassin de pente très large (plus de 20 km) plio-quadernaire. Ce bassin est peu déformé, mais est cependant affecté sur ses bordures par des chevauchements. Lewis et Pettinga (1993) attribuent la complexité de ce secteur **1)** aux interactions entre la déformation et les apports sédimentaires rapides liés à la proximité du pôle continental, **2)** à l'influence des oscillations eustatiques et **3)** aux déstabilisations gravitaires des pentes.

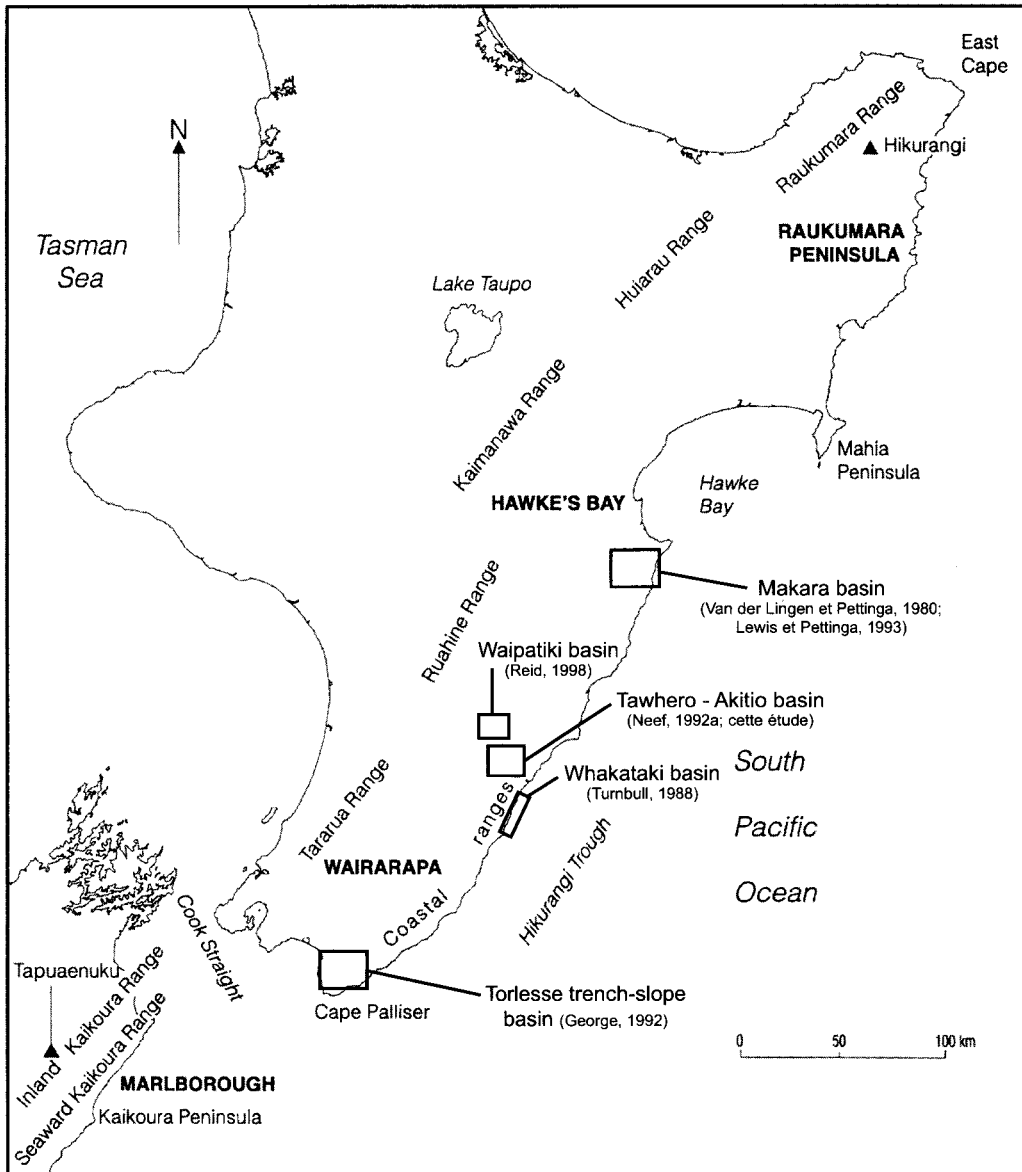


Fig.II-21. Localisation dans la Chaîne Côtière (Côte Est de l'île Nord de Nouvelle-Zélande) des affleurements de séries sédimentaires miocènes correspondant aux remplissages des bassins perchés de Makara, de Tawhero, de Whakataki et de Waipatiki. Fond cartographique d'après Field, Uruski *et al.* (1997).

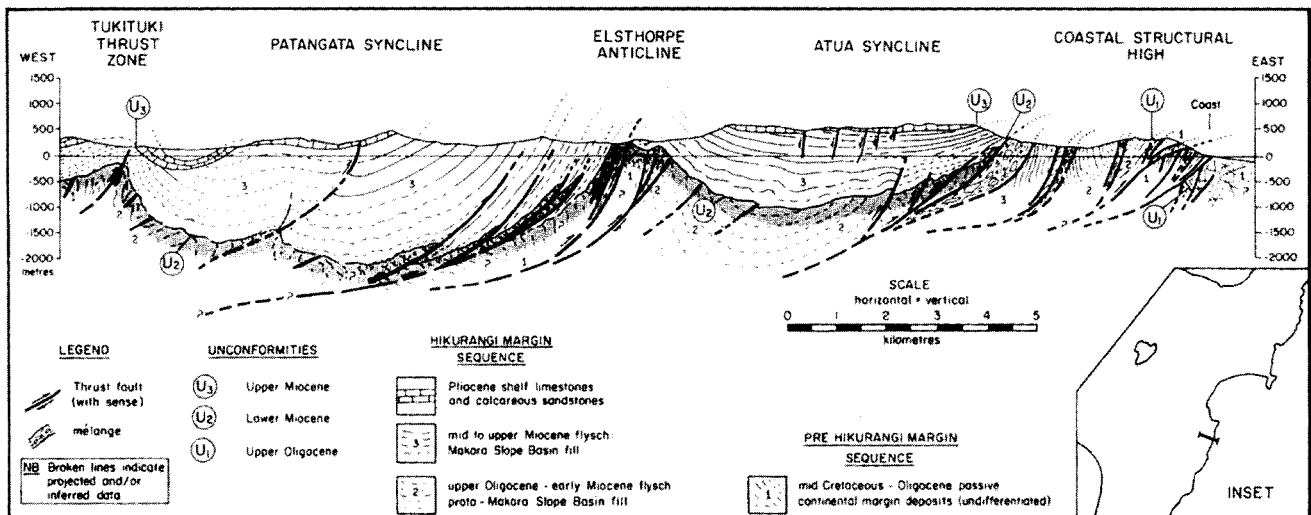


Fig.II-22. Coupe montrant la déformation du bassin perché miocène de Makara (Chaîne côtière, secteur Sud d'Hawke Bay - Localisation Fig.II-21). Lewis et Pettinga (1993), d'après Van der Lingen et Pettinga (1980).

B) À terre

L'émersion rapide des domaines les plus internes de la marge Hikurangi au cours du Quaternaire (Ghani, 1978; Cape *et al.*, 1990) a permis la mise à l'affleurement d'épaisses séries turbiditiques constituant le remplissage de bassins perchés miocènes (Van der Lingen et Pettinga, 1980; Pettinga, 1982 ; Van der Lingen, 1982, 1988; Neef, 1992a; Turnbull, 1988 ; Reid, 1998). Dans la région du Wairarapa, ces unités syn-subduction affleurent dans la Chaîne Côtière à la faveur de larges synclinaux dont les axes sont sub-parallèles à la marge (Fig. II-18). Ces synclinaux sont bordés par des lanières intensément déformées et composées de roches du soubassement. Il s'agit de formations sédimentaires anté-subduction d'âge Crétacé à Paléogène. La structuration de cette partie de la marge en lanières successives d'axe Nord-Est/Sud-Ouest résulte de la déformation compressive récente, encore active.

Plusieurs de ces bassins (Fig. II-21) ont déjà été étudiés d'un point de vue sédimentaire et/ou structural. Il s'agit des bassins de Makara (Van der Lingen et Pettinga, 1980 ; Pettinga, 1982 ; Van der Lingen, 1988 ; Lewis et Pettinga, 1993), de Whakataki (Turnbull, 1988), de Tawhero (Neef, 1992a), et de Waipatiki (Reid, 1998).

1) Le bassin de Makara

Le flysch de Makara (Fig. II-21) est interprété comme le remplissage d'un petit bassin, de 30 km sur 20 km, formé sur la pente du prisme d'accrétion. À l'affleurement, ces séries miocènes sont bordées par d'étroites lanières de sédiments très déformés datés du Crétacé supérieur au Tertiaire inférieur (Fig. II-22 ; Pettinga, 1982). Ces lanières sont interprétées comme d'anciens hauts structuraux, actifs au cours du Miocène, contrôlés par des chevauchements durant le remplissage du bassin au Miocène moyen et supérieur (Fig. II-23 et II-24 ; Van der Lingen et Pettinga, 1980 ; Pettinga, 1982 ; Lewis et Pettinga, 1993). Un troisième haut structural (Elsthorpe Anticline ; Pettinga, 1982) se développe plus tardivement, probablement au cours du Quaternaire (Pettinga, 1982), sous la forme d'un anticlinal au centre du bassin qui divise ainsi les séries turbiditiques miocènes en deux synclinaux dissymétriques (Fig. II-22). La sédimentation du bassin de Makara est dominée par des turbidites de faibles granulométrie (Van der Lingen et Pettinga, 1980 ; Van der Lingen, 1988) et présentant des séquences de Bouma bien développées. Van der Lingen et Pettinga (1980) puis Van der Lingen (1988) identifient également des argiles à galets et à slumps traduisant des dépôts de débris-flows grossiers issus de déstabilisations des bordures du bassin. Les 2200 m de série sédimentaire comprennent également des argiles hémipélagiques et des occurrences de tufs volcanoclastiques, témoins de l'activité de l'arc volcanique (Fig. II-24).

D'après Van der Lingen (1998), ces sédiments marins profonds ne présentent aucune des caractéristiques des faciès de cônes sous-marins profonds (*deep-sea fan*). Il explique cette observation par la taille réduite du réceptacle sédimentaire et par l'environnement structural particulier (*i.e.* gouttières structurales allongées ; Fig. II-24) qui ne seraient pas favorables à l'installation de grands systèmes turbiditiques bien organisés. Quoi qu'il en soit, à la fin du Miocène moyen cette sédimentation semble prendre le relais de celle du bassin d'Akitio (*cf.* ce manuscrit), situé plus au Sud (Fig. II-21), par migration du dépôt centre vers le bassin de Makara, donc vers le Nord (Van der Lingen et Pettinga, 1980).

2) Les bassins de la zone d'étude

Trois bassins (Whakataki, Tawhero et Waipatiki ; Fig. II-21) ont été précédemment signalés dans la littérature sur le secteur de ma zone d'étude (Wairarapa area, Fig. II-18).

Contrairement aux résultats concernant les environnements de dépôt du flysch de Makara, le flysch Miocène basal du bassin de Whakataki (Fig. II-18 et II-21) est considéré comme le témoin d'un système turbiditique de type *deep-sea fan* (Turnbull, 1988). Ce système, alimenté par des chenaux, montre une distalisation latérale le long de l'axe du bassin à partir des zones sources (Fig. II-25). Le système comprend l'ensemble des éléments qui constituent un *deep-sea fan* au sens de Walker (1978) : de l'*upper fan* au *lower fan*, puis au *basin plain*. Turnbull (1988) insiste également sur la présence de *fans* de plus petite taille traduisant des alimentations plus locales en provenance de la bordure Ouest du bassin (haut structural probablement contrôlé par la faille de Whakataki au Miocène inférieur).

D'après Neef (1992), le remplissage du bassin de Tawhero affleure au sein des synclinaux de Tawhero et d'Akitio (Fig. II-18 et II-21). Ce bassin comprend des sédiments âgés du Miocène inférieur au Miocène supérieur (*c.* 24 – 5 Ma ; Fig. II-26). Nous montrerons dans cette étude que les séries du bassin de Tawhero *sensu* Neef (1992) correspondent en réalité aux remplissages de deux bassins différents : **1)** le bassin Miocène inférieur-moyen d'Akitio, qui affleure principalement dans le synclinal d'Akitio (il s'agit de la base du bassin de Tawhero au sens de Neef, 1992), et **2)** le bassin Miocène supérieur de Tawhero proprement dit, qui affleure principalement dans le synclinal de Tawhero. Les séries sédimentaires du synclinal d'Akitio reposent sur les roches du soubassement du bloc de Pongaroa (*Pongaroa Block*) et du bloc côtier (*faulted Coastal Block*, Moore, 1988 ; ou *Coastal Hills*, Van der Lingen et Pettinga, 1980).

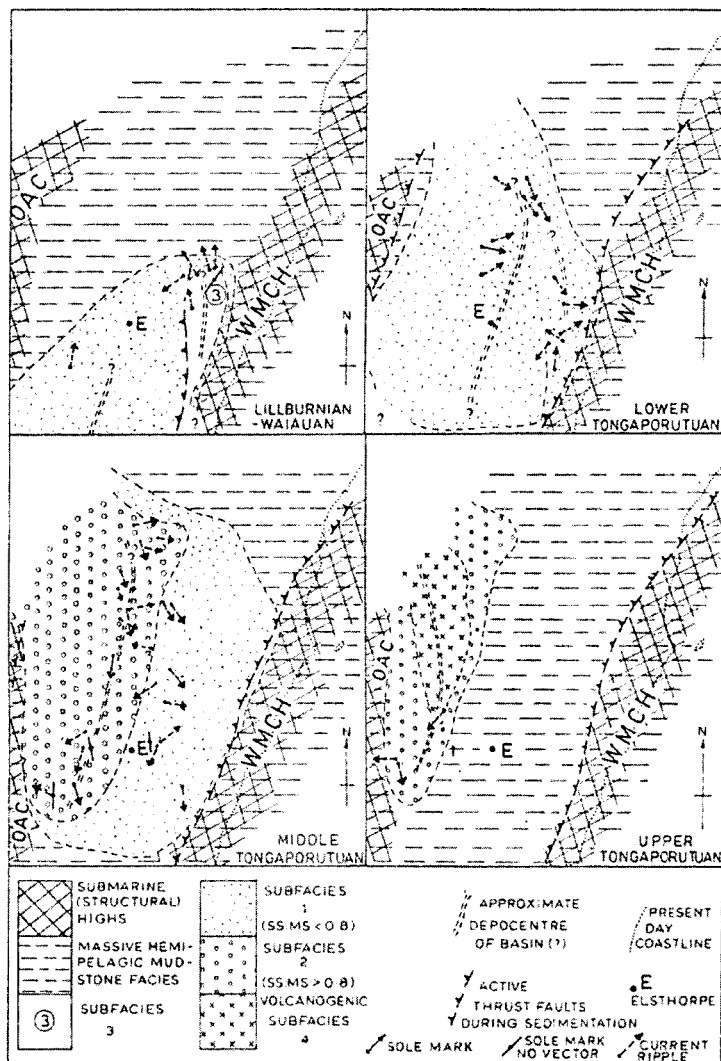


Fig.II-24. Cartes paléogéographiques du secteur Sud d'Hawke bay (Chaîne côtière - localisation Fig.II-21). Développement du bassin de Makara au cours du Miocène moyen et du Miocène supérieur. WMCH - Waimarama-Mangakuri Coastal High, OAC - Otane Anticlinal Complex, E - Elsthorpe. Van der Lingen et Pettinga (1980).

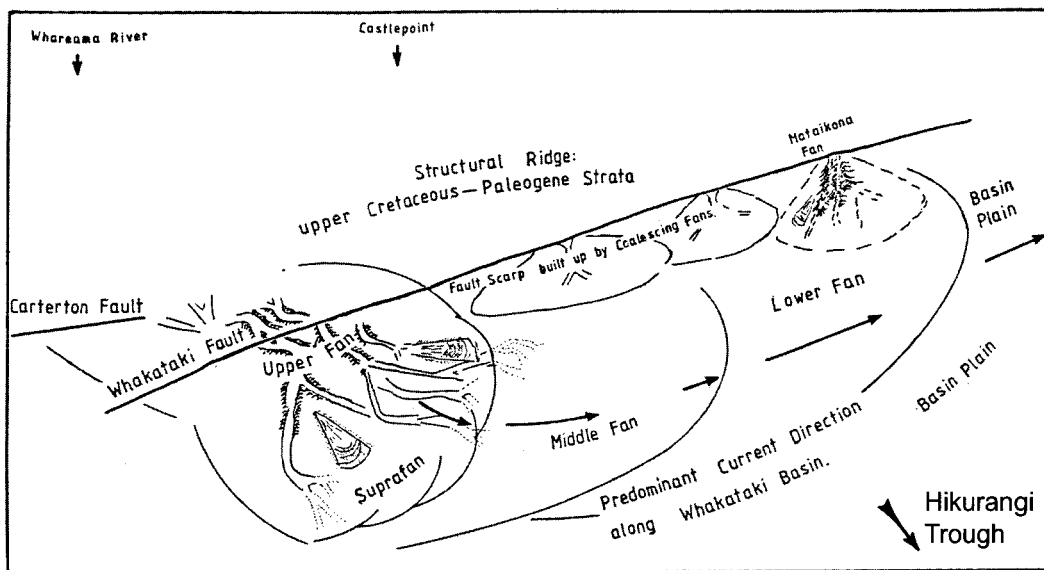


Fig.II-25. Reconstitution paléoenvironnementale du bassin de Whakataki (Chaîne côtière - localisation Fig.II-21). Ce bassin présente une sédimentation contrôlée par un système turbiditique de type deep sea fan. A l'exception du débouché des canyons, les directions de courant dominantes sont parallèles à l'axe du bassin. Turnbull (1988).

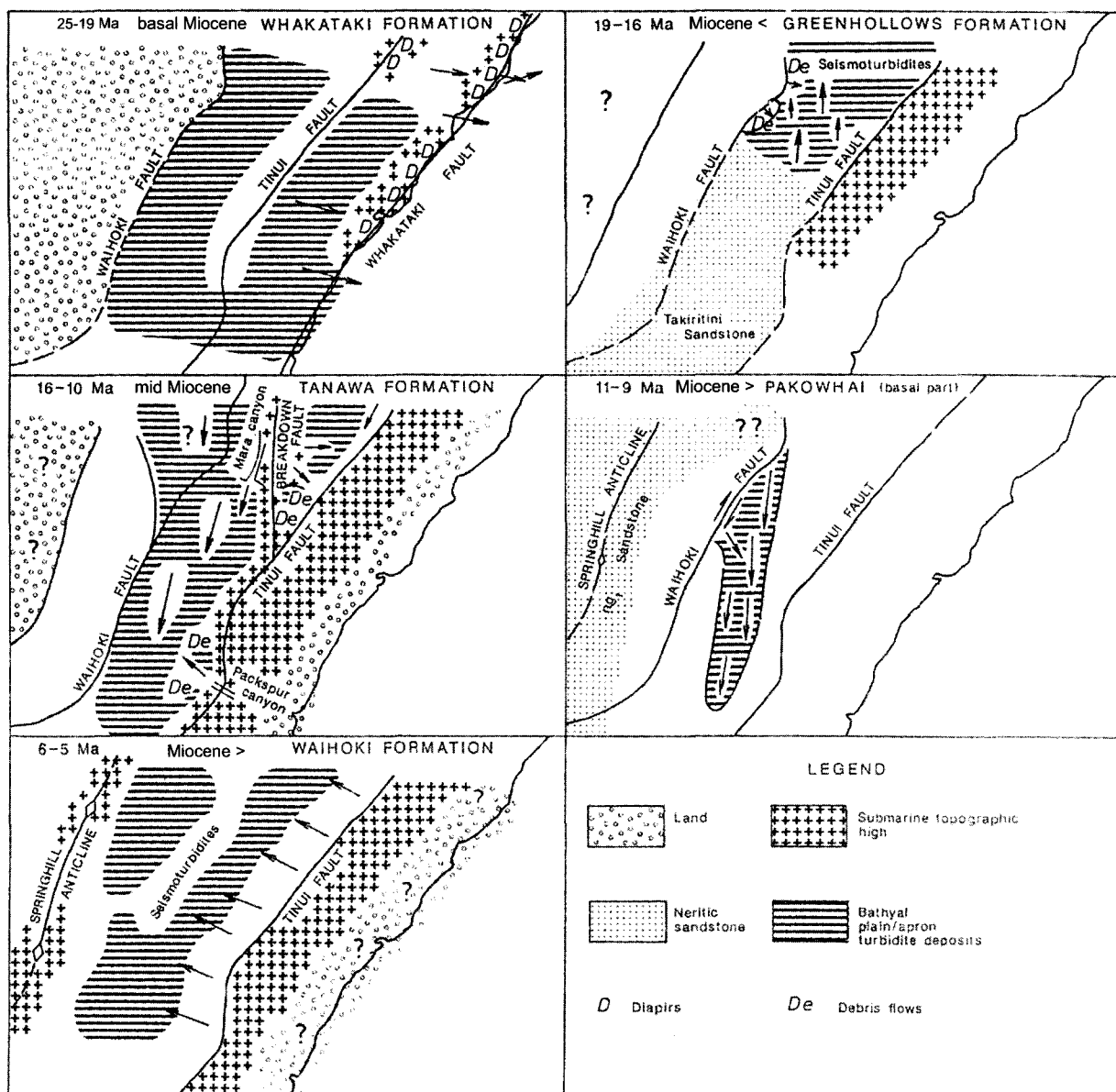


Fig.II-26. Cartes paléogéographiques du secteur de Pongaroa (Chaîne côtière - localisation Fig.II-21). Développement du bassin de Tawhero du Miocène basal au Miocène supérieur. D'après Neef (1992a). Dans notre étude nous différencierons d'une part, les séries du Miocène inférieur et du Miocène moyen qui appartiennent à un bassin confiné, le bassin que nous nommerons d'Akitio, et d'autre part, les séries du Miocène supérieur qui appartiennent à un bassin plus large et plus récent, le bassin de Tawhero proprement dit.

Fig.II-27. Représentation schématique des environnements de dépôt du secteur du synclinal de Waipatiki (Chaîne Côtière - localisation Fig.II-21) au Miocène inférieur. Le bassin de Waipatiki y est interprété comme un bassin perché (*slope basin*) daté du Miocène basal. Reid (1998).

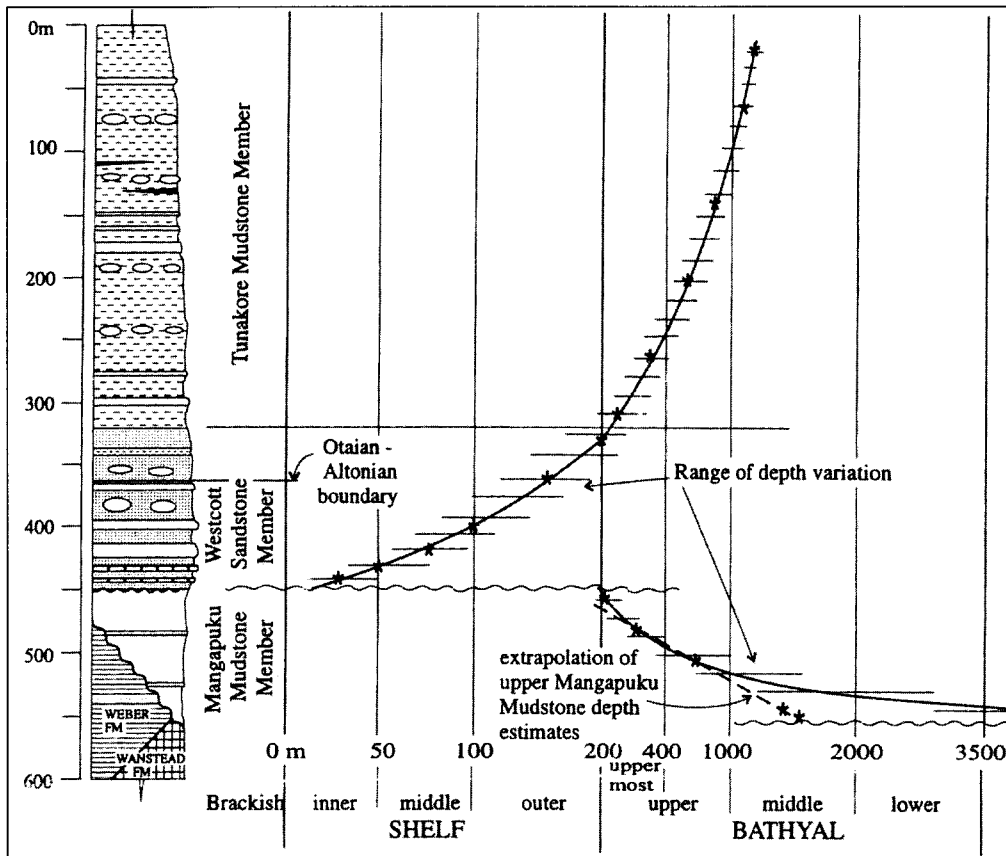
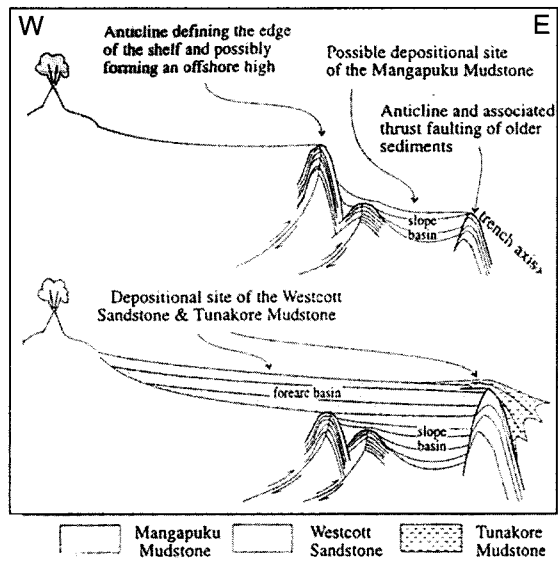


Fig.II-28. Lithostratigraphie et paléobathymétries du bassin de Waipatiki, Miocène inférieur (Chaîne Côtière - localisation Fig.II-21). Divisions bathymétriques d'après Hayward (1986). Reid (1998).

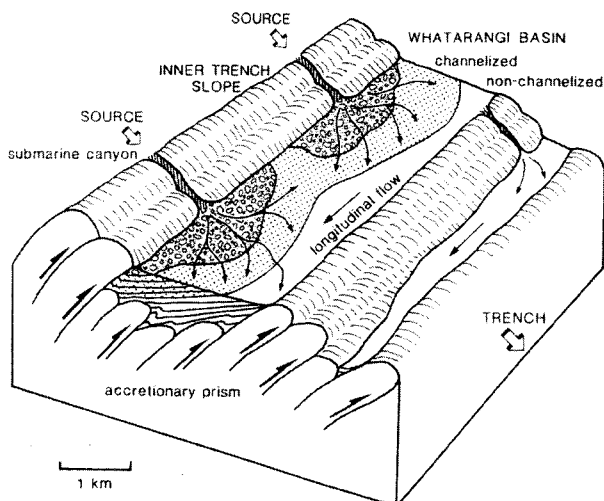


Fig.II-29. Reconstitution des environnements de dépôt de la Whatarangi Formation suggérant l'existence de bassins perchés au Crétacé inférieur sur le prisme d'accrétion du Torlesse (Sud-Est de l'île Nord de Nouvelle-Zélande - localisation Fig.II-21). George (1992).

Ces deux blocs déformés ont également été nommés respectivement *Forearc Ridge* et *Trench slope break* (Neef, 1997a,b). Dans ce mémoire, nous emploierons préférentiellement le terme *Coastal Block* pour le bloc le plus à l'Est car nous considérons l'ensemble de la Chaîne Côtière actuelle comme la plus haute ride du prisme (*i.e. trench slope break* ; Fig. II-5B). De plus, au Miocène inférieur et moyen, le *Coastal Block* constituait non pas la plus haute ride du prisme mais plus humblement la bordure externe (côté mer) d'un bassin perché. Suite au démarrage de la subduction, l'individualisation du bassin perché d'Akitio, long de 70 km pour 8 km de large (base du bassin de Tawhero *sensu* Neef, 1992a, 1997a), a été estimée à *c.* 22.4 Ma (Neef, 1999). À cette période et jusqu'à la fin du Miocène moyen, Neef (1999) considère le bloc de Pongaroa et le bloc Côtier, associés respectivement à la faille de Waihoki et à celle de Tinui (Fig. II-26), comme les bordures Ouest et Est du bassin.

Dans le bassin d'Akitio, Neef (1992a) identifie deux formations turbiditiques d'âge Miocène inférieur à Miocène moyen (*Greenhollow* et *Tanawa Formations*, Fig. II-26) qu'il décrit d'après la nomenclature de Pickering *et al.* (1989). Ces deux formations turbiditiques se sont déposées à des profondeurs de 200 à 1000 m (bathyal moyen à supérieur). D'après Neef (1992a), la *Greenhollow Formation* résulterait de courants non-confinés (*unconfined sheet flow*) sur une rampe sous-marine (*submarine ramp feeder system*) telle que définie par Heller et Dickinson (1985). La *Tanawa Formation* est attribuée à un système de pente à sources multiples (*multiple sources slope feeder system*) tel que défini par Reading (1991). Pour ces deux formations, les directions d'alimentation sont apparemment parallèles à l'axe du bassin (Fig. II-26).

Le bassin de Waipatiki, situé au Nord du bassin d'Akitio (Fig. II-18 et II-21), est interprété comme un bassin de pente du Miocène basal (Fig. II-27 ; Reid, 1998). Les séries sédimentaires (Fig. II-28 ; *Mangapuku Mudstone Member*) reposent en discordance angulaire sur le soubassement. L'érosion des séries sédimentaires du Miocène basal avant le dépôt des formations discordantes plus récentes (discordance angulaire également identifiée au toit du bassin) fait que l'épaisseur de l'enregistrement sédimentaire est faible, de 20 à 150 m (Fig. II-28). Les faciès observés pour ce bassin de pente du Miocène basal sont dominés par des argiles qui présentent des faunes remaniées et localement des débris-flows. De rares turbidites distales sont également identifiées. Grâce aux datations et à l'estimation des paléobathymétries sur la base des associations de foraminifères, Reid (1998) propose une estimation des taux de surrection pour ce bassin. Les résultats obtenus vont de 380 à 1100 m/Ma pour le Miocène basal, mais sont fortement sujets à caution du fait de l'érosion de la partie supérieure du remplissage du bassin.

Il est également à noter que des bassins perchés plus anciens (Crétacé inférieur) ont été identifiés au Sud de l'Ile Nord et sont supposés s'être développés sur la pente du prisme d'accrétion du Torlesse lors de l'orogénèse Rangitata (Fig. II-29 ; George, 1992 ; Leverenz 2000). Ces bassins anciens sont actuellement très déformés, affectés par plusieurs phases de déformation, et sont intégrés au soubassement de la marge active Hikurangi.

Chapitre III

Les systèmes turbiditiques du domaine avant-arc interne de la marge convergente Hikurangi (Nouvelle-Zélande): de nouvelles contraintes sur le développement des bassins perchés sur le prisme de subduction

Keywords: turbidites, deep-sea facies, trench-slope basins, subduction wedge, stratigraphy, Hikurangi subduction margin, New Zealand.

Mots clefs: turbidites, faciès marins profonds, bassins perchés, prisme de subduction, stratigraphie, subduction, marge Hikurangi, Nouvelle-Zélande.

Turbidite systems in the inner forearc domain of the Hikurangi convergent margin (New Zealand): new constraints on the development of trench-slope basins

JULIEN BAILLEUL¹, CECILE ROBIN², FRANK CHANIER¹, FRANÇOIS GUILLOCHEAU², BRAD FIELD³, AND JACKY FERRIERE¹

¹ UMR 8110 Processus et Bilans des Domaines Sédimentaires, Université des Sciences et Technologies de Lille1, France
e-mail : julien.bailleul@ed.univ-lille1.fr

² UMR 6118 Géosciences Rennes, Université de Rennes 1, France

³ Institute of Geological and Nuclear Sciences, Lower Hutt, New Zealand

ABSTRACT

The development and evolution of trench-slope basins on subduction wedges, are strongly related to subduction processes. These narrow elongated basins form on the lower trench slope and their edges consist of structurally controlled linear bathymetric highs. In this particular setting, sedimentary processes may be controlled both by tectonism and sea level changes. Thus, the study of the sedimentary record may give more accurate evaluation of the spatial and temporal contribution of tectonic activity on the development and stratigraphic evolution of trench-slope basins. During the last 25 My, the westward subduction of the Pacific plate beneath the North Island of New Zealand led to the development of trench-slope sedimentation related to the evolution of the Hikurangi margin. Recent uplift of the inner part of the subduction wedge has provided good exposure of the Miocene Akitio sedimentation area. Identification of the main sedimentary discontinuities, reconstitution of the geometry of the sedimentary units, and paleocurrent studies were undertaken. We propose a stratigraphic and structural scheme for the evolution of this region that may have application in other tectonically active regions.

Because the deep sea deposits are unusually very fine grained, a new facies model for lower trench-slope setting is proposed and comprises four main facies associations (Fa1 to Fa4). Two facies associations (Fa5 and Fa6) are also identified for shelf deposits. Deep sea facies associations are representative of three main depositional systems which may develop during trench-slope basin evolution. The first one corresponds to large submarine slides leading to deposition of local olistostromes at base of a slope (Fa3a). This depositional system generally marks early stages of basin development and is related to active thrust faulting during nappes emplacement episodes. Following this, the sedimentary pattern during the basin fill evolution is dominated by morphologic components of fine grained sand-rich submarine fans. This includes distal basin plain facies associations (Fa1b + distal Fa4),

depositional lobes (Fa1g), channel – lobe transitions (Fa1e); channel levee complexes (Fa1w) and small channels (Fa2a + Fa2c). Mud-rich slope facies associations (Fa3m) and sand-rich slope facies associations (Fa3s) are common and point out the important contribution of slope processes to the basin sediment budget in such a depositional setting. The third depositional system is a low gradient submarine ramp with sheet like turbidite (Fa1s), derived from unconfined turbidity currents, characterizing a late stage of the trench-slope basin fill. This filling-up megasequence constitutes a lowstand system tract which may be subdivided into basin floor fan, slope fan and prograding wedge complex.

We demonstrate that brutal facies changes (*e.g.* drowning of a mixed carbonaceous/siliciclastic shelf by basin plain facies associations) characterized five major discontinuities (D1 to D5) which are related to regional tectonic events (*i.e.* onset of subduction at 25 Ma, beginning of regional subsidence at 15 Ma) or local tectonic events (*i.e.* local uplift of structural edges of the Akitio trench-slope basin at 17.5 Ma and 16.5 Ma, acceleration of subsidence at 13.2 Ma). The tectonic control is apparently mainly expressed by slope creations leading to inversions of the vergence of sedimentary systems, by changes in turbidite facies, and by the creation of new sediment sources. Moreover, we show that the timing of development of some lowstand system tracts (*i.e.* of slope fans and of prograding wedge complexes) may also be largely controlled by changes in style and/or amplitude of tectonic activity.

I) INTRODUCTION

On an active margin, sedimentary basins form from various types of structural development depending on their location within the subduction complex. Four settings can be distinguished, in order, from outer to inner margins: trench, trench-slope basins, the forearc basin and the back-arc basin. These settings are generally parallel to the plate boundary and basin development within them is partially controlled by subduction processes. Trench-slope basins, perched on subduction wedges (for definition, *cf. infra*), are narrow elongated basins located on the lower trench slope, between the trench and the trench slope break (Underwood and Moore, 1995). If the geometry and subsidence of these basins are linked to the motion and coupling of the downgoing slab and to the evolution of the subduction wedge, their sedimentary infill may have recorded tectonic events, as well as climatic and eustatic signatures. Present-day examples of trench-slope basins are generally underwater and most knowledge on their development, evolution, geometry and tectonic/sedimentary processes is essentially based on seismic and drilling studies, mainly on the Aleutians (Moore and Karig 1976; Underwood and Norville 1986; Lewis et al. 1988; Underwood and Moore 1995), Barbados (Masle et al. 1990; Underwood and Moore 1995; Huyghe et al. 1996), Cascadia (Davis and Hyndman 1989; Underwood and Moore 1995; McAdoo et al. 1997), Hikurangi (Lewis 1980; Davey et al. 1986), Makran (White and Loudon 1982), Nankai and Japan (Moore and Karig 1976; Von Huene and Arthur 1982; Okada 1989; Underwood and Moore 1995; Underwood et al. 2003) and Sunda accretionary systems (Moore and Karig 1976; Karig et al. 1979, 1980; Stevens and Moore 1985; Underwood and Moore 1995). Along the eastern North Island of New Zealand, trench-slope basins have been identified in outcrop (van der Lingen and Pettinga, 1980; van der Lingen, 1980, 1982; Neef, 1992a; Turnbull, 1988; Lewis and Pettinga, 1993; Reid, 1998) as well as offshore (Lewis, 1980; Davey *et al.*, 1986; Lewis and Pettinga, 1993). This paper focuses on an outcrop study of a trench-slope basin, the Akitio basin, located in the Coastal Ranges (Fig. III-1). The development of this basin is related to the westward subduction of the Pacific plate beneath the North Island (Fig. III-1 and III-2A) characterized by the growth of an active subduction wedge (*e.g.* Lewis, 1980; Davey *et al.*, 1986; Lewis and Pettinga, 1993). Our aim is to characterise the development of trench-slope basins and their stratigraphic and structural evolution. We document the different facies in detail, particularly those from deep sea deposits. These sediments are unusually very fine grained for syn-tectonic turbidites and we propose therefore a new facies model for trench-slope basins. The facies characterization helps to constrain the vertical and lateral evolution of gravity driven systems, and enables evaluation of the spatial and temporal contribution of tectonic control on trench slope evolution.

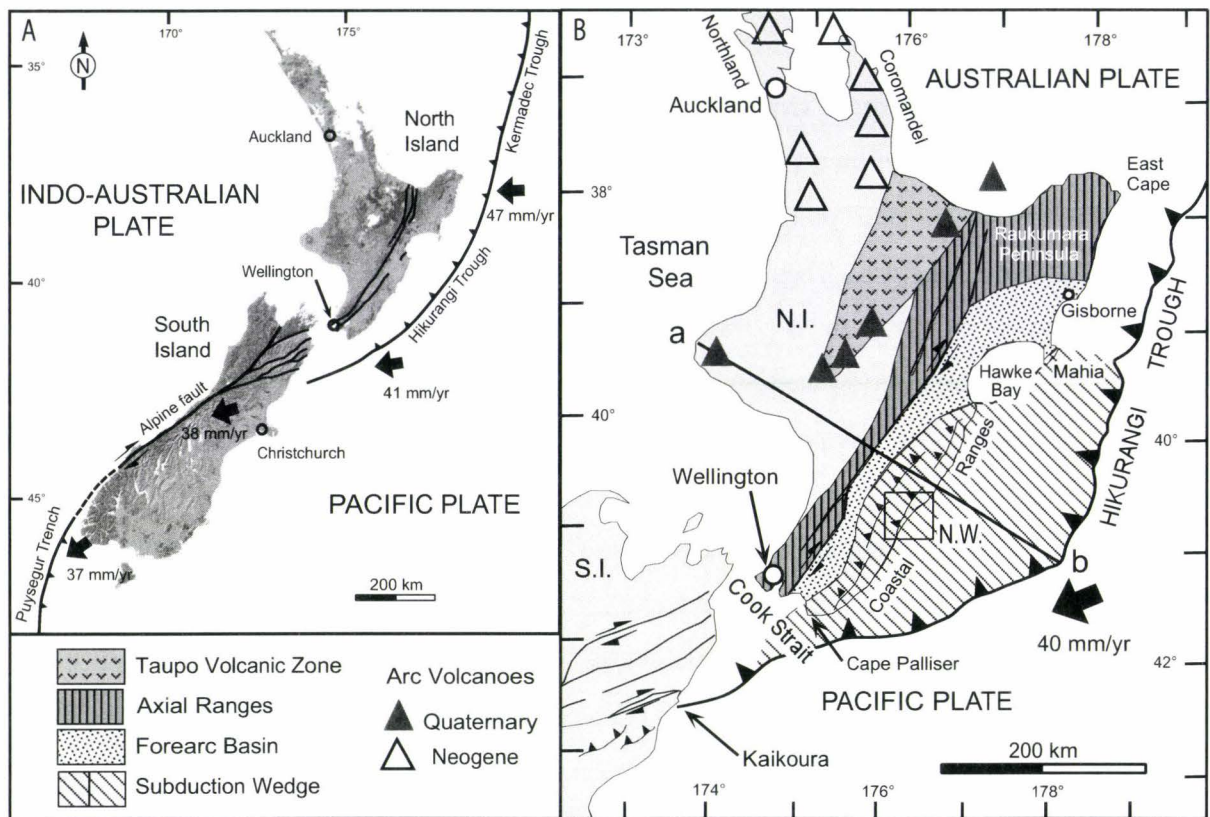


Fig.III-1. Plate tectonic setting of New Zealand (A) and major subduction related morphostructural features of the Hikurangi active margin (B). Black arrows show present-day relative plate motion between Pacific and Australian plates. See fig.2 for the a - b cross-section. N.I. - North Island, S.I. - South Island, N.W. - Northeastern Wairarapa. Modified after Chanier *et al.* (1999).

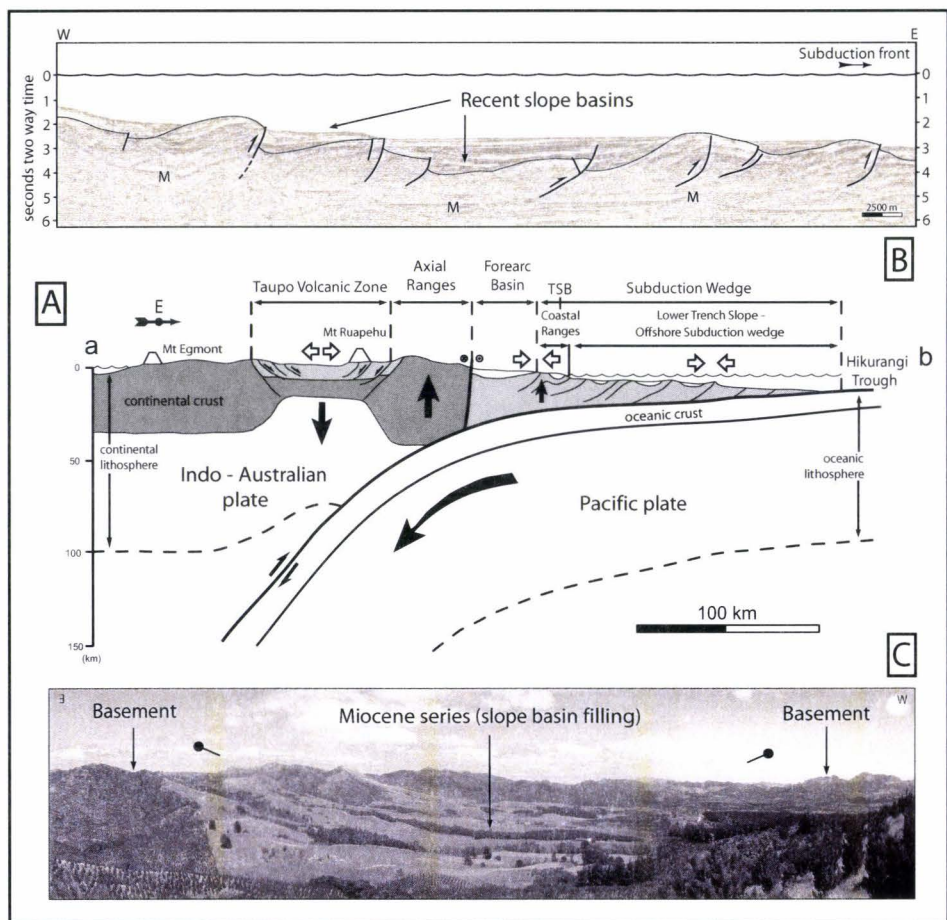


Fig.III-2. A - General cross-section of the Hikurangi subduction complex (TSB - Trench Slope Break). B - Seismic line Lee 203 (detail), location and geometry of offshore Quaternary trench-slope basins near the subduction front. Modified after Lewis and Pettinga (1993). C - Panorama of the Te Wharau syncline which presents Miocene trench-slope basin sediments cropping out onshore in the Coastal Ranges (southeastern Wairarapa).

II) STRUCTURAL CHARACTERISTICS AND GEOMETRY OF TRENCH-SLOPE BASINS

Trench-slope basins (Fig. III-2B), also called “accretionary basins” (Dickinson and Seeley, 1979), refer to small elongated structural depressions that form between linear bathymetric highs in lower trench slope settings of subduction margins (Moore and Karig, 1976, Underwood and Moore, 1995). These active narrow ridges are generally controlled by thrust faulting and/or growing folds within the underlying subduction wedge (Okada, 1989). Trench-slope basins are commonly 5 – 30 km wide, depending on the main thrust sheet spacing, and their sedimentary successions may reach 200 to 3000 m thick (Lewis, 1980; Stevens and Moore, 1985, Davey *et al.*, 1986, Okada, 1989; Mascle *et al.*, 1990) with a general increase in size, thickness and age up-slope (Karig *et al.*, 1980; Stevens and Moore, 1985). This distribution reflects the progressive uplift of trench-slope basins during deformation of the subduction wedge and the smothering of inactive structural ridges with increasing distance from the deformation front (Karig *et al.*, 1980). Before each thrust became inactive, the sedimentary fill of trench-slope basins is progressively back-tilted landward, with minor intra-basinal deformation (Moore and Karig, 1976; Lewis, 1980; Davey *et al.*, 1986, Underwood and Moore, 1995). This landward shift of the depocentre is associated with progressive onlap of sediments on the trenchward edge (Lewis, 1980; Stevens and Moore, 1985). This confers an asymmetric geometry to the basin. Seismic profiling of trench-slope basins also shows that the stratigraphic successions generally rest at an unconformity on the highly deformed basement of the subduction wedge (Fig. III-2B).

III) FACIES AND DEPOSITIONAL SYSTEMS WITHIN TRENCH-SLOPE BASINS

Underwood and Bachman (1982) have proposed a synthetic depositional model, based both on various geophysical studies and coring within recent trench-slope basins and outcrops of ancient analogues (Fig. III-3). This model proposes a predictive location for deep marine deposits within trench-slope basin domains. The seaward regional slope is cut by major submarine canyons and channels, which control the sedimentary input into the trench and trench-slope basins. Because of the structural grain, most of these canyons are blocked upslope by tectonic ridges and never reach the trench (Karig *et al.*, 1979; Underwood and Karig, 1980; Underwood and Bachman, 1982). The turbidites and other gravitational deposits are therefore preferentially ponded in upslope trench-slope basins (mature slope basins) which constitute local sedimentary traps for coarse sediments in close proximity to the trench slope

break (Moore *et al.*, 1980; Underwood and Bachman, 1982; Stevens and Moore, 1985). Downslope, trench-slope basins mainly contain hemipelagic deposits (immature slope basins). This up-slope increase in terrigenous turbiditic input is responsible for deposition of thickening- and coarsening-upward mega-sequences in trench slope basins, reflecting their gradual uplift (Moore *et al.*, 1980; Underwood and Bachman, 1982). However, this general stratigraphic model contrasts with some recent coring results in the Nankai subduction zone that show a thinning and fining upward trend within a trench-slope basin (Underwood *et al.*, 2003). Deposition of such a sequence may reflect a blockage of the previous feeder system (*e.g.*, due to out-of-sequence thrusting, or deformation of the margin in response to the subduction of sea mounts etc) or a disconnection of the canyon network from the shoreline (sea level rise or subsidence). For mature slope basins, the feeding directions may be perpendicular to the margin near the canyon mouths or parallel to the margin, reflecting the deflection of the sedimentary input along the axes of the basin (Underwood and Bachman, 1982). Although submarine canyons play an indisputable role in the distribution of sediments within trench-slope basins, other important contributions to the sediment budget are also identified. Thus, strong variations in detrital modes of turbidites on the lower slope of the eastern Aleutian trench (DSDP Leg 18, Site 181) suggest deposition by unconfined turbidity currents triggered in different source areas (Underwood and Norville, 1986). Likewise, local slope instability on adjacent ridges, caused by tectonic activity and/or eustatic fluctuations, can create significant sub-marine reworking from local sediment sources as identified in the Western Sunda arc (Stevens and Moore, 1985).

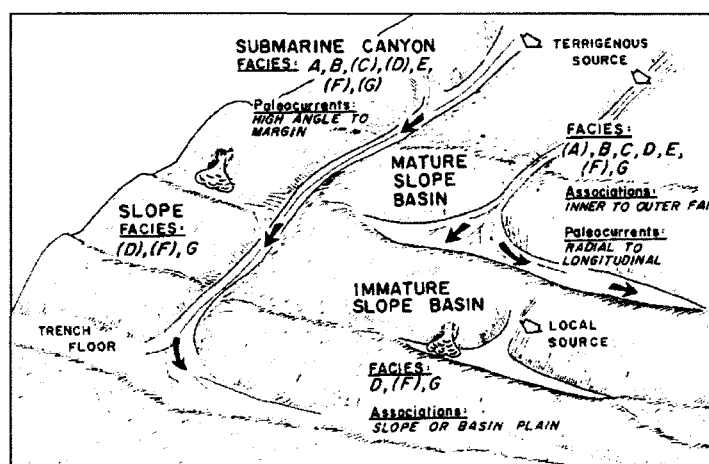


Fig.III-3. Synthetic model showing a predictive location for deep sea facies, included turbidites, and their relationships within trench-slope settings. The lithofacies code (letters) refers to the deep sea sedimentary facies model defined by Mutti and Ricci Lucchi (1978). After Underwood and Bachman (1982).

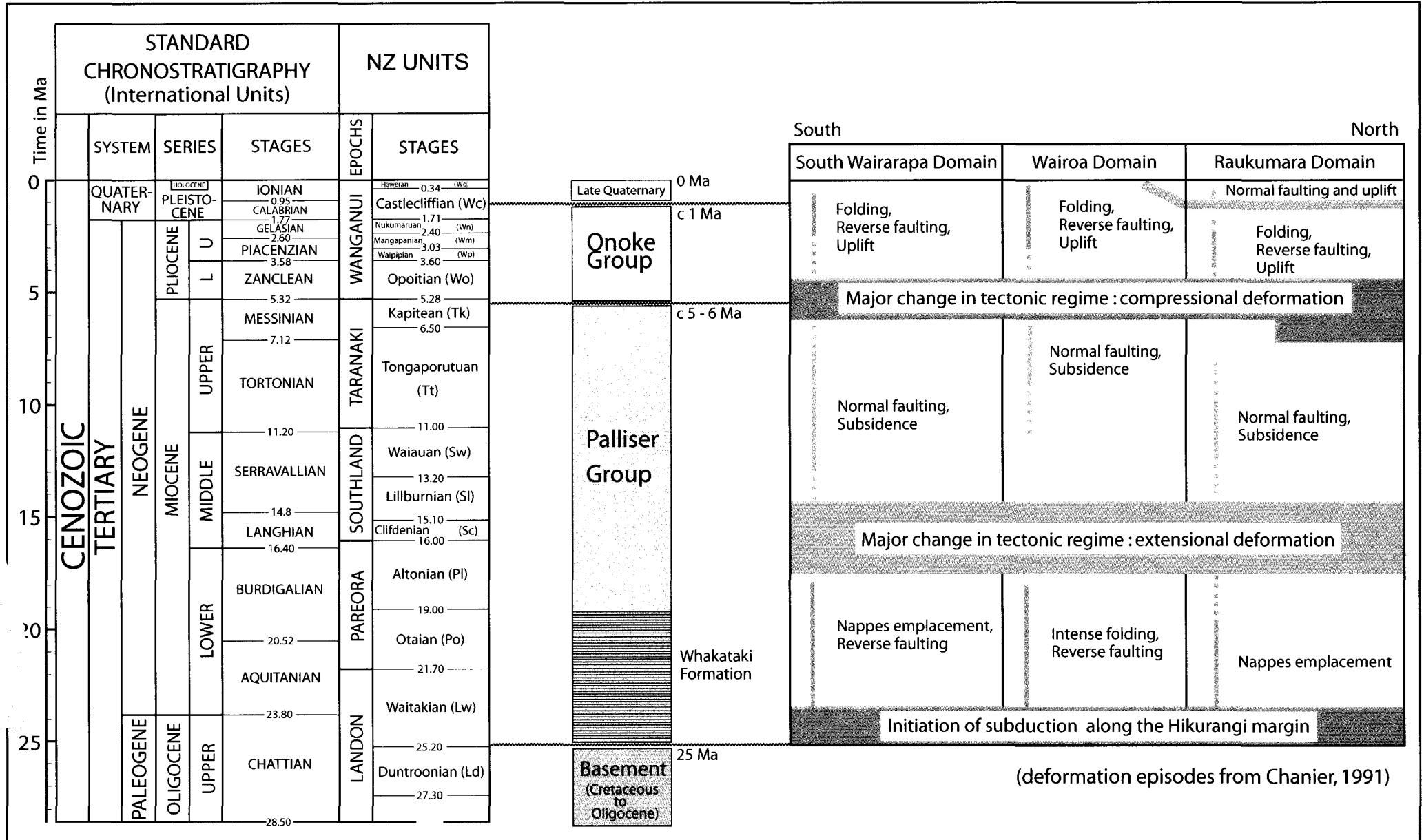
IV) STRUCTURAL SETTING

A) The Hikurangi Margin

The morphology of eastern North Island of New Zealand (Fig. III-1 and III-2A) is strongly controlled by the westward oblique subduction of the Pacific plate beneath the Indo/Australian plate (Hikurangi subduction zone; Spörli, 1980) and a pre-existing northeast-trending structural grain in the underlying Mesozoic rocks. The main particularity of this subduction zone is the relative thickness of the oceanic crust of the down-going slab: the 10 to 15 km thick Hikurangi Plateau (Davy and Wood, 1994; Mortimer and Parkinson, 1996; Collot *et al.*, 1996). This particularity is probably responsible for the recent uplift and exposure of basins on the overriding plate. Present-day major morpho-structural features of this active margin are from east to west (Fig. III-2A): **1)** the Hikurangi Trough, 2.5 to 3.5 km deep, supplied in sediments, mainly axially, from the South Island through large canyons (Lewis and Barnes, 1999), **2)** the Hikurangi subduction wedge, including elongated slope basins parallel to the trench axis. The highest ridges and basins of this subduction wedge form onland the Coastal Ranges, **3)** a forearc basin, developed on the back of the subduction wedge, **4)** the Axial Ranges (Tararua Ranges) which correspond to a mainly dextral strike-slip fault belt (Kingma, 1967; Lensen, 1969; Spörli, 1980; Cashman *et al.*, 1992), **5)** active volcanoes of the magmatic arc. In his paper, we introduce the term “subduction wedge” to refer, in subduction context, to the whole deformed area localized between the trench slope break and the trench. For the Hikurangi margin, this area is composed of **1)** the accretionary prism *sensus stricto*, localized close to the trench, and **2)** an inner highly deformed wedge, localized between the trench slope break and the accretionary prism. This inner wedge includes a deformed but non-accreted basement composed of pre-subduction series of the former margin (submitted to active deformation related to subduction processes).

Offshore, the upper part of the overriding plate is characterized by active imbricated thrusts (Fig. III-2B; Lewis, 1980; Davey *et al.*, 1986; Lewis and Pettinga, 1993). Onshore, the Coastal Ranges, also referred as the East Coast Deformed Belt (Spörli, 1980), lie from Cape Palliser to Hawke Bay and represent a 260 km long by 30 km wide northeast-southwest structural feature (Fig. III-1). In southern Hawke’s Bay, the Coastal Ranges have been considered as the highest ridge of the Hikurangi wedge, dominated by compressional features sub-parallel to the margin (Pettinga, 1982; Lewis and Pettinga, 1993). Detailed structural analysis suggests a succession of three main tectonic periods (Fig. III-4) rather than a homogeneous, continuous deformation since the onset of subduction (Chanier, 1991).

Fig.III-4. Main stratigraphic units of the Wairarapa area correlated to major deformation episodes recorded since the onset of subduction (basal Miocene, 25 Myr). Deformation episodes along the Hikurangi active margin after Chanier (1991). See the chronostratigraphic chart for equivalence between New Zealand stages (Cooper, 2004), used in this paper, and standard international stages.



(deformation episodes from Chanier, 1991)

The first tectonic regime is related to the onset of subduction responsible for seaward emplacement of thrust sheets, intense folding and reverse faulting along the Hikurangi margin (Chanier and Ferrière, 1989, 1991; Rait *et al.*, 1991). This early stage (*c.* 25 – 19 Ma) of subduction wedge development, in the region of the present Coastal Ranges, appears to have been followed by a significant period of relative tectonic quiescence, with normal faulting and syn-sedimentary gravitational collapse, as roll-over structures developing locally (Chanier *et al.*, 1999). This episode, mainly because it is contemporaneous with widespread subsidence of the whole margin (*c.* 15 – 5 Ma), has been attributed to a period of tectonic erosion (Chanier *et al.*, 1999). The third period, Pliocene and Quaternary, is characterized by the renewal of dominantly compressional deformation (Walcott, 1984; Lamb and Vella, 1987; Wells, 1989; Cape *et al.*, 1990; Chanier, 1991; Beanland *et al.*, 1998; Nicol *et al.*, 2002). This folding and reverse faulting event occurred over the entire region and led to the uplift and subsequent exposure of the Coastal Range area very recently, possibly about 0.3 My ago (Ghani, 1978). The recent tectonic development is also characterized, at least locally, by some strain partitioning (*e.g.* strike-slip vs compression) driven by the oblique convergence along the Hikurangi margin (Cashman *et al.*, 1992, Barnes *et al.*, 1998).

As seen previously, trench-slope basin development is strongly controlled by active margin tectonic activity. Therefore, since the onset of subduction, the succession of episodes of deformation must have strongly influenced sedimentation on the lower trench slope. The study of the sedimentary record within trench-slope basins may give more accurate constraints on local and regional tectonic activity. This work is based on an identification of the main sedimentary discontinuities, a reconstitution of the geometry of the sedimentary units (with a focus on their lateral thickness variations, which represent subsidence variations at the basin scale), and paleocurrent reorganization (and hence major paleogeographic changes).

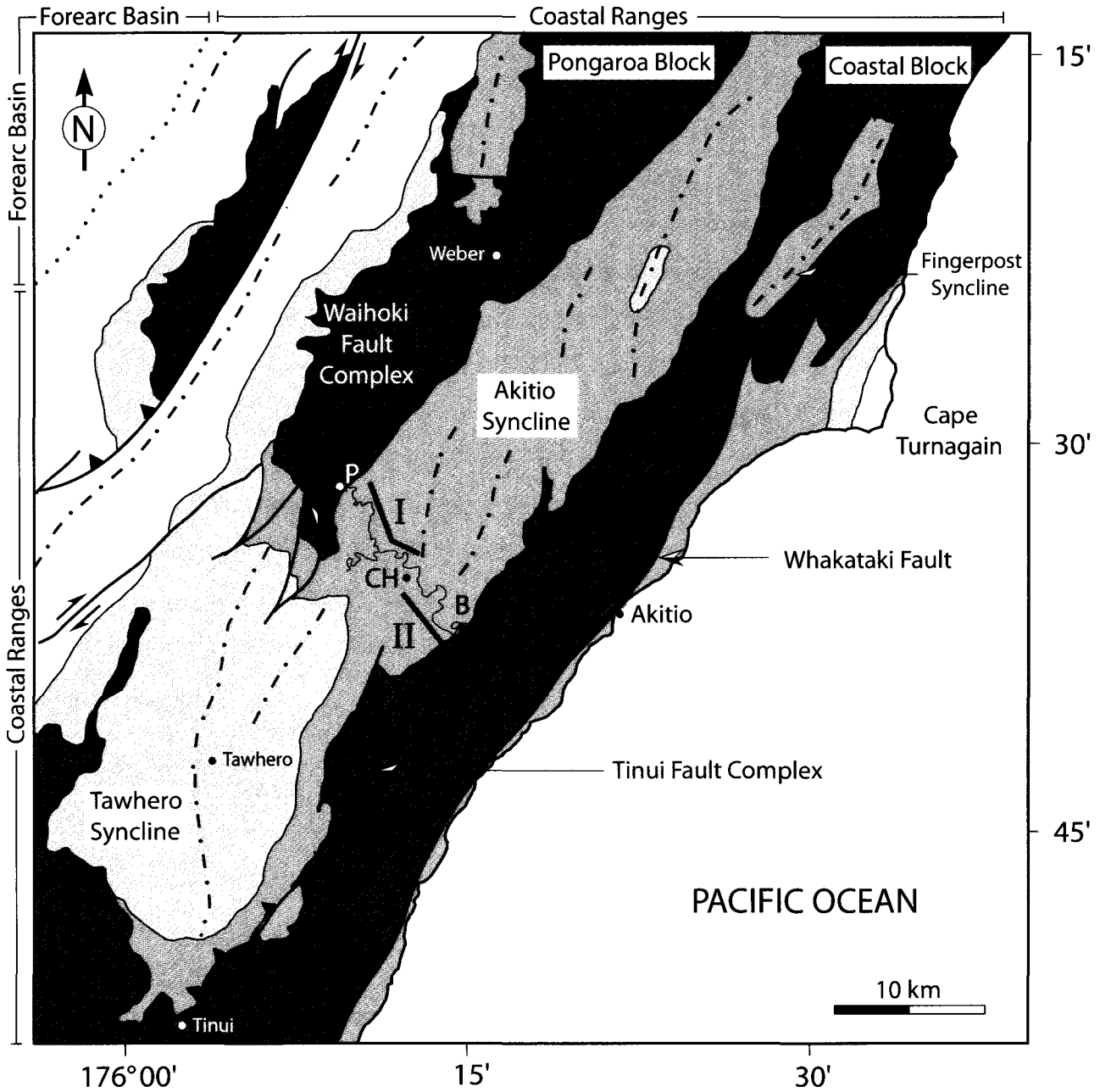
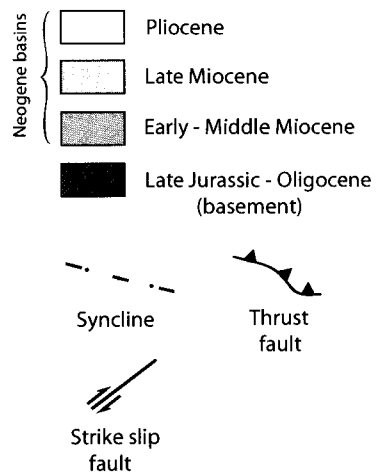


Fig.III-5. Structural map of the Pongaroa area, central eastern Wairarapa. Location of the sedimentological vertical sections within the Akitio syncline: I - Pongaroa section, II - Branscomb section. P - Pongaroa, CH - Cross Hills, B - Branscombe. After Lee and Begg (2002).



B) The Akitio Basin

Rapid uplift of the inner part of the Hikurangi margin during the Quaternary (Ghani, 1978; Cape *et al.*, 1990) has produced exposures of thick turbidite successions of Miocene trench-slope basins (van der Lingen and Pettinga, 1980; van der Lingen, 1982, 1988; Neef, 1992a; Turnbull, 1988). In the north-eastern Wairarapa (Coastal Ranges), elongate, wide synclines lie between highly deformed basement strips which comprise Cretaceous to Paleogene pre-subduction sedimentary rocks (Fig. III-2C and III-5). This succession of basement strips and synclines trend parallel to the margin (*i.e.*, mainly northeast-southwest).

The infill of the Tawhero-Akitio basin is exposed within two major synclines, the Tawhero syncline to the southwest and the Akitio syncline to the northeast (Fig. III-5). The sedimentary series of these synclines overlies basement rocks of the Pongaroa Block and of the faulted Coastal Block (Moore, 1988), also referred as the Forearc Ridge and the Trench Slope Break respectively (Neef, 1997a,b). In this paper, we favour the term "Coastal Block" because we consider the whole present day Coastal Ranges as the present trench slope break (Fig. III-2A) *i.e.* highest ridge lying between the forearc basin and the trench (Underwood and Moore, 1995). Moreover, during the early and middle Miocene, the Coastal Block (pre-subduction basement deformed during the onset of subduction) corresponded to the trenchward edge of the Akitio trench-slope basin and therefore was not the trench slope break.

The Tawhero syncline, includes all the Miocene series (*c.* 25 – 5 Ma) whereas the Akitio syncline comprises only early and middle Miocene sediments (*c.* 24 – 13 Ma). Following the onset of subduction, the period of development of the 70 km long, 8 km wide Tawhero trench-slope basin (Neef, 1992a, 1997a) has been estimated to start at *c.* 22.4 Ma (Neef, 1999). At that time, Neef (1999) considers the Pongaroa Block and the Coastal Block, uplifted along the Waihoki Fault Complex and the Tinui Fault Complex respectively, as the western and eastern edges of the basin until the end of the middle Miocene (Fig. III-5). Thus, nowadays, most of the early to middle Miocene sedimentary infill of the Tawhero trench-slope basin (Neef, 1992a, 1997a) seems to be confined to the Akitio syncline. Therefore, we prefer to rename this basin "Akitio basin" to avoid confusion with the Tawhero syncline. During the early and middle Miocene, turbidite fill accumulated in middle to upper bathyal depths (200 – 1000 m).

The particularly well exposed Akitio basin provides sufficient data to accurately describe the sedimentary pattern within a lower trench slope setting. Moreover, high resolution vertical section measurements give us a new approach to trench-slope basin development and evolution.

V) REGIONAL STRATIGRAPHIC AND SEDIMENTOLOGIC FRAMEWORK

Because of structural complexity and rapid lateral facies changes, the lithostratigraphic framework of the north-eastern and south-eastern Wairarapa is problematic. A large number of local group and formation names have been defined in the past (Vella and Briggs, 1971; Johnston, 1975, 1980; Crundwell, 1987, 1997; Neef, 1992a, 1992b, 1995, 1997a, 1997b). Further work for the synthesis of the Cretaceous – Cenozoic geology of the East Coast Region (Field, Uruski *et al.*, 1997) and for the Wairarapa 1:250000 Q-map (Lee and Begg, 2002) led to a clarification of the regional stratigraphy (Fig. III-4).

The whole Miocene sedimentary series are included in a single stratigraphic unit, the Palliser Group (modified after Vella and Briggs, 1971). This group includes at its base the early Miocene series of the Whakataki Formation (Johnston, 1975, 1980) which consists mainly of olistostrome and flysch deposits and contrasts with underlying Eocene-Oligocene pelagic sedimentation (marls and pelagic limestones). This sharp facies change, observed over the whole Coastal Ranges, is correlated with the onset of subduction (Chanier and Ferrière, 1991). However, the contact between the earliest Miocene sediments of the Whakataki Formation and Cretaceous to Oligocene basement is generally conformable. Regionally, the overlying middle and late Miocene sediments of the Palliser Group show successive discontinuities associated with a progressive onlap on basement (Fig. III-5). Vella and Briggs (1971) considered this sequence as the result of a major marine transgression during a period of broad subsidence of the margin. Middle and late Miocene units are composed mainly of turbidites, bathyal mudstones and neritic sandstones. Further work indicates that some facies changes within this sequence also record global sea level oscillations or local tectonic activity (Neef, 1997a).

The overlying latest late Miocene to early Quaternary (*c.* 6.5 – 1.5 Ma) marine sediments of the Onoke Group (Vella and Briggs, 1971; Lee and Begg, 2002) are unconformable on the Palliser Group and provide evidence of a regional marine regression. This shallowing event may be related to the beginning of the Plio – Quaternary uplift episode (Walcott, 1984; Lamb and Vella, 1987; Wells, 1989; Cape *et al.*, 1990; Beanland *et al.*, 1998; Nicol *et al.*, 2002).

The Akitio syncline contains sedimentary series of the lower Palliser Group (early – middle Miocene), including the Whakataki Formation.

VI) LOCATION AND METHODOLOGY

Near Pongaroa, the Pongaroa and the Owahanga rivers, which cut perpendicularly the structures of the Akitio syncline, provide good exposures of the Miocene sedimentary series of the Akitio basin (Fig. III-5). Two vertical sections have been measured on each limb of the Akitio syncline. To the southeast (Branscombe section), the sedimentary record represents 910 m of various deep sea sediments which crop out along the Owahanga River, from Branscombe to Cross Hills (Fig. III-5). To the northwest (Pongaroa section), a 1460 m long vertical section crops out along the Pongaroa River and the Owahanga River, from Pongaroa to Cross Hills (Fig. III-5). Correlations, combined with paleocurrent direction analysis (flute casts or unidirectional ripples measurements, all data backtilted to horizontal), highlight strong variations of the depositional environment through time.

Correlations between the two sections were first established using New Zealand stage boundaries, based on foraminiferal assemblages. Vertical successions of facies in each section were then used to identify major discontinuities (characterized by sharp facies changes). These sedimentary discontinuities bound the main stratigraphic units within the basin fill. Correlations of the discontinuities are firstly based on the biostratigraphic framework, which allows good dating of the unit boundaries for both sections. The significance of the facies changes for each discontinuity, as well as the distal/proximal trend of sedimentary systems within each unit, are also taken into account to improve the precision of our correlations.

In order to constrain the stratigraphic units and their significance in terms of depositional environment, the sedimentary systems had to be characterized. To do this, the sedimentary facies encountered in the eastern Wairarapa were identified, described and integrated into a facies model for turbidite and the related deep sea facies, as well as shelf facies. Our interpretation of deep sea sediments includes a distal/proximal zonation of facies within a turbidite system. Indeed, the presence of trench-slope basins at different bathymetries on the lower trench slope, the multiplicity of possible locations for sediment sources (which may be also affected by tectonic activity), as well as the existence of axial feeding processes, suggest that the facies or facies associations in this particular tectonic setting do not inevitably reflect paleobathymetry. This phenomenon is amplified by the fine grained character of the sediment, leading to deposition of fine grained turbidites even within the upslope trench-slope basins. Therefore, with the exception of the shallower water environments (neritic), for which we could determine the paleowater depth from facies analysis, paleobathymetries had to be

estimated from microfaunal assemblages (biofacies). Most paleontological data used in this study come from the New Zealand Fossil Record File held at the Institute of Nuclear and Geological Sciences (GNS, Fossil Record Electronic Database). Paleobathymetric classes are from Hayward (1986, 1987), King *et al.* (1993) and Crundwell *et al.* (1994): neritic 0-200 m (inner shelf 0-50 m, middle shelf 50-100 m, outer shelf 100-200 m), upper bathyal 200-600 m, middle bathyal 600-1000 m, and lower bathyal 1000-2000 m.

VII) FACIES ANALYSIS

Apparently homogeneous silty fine grained Miocene turbiditic series crop out in the Coastal Ranges in north-eastern and south-eastern Wairarapa (Fig. III-2B and III-5). High resolution section measurements from Akitio Syncline and surrounding areas allow us to propose an overview of Miocene deep marine facies and facies associations encountered within trench-slope basin environments (Table III-1, Plate III-1 and III-2). Shelf sediments also occur (Table III-2, Plate III-2). All these facies have been partially described by previous workers such as Lillie (1953), Vella and Briggs (1971), Johnston (1980), Moore (1980, 1988), Crundwell (1987, 1997), Turnbull (1988), Francis (1990), Chanier and Ferrière (1991), Neef (1992a, 1992b, 1995, 1997a, 1997b), Edbrooke and Browne (1996), Reid (1998), Johansen (1999) and Field (2005). Compilations of these previous studies have been undertaken by Field, Uruski *et al.* (1997) and Lee and Begg (2002). Authors have generally published regional and detailed maps, descriptions of the main regional and local stratigraphic units, and occasionally some localized facies descriptions (e.g. Neef, 1992a, 1997a). Most do not present large measured vertical sections and related facies analysis.

In this paper, descriptions of sedimentary facies are based on their lithology, grain size, sedimentary structures at different scales, stratification, and geometric relationships. Two major types of sedimentary environments have been identified: deep-sea gravitational deposits and shelf sediments. Deep sea deposits comprise (Table III-1): Fa1 - alternation of fine grained sandstones with siltstones; Fa2 - channelized facies; Fa3 - disorganized facies; and Fa4 - massive mudstones to siltstones. Shelf deposits include (Table III-2): Fa5 - limestones facies; and Fa6 - bioclastic siltstones to fine grained sandstones. These facies associations are interpreted in terms of sedimentary environments (with regard to gravity flow processes for deep marine deposits) and integrated into a depositional model based on turbidite system characteristics.

With the exception of sheet-like turbidites (Fa1s) and olistostromes (Fa3a), gravity flow deposit facies associations clearly fit the main characteristics of deep sea fan systems. Previous field work on turbiditic trench-slope basins attempted to apply a general submarine fan model (e.g. Mutti and Ricci Lucchi, 1978; Walker, 1978) with considerations to the specificities of the studied gravitary system (e.g. Smith *et al.*, 1979; Moore *et al.*, 1980; Turnbull, 1988). Since, it has become evident that a single model cannot be applied universally to the wide variety of depositional environments where deep sea sedimentary systems may develop (Shanmugam *et al.*, 1985). Deep sea fan models were constructed after observations on recent fans along a transform active margin (off California), and/or on ancient analogues within foreland basins (Apennines and Pyrenees). Compared to trench-slope basins, these depositional settings may present significant differences concerning the parameters that control the development of gravitary systems (e.g. geometry of the basin, tectonic activity, sediment flux). We characterize the studied turbidite system using the morphologic component approach described by Mutti and Normark (1987, 1991). At first pass, this provides a distal/proximal zonation for our facies associations: Fa1b and distal Fa4 - distal basin plain, Fa1g - depositional lobe, Fa1e - channel - lobe transition, Fa1w - channel levee complex, Fa2a and Fa2c - small channel infill, Fa3s and Fa3m - slope facies associations. Olistostromes and sheet-like turbidites as well as the main characteristics of the turbidite system and its evolution for the Akitio basin will be discussed in a later section of this paper.

Our facies zonation compared to the paleobathymetries obtained using the foraminiferal assemblages shows that the most distal and the most proximal facies are respectively generally the deepest and the shallowest. However, as expected in this particular tectonic setting, few examples clearly illustrate the difficulties in associating a facies to a paleobathymetry determination with certainty. Indeed, in the Akitio Basin, distal turbidites (Fa1b) may be encountered from middle or even lower bathyal to upper bathyal settings (Appendix 2). Moreover, a variety of facies can occur in a given paleowater depth; for example, middle bathyal settings can contain distal turbidites (Fa1b), slope facies associations (Fa3m) and massive siltstones (Fa4).

Table III-1. Characteristics and interpretation of the sedimentary facies for the turbidites and the related deep-sea deposits identified in this study

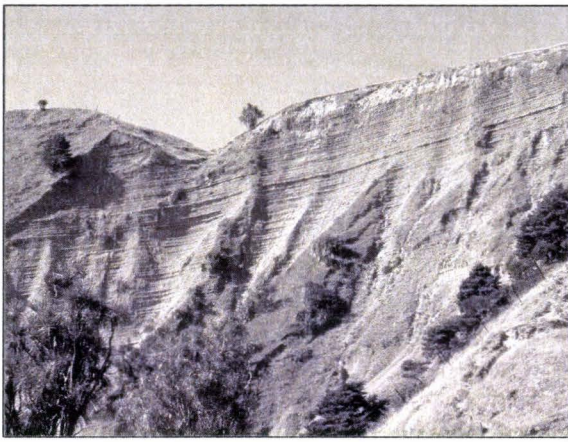
Facies code	Lithology	Stratification	Internal bedding	Gravity processes	Interpretation
<i>Alternation of fine grained sandstones with siltstones, Fa1</i>					
1b	Alternation of 1 to 50 cm thick siltstones with 1 to 50 cm thick fine grained sandstones, well sorted	Tabular, good lateral continuity of beds, sharp bases (rare flute casts) and gradational tops	Well developed Bouma sequences, Ta-e to Tc-e, most common Tb-e, systematic climbing ripples, common convolutions, local escape and load structures, sometimes non-erosive amalgamation surfaces	Low density turbidity currents (unsteady turbulent flows)	Deep sea plain like turbidites (Bouma type turbidites), distal basin plain
1g	Alternation of 5 mm to 5 cm thick siltstones with 0.5 to 2 m thick dirty fine grained sandstones, well sorted	Tabular, sharp bases and tops	Commonly massive, restricted intervals with plane laminations (traction) and well developed intervals with growing up hummocks (aggradation), sometimes non-erosive amalgamation surfaces	Low density turbidity currents (unsteady turbulent flows)	Depositional lobe
1e	Alternation of 1 to 50 cm thick siltstones with 1 to 30 cm thick dirty fine grained sandstones, well sorted	Laterally discontinuous beds, numerous erosive features at bed boundaries	Commonly massive, climbing ripples (Tc), rare plane laminations (Tb), systematic intra-beds erosive amalgamation surfaces and/or "reprises granulo"??	high density turbidity currents (unsteady turbulent flows), mostly erosive (low degree of sediment preservation)	Bypass (channel – lobe transition)
1w	Alternation of 10 cm to plurimetric thick siltstones with 1 to 20 cm thick bioturbated fine grained sandstones, well sorted, bioturbated	Wedge geometry (plurimetric scale), laterally discontinuous beds, local low angle unconformities, erosive bases and gradational tops	Massive (due to the bioturbation ?), sometimes climbing ripples, rare basal coarser intervals	Lateral spreading from a high density confined turbidity current (unsteady turbulent flows)	Channel levee (overbank deposits)
1s	Alternation of 5 to 50 cm thick siltstones with 5 cm to 2 m thick fine grained sandstones, well sorted, bioturbated	Tabular (sheets), good lateral continuity of beds, sharp erosive bases and gradational to sharp tops, local low displacement slumps and slump scours	Commonly massive, sometimes plane laminations, rare ripples and convolutions, intra-beds erosive to non-erosive amalgamation surfaces	Unconfined turbidity currents (unsteady turbulent flows)	Sheet like turbidites
<i>Channelized facies association, Fa2</i>					
2a	Alternation of 5 to 10 cm thick fine grained sandstones and 5 to 30 cm thick siltstones with scattered extraformational centimetric to decimetric clasts and broken bioclasts (bivalvia, gastropoda)	Lenticular (metric scale and poorly erosive) - laterally discontinuous beds		Mud-flows (cohesive flows) and turbidity currents (unsteady turbulent flows)	Small channel
2c	Conglomerates made up of broken bioclasts (bivalvia, rare gastropoda) and minor centimetric extraformational clasts	Lenticular ?		Debris-flows (cohesive flows)	Small channel ?
<i>Disorganized facies association, Fa3</i>					
3s	Disorganized facies, syn-sedimentary deformation of alternating 20 cm to 1 m thick sandstones and 10 cm to 2 m thick conglomerates	Large displacement slumps, low displacement slumps, slump scours	Shear and load structures	Slumping and debris-flows (cohesive flows)	"Sandrich" slope facies association
3m	Disorganized facies, syn-sedimentary deformation of alternating 1 to 20 cm thick sandstones and 10 cm to plurimetric thick siltstones with scattered centimetric to decimetric extraformational clasts and broken bioclasts (bivalvia, gastropoda and rare scleractinia)	Large displacement slumps, low displacement slumps, in situ slumps, slump scours		Slumping and mud-flows (cohesive flows)	"Mudrich" slope facies association
3a	Disorganized facies, syn-sedimentary deformation of conglomerates made up of centimetric to plurimetric extraformational clasts, sometimes punctuated by mudstones or siltstones with scattered extraformational centimetric clasts	Good lateral continuity of huge sedimentary volumes, large displacement slumps	Shear and load structures	Slumping, debris-flows and sometimes mud-flows (cohesive flows)	Olistostromes

Table III-1. (Contd.) Characteristics and interpretation of the sedimentary facies for the turbidites and the related deep-sea deposits identified in this study

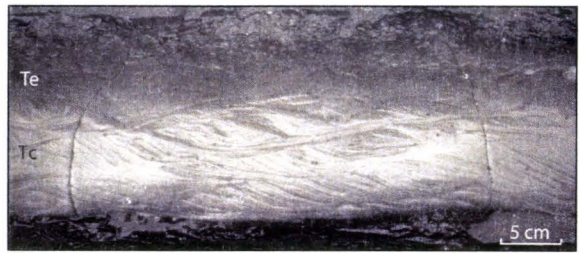
Facies code	Lithology	Stratification	Internal bedding	Gravity processes	Interpretation
<i>Massive mudstones to siltstones facies association, Fa4</i>					
4	Blue grey mudstones to siltstones, more or less carbonaceous and bioturbated, scattered foraminifera, sometimes wood, common indurated diagenetic concretions and pipes	Massive, no clear stratification		Pelagic to hemipelagic deposition	Slope to distal basin plain deposition (may be precised by palaeo-ecology on foraminifers)

Table III-2. Characteristics and interpretation of the sedimentary facies for the shelf deposits identified in this study

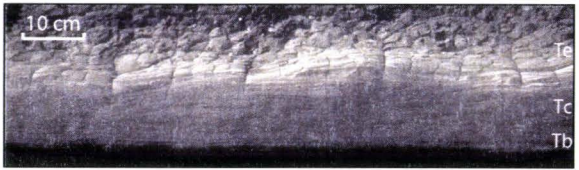
Facies code	Lithology	Stratification	Internal bedding	Interpretation
<i>Limestones facies association, Fa5</i>				
5	Alternation of 1 to 20 cm thick siltstones (scattered centimetric extraformational clasts and broken bivalvia bioclasts, common layers of red algae bowls) with 5 to 50 cm thick more or less clastic algal limestones. Less clastic limestones made up of abundant broken or encrusting red algae, amphistegimid foraminifers and broken bryozoa; common broken bivalvia, gastropoda; echinoderms, echinoid spines, benthic and planktonic foraminifers; rare encrusting foraminifers, oyster fragments and scaphopod molluscs; glauconite, rare quartz	Crudely stratified, lenticular, laterally discontinuous beds (lateral disappearance or shift to Fa6c or to a centimetric layer of algal layer bowls), erosive surfaces and scours	Red algae encrusting, sometimes polyphase, of reworked shelf bioclasts or aggregates (matrix and bioclasts): floatstone; micritic matrix or sometimes sparitic cement, bio-erosion	Bryozoa and amphistegimid red algae encrusted floatstone; high energy Outermost shelf
<i>Bioclastics siltstones to fine grained sandstones facies association, Fa6</i>				
6c	Well cemented 10 to 50 cm thick bioclastic fine grained sandstones (abundant broken and unbroken bivalvia, gastropoda), well sorted	Laterally discontinuous beds, generally associated at base or laterally to Fa5	Macrofauna scattered within the micritic cemented sandy component	High energy Outermost shelf
6b	Extensively bioturbated bioclastic siltstones to fine grained sandstones (bivalvia, gastropoda, scaphopoda), well sorted	Massive, may presents interstratified sub-facies: 6bs - HCS (well cemented and well sorted decimetric "en dôme" sandstone beds, erosive bases, scattered disarticulated fossils), 6bf - high flooding deposits (plurimetric beds of poorly sorted fine to medium grained sandstones, sharp bases, plane laminated, no bioclasts)	Fossils in live position, or highly concentrated within bioturbated pockets, or concentrated by storm waves within centimetric thick layers, or scattered and disarticulated.	No gravitary deposit Outer shelf (confirmed by palaeo-ecology on foraminifers) to Middle shelf (locally influenced by storm waves and high flood currents)



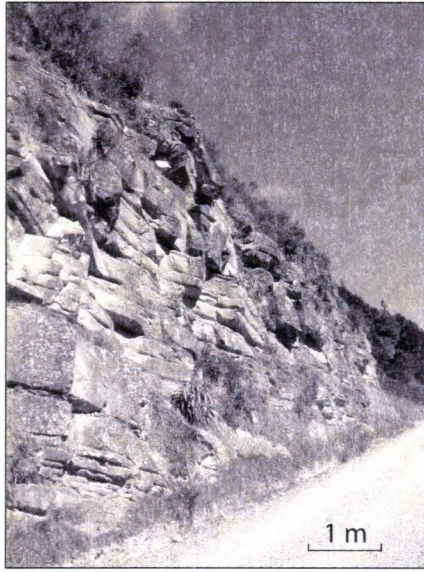
A - Fa1b



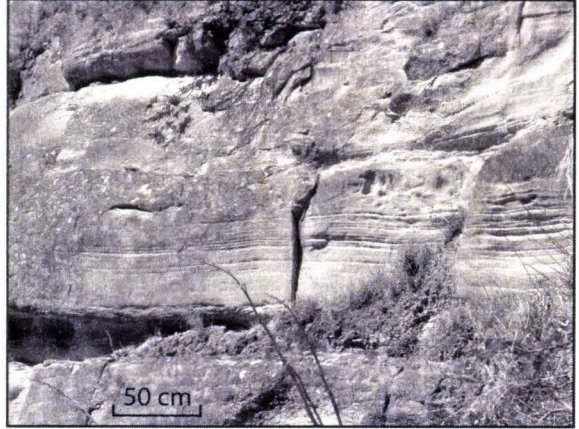
B - Fa1b



C - Fa1b



D - Fa1g



E - Fa1g



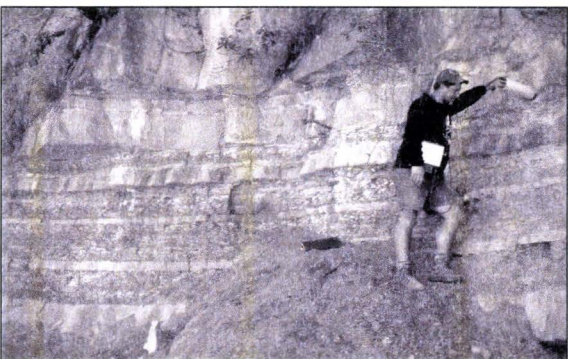
G - Fa1e



F - Fa1e



H - Fa1w



I - Fa1s



J - Fa2a

Plate III-1. Turbidites and related deep-sea sediments encountered within trench-slope basin environments (Fa1b to Fa2a). See tables III-1 and III-2 for description and interpretation of the facies.



K - Fa3s



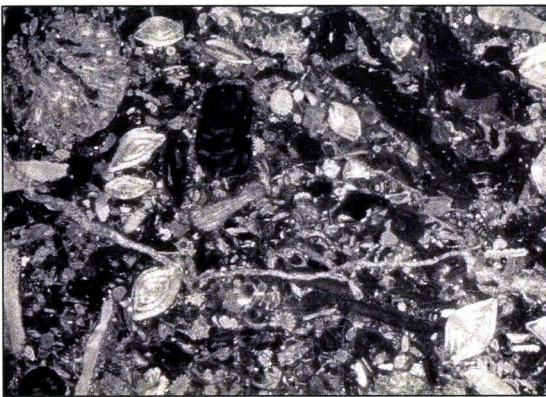
L - Fa3m



M - Fa3m



N - Fa5



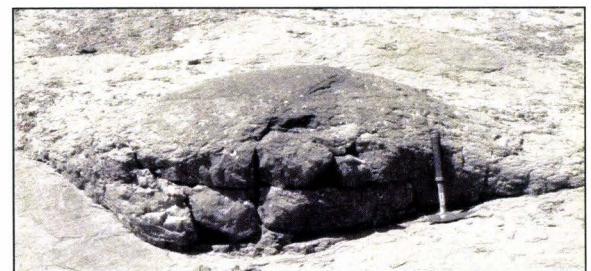
O - Fa5



P - Fa6b



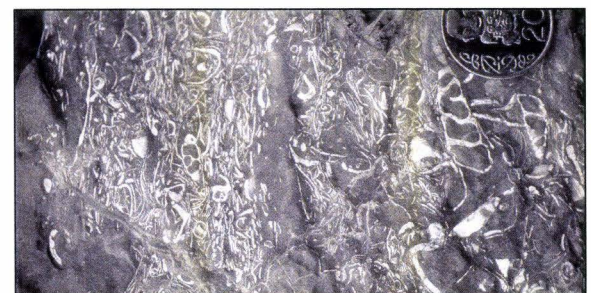
Q - Fa6b



R - Fa6bs



S - Fa6bf



T - Fa6c

Plate III-2. Turbidites and related deep-sea sediments encountered within trench-slope basin environments (Fa3s to Fa3m), and outer shelf to middle shelf deposits (Fa5 to Fa6c). See tables III-1 and III-2 for description and interpretation of the facies.

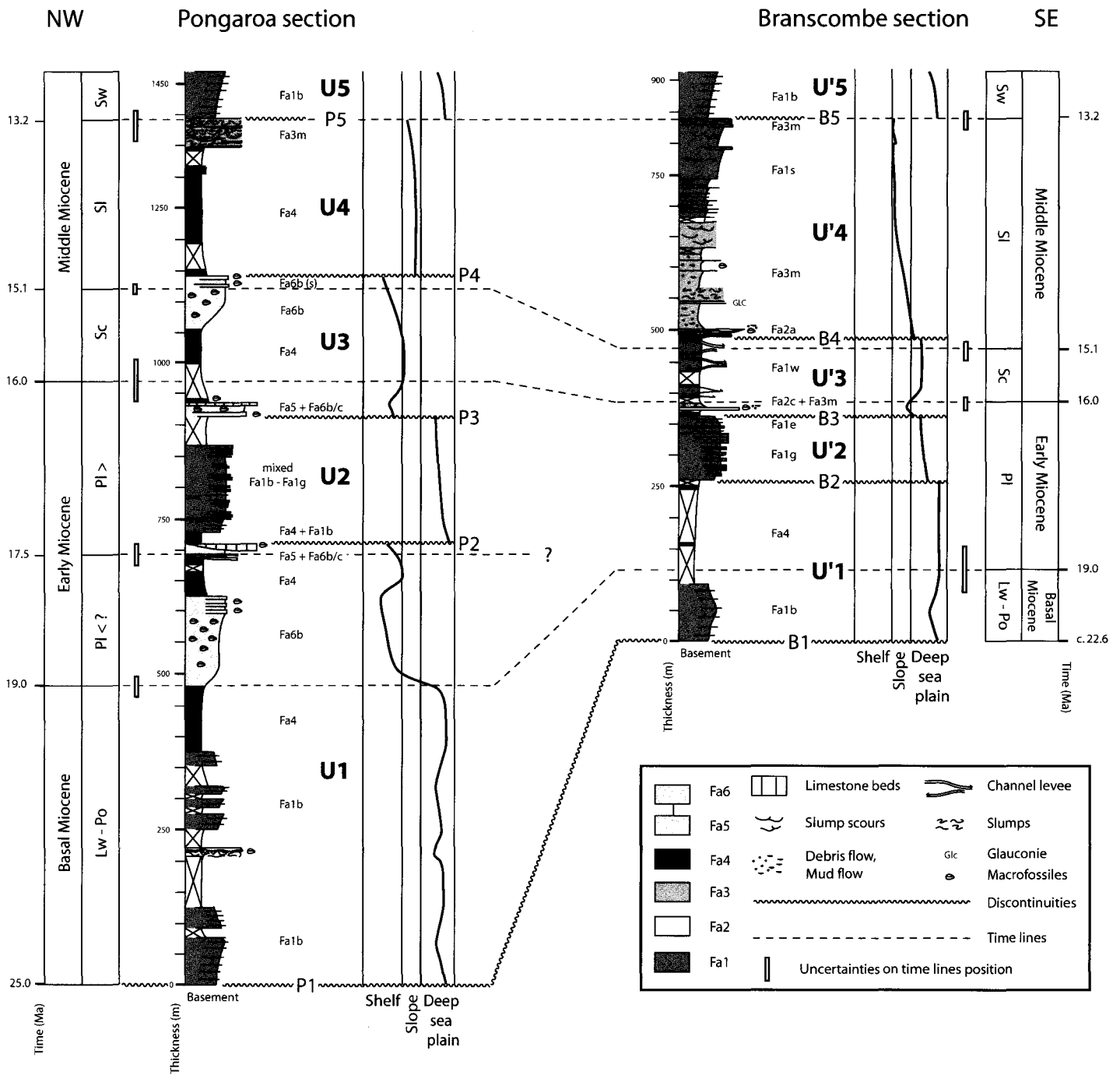


Fig.III-6. Time lines correlations of the Pongaroa and Branscombe sedimentological sections. B1-5, P1-5, U1-5 and U'1-5: see text. Refer to Fig.III-5 for location, Table III-1 and III-2 for facies code and Appendix 2 for datations.

VIII) STRATIGRAPHIC EVOLUTION OF THE AKITIO BASIN

A) Lithostratigraphy of the Akitio Basin

Sharp facies changes within the sedimentary series of the Akitio syncline mark five major sedimentary discontinuities which bound five main stratigraphic units for each section (Fig. III-6). The discontinuities and the main units are noted respectively P1 to P5, U1 to U5 for the Pongaroa section and B1 to B5, U'1 to U'5 for the Branscombe section.

1) Pongaroa section.

U1: This unit records progradation from a distal turbidite (Fa1b) to shelf (Fa5 - Fa6b/c - Fa4). The sediments can be subdivided into three sub-units (Fig. III-6). From oldest to youngest these are: (1) distal turbidites (Fa1b) deposited on a basin plain, and organized into a thickening-up then thinning-up section and punctuated at the top by slumps and megaturbidites; (2) the same facies as for sub-unit 1, but overlying the slumped strata; (3) a mixed carbonate and siliciclastic system with facies recording shallowing from bathyal to outer shelf settings. U1 thus contains two shallowing upward intervals, from mid-upper bathyal siltstones (Fa4) to outer shelf facies (Fa6b), across the transition from sub-unit 2 to sub-unit 3, and from upper bathyal siltstones (Fa4) to outer shelf facies (Fa5 - 6b/c) near the top of sub-unit 3. The lack of slumps and gullies suggests a low angle slope, perhaps a distally steepened ramp. The basal contact of U1 is an unconformity (P1) between the underlying Oligocene massive calcareous mudstones and U1 basal Miocene deep sea plain like turbidites (Fa1b).

U2: This unit consists of a turbidite sequence in which the beds thicken up-section (Fig. III-6). It comprises distal hemipelagic siltstones (Fa4) and distal turbidites (Fa1b) that evolve vertically to distal lobe facies (mixed Fa1b - Fa1g). The basal discontinuity (P2) shows the drowning of the mixed carbonaceous/siliciclastic outer shelf by distal basin plain, massive silty deposits (Fa4).

U3: This unit is characterized by outer shelf facies associations (Fa5 - Fa6b - Fa6c). U3 can be subdivided into three sequences (Fig. III-6): (1) a coarsening-up sequence showing the decrease of the siliciclastic input within a carbonated sequence on top of which pure algal limestone (Fa5) deposition occurs; (2) a fining-up sequence that includes shelly

(Terebratulidae) fine sands facies fining-up to upper bathyal – outermost shelf massive silty deposits (Fa4). This sequence shows an important decrease of the carbonated material; (3) a coarsening-up sequence characterized by a renewal of highly carbonated shelly sands (Fa6b) deposition. The shallowing-up trend is topped by a storm influenced shelf (Fa6b – s) on top of the sequence. U3 basal boundary corresponds to a sedimentary discontinuity (P3) with a sharp contact of outer shelf sediments (Fa5 + Fa6b/c) on U2 deep-sea turbidites.

U4: This unit is a coarsening-up sequence (Fig. III-6) which comprises massive silty hemipelagic deposits (Fa4) passing up to slope facies association (Fa3m). The slope facies is dominated by slumped turbidite strata and slump scours (headscarp erosional surfaces) intercalated within a fine grained silty matrix. The basal discontinuity of U4 (P4) marks the drowning of outer shelf facies (Fa6b – s) by upper bathyal silty sediments (Fa4).

U5: This unit comprises distal turbidites (Fa1b) on a deep sea plain-like sedimentary environment (Fig. III-6). These facies (Fa1b) are organized into a thickening-upward bed sequence. The sedimentary disruption from slope facies (Fa3m) to distal turbidites marks the U5 basal discontinuity (P5).

2) The Branscombe vertical section

U'1: This unit comprises a turbidite system that evolve from sandy distal turbiditic facies (Fa1b) to massive silty bathyal facies (Fa4). The extent of Fa4 is inferred partly from the Pongaroa section and partly on the basis that the poor outcrop is due to a lack of resistant sand beds. The distal turbidites (Fa1b) are organized into a thickening – thinning upward bed sequence. As for U1, the basal discontinuity for U'1 (B1) corresponds to the contact between Oligocene massive calcareous siltstones and the basal Miocene distal basin plain turbidites (Fa1b).

U'2: This unit is made up of a prograding turbidite system that can be subdivided into (1) a thickening upward bed depositional lobe sequence (Fa1g), and (2) a by-pass sequence (Fa1e). The U'2 basal contact is a sedimentary discontinuity (B2) that records renewed turbidite input to the basin, with deposition of lobe facies (Fa1g) over U'1 massive bathyal siltstones (Fa4).

U'3: As for U3, U'3 can be subdivided into three sequences: (1) a coarsening-up sequence characterized by debris-flows filled channels (Fa2c) and slope facies association (Fa3m) overlying silty deposits (Fa4); (2) a fining-up sequence which corresponds to the development

of a channel levee complex (Fa1w) that drowned the underlying slope deposits (Fa3m); (3) a coarsening-up channel levee complex (Fa1w). The U'3 basal discontinuity (B3) marks an important decrease in terrigenous input (prior to the renewal of turbidite deposition within the unit) compared to U'2. This decrease is characterized by the deposition of outer shelf to upper bathyal siltstones (Fa4) at the base of the unit.

U'4: This unit consists of a coarsening-up turbiditic sequence going from small channels (Fa2a) to slope facies (Fa3m) and sheet like turbidites (Fa1s). On top of this unit, intense syn-sedimentary deformation of the sheet like turbidites beds is observed. This facies is more sandy than the slope facies (Fa3m) identified in the Pongaroa section. U'4 basal contact (B4), marked by a distinctive channelized formation (Fa2a), corresponds to the transition between channel levee complex (Fa1w) and slope deposits (Fa3m).

U'5: This unit crops out in the axial part of the Akitio syncline and is therefore common to both sections (see U5 for details).

B) Biostratigraphy of the Akitio Basin

The New Zealand Fossil Record File has provided 45 foraminiferal age determinations for both sections (Appendix 2) using New Zealand biostratigraphic stages (Fig. III-6). Absolute ages used in this paper refer to the New Zealand Cretaceous-Cenozoic Timescale from Cooper *et al.* (2004). Four time lines are identified on both sections: the Waitakian/Otaian – Altonian boundary (19 Ma); the Altonian – Clifdenian boundary (16 Ma); the Clifdenian – Lillburnian boundary (15.1 Ma); and the Lillburnian – Waiauan boundary (13.2 Ma). The Altonian stage is divided in two sub-stages in the Pongaroa section and a time line marks the boundary between the early and late Altonian (*c.* 17.5 Ma) though this boundary could not be recognised at the Branscombe section.

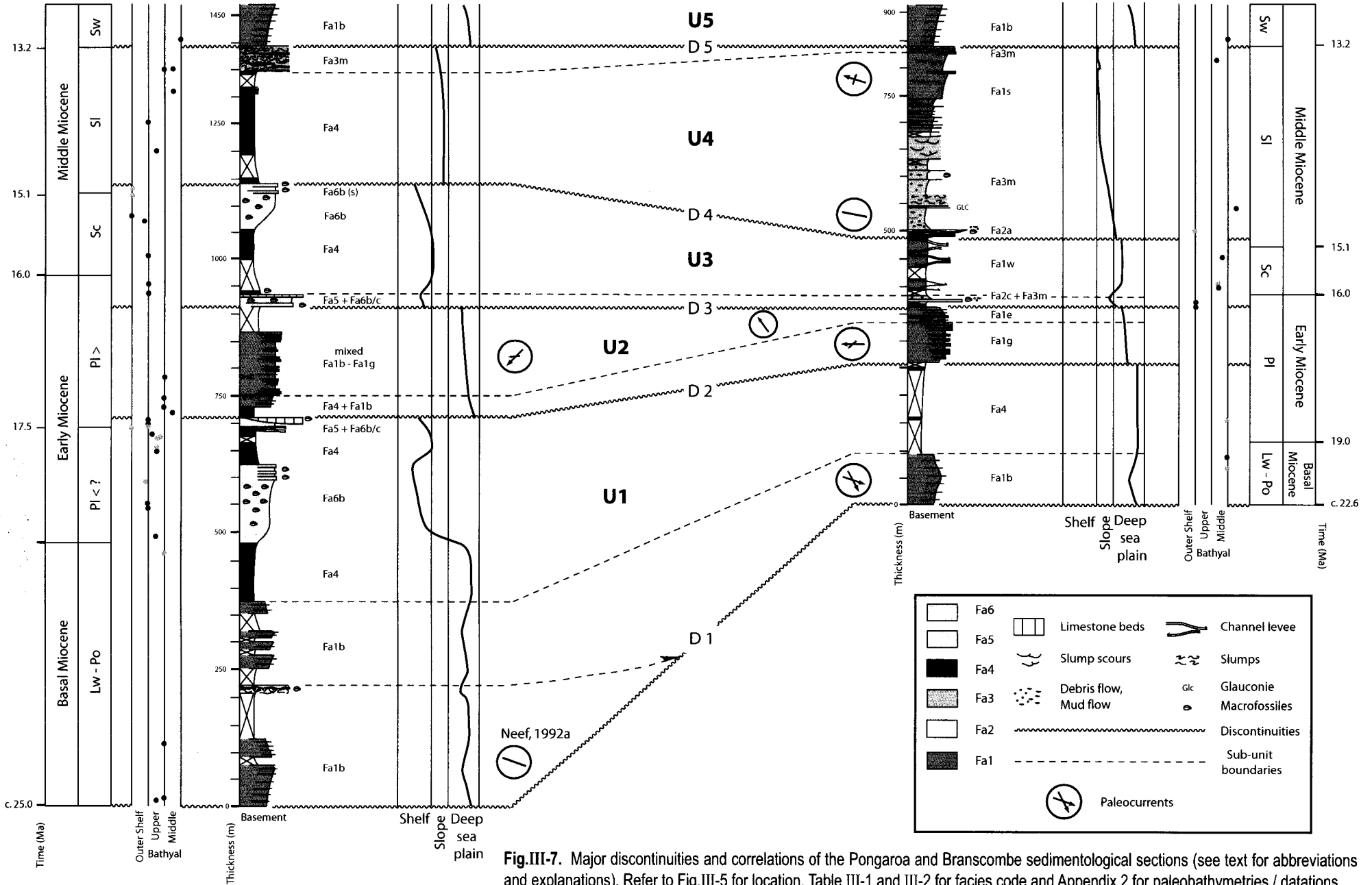


Fig.III-7. Major discontinuities and correlations of the Pongaroa and Branscombe sedimentological sections (see text for abbreviations and explanations). Refer to Fig.III-5 for location, Table III-1 and III-2 for facies code and Appendix 2 for paleobathymetries / datations.

XI) CORRELATIONS AND GEOMETRIC EVOLUTION OF THE AKITIO BASIN

Correlations are based firstly using biostratigraphy. Then, major discontinuities, identified by sharp facies changes, are dated and correlated. The main stratigraphic units between these discontinuities are then defined, subdivided and correlated. Using this approach, five dated sedimentary discontinuities are recognised at the basin scale (D1 to D5) and correspond, from base to top, to the correlations of P1 & B1 (D1, *c.* 25 Ma), P2 & B2 (D2, *c.* 17.5 Ma), P3 & B3 (D3, *c.* 16.5 Ma), P4 & B4 (D4, *c.* 15 Ma) and P5 & B5 (D5, *c.* 13.2 Ma). These discontinuities bound the five main stratigraphic units (U1 to U5) within the basal to middle Miocene series (Fig. III-7). In terms of duration, unit U1 represents 7.5 My (Waitakian/Otaian – early Altonian) whereas units U2, U3 and U4 represent 1 My (late Altonian), 1.5 My (latest Altonian – Clifdenian) and 1.8 My (Lillburnian) respectively. In the Pongaroa section, U1 can be divided in 3 sub-sequences which are of similar duration (*c.* 1 to 2 My) to the overlying stratigraphic units (U2, U3 and U4). U5 is restricted to the Waiau and its duration is unknown because the top of the unit is not seen in the study area.

A) U1: Waitakian/Otaian – Early Altonian (c. 25 – c. 17.5 Ma) – Southeastward prograding, mixed outer shelf/ramp

This unit records a progradation from fine-grained sandy deep-sea plain like turbidites (Fa1b) to mixed outer shelf/ramp facies (Fa5 - Fa6b/c - Fa4). U1 is delimited at its base by a discontinuity (D1), of basal Miocene age (*c.* 25 Ma), recording the onlap of the distal turbiditic system on the Oligocene passive margin deep sea sediments (middle bathyal calcareous mudstones). D1 is overlain by a wedge sub-unit on top of which disorganized facies associations are identified only to the northwest (Pongaroa section) suggesting the development of a southeastward facing paleoslope. This facies distribution is consistent with paleocurrent data from Neef (1992a) which indicate northwest to southeast feeding directions (Fig. III-7 and III-8 – stage 1). The second distal turbiditic sub-unit is the most extensive and homogeneous at the basin scale in the whole transect. Our paleocurrent measurements indicate flow to the southeast (Fig. III-7 and III-8 – stage 1). As well as the U1 progradational trend, the presence of the mixed outer shelf/ramp system in the third sub-unit to the northwest confirms that the sedimentary setting for U1 is likely to comprise a paleoslope to the southeast. The lateral thickness change within U1, which is less preserved to the southeast, is consistent with decreasing sedimentation rates due to increasing distality to the southeast. It can be explained by the progradation of the sedimentary system from northwest to southeast.

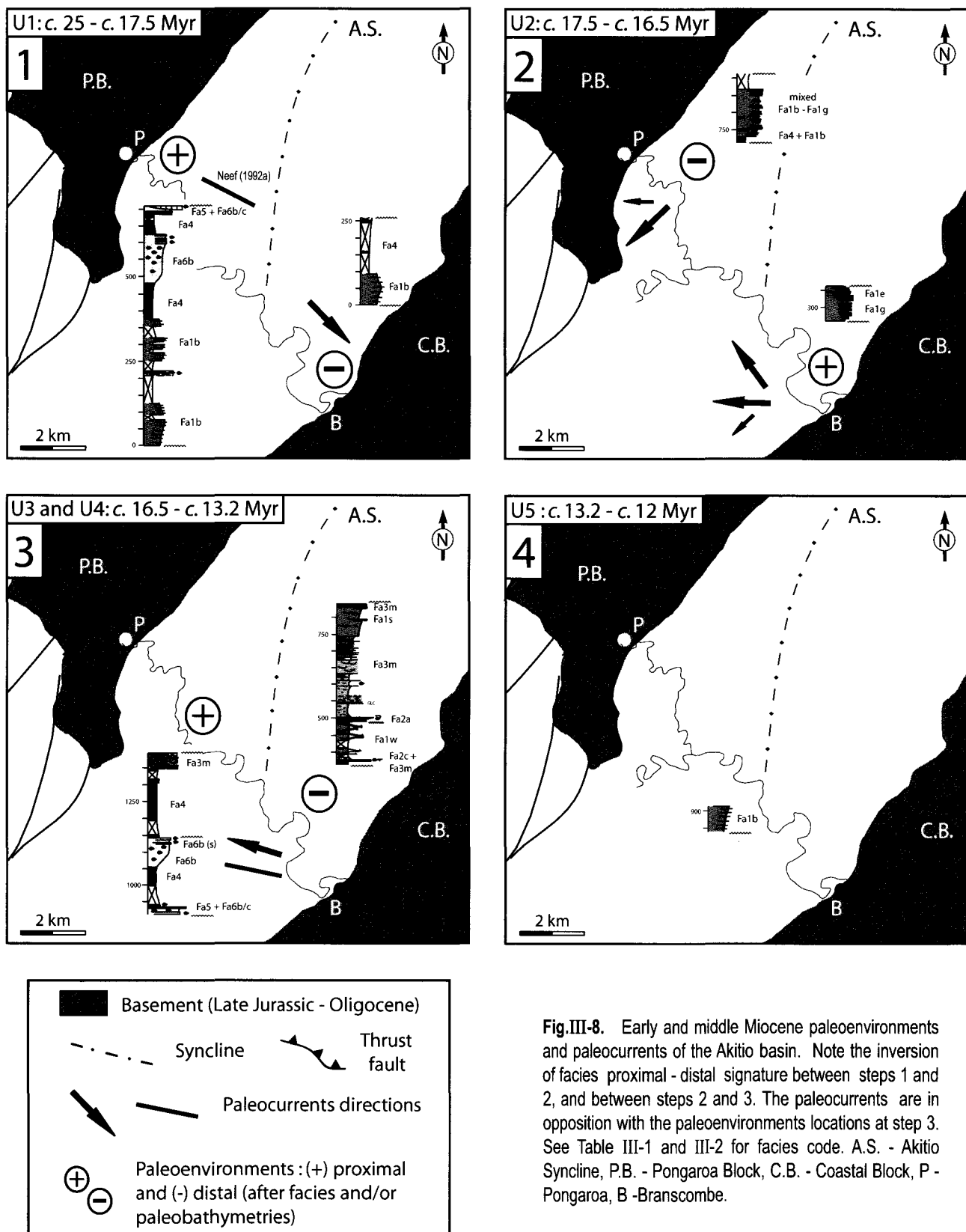


Fig.III-8. Early and middle Miocene paleoenvironments and paleocurrents of the Akitio basin. Note the inversion of facies proximal - distal signature between steps 1 and 2, and between steps 2 and 3. The paleocurrents are in opposition with the paleoenvironments locations at step 3. See Table III-1 and III-2 for facies code. A.S. - Akitio Syncline, P.B. - Pongaroa Block, C.B. - Coastal Block, P - Pongaroa, B - Branscombe.

B) U2 : Late Altonian (c. 17.5 – c. 16.5 Ma) - Westward prograding turbidite system

Unit U2 consists of a westward prograding turbidite system, reflecting a major change in the paleogeographic trend compared to the underlying unit (Fig. III-7 and III-8 – stage 2). The basal discontinuity (D2) records sudden development of the turbidite system in both sections with an important deepening to the northwest. As said previously, U2 has two components: (1) a thickening upward bed depositional lobe (Fa1g) thinning northwestward to more distal hemipelagic siltstones (Fa4) and deep sea plain like facies (Fa1b); (2) a by-pass (Fa1e) sequence thickening northwestward and passing through well preserved thickening upward bed distal lobe (mixed Fa1b - Fa1g). This partitioning of the sedimentary volumes is consistent with paleocurrent data, which indicates flow mainly toward the west. Thus this unit marks a major inversion of the paleogeography, with a westward shifting of facies (Fig. III-8 – stage 2). This indicates the presence of a bathymetric high to the east leading to the development of sediment sources that fed the basin via a westward paleoslope.

C) U3: Latest Altonian - Clifdenian (c. 16.5 – c. 15 Ma) - Disconnected outer shelf/westward prograding turbidite system

This unit shows disconnected sedimentary systems on both sides of the syncline. To the northwest, D3 records abrupt shallowing with a sharp transition to a mixed carbonated/siliciclastic shelf (Fa5 + Fa6b/c). To the southeast, the significant reduction in turbidites and deposition of massive siltstones (Fa4), can not be assessed in terms of paleobathymetry because of the lack of micropaleontological data within the underlying unit (U2). However, the appearance of slope facies (Fa3m) on top of the U3 basal silty interval favours a slight shallowing at D3. As seen previously, this unit is characterized by the sharp transition to a shelf setting in the Pongaroa section (Fig. III-7). This shelf seems to be disconnected from the southeastern turbidite system (dominated by a well developed channel levee complex) which was more likely fed from the east because of the broad continuity of the turbidite system (Fig. III-8 – stage 3). At D3, the development of a shelf, in the Pongaroa section, indicates the presence of a submarine high to the west of the Akitio syncline area. In the Branscombe section, the continuation of the westward progradation of the turbidite system suggests that the eastern submarine high, appeared at D2, still exist at that time. This shows the containment of an individual sedimentary basin, confined to the Akitio syncline area, called here the Akitio basin. During U3, three subdivisions of similar significance are recognised in both sections on the shelf as well as in the basin, despite the partitioning of the

sedimentary inputs. This suggests that the internal stratigraphic subdivisions of U3 are more likely related to regional tectonic or eustatic variations than to a local tectonic event (*e.g.* individual fault development or local folding).

D) U4: Lillburnian (c. 15 – c. 13.2 Ma) – Disconnected aggrading silty system/westward prograding turbidite system

As for U3, this unit has apparently disconnected facies associations on both sides of the Akitio syncline. On the southeastern limb, the U2 – U3 turbidite system is still active and did not extend to the massive silty facies (Fa4) observed on the northwestern limb (Fig. III-7 and III-8 – stage 3). On top of U4, similar facies in both sections suggests that the two sedimentary systems are connected again. The U4 basal contact is a discontinuity (D4) which has different characteristics on either side of the syncline (Fig. III-7). In the Pongaroa section, D4 corresponds to a rapid deepening with the appearance of upper bathyal silty facies (Fa4) over an outer shelf facies (Fa6b – s). In the Branscombe section, D4 is laterally correlated with the base of a channelized formation (Fa2a) suggesting a slight shallowing compared to U3. The Branscombe section comprises turbidites which are increasingly proximal through the top of U4. Despite this trend and measured paleocurrents toward the west-northwest (Fig. III-8 – stage 3), no prograding geometry is observed at the basin scale. Indeed, the Pongaroa section comprises hemipelagic deposits of massive siltstones (Fa4) at this time, with no sandy turbidites despite the continuation of the active turbidite system to the southeast. This aggrading sequence suggests that the Pongaroa section still marks the northwestern margin of the basin during deposition of the lower part of U4 (Fig. III-8 – stage 3). Moreover, U4 shows an increase in accommodation space contemporaneously with significant sedimentary flux. Terrigenous input is high enough to partly fill the basin, as observed in the Branscombe section. In the Pongaroa section, our estimates of paleobathymetry indicate a progressive deepening of water depth. All these observations means that the ratio accommodation: sedimentary flux is $0 < a/s < 1$ for the Branscombe section and $a/s > 1$ for the Pongaroa section. This signifies the onset of a period of increased subsidence affecting the basin and its edges.

On top of U4, the unit coarsens up to slope facies association (Fa3m). The simultaneous deposition of slope facies (Fa3m) in both sections suggests that the two sedimentary systems become connected again during an important slope destabilization episode. This episode may record an acceleration of basin subsidence.

E) U5: Waiauan (c. 13.2 – c. 12 Ma) – Deep sea plain like

This unit comprises deep sea plain like turbidites (Fa1b). The basal discontinuity (D5) over the underlying turbidite system marks a sharp deepening. This is confirmed by foraminiferal paleobathymetric data which indicate much deeper water depths (mid to lower bathyal) compared to the underlying unit (mid to upper bathyal; Fig. III-7). This deepening is consistent with an acceleration of basin subsidence around D5 as inferred by the slope destabilization episode identified on top of U4.

X) DISCUSSION

A) Turbidite systems and facies model within trench-slope basins

Most of field observations on ancient analogues of mature trench-slope basins show the development of deep sea fan at the canyon mouths (*e.g.* Smith *et al.*, 1979, Moore *et al.*, 1980, Turnbull, 1988). These results contrast with seismic surveys that suggest non-channelized sheet-like turbidites deposition rather than well-organized turbidite system development (Underwood and Moore, 1995) as described by Mutti and Normark (1987). Nevertheless, Stevens and Moore (1985) report, from seismic data, a possible submarine fan within a modern trench-slope basin in the western Sunda accretionary system. Moreover, except Neef (1992a) and Van der Lingen (1980, 1982), who considers these basins too small for submarine fan systems to develop, most of authors propose the existence of submarine fan facies associations from field analogues. Facies associations are generally described from the facies terminology of Mutti and Ricci Lucchi (1978) and are attributed to canyon, inner fan, middle fan, outer fan and basin plain depositional settings (*e.g.* Moore *et al.*, 1980; Turnbull, 1988). In trench-slope basins of central California, Smith *et al.* (1979) also report the settlement of a suprafan (Normark, 1970) that results from rapid deposition of coarse-grained sediments. Other described gravity system consists in channelized base-of-slope aprons identified within early Cretaceous trench-slope basins of the North Island of New Zealand (George, 1992). Nevertheless, the characterization of trench-slope basins turbidite systems from field analogues remains questionable as suggests by the rarity of well developed submarine fans offshore and because most of the field observations were carried out before the recent developments on turbiditic facies and on turbidite systems.

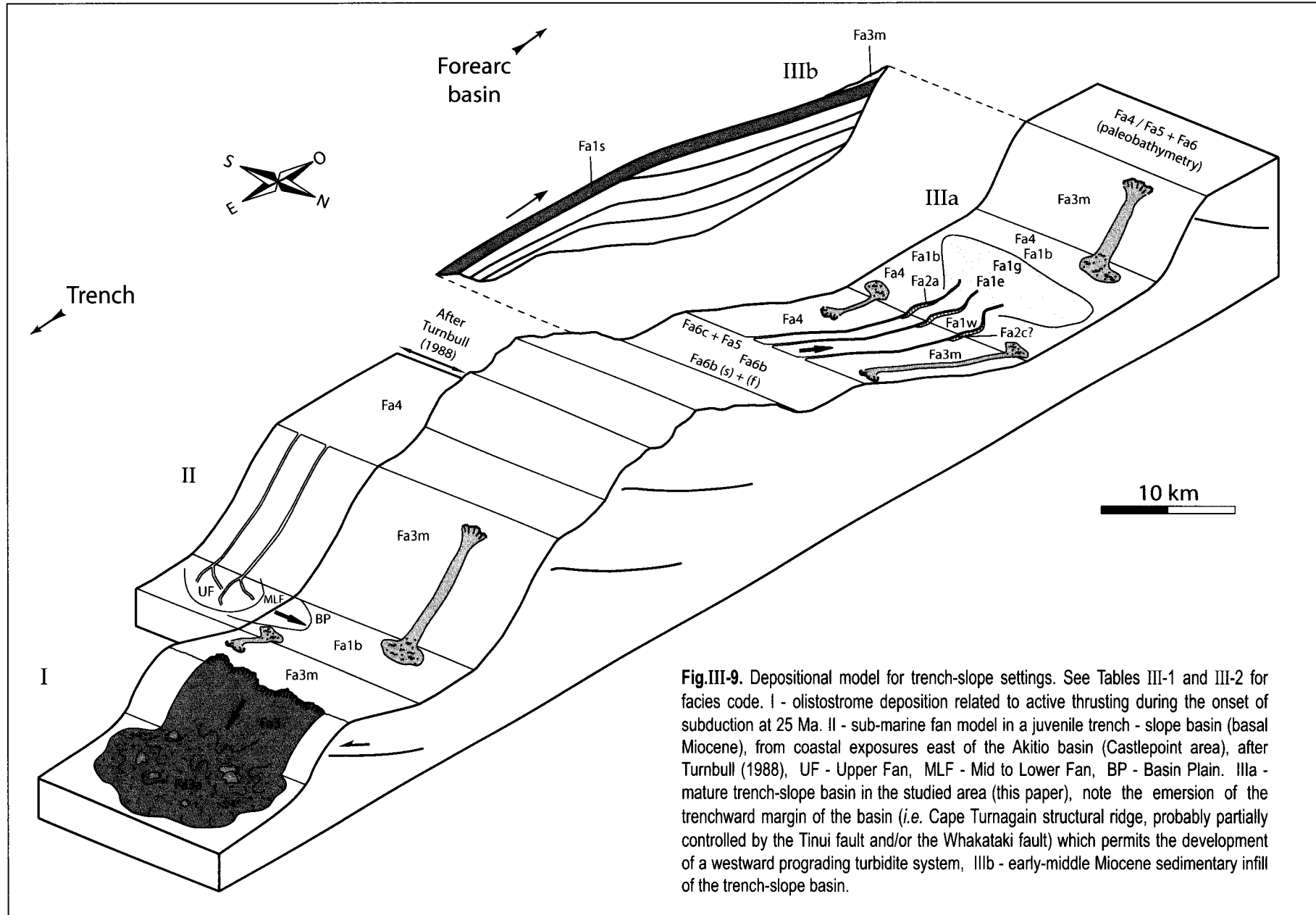


Fig.III-9. Depositional model for trench-slope settings. See Tables III-1 and III-2 for facies code. I - olistostrome deposition related to active thrusting during the onset of subduction at 25 Ma. II - sub-marine fan model in a juvenile trench - slope basin (basal Miocene), from coastal exposures east of the Akitio basin (Castlepoint area), after Turnbull (1988), UF - Upper Fan, MLF - Mid to Lower Fan, BP - Basin Plain. IIIa - mature trench-slope basin in the studied area (this paper), note the emersion of the trenchward margin of the basin (*i.e.* Cape Turnagain structural ridge, probably partially controlled by the Tinui fault and/or the Whakataki fault) which permits the development of a westward prograding turbidite system, IIIb - early-middle Miocene sedimentary infill of the trench-slope basin.

In the Akitio basin, between D2 and D5, the Branscombe section shows the westward deposition of turbidites and related deep sea sediments, in a mature slope basin (Fig. III-7). These turbidite systems rework some fine grained siliciclastic material coming from the erosion of an ancient accretionary prism (Ferrière, 1987), late Jurassic to early Cretaceous in age, and of the bathyal part of a relatively inactive margin (Karig, 1982; Chanier, 1991), late Cretaceous to Oligocene in age. Therefore, the deep sea facies deposited within the Miocene Akitio trench slope basin are generally very fine grained whatever the energy of transport. Because of this particularity, a new facies model (Table III-1 and III-2), taking into account the recent knowledge on turbiditic facies, has been applied in this study rather than the facies terminology of Mutti and Ricci Lucchi (1978).

In the study area, Neef (1992a) identified two turbidite formations (Greenhollows and Tanawa Formations) and described them on the basis of Pickering *et al.* (1989) nomenclature. According to Neef (1992a), the Greenhollows Formation (U2) results from unconfined sheet flow on a submarine ramp feeder system (as defined by Heller and Dickinson, 1985) and the Tanawa Formation (U3 to U5) represents a multiple source slope feeder system (as defined by Reading, 1991). We demonstrate that, between D2 and D5, three units (U2 to U4) are identified and can be characterized in term of sequence stratigraphy by their main facies associations (Fig. III-7). Rather than a submarine ramp, U2 shows the development of a basin floor fan, with deposition of sandy fine grain depositional lobes (morphologic component defined by Mutti and Ricchi Lucci, 1978; Fa1g in this paper) that evolve to by-pass facies (interpreted as a channel-lobe transition; Fa1e). U3 mainly comprises a channel levee complex (Fa1w) that we interpret as a slope fan. Finally, U4 represents a prograding wedge complex (Fa3m + Fa1s), characterized by the drowning of the basin floor fan and the slope fan by progradation of a slope (Fa3m). This interpretation suggests that the overall turbidite mega-sequence constitutes a lowstand system tract (Posamentier *et al.*, 1988). The prograding wedge complex also comprises sheet like turbidites (Fa1s) which result from distal unconfined turbidity currents. These facies were probably deposited on a low gradient submarine ramp developed on top of the prograding slope during a late stage of basin fill (Fig. III-9). The last facies observed on top of the mega-sequence consist of sheet like turbidite slumped strata (Fa3m). This may illustrates the end of the basin filling up history by syn-depositional deformation of sheet-like turbidite beds in a very restricted sedimentation area (Fig. III-9).

Thus, in the Branscombe section, we interpret the turbidite series between D2 and D5 as comprising two main types of depositional system constituting a filling up mega-sequence.

The first one presents the main morphologic components of deep sea fan depositional systems (Fig. III-9). The westward thinning from depositional lobe (Fa1g, Branscombe section) to massive siltstones (Fa4, Pongaroa section) and distal turbidites (Fa1b, Pongaroa section) shows that the lobes may be distally, and maybe laterally, associated with distal basin plain deposits (Fa4 + Fa1b). Mapping of lobe facies (Fa1g) indicates that their extent may reach several tens of kilometres laterally and around ten kilometres distally in the basin. This indicates that lobes have an elongated geometry, sub-parallel to the basin margins (Fig. III-9). In the Branscombe section, paleocurrents in lobe facies (Fa1g) are not longitudinal, as inferred in such an elongated lobe, but radial (Fig. III-8 – stage 2). This suggests that the studied section was located in close proximity of the feeder system. Other morphologic components observed in the Branscombe section are channel levee complex (Fa1w), small channels (Fa2a + Fa2c), and a mud-rich slope (Fa3m) (Fig. III-9). The presence of both levees (Fa1w) and well developed lobes (Fa1g) as well as the size and location of the system suggests a fine grained sand-rich submarine fan (Reading and Richards, 1994; Richards *et al.*, 1998). However, difficulties in reconstructing the geometries and identifying the feeder system in the field did not allow us to go further toward the characterization of the turbidite system.

The second depositional system is a low gradient submarine ramp developed on top of the previous prograding turbidite system during a late stage of the basin filling up (Fig. III-9). These observations show that both small scale submarine fan and submarine ramp systems may develop within the same trench-slope basin. Moreover, the analysis of the Branscombe filling up mega-sequence suggests that submarine ramp systems more likely settle in a late stage of the basin development.

Elsewhere in the Coastal Ranges, olistostrome deposits (Fa3a) have been identified at the base of the Whakataki Formation (*c.* 25 Ma). These facies, which record significant submarine reworking, result from large submarine slides with deposition of highly disorganized facies association at the bases of slopes (Fig. III-9). This depositional system is inferred to result from active thrust faulting during nappes emplacement episodes (Chanier and Ferrière, 1991). This suggests that olistostromal systems are active preferentially during the early stages of the trench-slope basins development.

B) Tectonic Control on turbidite systems

As seen previously, the overall Branscombe filling up mega-sequence comprises four discontinuities (D2 to D5). Correlations to eustatic curves (Hardenbol *et al.*, 1998) and mainly the amplitude and the rapidity of bathymetric and/or facies changes suggest that these discontinuities are more likely related to tectonic activity than to global sea-level changes. Indeed, D4 marks a rapid deepening at *c.* 15 Ma (Fig. III-7) and may be related to the onset of the widespread subsidence (*c.* 15 – 5 Ma) attributed to a period of tectonic erosion over the whole margin (Fig. III-4; Chanier *et al.*, 1999). D2, D3 and D5 don't seem to be correlated either to a global sea-level change nor to a major tectonic event affecting the whole margin. However, D2 leads to 1) a reversion of the paleocurrents, 2) an important inversion in facies distal/proximal signature within the basin, and 3) a northwestward increase of accommodation (Fig. III-7 and III-8 – stage 2). This demonstrates that D2 is of tectonic origin and can be related to a local uplift that occurred to the east of the studied area. An inversion in facies distal/proximal signature is also observed at D3 and is accompanied by an abrupt shallowing in the Pongaroa section (Fig. III-7 and III-8 – stage 3). This event marks a rapid uplift localized within the western part of the basin. Finally, D5 records a rapid deepening that is also observed elsewhere on the margin (*i.e.* Cape Turnagain; Fig. III-5). It may records acceleration of subsidence during the extensional deformation episode (*c.* 15 – 5 Ma).

None of these tectonic events is contemporaneous with the transition between the two different sedimentary systems identified within the Branscombe basin-fill mega-sequence (Fig. III-7). This suggests that, in the studied basin, the evolution from one type of turbidite system to another (*i.e.* deep sea fan vs sheet-like turbidites) is not only controlled by tectonism. However, tectonic events clearly lead to slope creations which may cause: 1) inversions of the vergence of the sedimentary systems as illustrate by the paleogeographic change at D2 (Fig. III-8 – stage 2); and 2) modifications of the turbiditic facies as suggests by the facies disruptions within the turbidite system at each discontinuity (Fig. III-7).

Moreover, this study shows that tectonic processes may control the timing of the evolution of a lowstand system tract. Indeed, the Branscombe basin floor fan developed originally above D2 in response to a tectonic event creating new sediment sources to the west of the study area (Fig. III-7 and III-8 – stage 2). As this turbidite succession is inferred to be a lowstand systems tract, it is not consistent with global sea level variations at this time (Hardenbol *et al.*, 1998) *i.e.* sea-level rise (lower lowstand) during the settlement of basin

floor fan and slope fan, and sea-level fall (upper lowstand) during development of the prograding wedge complex. However, the basal boundaries of the slope fan and of the prograding wedge complex are sharp and contemporaneous with D3 and D4 respectively (Fig. III-7). These discontinuities are well expressed at the basin scale. Indeed, both discontinuities are also recorded in the Pongaroa section in sedimentary environments different than those of the Branscombe section (Fig. III-7). D3 marks a rapid uplift characterized by the development of a carbonate-capped submarine high while D4 corresponds to its abrupt drowning. All these observations mean that **1)** the evolution of the turbidite system follows the ratio subsidence/regional sedimentary flux, but **2)** the timing of settlement of the sedimentary bodies that composed the lowstand system tract is controlled by local tectonic events related to structural development of the confined Akitio trench-slope basin.

C) Structural and stratigraphic evolution of the Akitio basin and regional structural history

Our analysis of the vertical and lateral distribution of facies demonstrates that sedimentation processes within the Akitio basin are strongly controlled by tectonic activity (which mainly controls the accommodation and the geometry of the basin borders). The Akitio basin has undergone several tectonic events that have constrained its asymmetric paleogeography. This results from the development of structural highs and their effects on paleoslopes. These important paleogeographic changes (Fig. III-8) are characterized by particular stratal discontinuities (Fig. III-7) which reflect the tectonic development of the area.

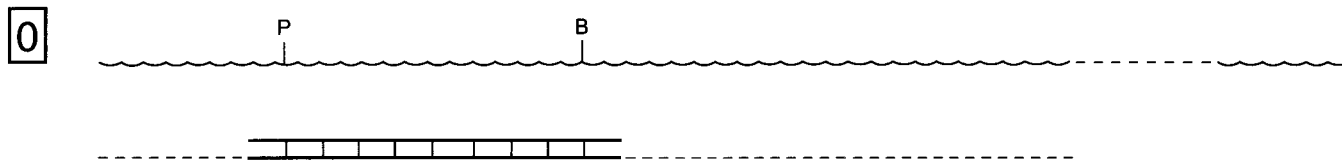
Prior to the onset of subduction, during the Oligocene, hemipelagic deposition of calcareous mudstones occurred on a bathyal plain (fig. III-10 – stage 0). Then, D1 is characterized by an abrupt increase in terrigenous input on the Oligocene passive margin (Fig. III-7). This discontinuity over the pre-Miocene basement is observed all along the East Coast and is contemporaneous with the onset of subduction (Fig. III-4; *c.* 25 Ma). U1 is characterized by the southeastward progressive progradation of a mixed siliciclastic–carbonate shelf during basal Miocene times (Fig. III-10 – stage 1). This can be related to the nappe emplacement episode identified by Chanier and Ferrière (1989, 1991; Fig. III-4). East of the Coastal Block, early stages of this first compressional episode are also accompanied by deposition of olistostromes (Fa3a). These facies are inferred to result from important submarine reworking related to active thrust faulting (Fig. III-9). This tectonism of the margin continued during deposition of U1 as suggested by the slumps and debris-flows in the

Pongaroa section (on top of U1 sub-unit 1) which traduce slope rejuvenation (Fig. III-7). A significant change in the sedimentary system occurred on top of U1 (U1 sub-unit 3) with a decrease in siliciclastic input within the distal basin plain associated to an increase in accommodation and carbonate production on the shelf (Fig. III-7). This produced the slightly progradational aggradation of the shelf (U1 sub-unit 3). This may be explained by a sea-level rise or by subsidence of the shelf. Indeed, both hypotheses suggest a decrease in tectonic activity during earliest Altonian (*c.* 19 – *c.* 17.5 Ma).

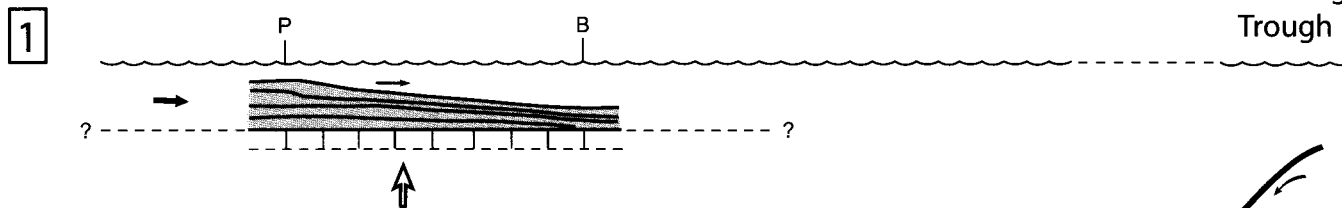
D2 records a major uplift that occurred to the east of the Akitio syncline area with the development of a structural high that probably resulted from a growing anticline associated with thrust faulting (Fig. III-10 – stage 2). This local tectonic event caused subsidence in the northwestern part of the area and led to a reversion of the sedimentary feeding directions within the depositional domain (Fig. III-8 – stage 2). U2 (late Altonian, *c.* 17.5 – *c.* 16.5 Ma) shows the establishment of an eastward fed turbidite system (basin floor fan), characterized by high siliciclastic input (Fig. III-7). At Cape Turnagain, the Waiuan series lie unconformably on the Oligocene marls and limestones. The late Altonian uplift in this area probably led to erosion of thick early Altonian and basal Miocene sedimentary series. To the west of Cape Turnagain, in the eastern limb of the Fingerpost syncline (Fig. III-5), algae limestone facies (Fa5), resting on top of Eocene formation, indicates that a shelf lay along the western border of the structural high. These observations suggest that the structural ridge was emergent during late Altonian with an onshore area probably located in the southward (or southwestward) continuity of Cape Turnagain (Fig. III-5). At that time, the western margin of the basin was located to the west of the Pongaroa block and its nature remains unclear.

D3 corresponds to an uplift of the western part of the basin which is responsible for important changes in the basin geometry (Fig. III-10 – stage 3). This uplift can be attributed to the growing of a local tectonic structure (*e.g.* anticline or out-of-sequence thrusting). Nevertheless, the tectonic event at D3 is responsible for the strong containment of the Akitio basin between two structural highs (Fig. III-10 – stage 3). Our reconstruction of the basin geometry shows that subsidence rates probably increase in close proximity of the western margin of the basin. U3 (latest Altonian – Clifdenian, *c.* 16.5 – *c.* 15 Ma) records the development of an outer shelf over basin floor fan facies association (Fig. III-7). Our paleocurrent data shows the Akitio basin was still dominantly fed from the east (Fig. III-8 – stage 3). Following disruption due to uplift with slopes modifications, the turbidite system evolved into a slope fan (Fig. III-7).

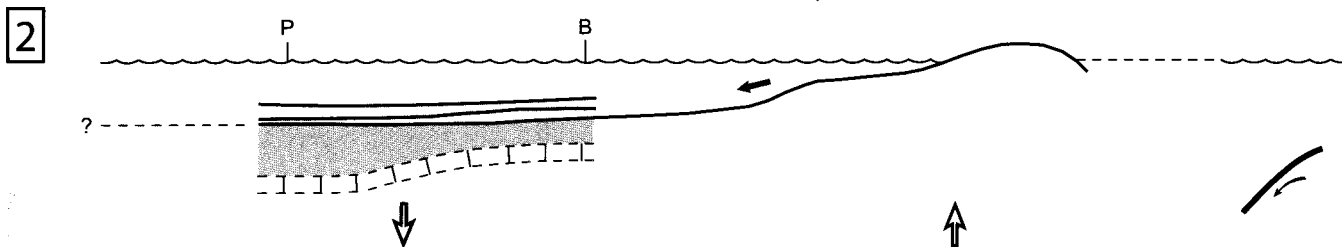
Oligocene (c. 27 Myr)



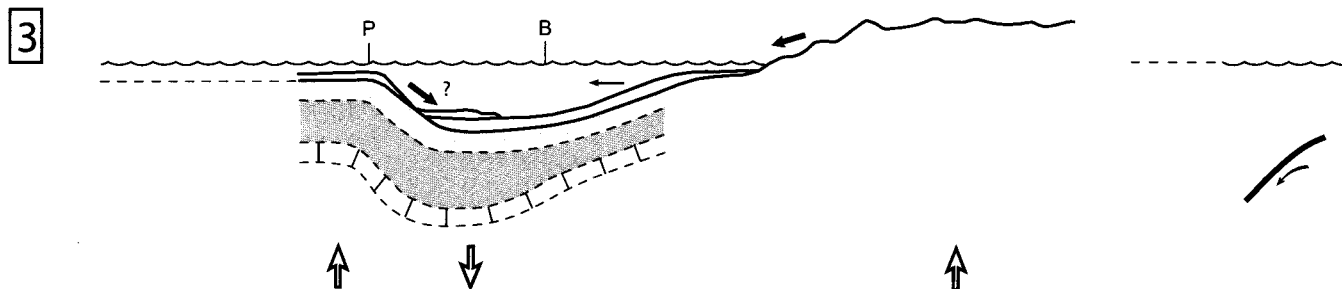
U1: Lw-Po/Early PI (c. 25 - c. 17.5 Myr)



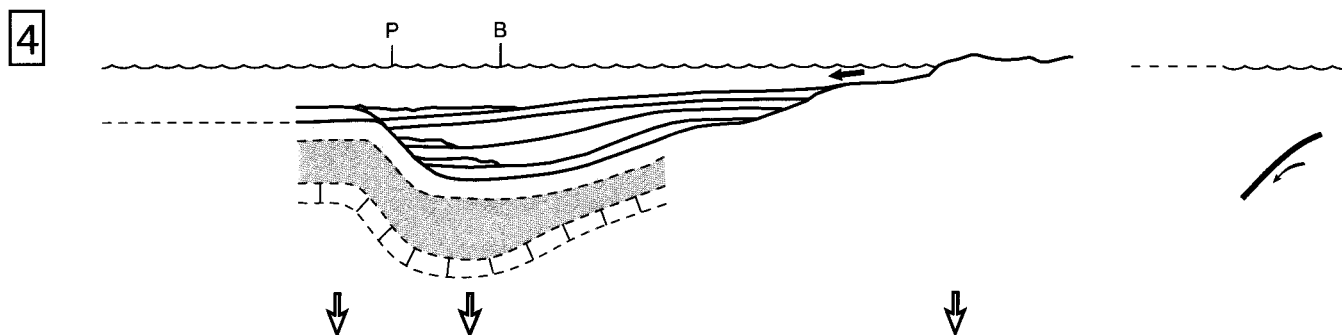
U2: Late PI (c. 17.5 - c. 16.5 Myr)



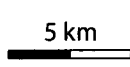
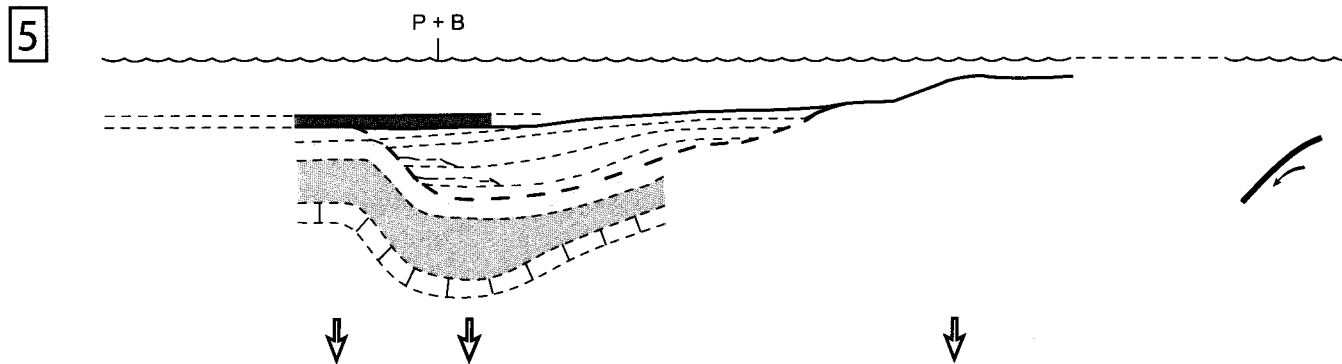
U3: Latest PI/Sc (c. 16.5 - c. 15 Myr)



U4: SI (c. 15 - c. 13.2 Myr)



U5: Sw (c. 13.2 - c. 12 Myr)



← Feeding directions
 ↑ ↓ Uplift / Subsidence

Fig.III-10. Stages of development of the Akitio trench-slope basin. Stage numbers also correspond to the five stratigraphic units identified in this study (comments in text). P - Pongaroa vertical section, B - Branscombe vertical section.

D4 is defined by a major deepening contemporaneous with the beginning of widespread subsidence over the whole margin (*c.* 15 – 5 Myr). This subsidence episode has been attributed to a period of tectonic erosion (Fig. III-4; Chanier *et al.*, 1999). Nevertheless, at this time, the uplift of the structural edges of the Akitio basin has stopped. U4 (Lillburnian, *c.* 15 – *c.* 13.2 Ma) consists of the progressive filling of the Akitio basin by siliciclastics derived from the eastern edge of the basin (Fig. III-10 – stage 4). The westward progradation of the turbidite system (Fig. III-8 – stage 3) led to a change in depositional system, signalled by the appearance of sheet-like turbidites (Fa1s) derived from unconfined turbidity currents (Fig. III-7 and III-9). In the Pongaroa section, Fa4 hemipelagic deposition (Fig. III-7) suggests that the western structural high was still a paleohigh, isolated from the eastern sediment source, at least during most of Lillburnian stage (Fig. III-10 – stage 4). The slope facies association (Fa3m) on top of the basin-fill mega-sequence are the last sediments ponded in the Akitio trench-slope basin (Fig. III-9 and III-10).



D5, following this period of basin infill, precedes a major change in the depositional setting that is accompanied by abrupt deepening (Fig. III-10 – stage 5). U5 (early Waiauan, *c.* 13.2 - 12 Ma) corresponds to the deposition of distal turbidites (Fa1b) on a basin plain (Fig. III-7). At Cape Turnagain (Fig. III-5), the unconformable deposition of Waiauan upper bathyal – outer shelf siltstones (Fa4) over the Oligocene indicates a re-drowning of the eastern structural high (Fig. III-10 – stage 5). These observations suggest a continuation of subsidence over the active margin during the Waiauan, maybe with an acceleration at D5. For this period, sediment sources are quite difficult to identify because of a lack of paleocurrent data.

Therefore, the earliest stage (D1, U1) of the high resolution sedimentologic evolution of the Akitio area is consistent with all the previous hypothesis on the margin development that infer an early major shortening event with thrust faulting and/or nappe emplacement accompanying the onset of subduction, 25 My ago (Pettinga, 1982; Van der Lingen, 1982; Chanier and Ferrière, 1989, 1991; Rait *et al.*, 1991; Delteil *et al.*, 1996; Field, Uruski *et al.*, 1997). Our study shows that D2 and D3 may be attributed to local tectonic deformation (growing folds, thrust or reverse faulting) leading to the containment of the Akitio trench-slope basin in the latest Altonian (*c.* 16.5 Ma). Basin tectonism is consistent with a compressional episode subsequent to the onset of subduction, as described by Chanier and Ferrière (1989, 1991) and Rait *et al.* (1991). Finally, the hypothesis of an extensional episode

affecting the whole margin after the first compressional episode (Chanier *et al.*, 1999) is favoured by D4 and D5 which are characterized by subsidence of the Akitio basin and its borders.

ACKNOWLEDGEMENTS

We gratefully acknowledge Geoffroy Mahieux and Christophe Buret for their work during field trips as well as for our numerous discussions on field. We are indebted to Alan Beu and Hugh Morgans, who have dated respectively the macrofossils and foraminifera that we have sampled on field. Thanks also go to Colin North, Michael Underwood, Gregory Moore and an anonymous reviewer for their comments and suggestions. Without the technical support and the free access to the New Zealand Fossil Record File given by the Institute of Geological and Nuclear Sciences (Lower Hutt, New Zealand), this work could not have been possible. We also thank Jean-Christophe Embry for its help in shelf facies analysis. A special thank to Pauline and George Wardle, and their sons, for their friendship, their helpfulness and their warm welcome, for weeks during three years, at Glenross lodge.

This research was supported in part by the BQR PhD student mobility program of the Université des Sciences et Technologies de Lille 1. Other funding supports has come from the program about active margin of the french research group GDR marges, from the French Embassy in New Zealand, and from New Zealand government FRST contract CO5X002.

Chapitre IV

Structure et stratigraphie sismique d'un bassin perché immergé, comparaison avec un analogue de terrain (marge active Hikurangi, Nouvelle-Zélande)

Keywords: trench-slope basins, seismic stratigraphy, subduction wedge, subduction, Hikurangi margin, New Zealand.

Mots clefs: bassins perchés, stratigraphie sismique, prisme de subduction, subduction, marge Hikurangi, Nouvelle-Zélande.

Structure and seismic stratigraphy of an offshore trench-slope basin, comparison with a field analogue (Hikurangi subduction margin, New Zealand)

Julien Bailleul⁽¹⁾, Frank Chanier⁽¹⁾, Christian Gorini⁽¹⁾, Geoffroy Mahieux⁽²⁾,
Cécile Robin⁽³⁾, and Jacky Ferrière⁽¹⁾

¹ UMR CNRS 8110, Processus et Bilan des Domaines Sédimentaires, Université des Sciences et Technologies de Lille1, France

e-mail : julien.bailleul@ed.univ-lille1.fr

² UMR CNRS 4110, Processus et Bilan des Domaines Sédimentaires, Université de Haute-Picardie, Amiens, France

³ UMR CNRS 4661, Géosciences Rennes, Université de Rennes 1, France

ABSTRACT

The tectonic of the North Island of New Zealand is dominated since 25 Myr by the oblique westward subduction of the Pacific plate. The detailed structural analysis of the emerged part of the margin suggests a succession of major tectonic events rather than an homogeneous continuous deformation since the onset of subduction. Contemporaneously, trench-slope basins have developed on the subduction wedge. These basins are structurally controlled and, therefore, their sedimentary infill has recorded regional or local deformational episodes. In this particular setting, the close interactions between deformational processes and basin development, particularly modalities of tectonic control on sedimentary processes and on basin stratigraphic evolution, may be accurately studied. Compilation of seismic stratigraphic and wireline logs (gamma ray and sonic) data, combined with lithostratigraphic and biostratigraphic data obtained from well Titihaoa-1, allows a detailed stratigraphic analysis of the offshore lower trench slope of the Hikurangi margin.

There, the development of highly confined trench-slope basins occurs during middle to late Miocene (*c.* 13.7 – 6.2 Ma) in lower bathyal sedimentary environment. The infill of the Titihaoa basin comprises six seismic units, 1 to 2 Myr in duration, characterized by important sedimentation rates variations through time. These units are delimited by unconformities related to tectonic activity. The depositional surfaces are seaward or landward tilted and therefore correspond to angular unconformities related to the development of the structural ridges that bound the basin. The comparison with the onshore Akitio trench-slope basin shows that the unconformable surfaces are associated to sedimentary discontinuities with rapid shifts of facies and important paleoenvironmental changes, which traduce slope creations or modifications. As long as the structural ridges develop, slopes are regularly rejuvenated favouring progradation of gravity systems in association with high sedimentary flux. The

very fine grained sedimentation within trench-slope basins is therefore dominated by filling processes leading to the development of well expressed fourth order scale coarsening-up sequences. In such basins, the preservation of fining-up sequences may reflect distality from sediment sources or a diminution of sediment influx in relation with stabilisation of slopes.

At the margin scale, the comparison of these two basins suggests that deformation, responsible for trench-slope basins development, has stopped during middle Miocene (*c.* 13.2 Ma) on the inner trench-slope (onland) while it has continued during late Miocene (*c.* 6.2 Ma) closer to the subduction front. Offshore, a major unconformity (*c.* 6.2 Ma) marks the drowning of trench-slope basins, including the Titihaoa basin, and some of their borders. This unconformity marks a stop in the development of some Miocene structural ridges. The subsequent sedimentation occurred within a larger depositional domain, the Turnagain slope basin, fill by thick prograding sedimentary series. The settlement of the Turnagain basin is contemporaneous with a shallowing event which may be attributed either to a continuation of global uplift of the Hikurangi margin, or to the filling up of the basin with very high sedimentation rates (400 – 450 m/Ma) during moderate margin subsidence.

I) INTRODUCTION

On subduction margin, the dynamic of the downgoing slab is responsible for the lower trench slope morphology. Indeed, major tectonic motions control the distribution of deformation and therefore the shape of sedimentary basins (uplift versus subsidence, horizontal tectonic shortening or stretching). Yet, detailed interplays between the parameters of subduction and the sedimentary/tectonic records on the lower trench slope are poorly constraint.

The North Island of New Zealand is characterized by the westward oblique convergence of the Pacific plate (Fig. IV-1A). The onset of subduction beneath the North Island, 25 My ago, led to the development of the Hikurangi subduction wedge (Bailleul *et al.*, submitted). There, the structure of the lower trench slope is inferred to result from a succession of deformational episodes (Chanier, 1991; Ferrière & Chanier, 1993) that are dominated by important shortening (25 – *c.* 15 Myr and *c.* 5 - 0 Myr) or by extension (*e.g.* *c.* 15 – *c.* 5 Ma). Compressional deformation related to accretionary processes is often responsible for uplift and contraction of sedimentary domains during the growth of the accretionary wedge. On this accretionary wedge, syn-subduction sedimentation occurs within small elongated structural depressions called trench-slope basins (Moore & Karig, 1976, Underwood & Moore, 1995). Widespread extensional deformation occurred during a period of important regional subsidence and has been therefore considered as associated with tectonic erosion processes (Chanier *et al.*, 1999).

The aim of this present study is to highlight the close interplay between tectonic activity and the stratigraphic pattern of an offshore lower trench slope in an active subduction setting. We describe in particular the deformational processes and stratigraphic evolution of the Titihaoa Miocene trench-slope basin. Moreover, we also compare this basin to an onshore analogue: the Akitio trench-slope basin. We therefore attempt to propose an overview of trench-slope basin development that includes our sedimentological data (descriptions and interpretations of turbidite facies and related deep sea facies, characterization of sedimentary systems), our stratigraphic interpretations (definition of sedimentary units and fining-up/coarsening-up sequences development and organisation), and our structural analysis (basin geometry and deformational processes).

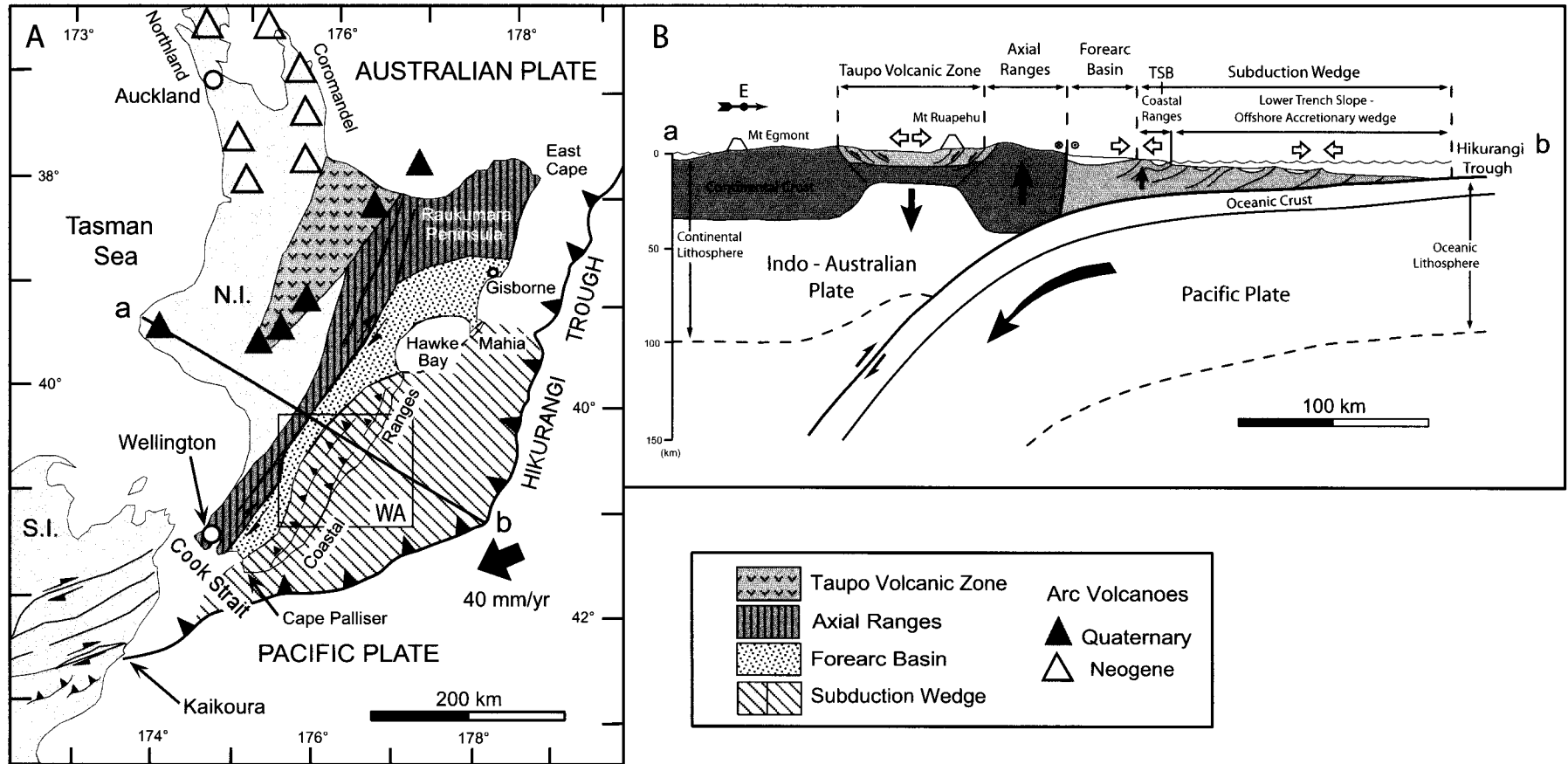


Fig.IV-1. A - Tectonic setting of the Hikurangi subduction zone, North Island of New Zealand (N.I. - North Island, S.I. - South Island, WA - Wairarapa Area). Black arrow shows present-day relative plate motion between Pacific and Australian plates. Modified after Chanier *et al.* (1999). **B** - General cross-section a - b of the Hikurangi subduction complex showing major subduction related morphostructural features of the Hikurangi active margin (TSB - Trench Slope Break).

II) MORPHOLOGY AND DEFORMATION OF TRENCH-SLOPE BASINS

In subduction contexts, the lower trench slope is located between the trench and the trench slope break (Fig. IV-1B), and is characterized by the development of linear submarine ridges (Fig. IV-2A). These ridges are structurally controlled by thrust faulting and/or growing folding during the growth of the accretionary wedge (Moore & Karig, 1976; Lewis, 1980; Stevens & Moore, 1985; Davey *et al.*, 1986; Lewis *et al.*, 1988; Okada, 1989). This structural grain, parallel to the plate boundary, individualizes narrow elongated basins called trench-slope basins (Moore & Karig, 1976; Stevens & Moore, 1985; Underwood & Moore, 1995). Structural ridges are generally seaward thrust and/or folded (Fig. IV-2A) and are therefore highly asymmetric (Moore & Karig, 1976; Lewis, 1980; Davey *et al.*, 1986; Okada, 1989). Because they are confined between these ridges, trench-slope basins are also dissymmetric with their seaward and arcward slopes characterized by a high gradient and a low gradient slope respectively. Trench-slope basins are commonly 5 – 30 km wide, depending on the main bathymetric highs spacing, and their sedimentary infill may reach 200 to 3000 m thick (Lewis, 1980; Stevens & Moore, 1985, Davey *et al.*, 1986, Okada, 1989; Mascle *et al.*, 1990).

Seismic profiling shows that sedimentary series of trench-slope basins rest in an unconformity on the basement of the accretionary wedge (Fig. IV-2A). This unconformity is pointed out by the onlap of the sedimentary series on the trenchward edge of the basin (Moore & Karig, 1976; Lewis, 1980; Stevens & Moore, 1985). In the vicinity of the arcward edge, intense deformation within the basin suggests a faulted contact with seaward thrusting of the basement over basin strata (Moore & Karig, 1980; Stevens & Moore, 1985). The basement of trench-slope basins is generally composed of highly deformed turbidites and deep sea deposits accreted from the trench (Moore & Allwardt, 1980). Because these sediments may be very similar to those deposited within the basins themselves, the distinction between trench slope basin infilling and basement units is also based on deformation criteria and age (basement older and much more deformed than the basin infilling; Lewis *et al.*, 1988). Indeed, there is little intra-basinal deformation during the trench-slope basin evolution (Fig. IV-2A; Stevens & Moore, 1985; Okada, 1989). Therefore, the stratigraphic succession within trench-slope basins is less deformed than the underlying accreted sediments (Smith *et al.*, 1979; Moore & Karig, 1980; Moore & Allwardt, 1980; Stevens & Moore, 1985; Okada, 1989). Further works (Bailleul *et al.*, submitted) have shown that, in the inner part of the accretionary wedge, trench-slope basins may also develop over highly deformed pre-subduction sediments corresponding to the deformation of a previous passive margin. They can be distinguished from syn-subduction sedimentation by age and by both sedimentological and deformation analysis.

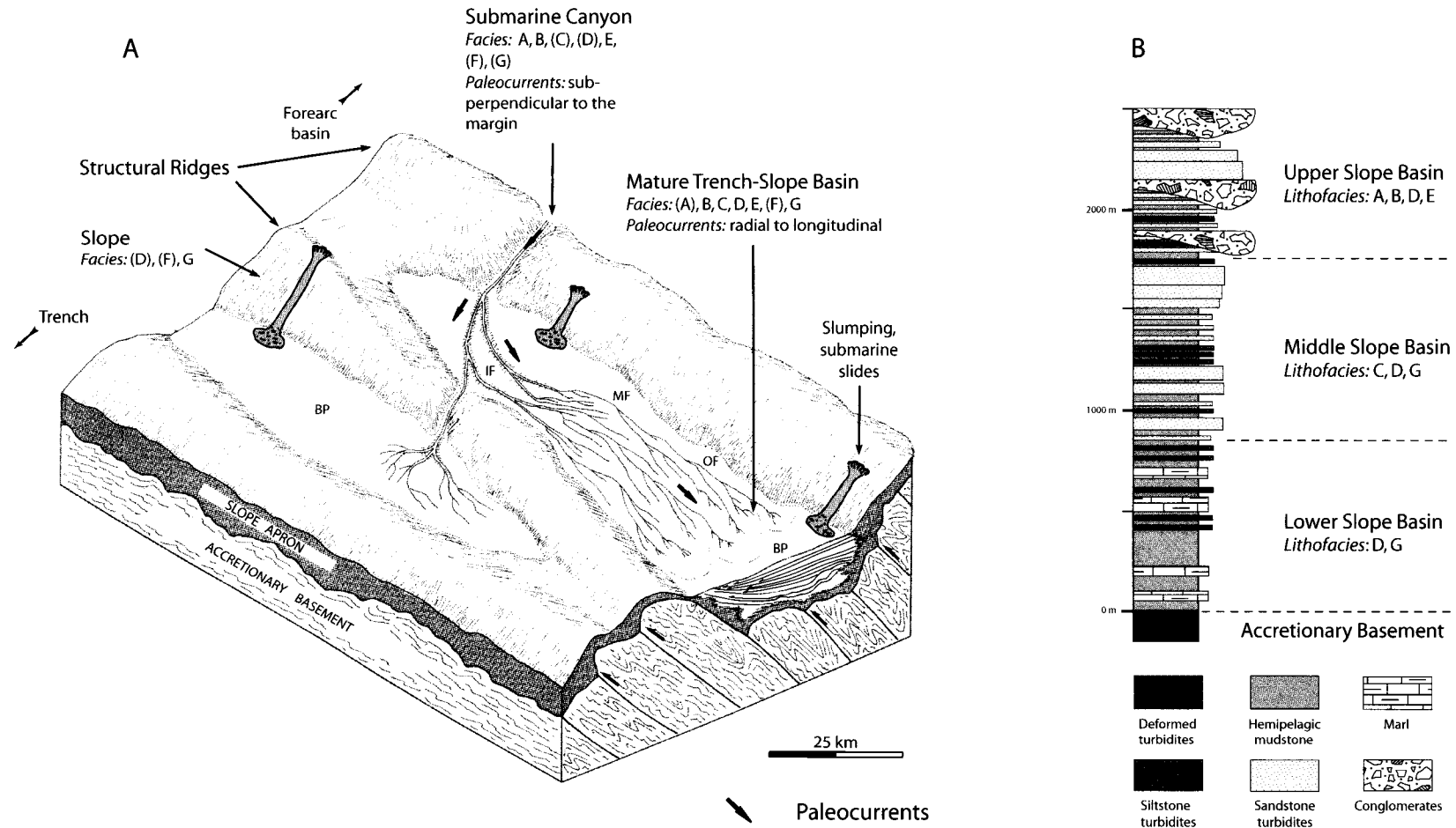


Fig.IV-2. Conceptual model showing morphology, structure and sedimentology of trench-slope basins. **A** - Bloc 3D after Underwood (1985), reflector within the basin after Stevens & Moore (1985), turbidites and depositional system after Underwood & Bachman (1982) (Letters refers to the deep sea lithofacies nomenclature defined by Mutti & Ricci Lucchi (1978), (IF - Inner Fan, MF - Middle Fan, OF - Outer Fan, BP - Basin Plain). **B** - Stratigraphic model for the evolution of a trench-slope basin. The upward coarsening and thickening trend reflects the progressive uplift of the basin which is associated to an increase in siliciclastic input. Sedimentological vertical section after Underwood *et al.* (2003), and Underwood & Moore (1995). Synthesis based on observations of Moore *et al.* (1980) on Nias Island, Indonesia.

In most of the studies on trench-slope basin structural development, the basement results (or is inferred to result) from accretion *sensu-stricto* (e.g. Moore & Karig, 1976; Moore & Karig, 1980; Davey *et al.*, 1986; Okada, 1989). Thus, first stages of trench-slope basin evolution occur in close vicinity of the trough following thrusting of the seaward slope of the trench. Then, the basins are progressively uplifted during the growth of the accretionary prism (Moore & Karig, 1976; Lewis *et al.*, 1988). With increasing the distance from the deformation front, the development of the structural edges leads to a progressive landward back-tilt of the basin sedimentary succession (Fig. IV-2A; Moore & Karig, 1976; Moore & Karig, 1980; Lewis, 1980; Stevens & Moore, 1985; Davey *et al.*, 1986, Lewis *et al.*, 1988; Underwood & Moore, 1995). Upslope, thrusting may stop and inactive structural ridges are drowned by sediments (Moore & Karig, 1976; Karig *et al.*, 1980; Lewis, 1980). This structural evolution is responsible for a general increase in size, thickness and age of trench-slope basins upslope (Moore & Karig, 1976; Karig *et al.*, 1980; Stevens & Moore, 1985).

On an active subduction setting, the development of trench-slope basins is therefore undoubtedly related to the structural evolution of the underlying accretionary prism. We carry out a detailed stratigraphic analysis of a Mio-Pliocene lower trench slope setting (Hikurangi margin, north-eastern New Zealand) to precise the stratigraphic signature of such tectonically active basins.

III) DEPOSITIONAL MODELS FOR TRENCH SLOPE BASINS

Underwood & Bachman (1982) have proposed a synthetic depositional model, based both on various geophysical studies and coring within recent trench-slope basins and outcrops of ancient analogues (Fig. IV-2A). This model proposes a predictive location for deep marine deposits within trench-slope basin domains. The seaward regional slope is cut by major submarine canyons and channels, which control the sedimentary input into the trench and trench-slope basins. Because of the structural grain, most of these canyons are dammed upslope by tectonic ridges and never reach the trench (Karig *et al.*, 1979; Underwood & Karig, 1980; Underwood & Bachman, 1982). The turbidites and other gravitational deposits are therefore preferentially ponded in upslope trench-slope basins (mature slope basins), which constitute local sedimentary traps for coarse sediments in close proximity to the trench slope break (Moore *et al.*, 1980; Underwood & Bachman, 1982; Stevens & Moore, 1985). Downslope, trench-slope basins mainly contain hemipelagic deposits (immature slope basins).

This up-slope increase in terrigenous turbiditic input is responsible for deposition of thickening- and coarsening-upward mega-sequences in trench slope basins (Fig. IV-2B), reflecting their gradual uplift (Moore *et al.*, 1980; Underwood & Bachman, 1982). However, this general stratigraphic model contrasts with some recent coring results in the Nankai subduction zone that show a thinning and fining upward trend within a trench-slope basin (Underwood *et al.*, 2003). Deposition of such a sequence may reflect a blockage of the previous feeder system (*e.g.*, due to out-of-sequence thrusting, or deformation of the margin in response to the subduction of sea mounts etc) or a disconnection of the canyon network from the shoreline (sea level rise or subsidence). For mature slope basins, the feeding directions may be perpendicular to the margin near the canyon mouths or parallel to the margin (Fig. IV-2A), reflecting the deflection of the sedimentary input along the axes of the basin (Underwood & Bachman, 1982). Although submarine canyons play an indisputable role in the distribution of sediments within trench-slope basins, other important contributions to the sediment budget are also identified. Thus, strong variations in detrital modes of turbidites on the lower slope of the eastern Aleutian trench (DSDP Leg 18, Site 181) suggest deposition by unconfined turbidity currents triggered in different source areas (Underwood & Norville, 1986). Likewise, local slope instability on adjacent ridges, caused by tectonic activity and/or eustatic fluctuations, can create significant sub-marine reworking from local sediment sources (Fig. IV-2A), as identified in the Western Sunda arc (Stevens & Moore, 1985).

On the Hikurangi active margin, the sedimentological study of the onshore Akitio basin has permitted to describe deep-sea facies that were interpreted in terms of depositional environments (Bailleul *et al.*, submitted). The accurate knowledge of gravitary systems within the studied trench-slope basins, onshore and offshore, allows us to evaluate the impact of deformational processes on their stratigraphic architecture.

IV) HIKURANGI SUBDUCTION WEDGE

Oblique convergence between the Australian and Pacific plates is responsible for the westward subduction of the thick Hikurangi oceanic plateau (10 to 15 km thick; Davy & Wood, 1994, Mortimer & Parkinson, 1996, Collot *et al.*, 1996) beneath the North Island, New Zealand (Fig. IV-1). The morphology of the lower trench slope of the Hikurangi Trough results from the Hikurangi subduction wedge (Bailleul *et al.*, submitted) development and evolution since the onset of subduction, 25 Myr ago (Fig. IV-1B). Now-a-days, the subduction wedge extends, onshore and offshore, along eastern North Island from Cape Palliser to Hawke Bay (Fig. IV-1A). It can be subdivided onto two main structural domains, from the trench to the forearc basin: the outer subduction wedge and the inner subduction wedge.

The outer subduction wedge is constituted by recent (mainly quaternary) accreted trench-fill sediments (Lewis, 1980; Collot *et al.*, 1999; Lewis *et al.*, 1999). This domain corresponds to the accretionary prism *sensu-stricto* (Seely *et al.*, 1974 ; Karig & Sharman, 1975 ; Moore & Karig, 1976 ; Scholl *et al.*, 1977 ; Seely, 1979). It is characterized by active imbricated thrusts and by the development of quaternary trench-slope basins offshore, near the subduction front (Lewis, 1980; Davey *et al.*, 1986; Lewis & Pettinga, 1993).

The inner subduction wedge includes the Coastal Ranges onshore and the upper slope of the active margin offshore (Fig. IV-3). It is more deformed than the outer subduction wedge and comprises a basement composed of pre-subduction sediments (Cretaceous to Paleogene). Syn-subduction sedimentary formations, including neogene trench-slope basins infill, overly this basement (Fig. IV-3). Although, the oblique convergence is responsible for some strain partitioning (Cashman *et al.*, 1992, Barnes *et al.*, 1998), the inner subduction wedge presents mainly contractional structures sub-parallel to the active margin. Indeed, the strike-slip component of the oblique convergence is mainly accommodated by dextral strike-slip faulting located behind the forearc basin (Fig. IV-1), within the Axial Ranges (Kingma, 1967; Lensen, 1969; Spörli, 1980, Cashman *et al.*, 1992). Offshore, the acoustic basement of the inner subduction wedge also contains middle, and probably early, Miocene sediments (Biros *et al.*, 1995; Field, Uruski *et al.*, 1997). The onshore inner subduction wedge constitutes the highest ridges and basins of the subduction wedge (Pettinga, 1982; Lewis & Pettinga, 1993) forming the East Coast Deformed Belt (Spörli, 1980), or Coastal Ranges (Figs IV-1B and IV-3).

Since the onset of subduction, the Hikurangi margin has undergone three main deformational episodes deduced from onshore structural analysis (Chanier, 1991).

First, the initiation of subduction along the Hikurangi margin, 25 Myr ago, has induced intense compressional deformation characterized by nappes emplacement: seaward thrusting, reverse faulting and folding (Chanier & Ferrière, 1989, 1991; Rait *et al.*, 1991). This tectonic episode (*c.* 25 – 19 Ma) is responsible for important deformation of the previous inactive margin that marks the onset of the inner subduction wedge development. In the Coastal Ranges, tectonism is associated with a sharp facies change from Eocene – Oligocene pelagic sedimentation (marls and pelagic limestones) to early Miocene olistostromes and turbidites of the Whakataki Formation (Johnston, 1975, 1980). The Whakataki Formation corresponds to the first sediments included within the Miocene Palliser Group (Lee & Begg, 2002; modified from Vella & Briggs, 1971). In the Pongaroa area, sedimentological study of the onshore Akitio trench-slope basin (Fig. IV-3) shows that the uplift of its structural edges still occurred before 19 Ma (Bailleul *et al.*, submitted). The timing of deformation of the Akitio basin therefore suggests the continuation of compressional deformation after the first paroxysmal phase of nappes emplacement, maybe till 16.5, even 15 Ma, at least locally.

The second tectonic period is dominated by normal faulting and local syn-sedimentary gravitational collapse. This deformation is contemporaneous with the progressive overlap on the basement, pointed out by successive discontinuities, of the middle and late Miocene marine sediments of the Palliser Group (Fig. IV-3). This provides evidence of a regional marine transgression during a period of broad subsidence of the margin (Vella & Briggs, 1971). All these observations led Chanier *et al.* (1999) to relate the extensional and subsiding episode (*c.* 15 - 5 Ma) to a period of tectonic erosion.

The third episode (*c.* 5 - 0 Ma) consists in renewed mainly compressional deformation characterized by reverse faulting and folding over the East Coast region (Walcott, 1984; Lamb & Vella, 1987; Wells, 1989; Cape *et al.*, 1990; Chanier, 1991; Beanland *et al.*, 1998; Nicol *et al.*, 2002). Unconformable on the Palliser Group, latest late Miocene to early Quaternary marine sediments of the Onoke Group (Vella & Briggs, 1971; Lee & Begg, 2002) traduce a major marine regression. This third tectonic episode is finally responsible for the rapid uplift and subsequent emersion of the inner subduction wedge during the Quaternary (Ghani, 1978; Cape *et al.*, 1990).

The recent emersion of the inner subduction wedge has permitted studies on outcrops of the turbidite infill of Miocene trench-slope basins. The compilation of these outcrop data with our geophysical study of similar basins, located offshore, allows a multidisciplinary analysis of the structural and stratigraphic development of such ponded basins. Moreover, we propose to compare and correlate the Mio-Pliocene tectonic history of the Hikurangi margin, deduced from onshore tectonic and sedimentological analysis, to seismic stratigraphy analysis of the Hikurangi offshore lower trench slope.

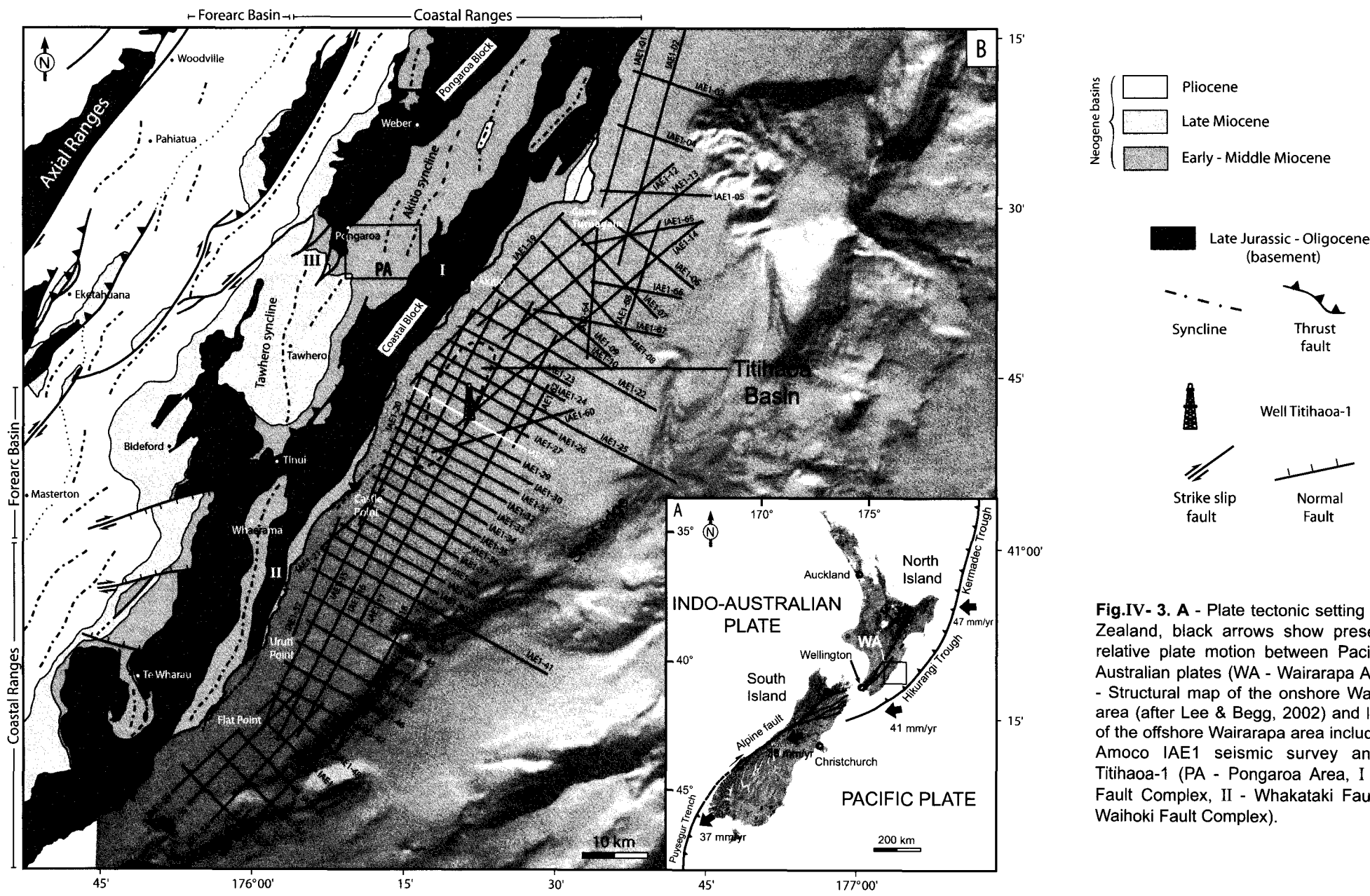


Fig.IV- 3. A - Plate tectonic setting of New Zealand, black arrows show present-day relative plate motion between Pacific and Australian plates (WA - Wairapa Area). **B** - Structural map of the onshore Wairapa area (after Lee & Begg, 2002) and location of the offshore Wairapa area including the Amoco IAE1 seismic survey and well Titihaoa-1 (PA - Pongaroa Area, I - Tinui Fault Complex, II - Whakataki Fault, III - Waihoki Fault Complex).

V) LOCATION, DATA AND METHODOLOGY

A) Location

Miocene and Pliocene lower trench slope sediments of the inner subduction wedge are encountered, onshore and offshore, in the Wairarapa area (Figs IV-1 and IV-3).

Onshore, within the Coastal ranges, highly deformed Cretaceous-Paleogene pre-subduction sediments constitute elongated basement structural highs with a northeast – southwest trend (Fig. IV-3). Between these structural highs, elongated wide synclines comprise Miocene syn-subduction sedimentary series (Palliser Group: Vella & Briggs, 1971; modified by Lee & Begg, 2002). These series are inferred to be partly deposited within ancient trench-slope basins (Bailleul *et al.*, submitted). The latest Late Miocene to Pliocene marine sediments (Onoke Group: Vella & Briggs, 1971; Lee & Begg, 2002) rest unconformably on this succession of basement strips and synclines. The sediments of the Onoke group were slightly landward backtilted during recent compressive deformation and consist mainly of shallow shelf sediments including coquina limestones.

Offshore, the inner subduction wedge (Fig. IV-3) benefits from a seismic coverage (IAE1 seismic survey) and from drillhole data (well Titihaoa-1). The area covered by geophysical survey (Wairarapa offshore area) is restricted between the coast and the first major structural feature affecting the seafloor. This submarine structural feature, still active, coincides with the shelf edge (Fig. IV-3) suggesting that the shelf geometry is partially controlled by tectonic activity. To the east of the shelf edge, the extent of the inner subduction wedge is not clearly defined. The Wairarapa offshore area consists in a smooth shelf, 20 - 40 km wide, which gently deepens from shore to *c.* 200 - 500 m of water depth. Seismic profiling shows that the structure of the shelf consists in a succession of acoustic basement ridges and sedimentary depressions overlaid by a less deformed, thick and continuous sedimentary cover.

This paper is based on a detailed stratigraphic analysis of the Titihaoa offshore area. The compilation of seismic stratigraphy and wireline logs (gamma ray and sonic) data, combined with the lithostratigraphy and the biostratigraphy obtained from well Titihaoa-1, permits to characterize and to organize hierarchically major sedimentary units and their bounding unconformities within the sedimentary infill of the lower trench slope. An offshore trench-slope basin (the Titihaoa basin), embedded between structural ridges, is then compared to an older onshore analogue (the Akitio basin).

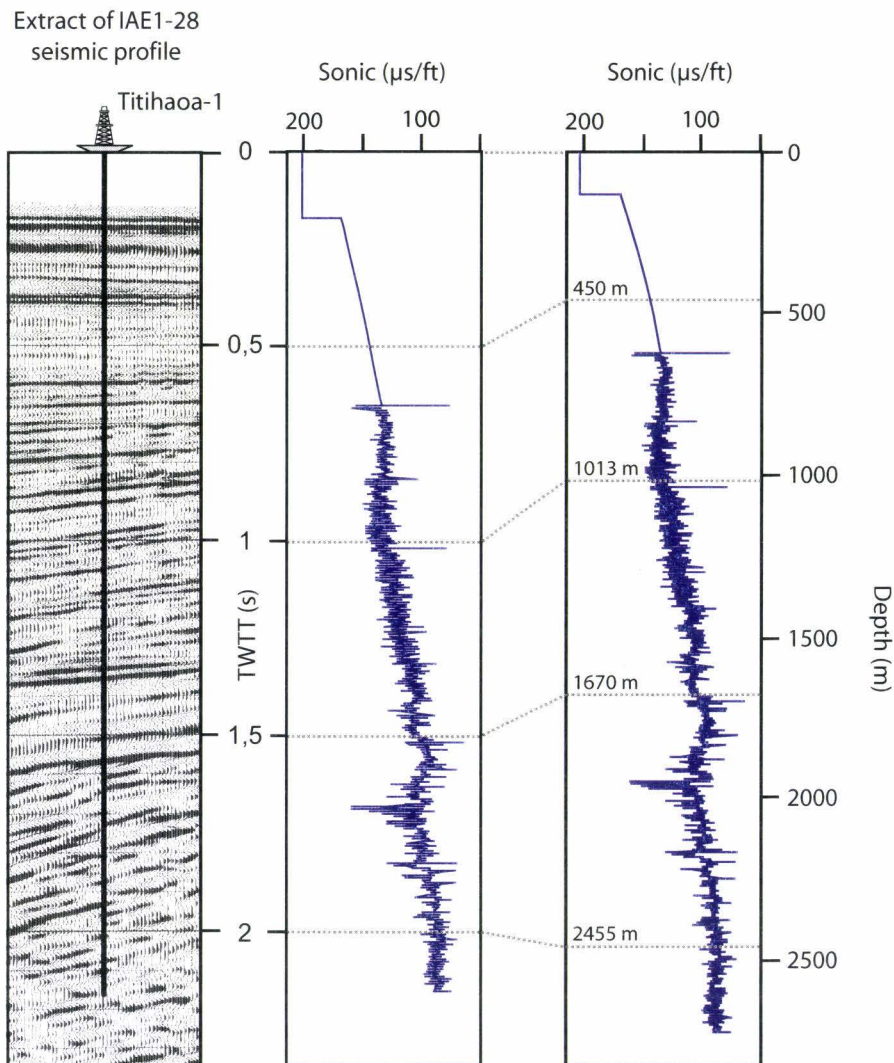


Fig. IV-4. Correlation between IAE1-28 seismic profile and Titihaoa-1 sonic logs (twtt (s) and m). See text for explanations.

B) Data and Methodology

1) Analysis of the offshore seismic profile (IAE1 seismic survey)

A 2D marine seismic survey, IAE1, has been carried out offshore Wairarapa by the Amoco New Zealand Exploration Company (Fig. IV-3). Seismic lines IAE1 were recorded and processed in 1990 and are now open file at the New Zealand Ministry of Commerce, Wellington (Adams & Sullivan, 1990). The survey consists in 1574 line kms (67 seismic lines) recorded, from Cape Turnagain to Flat Point, using conventional multichannel seismic reflexion. For this study, we present seismic line IAE1-28, perpendicular to the coast line, which is representative of the main structural grain of the margin (Fig. IV-3).

Because deformation in such an active margin setting can affect sequence geometries, we based our seismic analysis on the principles of seismic stratigraphy (Vail *et al.*, 1977; Mitchum *et al.*, 1977a) rather than on those of sequence stratigraphy (Posamentier & Vail, 1988). The methodology consisted to identify major seismic units that are characterized by their layered configurations (seismic facies) and are bounded by unconformities (*e.g.* prograding surfaces, aggrading surfaces, erosional surfaces ...). Unconformities are identified by the geometries of reflector terminations (Mitchum *et al.*, 1977b) and can be represented or not by a reflective horizon depending on the acoustic impedance contrast between seismic units. Within major seismic units, intra-unit unconformities were used to define seismic sub-units. Sequential analysis of the seismic units and sub-units was performed on the basis of drillhole data interpretations (see further sections of this paper).

2) Analysis of the well logs (Titihaoa-1 Exploratory Well)

The Titihaoa-1 petroleum exploration well was drilled 13 km offshore East Coast, North Island, using Neddrill 1 drillship (Fig. IV-3). Drilling operations were undertaken in 1994 by the Amoco NZ Exploration Company and data are now available at the New Zealand Ministry of Commerce, Wellington (Biros *et al.*, 1995). The borehole is located at the junction between seismic lines IAE1-28 and IAE1-17 (precise coordinates are Lat. 40°, 48', 5.20" S, Long. 176°, 25', 40.65" E). The well reached a total depth of 2740 m (meters below derrick floor) including 125.7 m of Water depth and 13.1 m of derrick platform elevation. Titihaoa-1 is a destructive drilling and therefore most of data on lithostratigraphy, biostratigraphy and paleoenvironments are provided by well-cuttings.

Accurate cuttings descriptions and wireline logs (resistivity, gamma ray and sonic) are only available from 625 m to total depth. For this study, we have digitalised sonic (DT) and gamma-ray (GR) logs in order to correlate well data and seismic profiles. The velocity analysis provided by the sonic gives a robust velocity profile from 625 m to total depth (Fig. IV-4). Above 625 m, the velocity profile comes from seismic wave velocity measurements available on seismic line IAE1-28. This part of the velocity profile has been confirmed by the upward interpolation of the sonic log. This methodology permits to construct an accurate time to depth model for the whole well. This model was then applied to precisely tie Titihaoa-1 well and IAE1-28 seismic profile (Fig. IV-4).

Using our time to depth model, the correlation between seismic profile IAE1-28 and well Titihaoa-1 (Fig. IV-4) permits to tie seismic unconformities and well logs. Using gamma ray and sonic logs and referring to the sequence stratigraphy methodology described by Cross *et al.* (1993) and Homewood *et al.* (1992), we were able to determine lower order fining-up/coarsening-up sedimentary sequences that composed our seismic units and sub-units. On wireline logs, the unit and sub-units boundaries, defined in the marine sedimentary infill, were found to correspond either to diachronous boundaries at base of coarsening-up sequences for prograding surfaces (downlap surfaces), or to the basal limits of fining-up sequences for aggrading surfaces and/or erosional surfaces. In sequence stratigraphy the base of coarsening-up sequences (progradation) are considered as maximum flooding surfaces (Galloway, 1989), while the base of fining-up sequences (retrogradation) are considered as flooding surfaces. However, as on active margins some of these surfaces may be related to tectonic activity, we prefer to use our seismic stratigraphy terminology (unit boundaries or unconformities) rather than the sequence stratigraphy nomenclature. The sedimentary facies intersected by the offshore well Titihaoa-1 were evaluated from the wireline logs pattern, which characterizes the bases, fining-up/coarsening-up pattern, and tops of the sedimentary sub-units, combined with the lithological informations obtained from determination of the well-cuttings. These interpretations were compared to the facies and depositional environments determined at outcrop in similar basins. Dating was also precisely established from the well micropaleontological data (Morgans *et al.*, 1995) using the New Zealand Cretaceous-Cenozoic Timescale (Cooper *et al.*, 2004).

VI) STRATIGRAPHY OF THE TITIHAOA AREA

A) Seismic stratigraphy

Seismic line IEA1-28 shows the vertical succession of three major seismic units: SI to SIII (Fig. IV-5). From base to top, SI is characterized by highly disorganised internal seismic reflectors, SII by irregular and discontinuous internal reflections, and SIII by relatively continuous parallel to sub-parallel internal reflections. Within SII and SIII, other unconformities permit to define internal seismic sub-units of same layered configuration (Figs IV-5 and IV-6).

1) Highly disorganised seismic unit (SI)

This basal unit is composed of chaotic internal reflections that traduced relative deformation of the unit compared to the overlying seismic units (Fig. IV-5). SI is crossed by strong west-dipping oblique reflectors interpreted by Field, Uruski *et al.* (1997) as major thrust zones. Above each west-dipping reflectors the seismic unit SI is uplifted forming structural ridges (SR1 to SR4). The relationships between structural ridges and the west-dipping reflectors suggest that deformation of this unit results from hanging wall anticline development over landward-dipping thrust faults (Field, Uruski *et al.*, 1997). This landward-dipping thrusts sheets imbrication is typical of substratum of subduction wedges. Nevertheless, this unit constitutes the acoustic basement of the overlying sedimentary units (Fig. IV-5).

2) Irregular and discontinuous seismic unit (SII)

This second unit mainly consists of low amplitude, irregular and laterally discontinuous reflectors (Figs IV-5 and IV-6 - enlargements 1 and 2). SII unconformably overlies the acoustic basement with a highly undulating basal boundary (B1) that reflects the deformation within the underlying unit (SI). The lower part of SII is confined between major acoustic basement structural ridges (SR2 and SR3) while its upper part shows their drowning (Fig. IV-5). Therefore, the unit presents a better lateral extent in its upper part. The complex layered configuration of the overall unit is also expressed by a divergent configuration of seismic reflectors. This characterizes a progressive thickening of the unit away from major acoustic basement ridges. Divergent arrangements of seismic reflectors suggest strong variations in the rates of deposition, or subsidence with progressive tilting of the depositional surfaces, or a combination of those factors.

SII can be subdivided into six sub-units (SII-1 to SII-6) on the basis of observed internal unconformities (B2 to B6). Divergent organisation of seismic reflectors is particularly well expressed within sub-units SII-1 and SII-2 (Figs IV-5 and IV-6 – enlargements 1 and 2).

- **SII-1** rests unconformably on the acoustic basement and is only restricted to the bathymetric depressions that have developed between major acoustic basement ridges (SR2 and SR3). To the west of SR2, this sub-unit cannot be clearly described as strata are apparently deformed by the growth of SR1 (Fig. IV-6 – enlargement 2). To the east of SR2, strata are better preserved showing discontinuous reflectors passing through laterally to small lenticular and reflection free seismic bodies and rare incised geometries (Fig. IV-6 – enlargement 1).

- **SII-2** directly overlies the basement above structural highs and is elsewhere unconformable on SII-1 that forms the basal infill of the bathymetric depressions (Fig. IV-5). Therefore, the upper part of SII-2 drowned major acoustic basement ridges (SR2 and SR3). SII-2 basal boundary (B2) above SII-1 is an irregular surface characterized by gullies (*e.g.* to the east of SR2), by the local onlap of SII-2 seismic reflectors, and by the toplap geometry of the seismic reflectors within the underlying sub-unit SII-1 (*e.g.* to the west of SR2). Sub-unit SII-2 internal cycle configuration is somewhat similar to SII-1 (Fig. IV-6 – enlargements 1 and 2).

- **SII-3** basal boundary (B3) develops on toplaps of SII-2 strata (Fig. IV-6 – enlargement 2). These toplaps are localized to the west of SR2 suggesting that B3 is still affected by the deformation related to the SR2 development. Between each ridge (SR2), or each paleoridge (SR3), the surface is slightly undulated. In close proximity of SR2 and SR3, SII-3 internal seismic reflections onlap over B3 (Fig. IV-6 – enlargements 1 and 2). Above and to the west of SR2, the sub-unit is condensed while to the east it shows a progressive eastward thickening (Fig. IV-5). This thickening traduces an eastward migration of the depot centre compared to SII-2. The migration of the depot centre is subsequent to the drowning of SR3 by SII-2. SII-3 is dominated by reflection free cycle configuration within the most condensed part of the sub-unit and by low amplitude seismic reflectors where the sub-unit thickened (Fig. IV-6 – enlargement 1 and 2).

- **SII-4** basal boundary (B4) presents local downlaps of SII-4 seismic reflectors in the eastern part of the profile (Fig. IV-6 – enlargement 1). Although SII-4 is apparently the most condensed seismic sub-unit of SII, it presents a good lateral continuity over the studied transect (Fig. IV-5). Internal cycle configuration is reflection free with rare low reflective seismic horizons (Fig. IV-6 – enlargements 1 and 2).

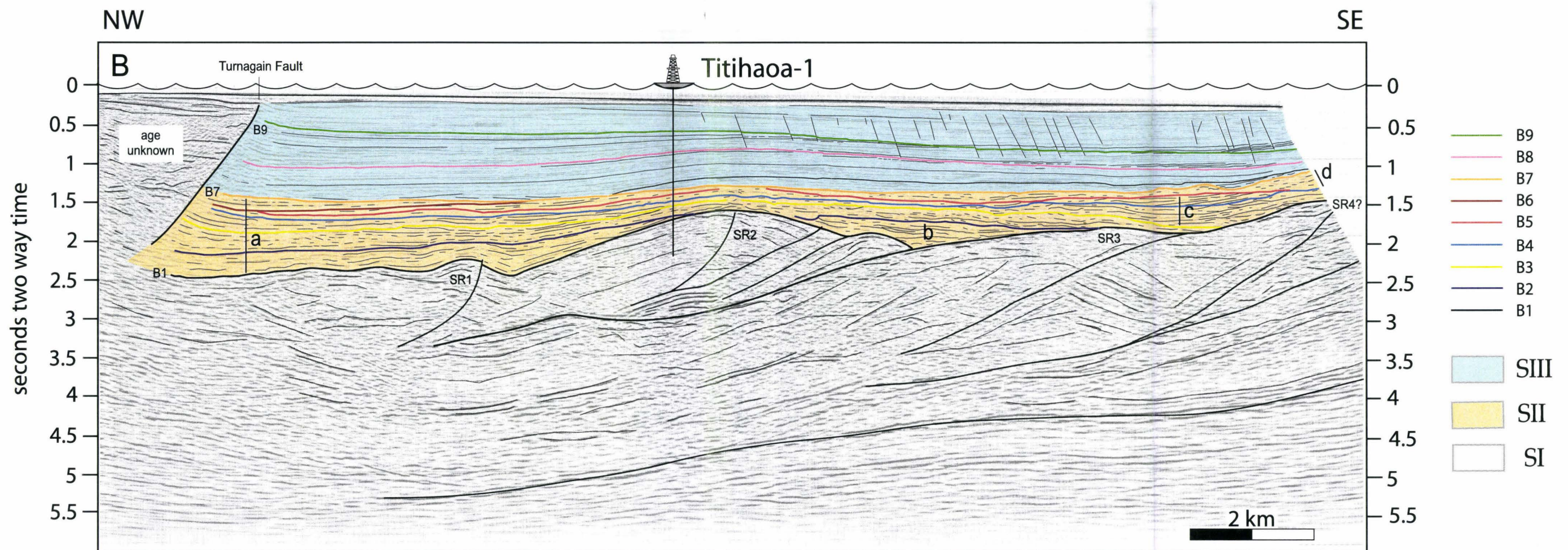
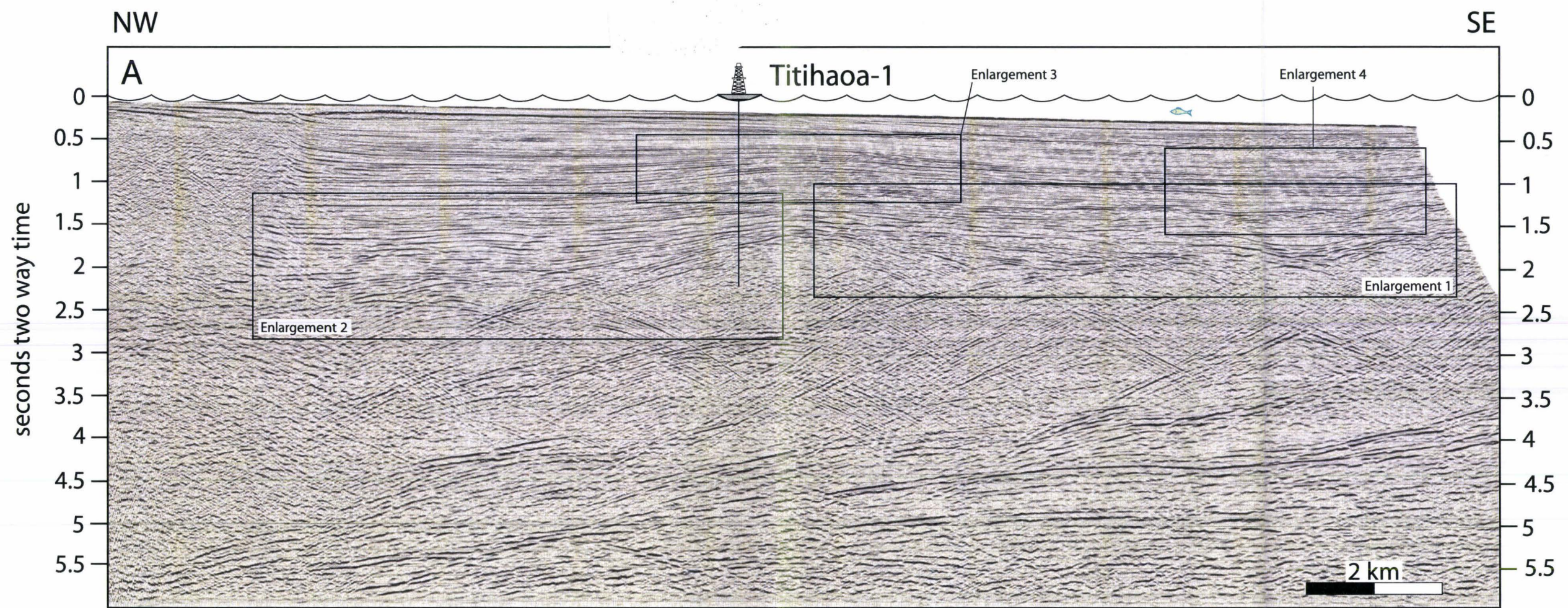


Fig.IV-5. IAE1-28 seismic line (A) and line drawing (B). SI - Highly disorganised seismic unit (deformed acoustic basement), SII - Irregular and discontinuous seismic unit (trench-slope basin infill) , SIII - Well organised and continuous seismic unit. "a", "b", "c" and "d" - trench-slope basins. B1 to B9 - seismic units/sub-units boundaries. See figure IV-6 for enlargements.

- **SII-5** basal boundary (B5) is laterally discontinuous with a gap above SR2 (Fig. IV-5). B5 is characterized by the downlap of SII-5 seismic reflectors (Fig. IV-6 – enlargements 1 and 2). This is particularly well expressed in the eastern extremity of the IAE1-28 seismic line (Fig. IV-6 – enlargement 1). Internal cycle configuration is comparable to this described for SII-3.

- **SII-6** basal boundary (B6) shows the onlap of SII-6 seismic reflectors and constitutes an angular unconformity over SII-5 and SII-4 (Fig. IV-6 – enlargement 2). Sub-unit SII-6 is confined to the western part of the profile (Fig. IV-5). It comprises slightly more reflective seismic horizons than the underlying sub-units.

3) Well organised and continuous seismic unit (SIII)

This third unit is made up of high amplitude and laterally continuous parallel to sub-parallel seismic reflectors (Fig. IV-5). SIII is bounded at base by a downlap surface (B7) traducing the westward progradation of SIII sedimentary series over a major discontinuity on top of the underlying unit (Figs IV-5 and IV-6 – enlargements 1 and 2). This erosive discontinuity (B7) is responsible for the truncation of B5 above SR2 and of B6 to the west of SR2 (Fig. IV-5). In the eastern part of seismic line IAE1-28, B7 is also highly undulated and shows small incised geometries (Fig. IV-6 – enlargement 1). The top of SIII is the seafloor reflector. As for SII, this unit can be subdivided into sub-units (SIII-1 to SIII-3) delimited by internal unconformities (B8 and B9). These sub-units are the most laterally continuous of the studied transect (Fig. IV-5).

- **SIII-1** basal boundary corresponds to B7 as described above. This sub-unit is characterized by sigmoidal prograding clinofolds particularly well expressed in the western part of the studied profile (Fig. IV-5).

- **SIII-2** is bounded at base by an onlap surface (B8). To the west of SR2, this surface is sub-parallel to the seismic reflectors of the underlying sub-unit (SIII-1). However, to the east of SR2, B8 clearly truncates the underlying sedimentary series (Fig. IV-6 – enlargement 3). Away from SR2, SIII-2 comprises sub-horizontal seismic reflectors (Fig. IV-5).

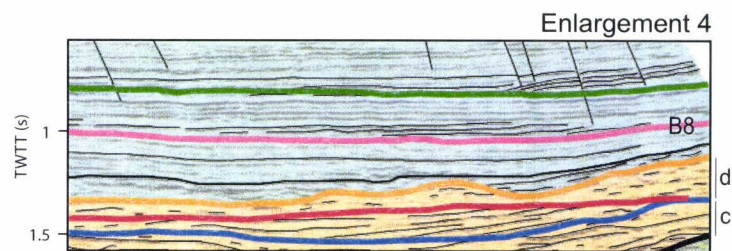
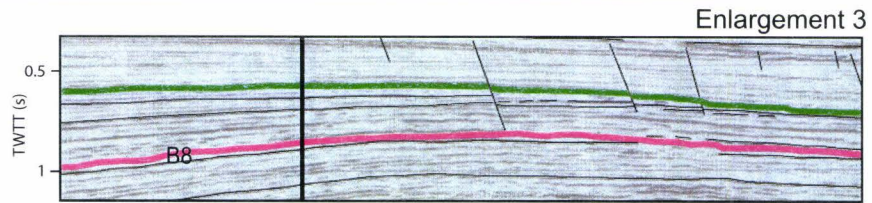
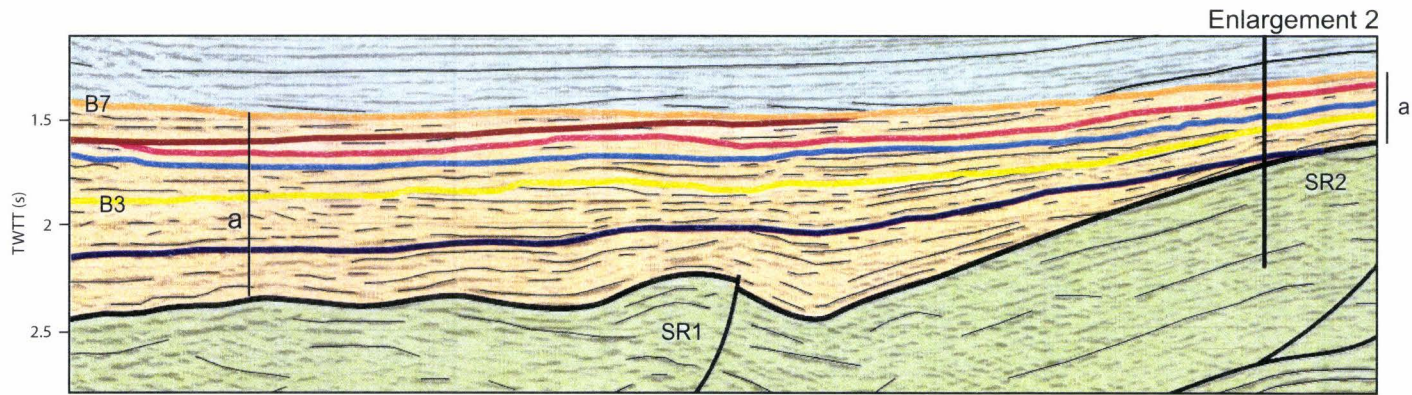
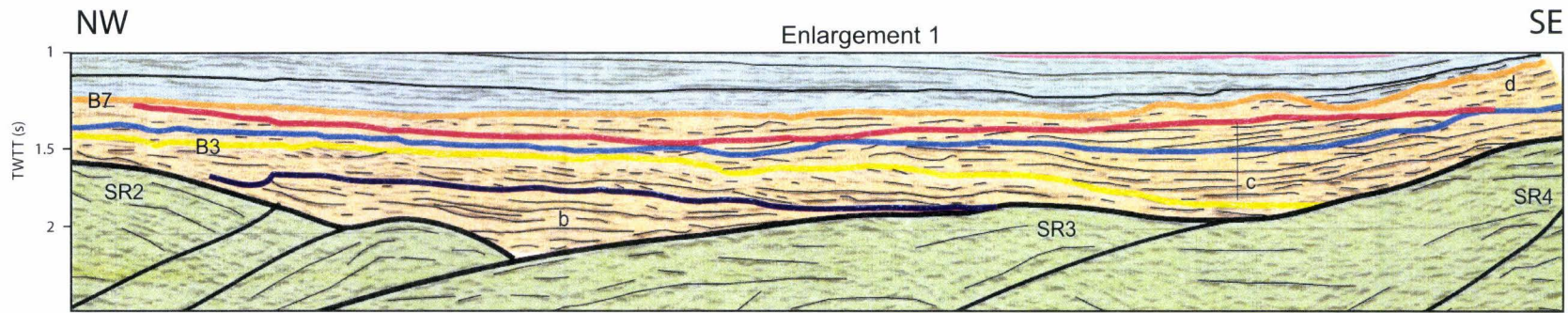


Fig.IV-6. Parts of the IAE1-28 seismic line and interpretations. Location of the enlargements is shown figure IV-5. Their numerotation also refers to figure IV-5. SI - Highly disorganised seismic unit (deformed acoustic basement), SII - Irregular and discontinuous seismic unit (trench-slope basin infill), SIII - Well organised and continuous seismic unit. "a", "b", "c" and "d" - trench-slope basins. B1 to B9 - seismic units/sub-units boundaries.

	SI		SII		SIII
--	----	--	-----	--	------

Zoom x2
1 km

- **SIII-3** basal boundary (B9) is a complex surface that shows downlaps in the eastern extremity of the profile (Fig. IV-6 – enlargement 4) and slight onlaps in its middle part (Fig. IV-6 – enlargement 3). In this last area, B9 is somewhat truncative over the underlying sub-unit SIII-2 (Fig. IV-6 – enlargement 3). SIII-3 is dominated by sub-horizontal seismic reflections that are slightly less reflective than in the underlying sub-units. In the eastern extremity of the profile, the basal part of SIII-3 shows very low angle clinoforms (Fig. IV-6 – enlargement 4).

B) Lithostratigraphy

The lithostratigraphy of the area was established from facies changes observed from cuttings of well Titihaoa-1. The whole well data led to distinguish two formations, from top to base: the *Whangaehu Mudstone Formation* (which includes the *Calcareous Mudstone Member* at its base) and the *Whakataki Formation* (Biros *et al.*, 1995). Formations names used there were based on the onshore lithostratigraphic framework of the eastern Wairarapa. Because of tectonic deformation, of rapid lateral facies changes, and of differences in age, the extent offshore of these formations appears uncertain. For example, the onshore Whakataki formation consists of Early Miocene turbidites while on well Titihaoa-1, turbidites of this formation are Middle Miocene in age. Moreover, the comparison between sedimentary facies on onshore outcrops and cuttings from well Titihaoa-1 remains uncertain. For this study, we therefore subdivide the strata onto three lithostratigraphic units (from top to base: L1 to L3) without references to the onshore lithostratigraphy (Fig. IV-7). Estimations of paleobathymetries mainly follow Crundwell *et al.* (1994) and Hayward (1986) from foraminiferal assemblages. The bathymetric divisions (Fig. IV-7) are: neritic 0-200 m (inner shelf 0-50 m, middle shelf 50-100 m, outer shelf 100-200 m), upper bathyal 200-600 m, middle bathyal 600-1000 m, and lower bathyal 1000-2000 m.

The lithostratigraphic units are, from base to top (Fig. IV-7):

L1: This unit extends from 1935 m to total depth (2740 m). L1 is constituted by slightly calcareous massive mudstones alternating with thin beds of siltstones and/or very fine to fine grained sandstones. Some intervals within the unit are dominated by the interbedded lithology while for others, the most common lithology consists of massive mudstones with a few sandstone beds.

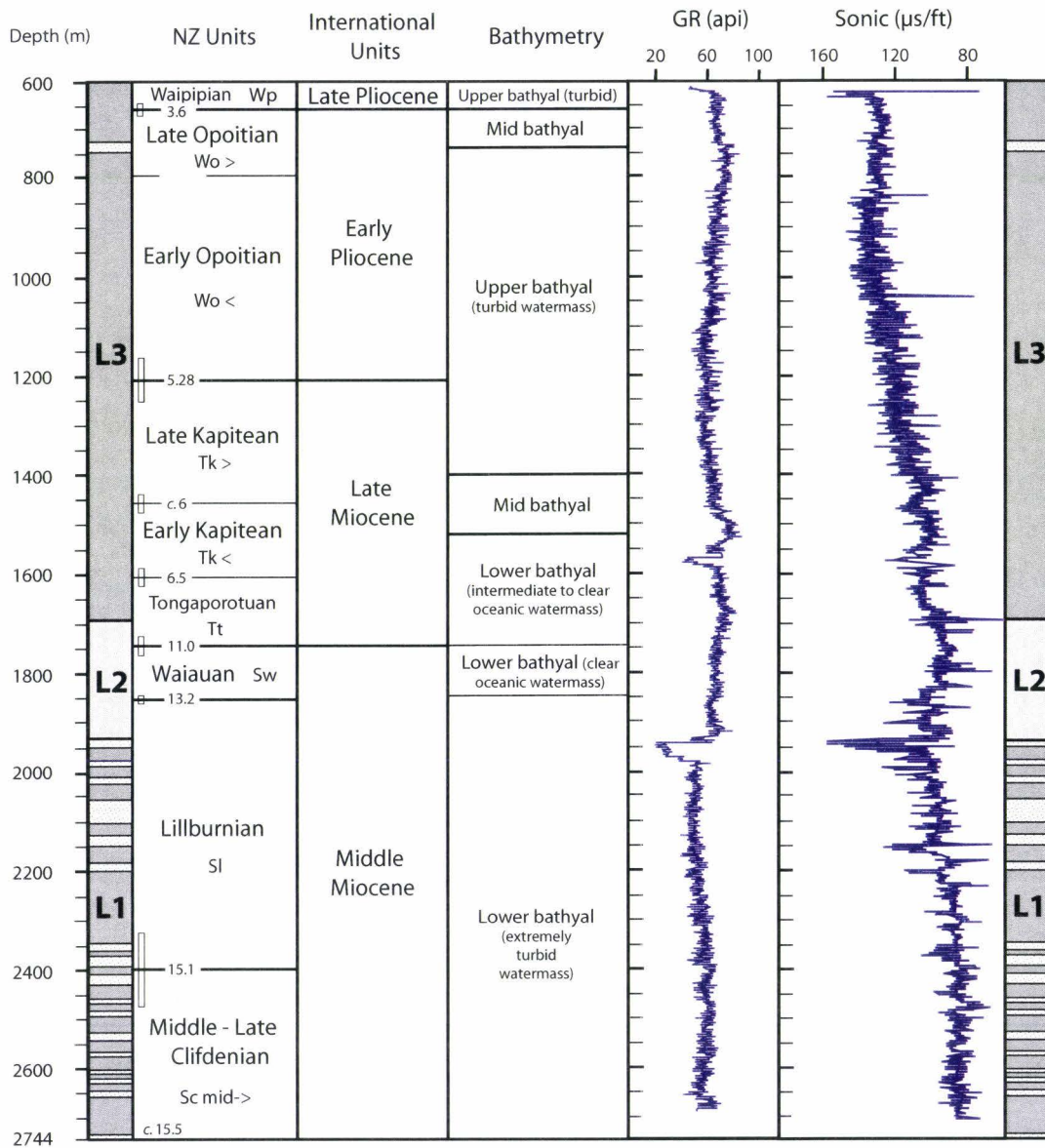
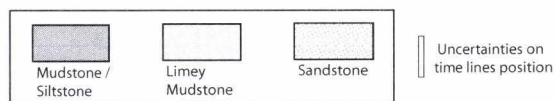


Fig. IV-7. Data compilation from well Titihaoa-1: lithologic log, paleobathymetry and wireline logs (GR , sonic). Lithologic and wireline logs after Biros *et al.* (1995), Biostratigraphy and paleobathymetries estimations (from foraminiferal assemblages) after Morgans *et al.* (1995).



These sediments are inferred to be deposited in a lower bathyal environment characterized by extremely turbid watermass (Morgans *et al.*, 1995). This is supported, especially between 2400 m and total depth, by the high rates of downslope reworking pointed out by reworked shelf and upper slope taxa. Despite no shows notification from drill cuttings data, sandstone beds have close affinities with distal turbidites. However, the presence of some thicker sandstone beds (up to 2m thick) within the thick turbidite sequence indicates that other turbidite facies (*i.e.* depositional lobes) may be encountered within the unit.

L2: This unit extends from 1692 m to 1935 m. L2 is also dominated by massive calcareous mudstones (8% to 15% CaCo₃), defining the previously named *Calcareous Mudstone Member* (Biros *et al.*, 1995). Paleoenvironmental interpretations show that L2 reflects a lower bathyal depositional setting (Morgans *et al.*, 1995; Crotty, 1995). The abundance in planktonic foraminifera and calcareous nannofossils suggests an open oceanic setting characterized by very low siliciclastic input (Morgans *et al.*, 1995). The low siliciclastic component within L2 is supported by the lithology, which presents a low sand/silt content. L2 basal boundary corresponds to the top of the last significant sandstone drill cuttings appearance (within L1) and was confirmed using correlations with well logs (Biros *et al.*, 1995).

L3: This last unit extends from 625 m to 1692 m. Lithology mainly comprises massive mudstone, with low carbonate content (1 to 3 % CaCo₃), that may be interpreted as pelagic to hemipelagic mud deposited on slopes or in distal basin plains. Paleontological data (Morgans *et al.*, 1995) indicate that L3 recorded three paleobathymetric changes, from base to top: a first shallowing from lower-middle bathyal to upper bathyal depths, then a deepening from upper to middle bathyal depths, and finally a second shallowing from middle to upper bathyal depths. Rare traces of very fine grained sandstones are also identified, especially between 625 m and 810 m. Despite no shows, deposition at bathyal depths of sandy layers within a massive mudstone sequence suggests that sandstone beds should be distal turbidites. A discontinuity, described as a probable hiatus by Biros *et al.* (1995), is recognised at 735 m from the presence of minor sandy lithology and scattered glauconite grains (up to 5% in cuttings). This discontinuity is contemporaneous with the deepening from upper to middle bathyal depth observed around 740 m.

C) Biostratigraphy

Sediments of well Titihaoa-1 range in age from late Pleistocene to middle Miocene (Fig. IV-7). Foraminifera and nannofossils from the drill cuttings have provided precise age determinations between 625 m and total depth (Morgans *et al.*, 1995). The IGNS (Institute of Geological and Nuclear Sciences) micropaleontology laboratory analysed 4 sidewall cores and 246 cutting samples for foraminiferal assemblages. Nannofossils were examined by Stratigraphic Solutions Limited from 4 sidewall cores and 109 cutting samples. Biostratigraphic determinations are based on the standard New Zealand Cenozoic stage classification of Edwards *et al.* (1988). Absolute ages used in this paper refer to the recent New Zealand Cretaceous-Cenozoic Timescale from Cooper *et al.* (2004).

Several datums allow to constraint New Zealand biostratigraphic stages and substages (Fig. IV-7). The Waipipian (late Pliocene) – Opoitian (early Pliocene) boundary (3.6 Ma) is located at *c.* 660 m, the Opoitian - late Kapitean (late Miocene) boundary (5.28 Ma) at *c.* 1210 m, the late Kapitean – early Kapitean (late Miocene) boundary (*c.* 6 Ma) at *c.* 1460 m, the early Kapitean – late Tongaporutuan (late Miocene) boundary (6.5 Ma) at *c.* 1600 m, the late Tongaporutuan – early Tongaporutuan (late Miocene) boundary (*c.* 8.5 Ma) at *c.* 1670 m, the early Tongaporutuan – Waiauan (middle Miocene) boundary (11 Ma) at *c.* 1750 m, the Waiauan – Lillburnian (middle Miocene) boundary (13.2 Ma) at *c.* 1854 m, and the Lillburnian – Clifdenian (middle Miocene) boundary (15.1 Ma) at *c.* 2400 m. The Clifdenian (15.1 – 16 Ma) finally extends to total depth. Concerning the Lillburnian and the Clifdenian, no substages were recognised because the abundance and preservation of microfossils decrease markedly below 2000 m. However, Morgans *et al.* (1995) have suggested that only middle-late Clifdenian sediments are reached at base of the well.

VII) AGE AND SEDIMENTOLOGICAL CHARACTERISTICS OF THE SEISMIC UNITS

Well Titihaoa-1 was drilled on the western flank of a buried structural high, SR2 (Fig. IV-5). The well has penetrated each defined seismic units and has reached the acoustic basement (seismic unit I). With the exception of B6 which is truncated by B7 to the west of the well, and of B9 which do not appear on well logs because it is located above 625 m, each of our seismic unit and sub-unit boundaries are tied precisely on well logs (Fig. IV-8). The adopted ages for the unit boundaries are: B1 *c.* 14.2 Ma, B2 *c.* 13.7 Ma, B3 *c.* 11.3 Ma, B4 *c.* 8.7 Ma, B5 *c.* 6.5 Ma, B7 *c.* 6.2 Ma and B8 *c.* 4.2 Ma. The correlations couldn't allow us to calibrate precisely B6 and B9. However, B6 is between 6.5 and 6.2 Ma and B9 is late Pliocene in age.

The boundaries of seismic units and sub-units were characterized and hierarchized using both wireline logs (gamma-ray and sonic) and the lithostratigraphic and paleobathymetric vertical evolution. Our interpretations of wireline logs permit to characterize the fourth order scale fining-up/coarsening-up pattern within the sedimentary infill of each seismic sub-unit (Fig. IV-8). The boundaries of the fining-up or coarsening-up sequences define new sub-unit internal surfaces that were not identified by our seismic stratigraphy analysis.

For each sub-unit we also calculate a sedimentation rate deduced from biostratigraphic data and from sub-unit vertical thickness estimation from well Titihaoa-1. Sedimentary units have been decompacted by the use of the porosity-depth parameters defined by Sclater & Christie (1980) for each lithologies. Given that some of the sub-units are bounded at top by truncative surfaces, their true sedimentation rates may differ slightly. Indeed, in spite of no major time gap (no missing biozones) identified in the biostratigraphic record (Morgans *et al.*, 1995), important sediment thickness may be missed by erosional processes. We present therefore minimum estimations of sedimentation rates.

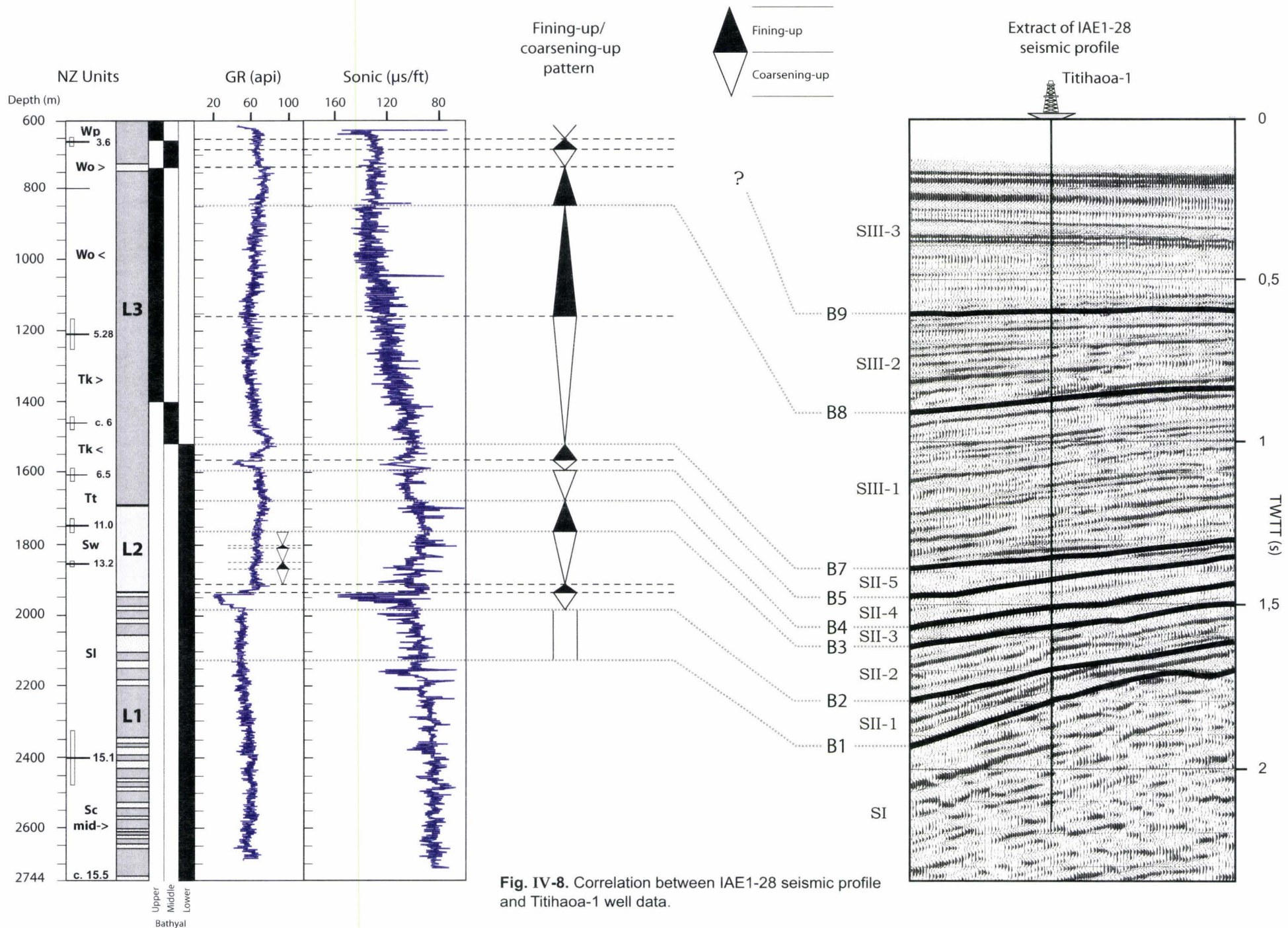


Fig. IV-8. Correlation between IAE1-28 seismic profile and Titihaoa-1 well data.

A) SI - acoustic basement (middle Miocene – stage unknown/SI <, c. age unknown-14.2 Ma)

The upper part of the acoustic basement is middle-late Clifdenian to early Lillburnian in age (Fig. IV-8). This part of the unit contains distal turbidites, deposited at lower bathyal depth, which have close affinities with the basal Miocene turbidites of the onshore *Whakataki Formation* (Biros *et al.*, 1995). Because of intense deformation of the unit, it is questionable to propose a fining-up/coarsening-up pattern for this interval. This overall unit certainly contains older rocks that are not reached by the well. These series are possibly basal Miocene to Cretaceous in age (Field, Uruski *et al.*, 1997). To the west of the profile, a major reverse fault (Turnagain fault, new name) is responsible for the seaward thrusting of an undetermined (age unknown) acoustic basement over basin strata of SII and SIII (Fig. IV-5).

B) SII - ponded sedimentary unit (middle Miocene to late Miocene – SI >/Tk <, c. 14.2-6.2 Ma)

This unit represents 8 Ma and comprises 600 m of sediments (Fig. IV-8), which are ponded between structural ridges (Fig. IV-5). On seismic data, the basal boundary, B1, clearly marks an angular unconformity. However, B1 is not well expressed on well data and no time gap (no missing biozones) was recorded between the acoustic basement and the overlying sedimentary infill (Morgans *et al.*, 1995). The lack of gamma ray or sonic signature (Fig. IV-8) for B1 may be explained by the apparent facies homogeneity (turbidites) through the underlying unit (SI) and the base of the overlying unit (SII-1). Moreover, even if a slight modification of the sedimentation occurred at B1, the poor resolution of facies identification after well-cuttings didn't allow to identify a possible shift of turbidite system. B1 is also not characterized by a bathymetric change but such a change may be not recorded at lower bathyal depth.

Five of the six sedimentary sub-units of SII have been tied on well Titihaoa-1 (Fig. IV-8). These sub-units (SII-1 to SII-5) are 0.3 to 2.6 Ma in duration and present important sedimentation rates variations through time. With the exception of SII-1, which is aggradational, each sub-unit comprises one or several fining-up and/or coarsening-up sequences:

SII-1: 0.5 Ma in duration and 140 m (225 m, decompacted) of sedimentary infill. The sedimentation rate is about 450 m/Ma. This sub-unit is bounded at base by B1 and is characterized by aggradation on wireline logs.

SII-2: 2.4 Ma in duration and 213 m (325 m, decompacted) of sedimentary infill. The sedimentation rate estimate is 135 m/Ma. The basal boundary, B2, is contemporaneous with the base of a coarsening-up sequence. This coarsening-up sequence is characterized by an important decrease of the gamma ray that we interpret as a sand-rich sedimentary body. The lithostratigraphic unit L2 whose base corresponds to a condensed fining-up sequence covers this sandy interval. Then, sedimentation within SII-2 evolves in a second coarsening-up sequence that is also included within L2. Detailed analysis of gamma ray log suggests that the basal coarsening-up of SII-2 also comprises low order sequences.

SII-3: 2.6 Ma in duration and 80 m (120 m, decompacted) of sedimentary infill. The sedimentation rate is around 50 m/Ma. SII-3 is bounded at base by B3, which constitutes the basal limit of a fining-up sequence. This condensed fining-up trend occurs through the entire sub-unit SII-3 and characterizes the upper part of the lithostratigraphic unit L2.

SII-4: 2.2 Ma in duration and 80 m (120 m, decompacted) of sedimentary infill. The sedimentation rate estimate is 55 m/Ma that is very similar to this of SII-3. B4 corresponds to the base of the lithostratigraphic unit L3 and is therefore contemporaneous with a brutal decrease of sediments calcareous content. B4 is overlaid by a condensed coarsening-up sequence that forms the overall sub-unit SII-4.

SII-5: 0.3 Ma in duration and 80 m (120 m, decompacted) of sedimentary infill. The sedimentation rate is about 400 m/Ma. B5 constitutes a basal discontinuity, which shows the brutal development of a coarsening-up sand-rich sedimentary body. SII-5 comprises a complete coarsening-up/fining-up sequence. Depths of deposition are still lower bathyal.

*C) SIII - laterally continuous sedimentary unit (latest Miocene to present day –
Tertiary/Quaternary, c. 6.2-0 Ma)*

This unit is 6.2 Ma in duration and contains 1525 m of sedimentary series (Fig. IV-8). The basal boundary (B7) marks a rapid shallowing from lower bathyal to middle bathyal depths. This transition is accompanied by the development of a coarsening-up sequence consistent with the progradation of SIII-1 sedimentary system as identified on seismic profiles (Fig. IV-5). Sub-units within SIII are around 2 Ma in duration and none of them are condensed. As for SII, each sub-unit may be sub-divided in fining-up and coarsening-up sequences (Fig. IV-8).

SIII-1: 2 Ma in duration and 670 m (900 m, decompacted) of sedimentary infill. The sedimentation rate estimate is 400 to 450 m/Ma, the highest recorded for the whole sedimentary succession within well Titihaoa-1. The sub-unit basal boundary is B7 as described previously. SIII-1 comprises a complete coarsening-up/fining-up sequence. A shallowing event, from middle bathyal to upper bathyal depths, occurred during deposition of the basal part of the coarsening-up sequence.

SIII-2 and SIII-3: 4.2 Ma in duration for the whole two sub-units and a total thickness of 825 m (925 m, decompacted). The mean sedimentation rate for both units is in the order of 200 m/Ma. B8 is a seismic discontinuity between two fining-up sequences. The base of SIII-2 shows a succession of fining-up/coarsening up sequences that are contemporaneous with rapid bathymetric changes, from upper bathyal to middle bathyal and from middle bathyal to upper bathyal. The deepening event is associated to a lithologic discontinuity, which is described by *Biros et al.* (1995) as a probable hiatus with minor sandy lithology and scattered glauconite grains. Despite this deepening, the discontinuity is overlaid by a coarsening-up sequence.

VIII) DISCUSSION

A) Deformational processes and stratigraphic evolution of the Titihaoa area

Our seismic and stratigraphic analysis over the Titihaoa area shows that the seismic unit SII is clearly a syntectonic sedimentary unit deposited in middle – late Miocene (c. 14.2 – 6.2 Ma) ponded basins (Fig. IV-5; basins “a”, “b”, “c”, and “d”). These basins develop above an acoustic basement in relation with the growth of anticline ridges. The acoustic basement incorporates middle Miocene (c. 15.5 - 14.2 Ma) and maybe older syn-subduction sediments (Field, Uruski *et al.*, 1997). Therefore, in the study area, the depositional environments that have existed from the onset of subduction to B1 (c. 25 – 14.2 Ma) cannot be constrained. The end of the confined basin infill is marked by a major angular unconformity (B7, c. 6.2 Ma) that also corresponds to a brutal change in depositional environments.

1) The Miocene Titihaoa Basin (basin “a”)

Because sedimentary series of basin “a” are penetrated by well Titihaoa-1 (Fig. IV-5), we have named it *Titihaoa basin*. The Titihaoa basin is located about 10 km offshore East Coast (Fig. IV-3). The basal infill of the Titihaoa basin is characterized by a westward thickening of seismic sub-units away from its eastern border, SR2 (Fig. IV-5). The bases and tops of seismic sub-units are angular unconformities associated to a landward tilt of depositional surfaces in close proximity of SR2 (Fig. IV-6 – enlargement 2). The sub-units are clearly syn-tectonic and associated to the growth of SR2, which forms the eastern edge of the Titihaoa basin. Deformation of SR2 seems to have occurred at least till B4 (c. 8.7 Ma) that is the youngest surface characterized by toplaps (Fig. IV-6 – enlargement 2).

The western border of the Titihaoa basin is more difficult to identify clearly, because of recent (post-Pliocene) tectonic activity. However, the angular unconformity of SII-6 (B6) above SII-5 and SII-4 (Fig. IV-6 – enlargement 2) suggests that the Turnagain Fault zone is responsible for folding of SII sedimentary series before B6 (c. 6.4 – 6.3 Ma). Then, the reverse motion has stopped and unconformable deposition of SII-6 occurred. During early and middle Miocene, the Cape Turnagain Structural High (now emerged, Fig. IV-3) has formed the eastern edge of the onshore Akitio basin (Bailleul *et al.*, submitted). Its uplift was recorded in the Akitio basin at c. 17.5 Ma. If the Turnagain Fault is responsible for this uplift, its reverse motion may have occurred as soon as c. 17.5 Ma. Nevertheless, the Cape

Turnagain Structural High may have also constituted the western edge of the Titihaoa basin during middle-late Miocene. The landward tilting of B6 may translate a renewal of SR2 deformation to the east of the Titihaoa basin.

Early deformation of the Titihaoa basin also includes the development of SR1, which is responsible for the division of the early Titihaoa basin into two sub-basins (Fig. IV-6 – enlargement 2). This deformation occurred during deposition of SII-1 that forms an anticline above SR1. The erosional surface (B2) on top of that anticline shows that deformation of SR1 stopped before *c.* 13.7 Ma.

Considering that the Titihaoa basin hasn't undergone much shortening and that SR2 and the Turnagain Fault have constituted its borders during its sedimentary evolution, we show that the late Miocene Titihaoa basin was about 5 km wide.

2) Development of eastern Miocene basins (basins “b”, “c” and “d”)

In the Eastern part of IAE1-28 seismic line, the first sediments observed above the acoustic basement (basin “b”) are localized on the eastern side of SR2 and onlap on the acoustic basement (B1) toward the east (Figs IV-5 and IV-6 – enlargement 1). Basin “b” forms a small depression between SR2 to the west and SR3 to the east. Sedimentary series of basin “b” are seaward tilted, probably in association with the growth of SR2. This suggests that uplift of SR3 stops before that of SR2, during deposition of SII-1. Then, SR3 is progressively drowned, by the eastward onlap of SII-2 sedimentary series. This is followed by an eastward migration of depot-centres with the shift of sedimentation to basin “c” then to basin “d”. These basins therefore present a westward migration of their sedimentary infill. The eastward migration of depot-centres seems to be related to the development to the east of a structural ridge (SR4) that succeeds to SR3 as an eastern basin edge. The growth of SR4 provokes synclinal folding of SII-3 sedimentary unit. Nevertheless, sedimentary units within basin “c” and “d” are bounded by angular unconformities (B3, B4, and B5), sometimes deformed (B4). All these observations suggest that the location of depot-centre is controlled by the development of basin borders. At base of basin “c”, the western edge of the basin corresponds to SR3. Then, SR3 is rapidly drowned and the depositional environment becomes more open to the west with SR2, then the Cape Turnagain structural high, constituting the western edge of the subsequent sedimentation area.

3) The Plio-Quaternary Turnagain slope basin

B7 (*c.* 6.2 Ma) is a major angular and erosional unconformity, which is contemporaneous with an important change in depositional environments. Indeed, all middle-late Miocene ponded basins, as well as some of their borders, are drowned (Fig. IV-5). The sedimentation over B7 reveals an important enlargement of the sedimentary domain (the Turnagain slope basin) with westward progradation of thick sedimentary series. The B7 event is accompanied by a rapid shallowing from lower bathyal to middle bathyal depths in association with the development of a coarsening-up sequence (Fig. IV-8). This suggests that, if local relative subsidence occurred within the large Plio-Quaternary basin, global uplift of the whole margin may still continue. However, this shallowing may also have occurred during global moderate margin subsidence, reflecting the very high sedimentation rates (400 – 450 m/Ma) which has led to the filling-up of the Turnagain basin.

The sedimentary unit SIII shows synclinal folding to the west, probably related to recent motion on the Turnagain Fault (Fig. IV-5). This suggests that the Cape Turnagain High may still constitute the western edge of the Turnagain large sedimentary domain. To the East, the eastern border of the Turnagain basin is not visible on profile IAE1-28 but may correspond to the deformed edge of the shelf (Fig. IV-3). In this case, the basin was about 40 km wide during the Plio-Quaternary. Nevertheless, the infill of the Turnagain basin comprises two unconformities, B8 and B9 (Fig. IV-5). These unconformities are locally angular, notably above SR2 structural ridge (Figs IV-5 and IV-6 – enlargement 3). Considering the location of the erosion of surfaces and the absence of global eustatic events contemporaneously with these unconformities, these geometries may be attributed to a late stage of SR2 development. This deformation affects the Plio-Quaternary Turnagain basin and is responsible for slight folding of its sedimentary series. The growth of this recent anticline above SR2 could be responsible for normal faulting on the eastern limb of SR2 (Fig. IV-5). Implied processes may be gravitational collapse of recently deposited poorly indurated sediments.

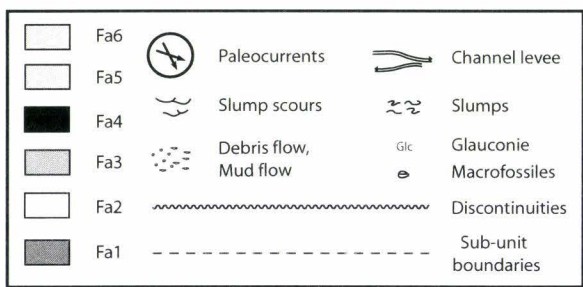
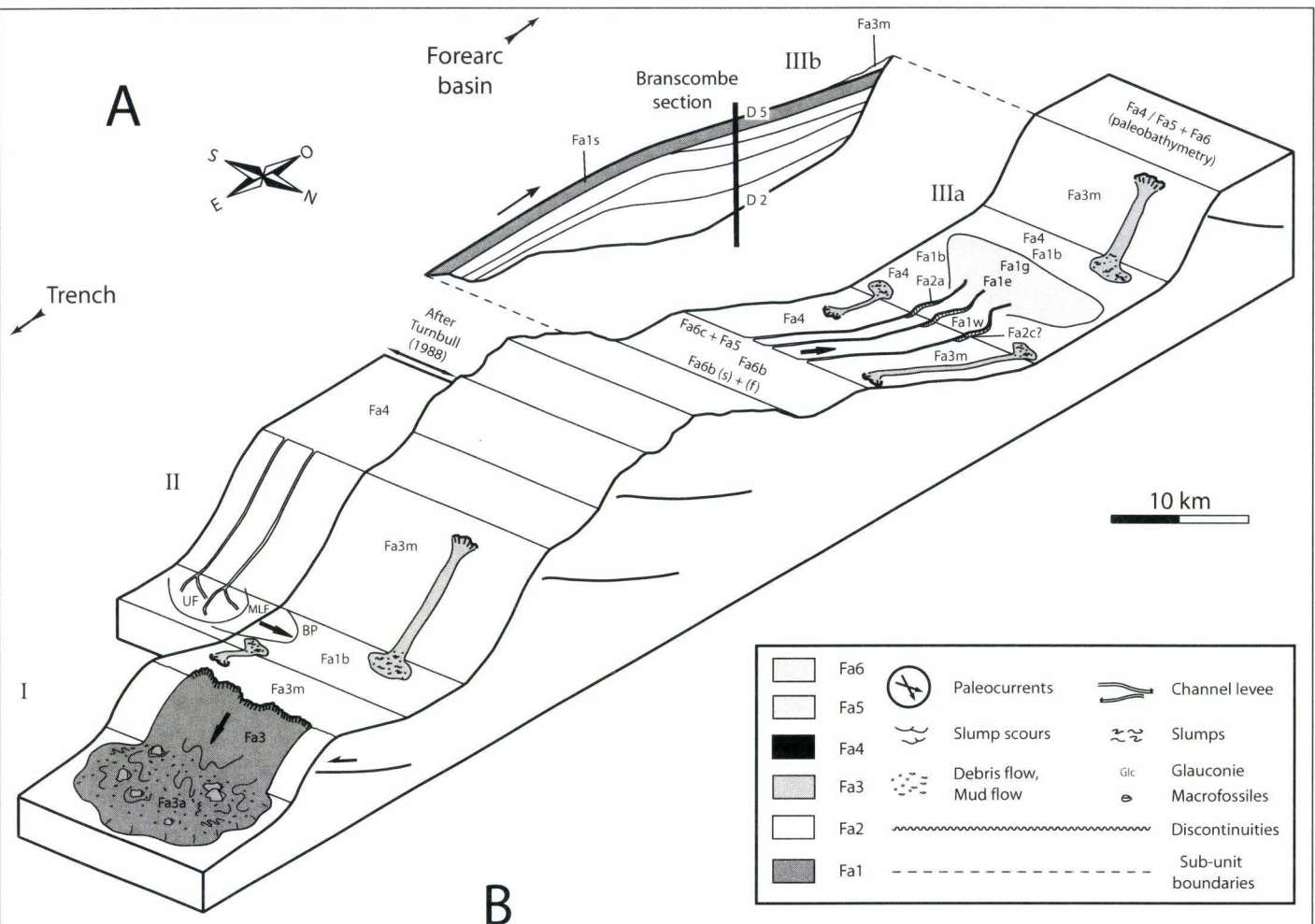
*B) Comparison of the offshore Titihaoa basin with
an older onshore analogue, the Akitio basin*

Our study of the offshore seismic survey shows that the seismic unit SII corresponds to the infill of trench-slope basins (Fig. IV-5; basins “a” – the Titihaoa basin, “b”, “c” and “d”) ponded between structural ridges (Fig. IV-5; Cape Turnagain structural high to SR4). The Titihaoa trench-slope basin (basin “a”) structural and stratigraphic evolution is well constrained by both seismic coverage (Figs IV-5 and IV-6 – enlargement 2) and well data (Fig. IV-8). We propose here to compare its development with the evolution of the very similar Akitio trench-slope basin located on the same transect, onshore (Fig. IV-9). Because these basins are not of the same age, we didn’t propose correlations between the two basins but a comparison of their stratigraphic architecture (which comprises in both cases unusual very fine grained facies) and of their mode of deformation (Fig. IV-10).

1) The onshore Miocene Akitio basin

In the north-eastern Wairarapa (Coastal Ranges), the recent uplift of the subduction wedge is responsible for the emersion of thick Miocene turbidite series. These sediments crop out within elongated wide synclines overlying pre-subduction basement units (Fig. IV-3). In the Akitio syncline (Fig. IV-3), middle to upper bathyal turbidite formations were deposited in the Akitio trench-slope basin during early and middle Miocene (*c.* 24 – 13 Ma; Fig. IV-9; Bailleul *et al.*, submitted). In the Pongaroa area (Fig. IV-3), the high resolution study of the sedimentary record (identification of the main sedimentary discontinuities, reconstitution of the geometry of the sedimentary units, and paleocurrents analysis) has given accurate evaluation of the spatial and temporal contribution of tectonic activity on the development and stratigraphic evolution of the Akitio trench-slope basin (Fig. IV-9; Bailleul *et al.*, submitted). This work has permitted to propose a structural and stratigraphic scheme for the evolution of this basin and its borders.

Because the deep sea deposits are unusually very fine grained, a new facies model (Table III-1) for lower trench-slope setting has been proposed and comprises four main facies associations (Fa1 to Fa4). Two facies associations (Fa5 and Fa6) were also identified for shelf deposits (Table III-2). Deep sea facies associations (Table III-1) are representative of three main depositional systems, which may develop during trench-slope basin evolution (Fig. IV-9).



B

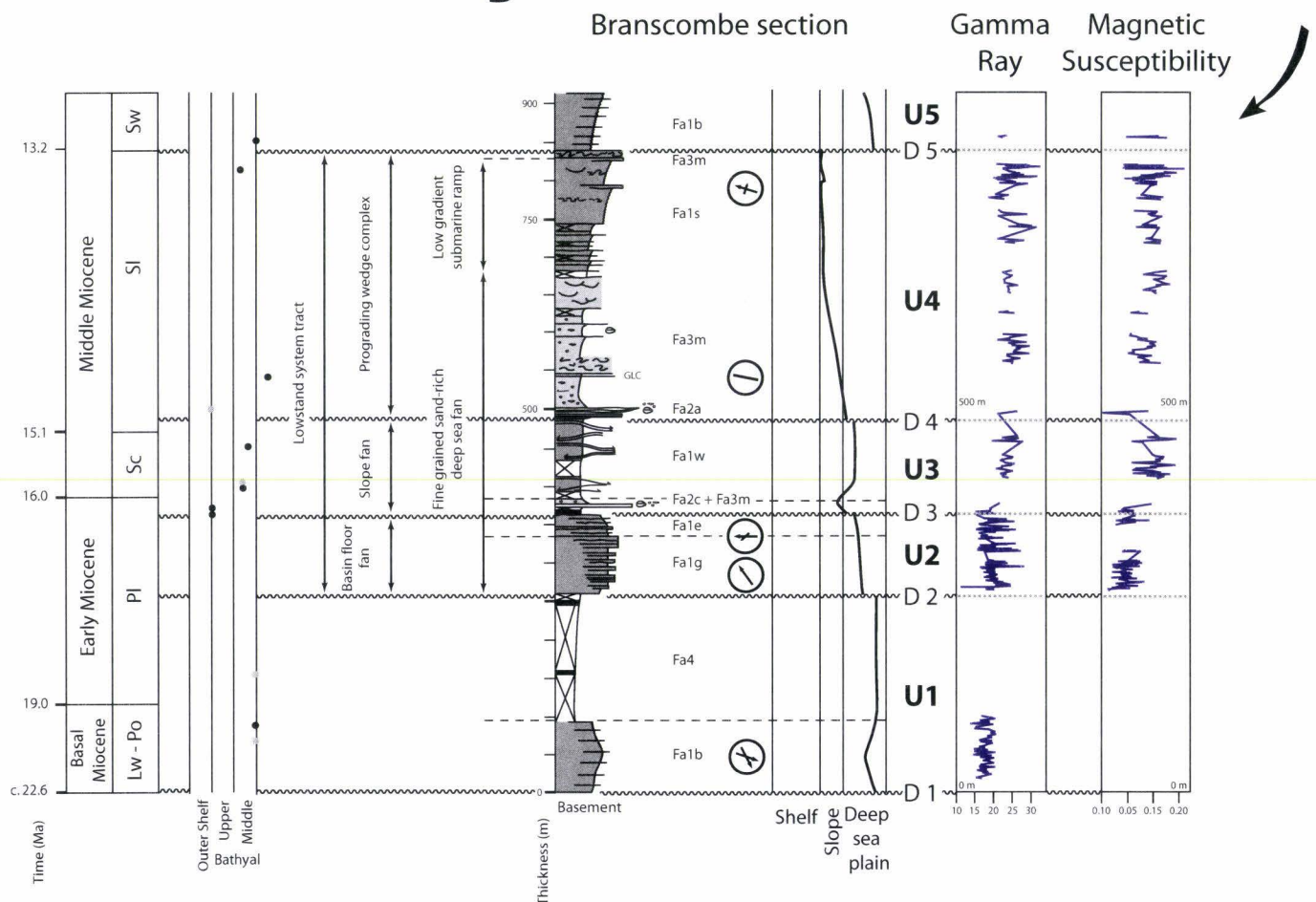


Fig. IV-9. A - Depositional model for trench-slope settings. I - olistostrome deposition related to active thrusting during the onset of subduction at 25 Ma. II - sub-marine fan model in a juvenile trench - slope basin (basal Miocene), from coastal exposures east of the Akitio basin (Castlepoint area), after Turnbull (1988), UF - Upper Fan, MLF - Mid to Lower Fan, BP - Basin Plain. IIIa - the Akitio mature trench-slope basin (Bailleul *et al.*, submitted; see chapter III of this manuscript), note the emersion of the trenchward margin of the basin (*i.e.* Cape Turnagain structural ridge, probably controlled by the main thrust faults: the Tinui Fault, the Whakataki Fault and the Turnagain Fault) which permits the development of a westward prograding turbidite system, IIIb - early-middle Miocene sedimentary infill of the trench-slope basin. **B** - Major discontinuities and correlations of the Branscombe sedimentological section (see text for abbreviations and explanations). Refer to figure IV-1 for location, and tables III-1 for facies code.

The first one corresponds to large submarine slides leading to deposition of local olistostromes at base of a slope (Fa3a). This depositional system generally marks early stages of basin development and is related to active thrust faulting during nappes emplacement episodes. Following this, the sedimentary pattern during the basin fill evolution is dominated by morphologic components of fine grained sand-rich submarine fans (Reading and Richards, 1994; Richards *et al.*, 1998). This includes distal basin plain facies associations (Fa1b + distal Fa4), depositional lobes (Fa1g), channel – lobe transitions (Fa1e); channel levee complexes (Fa1w) and small channels (Fa2a + Fa2c). Mud-rich slope facies associations (Fa3m) and sand-rich slope facies associations (Fa3s) are common and point out the important contribution of slope processes to the basin sediment budget in such a depositional setting. The third depositional system is a low gradient submarine ramp with sheet like turbidite (Fa1s), derived from unconfined turbidity currents, characterizing a late stage of the trench-slope basin fill. This filling-up megasequence constitutes a lowstand system tract, which may be subdivided into basin floor fan, slope fan and prograding wedge complex.

Bailleul *et al.* (submitted) have also demonstrated that brutal facies changes (*e.g.* drowning of a mixed carbonaceous/siliciclastic shelf by basin plain facies associations) characterized five major discontinuities (Fig. IV-9B; D1 to D5) which are related to regional tectonic events (*i.e.* onset of subduction at 25 Ma, beginning of regional subsidence at 15 Ma) or local tectonic events (*i.e.* local uplift of structural ridges on the edges of the Akitio trench-slope basin at 17.5 Ma and 16.5 Ma, local acceleration of subsidence at 13.2 Ma). The tectonic control is apparently mainly expressed by slope creations leading to inversions of the vergence of sedimentary systems, by changes in turbidite facies, and by the creation of new sediment sources. Moreover, we have showed that the timing of development of some lowstand system tracts (*i.e.* of slope fans and of prograding wedge complexes) may also be largely controlled by changes in style and/or amplitude of tectonic activity.

These results concerning the onshore Akitio trench-slope basin may be compared to this analysis of the offshore Titihaoa trench-slope basin (Fig. IV-10) allowing a multidisciplinary analysis of tectonically active ponded basins, from the scale of facies on outcrops to this of seismic units.

NW

Onshore: Akitio basin (c. 17.5 - 13.2 Ma)

Offshore: Titihaoa basin (c. 13.7 - 6.2 Ma)

SE

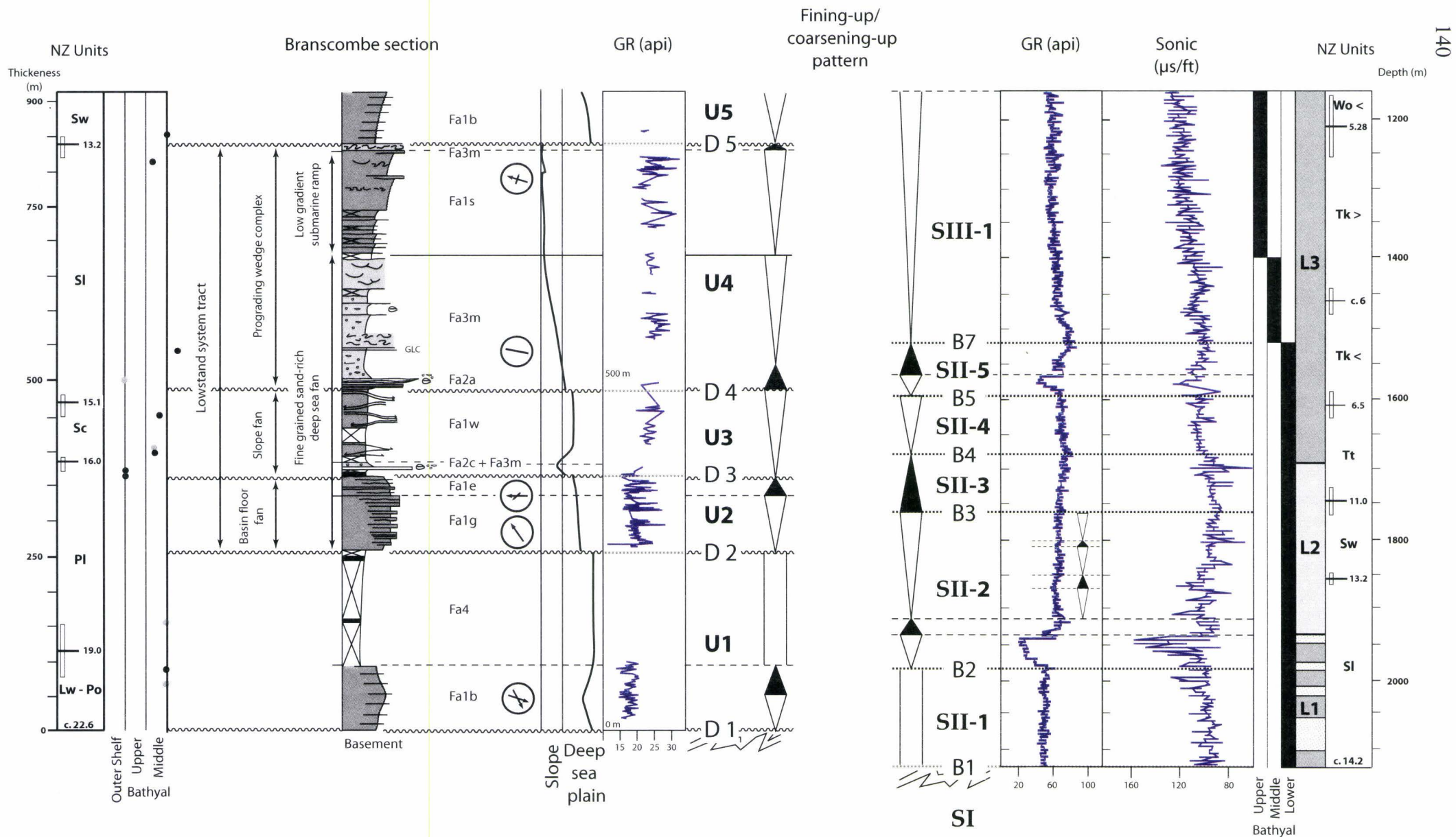


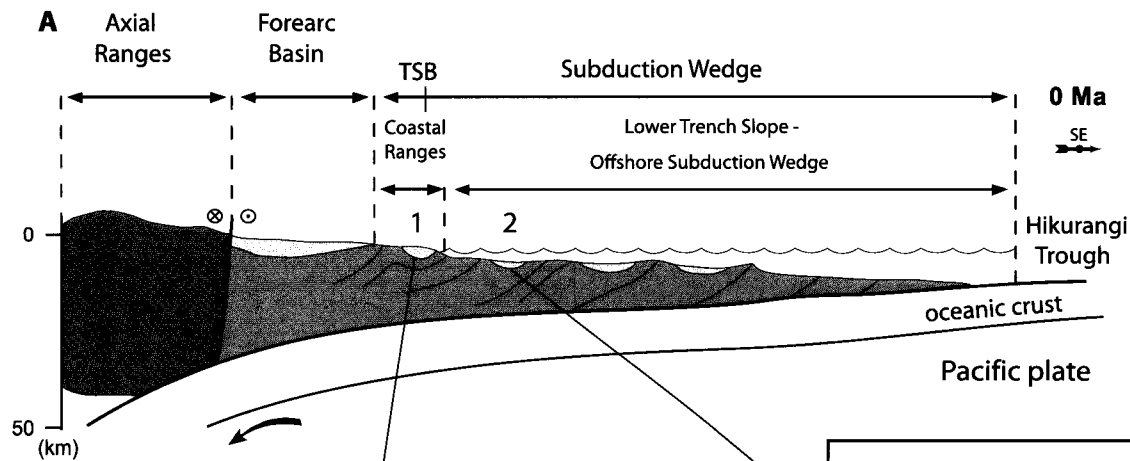
Fig.IV-10. Comparison between the Akitio onshore trench-slope basin and the younger Titihaoa offshore trench-slope basin. See figure IV-9B for legend of the Branscombe section and table III-1 for facies code.

2) Comparison with the Titihaoa offshore basin

a) Basal and upper boundaries of the basin infills

Onshore the Akitio basin develops from 17.5 to 13.2 Ma and contains 580 m of turbiditic fine-grained sediments deposited in 4.3 Ma (Figs IV-9 and IV-10). Offshore, the Titihaoa basin is a younger long-lived trench-slope basins, also characterized by very fine grained sedimentation. The Titihaoa basin total thickness is at least 460 m deposited in 7.5 Ma, from *c.* 13.7 to 6.2 Ma (Fig. IV-10). These new dating of basin limits suggest that the beginning of the Titihaoa basin development is approximately contemporaneous with the end of the Akitio basin filling (Fig. IV-11). This gives that the last highly confined trench-slope basins preserved before enlargement of sedimentary domains are younger to the East (closer to the subduction front) than to the West (closer to the trench-slope break). This eastward youngening of confined basin preservation is accompanied by a youngening of the acoustic basement. Indeed, we noticed offshore that B1 marks the base of the sedimentation over a highly deformed and faulted acoustic basement (Fig. IV-5). Onshore, the surface D1 is equivalent with deposition of distal turbidites (Fa1b) over the Cretaceous to Oligocene deformed series of the faulted Coastal Block (Fig. IV-10). In its upper part, the basement of the Titihaoa basin incorporates youngest rocks (middle Miocene for the youngest) than those of the Akitio basin (Oligocene for the youngest). All these observations suggest that deformation of bounding bathymetric highs at the origin of trench-slope basins containment may has continued to the east during late Miocene while it has stopped to the west during middle Miocene (Fig. IV-11). However, as we don't know the depositional environments before the development of the Titihaoa basin, we can't conclude about a possible eastward migration through time of depot-centres. The recognition of basal and upper boundaries of both onshore and offshore trench-slope basins allows better constraints on the characteristics and significance of these basin limits.

Onshore, the base of the Akitio basin (as a confined basin) is characterized by D2 (Fig. IV-10). D2 marks a major paleogeographic change characterized by the inversion of paleocurrents and development of a thick sand-rich sedimentary body. This surface may also correspond to an angular unconformity between U1 (dipping 40-45°W at base) and U2 (dipping 20-25°W). Unfortunately, the top of U1 is composed of massive siltstones and the inferred unconformable contact is therefore not visible on field.

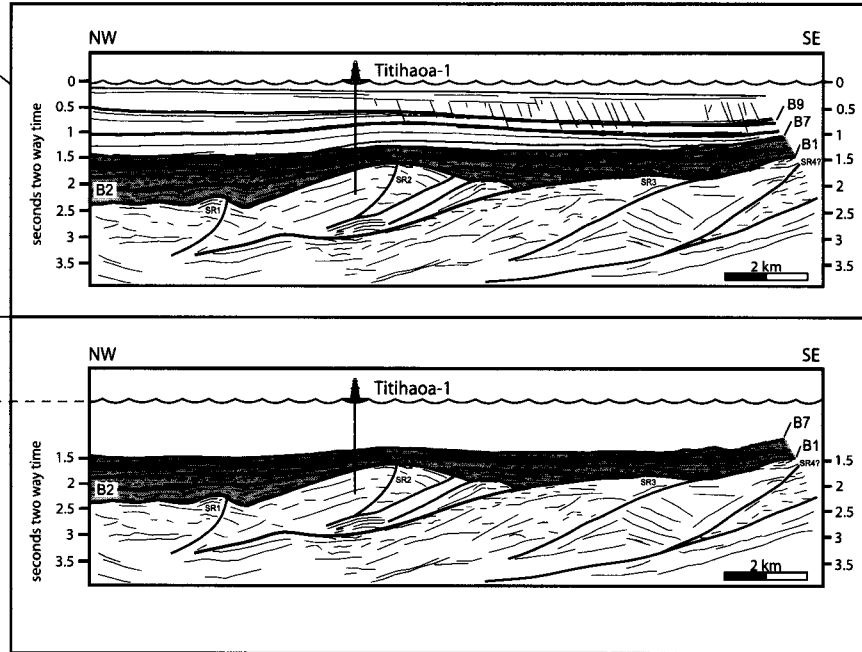
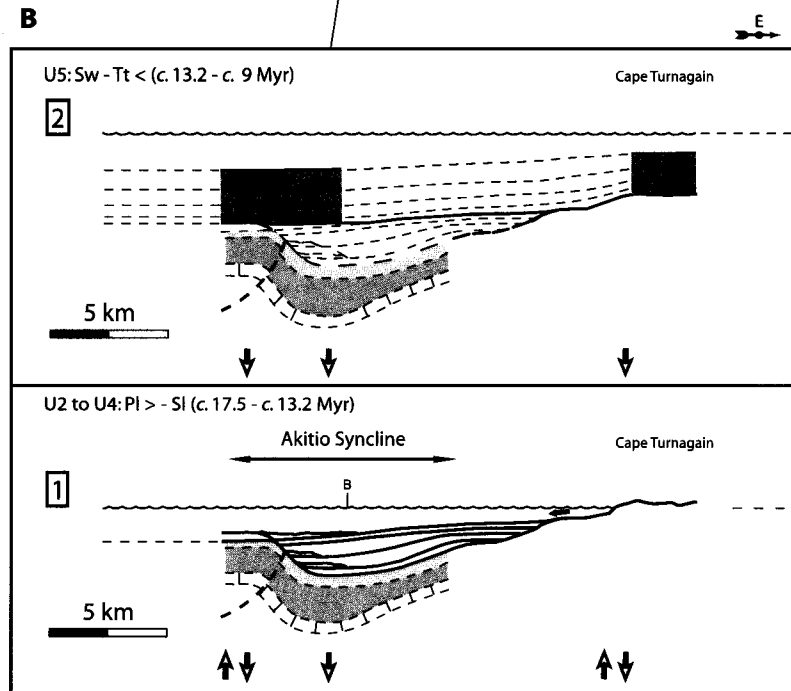


Onset of subduction (25 Ma) Feeding directions

Uplift / Subsidence

SIII
 SII
 SI

Fig.IV-11. Location and ages of trench-slope basins on the lower trench slope of the Hikurangi active margin. **A** - general cross section of the Hikurangi margin (TSB - trench-slope break), **B** - Middle and late Miocene cross-sections of the onshore Akitio basin (B - Branscombe vertical section, U2 to U5 - sedimentary units identified in the Branscombe vertical section, see Fig.IV-9B), **C** - Late Miocene and Plio-Quaternary line drawings (from IAE1-28 seismic profile) of the offshore Titihaoa basin (B1 to B9 - seismic units and sub-units boundaries, SR1 to SR4 - structural ridges).



CHRONOSTRATIGRAPHY		Time in Ma
NZ Stages	International Units	
Wg	0.34	QUATERNARY
Wc	1.71	
Wn	2.40	
Wm	3.03	
Wp	3.60	PLIOCENE
Wo	5.28	
Tk	6.50	UPPER
Tt	11.00	
Sw	13.20	MIDDLE
SI	15.10	
Sc	16.00	LOWER
PI	19.00	
Po	21.70	
Lw	25.20	

The rapid change in dipping between the two units is however probably an expression of such an angular unconformity, more than just a change in dipping related to recent folding of the Akitio area.

Offshore, B2 is a surface that presents strong similarities with D2. Indeed, B2 shows a landward tilting, erosion and the subsequent installation of sandy sediments (Figs IV-5, IV-6 – enlargement 2, and IV-10). We attribute this landward tilting to the growth of SR2 that is consistent with our onshore interpretation of D2 *i.e.* development of a structural ridge to the east of the Akitio sedimentation area (Cape Turnagain Structural High). These similarities between D2 and B2 suggest that, even if the uplift of the offshore structural ridge SR2 apparently begins before B2 (*i.e.* deformation occurs during deposition of SII-1), B2 really marks the development of SR2 as a well defined basin edge (Fig. IV-5). This seems to be confirmed by the deposition above B2 of the most condensed sedimentary sub-units of well Titihaoa-1 (Fig. 8). Indeed, this may traduces by-pass processes on the westward slope of the bathymetric high.

The end of the Akitio onshore trench-slope basin filling is marked by D5 (Fig. IV-10). D5 marks a rapid subsidence, contemporaneous with an abrupt deepening, that precedes deposition of thick prograding turbidite series. This subsequent sedimentation corresponds to more than 1000 m of late Miocene distal turbidites (Fa1b) and massive siltstones (Fa4). Offshore, the Titihaoa basin upper boundary is also characterized by the progradation of thick sedimentary series (SIII, Fig. IV-5) over a major discontinuity (B7, Fig. IV-10) that sealed the Miocene ponded basins and their structural edges. However, as it is contemporaneous with a rapid shallowing, B7 differs from the Akitio basin upper boundary (D5). Nevertheless, in both cases, the basins upper boundary corresponds to a major discontinuity, which sealed the basins and their bounding structural highs (Fig. IV-11). This discontinuity is angular (as outline on seismic profile IAE1-28, Fig. IV-5) and announced a brutal enlargement of depositional domains where deposition of thick prograding sedimentary series occurred. The onshore facies analysis shows that first sediments deposited in the larger basin are characterized by more distal turbidite facies (Fa1b) than the last facies ponded in the trench-slope basins (Fa1s-Fa3m). This reflects a relocation of sediment sources further from depositional areas.

b) Basins stratigraphic architecture and deformation

The filling of both basins comprises sedimentary units composed of fourth order scale fining-up and coarsening-up sequences (Fig. IV-10). The stratigraphic succession is disrupted by several discontinuities. Onshore, these discontinuities are characterized by rapid shift of facies and paleoenvironmental changes (pointed out by inversions of paleocurrent and of facies proximal-distal signature). Offshore, the discontinuities show landward or seaward tilting as well as erosions and local angular unconformities (Figs IV-5 and IV-6 – enlargement 2). In both cases, these surfaces are related to tectonic activity associated to the growth of bounding structural ridges. Onshore this has been demonstrated (Bailleul *et al.*, submitted) that the development of basin borders leads to slope creations or modifications that strongly influenced sedimentary systems (inversions of the vergence of sedimentary systems, changes in turbidite facies, creation of new sediment sources). Offshore, this structural and sedimentary evolution is associated to tilting of depositional surfaces which are determined by the development of bounding structural highs. These tiltings are responsible in particular for the location of depot-centres within the basins and therefore control their migrations through time. As long as the structural ridges develop, slopes are regularly rejuvenated favouring progradation of the sedimentary systems in association with high sedimentary flux.

The duration of the sedimentary units bounded by discontinuities of tectonic origin is from 0.5 to 2.5 Ma offshore, and from 1 to 2 Ma onshore (Fig. IV-10). This suggests that the development of the trench-slope basins on the Hikurangi active margin is controlled by tectonic pulsations affecting their edges each 1 or 2 Ma.

The fourth order scale fining-up/coarsening-up pattern within the basins shows that they are dominated by coarsening-up trends (Fig. IV-10). This partitioning between coarsening-up and fining-up sequences reflects the strong influence of filling processes, related to important sedimentary flux, during the basin development. We also notice that the fining-up sequences are slightly more expressed in the Titihaoa basin than in the Akitio basin (Fig. IV-10). This may be traduced in terms of proximal/distal signature for trench-slope basins which seems to be always dominated by coarsening-up sequences but with an increase of fining-up sequences preservation distally from terrigenous sources.

c) Facies

The comparison of our data between the onshore and offshore domains may also help in the interpretation of offshore facies. For example, the first coarsening-up/fining-up sequence at base of both basins (sedimentary unit U2 onshore and base of sedimentary unit SII-2 offshore) is characterized by deposition of a sand-rich sedimentary body overlaid by a condensed interval (Fig. IV-10). Considering these similarities and by analogy with our facies analysis onshore, we interpret the first offshore coarsening-up sequence as a depositional lobe (Fa1g) overlaid by fining-up by-pass facies (Fa1e).

IX) CONCLUSIONS

The structure of the offshore Wairarapa shelf shows a succession of acoustic basement ridges which bound middle-late Miocene (*c.* 13.7 – 6.2 Ma) confined trench-slope basins. The geometry and the evolution of these narrow basins, as well as the unusual very fine grained sedimentation, are very similar to those of older (*c.* 17.5 – 13.2 Ma) onshore analogues, known in outcrops in the Wairarapa region. The detailed study of the Titihaoa (offshore) and of the Akitio (onshore) highly confined trench-slope basins shows that:

1) These basins are bounded by growing submarine structural ridges that control their shape and size. The first sediments ponded between these structural highs constitute deformed sedimentary sequences, which develop between the underlying more deformed basement and the overlying unconformable trench-slope basins.

2) The basal limit of the basins corresponds to a landward tilted angular unconformity resulting from the development of bounding structural ridges. This basal angular unconformity is overlain by the settlement of well organised turbidite systems (fine grained sand-rich submarine fans). At this stage, trench-slope basins eastern structural ridges constitute well defined basin edges on their oceanic borders. This early stage of basin development is accompanied by modifications of paleocurrents traducing the major paleogeographic changes related to the deformation of the subduction wedge.

3) The infill of trench-slope basins is disrupted by landward or seaward tilted surfaces, sometimes erosional, and characterized by local angular unconformities near major structural ridges. These unconformities are related to the growth of structural ridges and are associated to rapid shift of facies and paleoenvironmental changes (pointed out by inversions of paleocurrents and of facies proximal-distal signature). Thus, the development of basin borders leads to slope creations or modifications that strongly influenced sedimentary systems (inversions of the vergence of sedimentary systems, changes in turbidite facies, creation of new sediment sources). As long as the structural ridges develops, slopes are regularly rejuvenated favouring progradation of the sedimentary systems in association with high sedimentary flux.

4) Unconformities within the basin infill define their main sedimentary/seismic units. The mean duration of these sedimentary units is 1 to 2 Myr. This suggests that tectonic pulses which affect basin borders have occurred every 1 or 2 Ma.

5) The fourth order scale fining-up/coarsening-up pattern within the sedimentary units shows that the studied basins are dominated by coarsening-up trends. This partitioning between coarsening-up and fining-up sequences reflects the strong influence of filling processes, related to important sedimentary flux, during the basin development.

6) The narrow trench-slope basins, as well as their borders, are sealed by a major angular unconformity (*c.* 6.2 Ma offshore and *c.* 13.2 Ma onshore) which marks the end of their filling-up before important enlargement of depositional domains. This reflects the stop of structural highs development and a relocation of sediment sources further from depositional areas. However, structural ridges may be reactivated later, provoking slight folding and local angular unconformities within the more recent and less deformed infill of the overlying larger slope basins.

7) Finally, at the margin scale, the last narrow trench-slope basins preserved before enlargement of sedimentary environments are younger to the East (closer to the subduction front) than to the West (closer to the trench-slope break). This eastward youngening of basin preservation is accompanied by a youngening of the acoustic basement. All these observations suggest that deformation of bounding bathymetric highs at the origin of trench-slope basins containment may have continued to the east during late Miocene while it has stopped to the west during middle Miocene.

ACKNOWLEDGEMENTS

This work has benefited from our discussions with Brad Field and Andy Nicol on the North Island geology and with François Guillocheau on the turbidite facies and sedimentary systems. We thank gratefully Christophe Buret for its efficient work during field trips. We also acknowledge Alan Beu and Hugh Morgans, who have dated respectively the macrofossils and foraminifera that we have sampled on field in the Akitio basin. Without the technical support and the free access to the New Zealand Fossil Record File given by the Institute of Geological and Nuclear Sciences (Lower Hutt, New Zealand), this work could not have been possible. We are grateful to the Wardle family for their warm friendship during our stays at Glenross lodge. This research was supported by the BQR PhD student mobility program of the Université des Sciences et Technologies de Lille 1, by the french research group GDR marges, and UMR-CNRS 8110 (Processus et Bilan des Domaines Sédimentaires).

Chapitre V

Déformation discontinue d'un prisme de subduction : Evolution de la marge Hikurangi (Nouvelle-Zélande) au cours des dernier 25 Ma

Keywords: trench-slope basins, seismic stratigraphy, stratigraphy, deformation analysis, subduction wedge, subduction, Hikurangi margin, New Zealand.

Mots clefs: bassins perchés, stratigraphie sismique, stratigraphie, analyse de la déformation, prisme de subduction, subduction, marge Hikurangi, Nouvelle-Zélande.

Deformation of the lower trench-slope in a subduction setting for the last 25 Myr: Hikurangi margin, New Zealand

Julien Bailleul⁽¹⁾, Frank Chanier⁽¹⁾, Jacky Ferrière⁽¹⁾, *et al.*

¹ UMR Processus et Bilan des Domaines Sédimentaires, Université des Sciences et Technologies de Lille1, France
e-mail : julien.bailleul@ed.univ-lille1.fr

ABSTRACT

The stratigraphic and structural analysis of a complete transect of the Hikurangi convergent margin (eastern North Island, New Zealand), based on both offshore and onshore data, permitted to constrain the tectonic evolution of the Hikurangi subduction wedge since the onset of subduction, 25 Myr ago. Three main morpho-structural domains may be distinguished within the Hikurangi subduction wedge. These are, from the trench to the forearc basin, the accretionary prism *sensu-stricto*, the Wairarapa shelf and the present-day emerged trench-slope break of the Hikurangi margin (Coastal Ranges). The differences between these domains are to relate to both their difference in age and their relative position in the subduction wedge trough times. The boundaries between the present-day morpho-structural domains correspond to major thrust faults, related to the subduction-related shortening episodes, such the Whakataki, Turnagain and Shelf Edge Faults. These Faults had controlled the growth of structural ridges (the Cape Turnagain Structural High and the Shelf Edge Structural High) that have bounded Mio-Pliocene slope basins: the highly confined Akitio and Titihaoa trench-slope basins, and the large Tawhero and Turnagain slope basins. The Turnagain fault zone and the Shelf Edge fault zone have been reactivated during the most recent contractional episode. The location of these major fault zones coincides with present-day geographic boundaries: the Wairarapa coast-line and the Wairarapa shelf edge.

The evolution of the Hikurangi subduction wedge is discontinuous and was controlled by successive tectonic periods identified across the Akitio transect: **1)** A basal Miocene phase of nappes emplacement (*c.* 25 – *c.* 18 Ma), **2)** An early-middle Miocene E-W compressional episode responsible for the development of structural highs and trench-slope basins (*c.* 17.5 – *c.* 15 Ma), **3)** A major subsidence episode associated with extensional deformation (*c.* 15 – *c.* 6.5 Ma) and probably related to tectonic erosion, and **4)** a latest Miocene-Quaternary period dominated by short-term (*c.* 1 Ma) episodes of E-W to NW-SE shortening (*c.* 6.5 – *c.* 0 Ma). That last tectonic period is accompanied by overall uplift of the margin leading to the emersion of the inner subduction wedge during the Quaternary. Changes in the tectonic

regime may have been induced by modifications of the terrigenous flux within the Hikurangi Trough or by variations in thickness and coupling of the downgoing slab. We demonstrate that the complex structural pattern of the Hikurangi subduction wedge results not only from this polyphased tectonic history, but also from transverse variations in style and amplitude of the deformation during a single tectonic episode. We show notably that some frontal accretion can occur close to the subduction front while extensional deformation and subsidence develops upslope during the period of tectonic erosion.

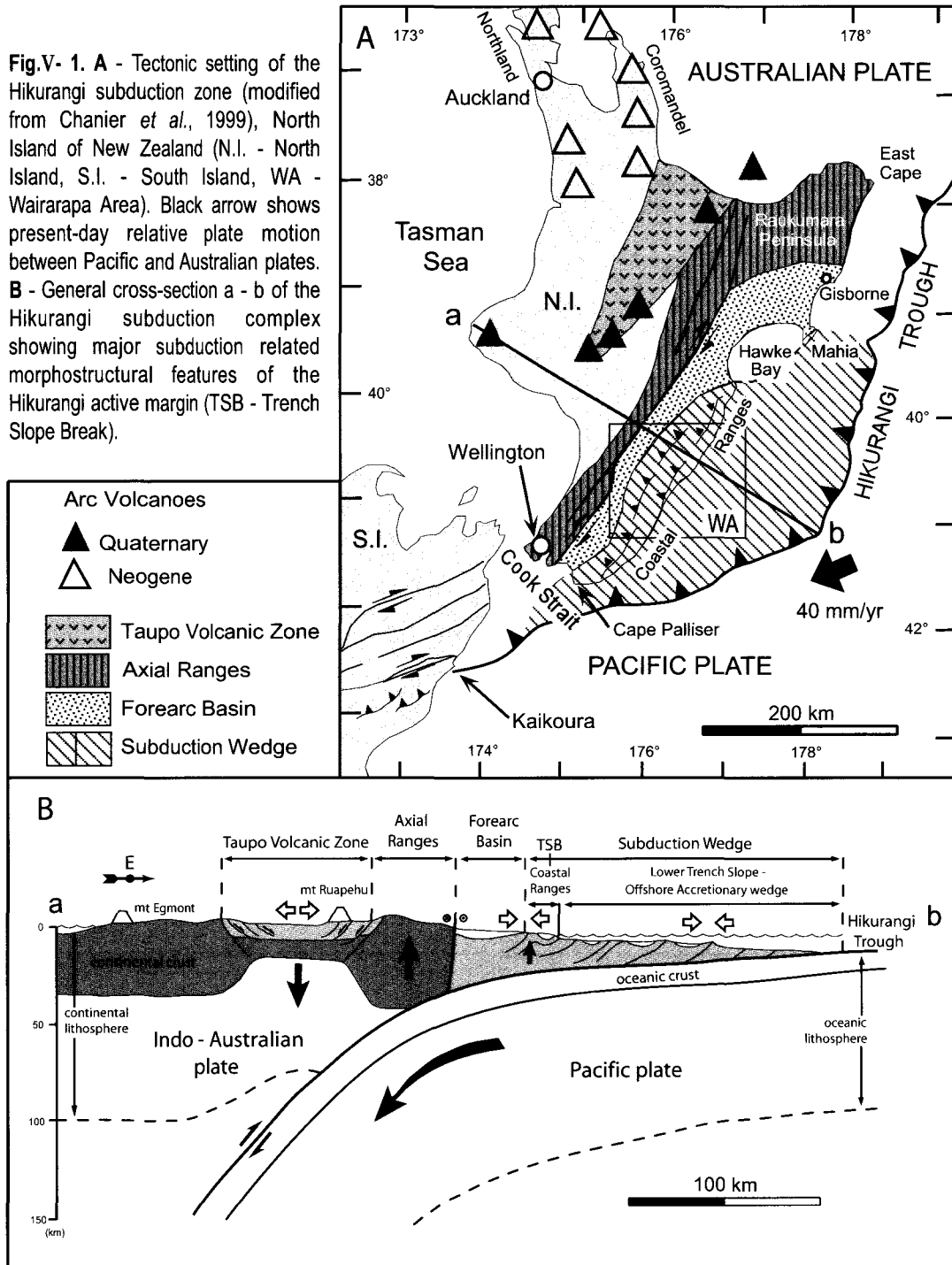
I) INTRODUCTION

On active margins, the morphology of the lower trench slopes (*i.e.* slope between the trench and the highest ridge of the subduction wedge) result from subduction wedges development that is controlled by the motion and coupling of the downgoing slab. Subduction activity is therefore responsible for the distribution and the evolution of lower trench slope sedimentation areas (*e.g.* trench-slope basins). In this context, the syn-subduction sedimentary infill may record the variations of regional tectonic regimes (*i.e.* compression, responsible for uplift and contraction of sedimentary domains; extension, responsible for subsidence and widening of sedimentary basins), but may also reflect more local deformation processes during a single tectonic episode.

Since 25 Myr, oblique convergence between the Australian and Pacific plates is responsible for the westward subduction of the thick Hikurangi plateau (10 to 15 km thick) beneath the North Island of New Zealand (Fig. V-1). At present time, the Hikurangi subduction wedge extends, onshore and offshore, along eastern North Island. There, trench-slope basins are known onshore, within the Coastal Ranges (van der Lingen and Pettinga, 1980; van der Lingen, 1982, 1988; Neef, 1992a; Turnbull, 1988; Lewis and Pettinga, 1993; Reid, 1998) as well as offshore (Lewis, 1980; Davey *et al.*, 1986; Lewis and Pettinga, 1993). We attempt to reconstitute the evolution through time of the repartition and geometry of these basins, as well as the modifications in location and structural development of their borders.

This study has been undertaken along a 130 km long transect (the Akitio transect) extending over the whole Hikurangi lower trench-slope, from the Hikurangi Trough to the onshore Coastal Ranges (Figs V-1 and V-2). The Akitio transect is subdivided into three distinct domains. These domains may be differentiated both by age and deformation of observed slope basins as well as by the nature and age of their basement. These are, from east to west: **1)** The lower part of the lower trench-slope (between the subduction front and the shelf edge, *i.e.* outer subduction wedge) which is constituted by accreted trench-fill turbidites overlain by mainly Quaternary trench-slope basins (Lewis *et al.*, 1999); **2)** The upper part of the lower trench slope (Wairarapa shelf, *i.e.* inner subduction wedge) which comprises Miocene to recent deformed trench-slope basin and shelf strata overlying an older acoustic basement. This basement possibly includes early Cretaceous to Oligocene pre-subduction sedimentary rocks (Field, Uruski *et al.*, 1996; Lewis *et al.*, 1999); and **3)** The trench-slope break (emerged Coastal Ranges) which is the most deformed part of the Hikurangi subduction wedge.

Fig.V- 1. A - Tectonic setting of the Hikurangi subduction zone (modified from Chanier *et al.*, 1999), North Island of New Zealand (N.I. - North Island, S.I. - South Island, WA - Wairarapa Area). Black arrow shows present-day relative plate motion between Pacific and Australian plates. **B** - General cross-section a - b of the Hikurangi subduction complex showing major subduction related morphostructural features of the Hikurangi active margin (TSB - Trench Slope Break).



In these Coastal Ranges, basement rocks are pre-subduction early Cretaceous to Oligocene highly deformed sedimentary formations. This basement forms elongated faulted strips, sub-parallel to the subduction front, which alternate with gently folded Miocene trench-slope basin strata (Fig. V-2).

We analyse slope basins and characterize their structural edges within these three morphostructural domains, from the subduction front (Hikurangi Trough) to the trench-slope break (Coastal Ranges), in order to reconstitute the geometric and structural evolution of the Hikurangi subduction wedge since the onset of subduction, 25 Myr ago.

II) GEOLOGICAL SETTING

The Eastern margin of North Island, New Zealand, corresponds to the forearc domain of the Hikurangi subduction zone. The present-day Hikurangi subduction margin extends from East Cape, at the southern end of the Tonga-Kermadec subduction zone, to Kaikoura, at the northern tip of the South Island (Fig. V-1). Along the whole Hikurangi subduction zone, the downgoing Pacific lithosphere includes the Hikurangi Plateau with 10 to 15 km thick oceanic crust thickened with seamount ridges, lava flows and Cretaceous sedimentary basins (Davy, 1993; Davy and Wood, 1994). Further south, the Pacific lithosphere comprises continental crust, which collides into the Australian Plate with a strong dextral component along the Alpine Fault in the Southern Alps (Fig. V-1).

The lower trench slope of the subduction zone presents three different segments in terms of active deformation (Fig. V-1). The northern segment, from East Cape to the southernmost Raukumara Peninsula, is characterized by a steep slope, no significant frontal offscraping, and possible active normal faults. This northern segment is probably mainly controlled by tectonic erosion related to the successive subduction of numerous seamounts (Collot *et al.*, 1996). The central segment, from the Mahia Peninsula to the Cook Strait, presents well-developed imbricated thrusts forming a growing accretionary prism, as clearly evidenced by seismic data (Davey *et al.*, 1986; Lewis and Pettinga, 1993; Collot *et al.*, 1996). This central segment includes the study area, the northeastern Wairarapa Region (Fig. V-1). The southern segment, from Cook Strait to Kaikoura, presents much less evidence of offscraping than the central segment and the behavior seems to be essentially transpressional (Lewis and Pettinga, 1993; Collot *et al.*, 1996). Various factors are probably responsible for

this latitudinal segmentation: **1)** the change in orientation of the relative plate motion, from an almost frontal convergence to the North to a highly oblique convergence in the South (Fig. V-1A); **2)** the southward increase in sediment supply into the trench along the margin; **3)** the important inhomogeneity in sediment thickness and lithology (presence of sedimentary basins, seamounts, *etc.*) of the downgoing Hikurangi Plateau (Davy, 1993); **4)** the occurrence of transverse morphological steps caused by major fractures in the downgoing slab, as suggested beneath the Cook Strait through seismological studies (Robinson, 1986).

The westward subduction of the Pacific plate along the Hikurangi margin started in the latest Oligocene to earliest Miocene, about 25 Ma ago. The age of the onset of subduction is documented by the beginning of calc-alkaline volcanism (Ballance *et al.*, 1985; Ballance, 1988), by the beginning of a period of intense compressional deformation over the whole margin (Pettinga, 1982; Spörli, 1987; Chanier and Ferrière, 1991; Rait *et al.*, 1991), and also by an abrupt change in sedimentation rate and nature (van der Lingen, 1982; Chanier and Ferrière, 1991; Ballance, 1993). The continuity of arc volcanism during the whole Neogene (the Northland - Coromandel arc) and Quaternary (the Taupo Volcanic Zone) also reveals continuous subduction beneath North Island (Cole, 1986; Ballance, 1988; Herzer, 1995), despite possible changes in rate and obliquity. The Quaternary opening of a back-arc basin in the Taupo Volcanic Zone, at the southern termination of the Lau-Havre Basin (Cole, 1984), is responsible for the separation between the Neogene and Quaternary volcanic centers (Fig. V-1).

From 25 Ma to present-day, the deformation of the margin has been continuous, but major variations in the deformational regime occurred with a succession of mainly contractional (*c.* 25-19 Ma and *c.* 5-0 Ma) and extensional (*c.* 15-6 Ma) episodes (Chanier, 1991; Chanier *et al.*, 1999).

III) DEFORMATION HISTORY IN THE NORTHERN WAIRARAPA REGION

The north-eastern Wairarapa region, corresponding to this study, is located in the middle of the central segment of the Hikurangi margin in eastern North Island. The present deformation across the lower trench slope is mainly compressional, related to the development of an accretionary prism (Davey *et al.* 1986; Lewis and Pettinga, 1993). Offshore data suggest a recent development of the present accretionary prism, during the last 0.5 Ma (Barnes and Mercier de Lépinay, 1997). Onland, in the Coastal Ranges and forearc basin (Fig. V-1), the Neogene and Early Quaternary deposits are folded and affected by reverse faulting (Lamb and Vella, 1987; Cape *et al.*, 1990; Chanier, 1991; Beanland *et al.*, 1998; Nicol *et al.*, 2002). Further west, at the western border of the forearc basin and in the Axial Ranges (Fig. V-1), the present-day deformation is dominated by dextral wrench faulting (Lewis, 1980; Lamarche *et al.*, 1995; Kelsey *et al.* 1995). Strike-slip motion along this zone accommodates most of the dextral component of the oblique displacement of the Pacific plate relative to the Australian plate (Lamb and Vella, 1987; Chanier, 1991).

In eastern Wairarapa, structural studies within the Coastal Ranges showed that the first episode of deformation related to the Late Cenozoic subduction, at *c.* 25 – 20 Ma, is contractional. This event induced the seaward-directed emplacement of imbricated thrust sheets. Thrusting and shortening were accompanied by syndepositional deformation of Early Miocene flysch deposits (Chanier and Ferrière, 1989; 1991). The minor structures that developed during this event are low-angle reverse faults and seaward-verging metric scale folds. Stress tensor analyses from data on these reverse faults and near the soles of major nappes indicate a NW-SE to N-S direction of shortening (Chanier, 1991). This thrusting episode started with the Hikurangi subduction, 25 Myr ago, as demonstrated by the inception of flysch sedimentation that abruptly followed the previous Paleogene pelagic series. The end of this phase is marked by an unconformity of the latest Early Miocene deposits (base of Altonian stage, *i.e.* 19 Ma) above major thrust faults (Fig. V-2).

From the end of early Miocene (*c.* 19 Ma) to Late Miocene, sediments are mainly massive siltstones and turbidites. The biofacies indicate a clear overall deepening related to major subsidence of the Wairarapa Domain (Crundwell, 1987; Wells, 1989). This subsidence was accompanied by widespread normal faulting observed in both Miocene and pre-Miocene rocks (Chanier *et al.*, 1999). The existence of large-scale high angle faults with a dip-slip motion is supported by sedimentological analyses, revealing contrasts between areas of thick deep-water Miocene strata and areas with thinner shallow-water strata of the same age.

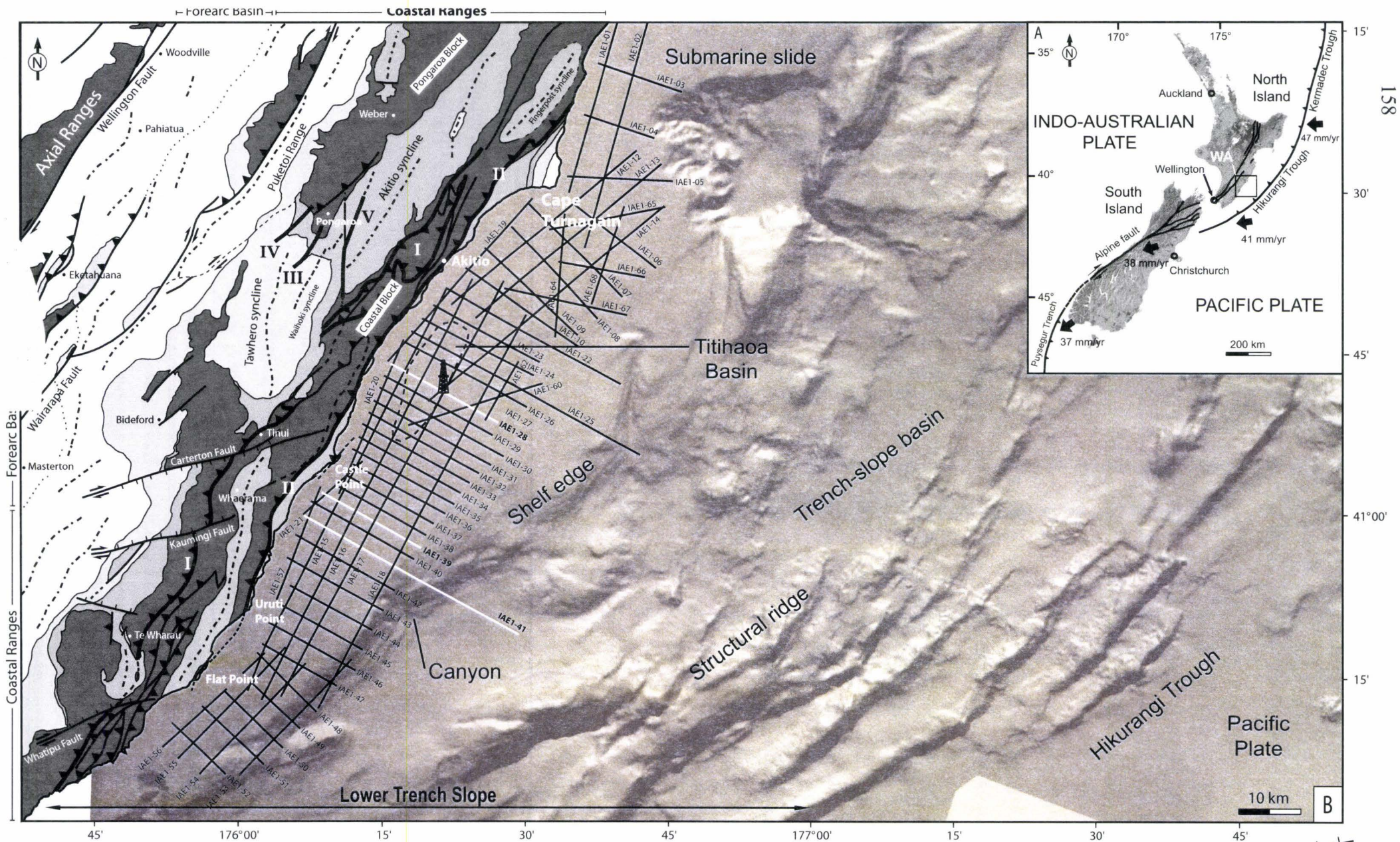


Fig.V- 2. A - Plate tectonic setting of New Zealand, black arrows show present-day relative plate motion between Pacific and Australian plates (WA - Wairarapa Area). **B -** Bathymetric map (Lewis *et al.*, 1999) and onshore structural map (modified from Lee and Begg, 2002) of the Wairarapa area. The offshore Wairarapa area includes location of the Amoco IAE1 seismic survey and well Titihaoa-1 (I - Tinui Fault Complex, II - Whakataki Fault, III - Waihoi Fault, IV - Mangatitahi Fault, V - Breakdown Fault).

Such contrasts are well illustrated in the Middle to Late Miocene sedimentation of eastern Wairarapa, suggesting a strong normal motion on some of these high angle faults at that time (Crundwell, 1987). The orientation of these large faults (Carterton Fault, Kaumingi Fault, Whatipu Fault; Fig. V-2) is consistent with most of the extensional axis determined from paleostress analysis on small-scale normal faults attributed to the same period. The large-scale high angle faults can thus be considered as normal faults that have been active during the Middle-Late Miocene as suggested by Crundwell (1987) for Kaumingi Fault. Some of these faults, trending E-W to NE-SW, have been later reactivated as dextral strike-slip faults, two of which are still active (Carterton and Kaumingi faults, Fig. V-2). Stress tensor analyses from sets of minor normal faults indicate two trends of extension for the Middle to Late Miocene times : one, dominant, is nearly parallel to the margin (σ_3 axis ranging from N170°E to N040°E), and another is perpendicular (σ_3 : N100°E to N116°E). Some authors (Delteil *et al.*, 1996) proposed alternatively the development of large-scale dextral strike-slip faults (*e.g.* Tinui Fault; Fig. V-2) during the Miocene in the Coastal Ranges of eastern Wairarapa. These faults developed after the southward emplacement of basal Miocene large nappes and are supposed to be active during most of the Miocene (Delteil *et al.*, 1996). This interpretation suggests that strain partitioning associated with oblique subduction could have started in the early Miocene.

The Neogene series, and the sets of normal faults as well, are now tilted because of folding postdating the extension discussed above. This recent folding affects the whole Neogene and Early Quaternary series. Folding is still active in the coastal ranges and folding rates have been estimated from progressive tilting of Quaternary marine terraces (Ghani, 1978), from field observations of progressive unconformities (Lamb and Vella, 1987; Nicol *et al.*, 2002), and from seismic data across the forearc basin (Cape *et al.*, 1990; Beanland *et al.* 1998; Nicol *et al.*, 2002). The results strongly suggest that most of the folding occurred during the Late Quaternary, since 1 Myr, with most of it possibly during the last 0.3 Myr (Ghani, 1978). Precise studies of seismic data and outcrops (Nicol *et al.*, 2002) showed that recent compressional deformation of the forearc domain occurred not only during this active episode, but also mainly during three rapid and short contractional events (0-1.8 Ma; 2.3-3.4 Ma; 5.5-7.5 Ma). However, the Plio-Quaternary period is overall dominated by NW-SE compressional deformation, with major regional folding and seaward reverse faulting. This period is also marked by the development of dextral strike-slip faults trending parallel to the margin in the forearc basin (*e.g.* Wellington Fault, Wairarapa Fault; Fig. V-2) and trending ENE-WSW in the Coastal Ranges (*e.g.* Carterton Fault, Fig. V-2).

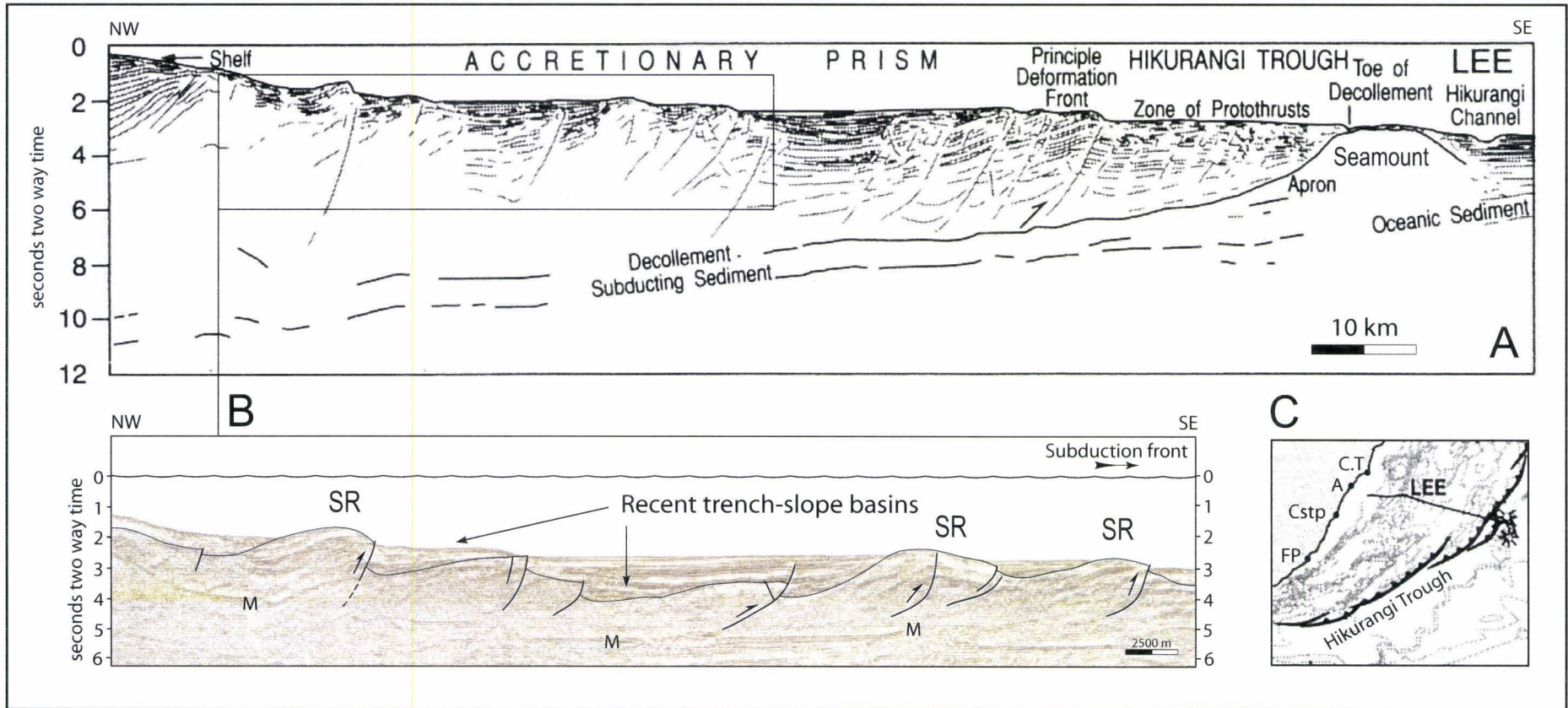


Fig.V- 3. A - Line drawing of seismic lines Lee 201 and 203, and **B** - Enlargement of seismic line Lee 203 : location and geometry of offshore Quaternary trench-slope basins near the Hikurangi subduction front. SR - Structural Ridges, M - Multiple. **C** - Location of seismic line Lee 203. C.T - Cape Turnagain, A - Akitio, Cstp - Castlepoint, FP - Flat Point. Modified from Davey *et al.* (1986) and Lewis and Pettinga (1993).

Since 25 Ma, the tectonic evolution and structural style of the Hikurangi margin has strongly influenced the location and geometry of depositional areas as illustrated onshore by the complexity of the stratigraphic framework (Vella and Briggs, 1971; Johnston, 1975, 1980; Crundwell, 1987, 1997; Neef, 1992a, 1992b, 1995, 1997a, 1997b; Field, Uruski *et al.* 1997; Lee and Begg, 2002). We analyse slope basins, perched on the subduction wedge, and characterize their structural edges from east to west, beginning with the offshore domains, which benefit from a seismic reflexion coverage (IAE1 seismic survey and lines LEE 201 and 203).

IV) THE OFFSHORE LOWER TRENCH-SLOPE

Offshore Wairarapa, notably on the Akitio transect, the Hikurangi subduction wedge is particularly well developed compared to North of Hawke Bay and South of Cook Strait (Fig. V-1; Lewis and Pettinga, 1993). The growth of a large accretionary body is favoured by the presence of the *c.* 3 kms thick turbidite sedimentary cover on top of the Hikurangi Plateau (Collot *et al.*, 1996). Across the Akitio transect, the offshore lower trench slope of the Hikurangi active margin is 100 km wide. In its lower part, close to the subduction front, the structure of the margin and the associated depositional environments have been described by Lewis (1980), Davey *et al.* (1986), and Lewis and Pettinga (1993). We first summarize their observations before our analysis of the more deformed upper part of the lower trench-slope.

A) Trench-slope basins close to the subduction front

The basement of the outer subduction wedge, near the subduction front, mainly comprises accreted trench-fill sediments. This structural domain therefore corresponds to an accretionary prism *sensu-stricto* (Seely *et al.*, 1974 ; Karig and Sharman, 1975 ; Moore and Karig, 1976 ; Scholl *et al.*, 1977 ; Seely, 1979). It is characterized by active imbricated thrust faults and by the development of Quaternary narrow trench-slope basins (Fig. V-2; Lewis, 1980 ; Davey *et al.*, 1986 ; Lewis and Pettinga, 1993). Lewis (1980) and Davey *et al.* (1986) have described the main characteristics of these basins on the bases of seismic reflexion profiling (Fig. V-3).

Quaternary trench-slope basins are sub-parallel to the Hikurangi Trough (Fig. V-2) and are particularly well developed between the longitudes of Hawke Bay and Uruti Point. These asymmetric sub-marine depressions are 5 to 30 km wide and 10 to 60 km long (Figs V-2 and V-3). Their sedimentary infill is unconformable over the basement of the underlying accretionary prism (Fig. V-3) and reaches 200 to 2000 m thick. Sedimentary series are landward tilted with minor internal deformations (Lewis, 1980). The tilting of basin strata generally increase progressively with toward the basin floor. The edges of the basins correspond to anticlinal ridges which show onlaps of basin strata on their western sides (Lewis and Pettinga, 1993). Structural bathymetric highs are associated to landward-dipping thrust faults (Lewis, 1980). Davey *et al.* (1986) has demonstrated that these major thrust faults, which control the growth of structural ridges, are connected at depth with a major landward-dipping decollement (Fig. V-3). Some basins may be subdivided later into several sub-basins by reverse faulting affecting their sedimentary infill (Davey *et al.*, 1986). With basins being progressively uplifted, they amalgamate (*i.e.* filling-up of the basins after the end of their structural edges development) or are subdivided into synclines or subbasins. The distinction between their infill and the sediments accreted from the trench becomes therefore less defined from seismic data (Davey *et al.*, 1986 ; Lewis and Pettinga, 1993).

These basins present the typical characteristics of trench-slope basins, as described from seismic and drilling studies on other accretionary margins (*i.e.* **Aleutians** - Moore and Karig, 1976; Underwood and Norville, 1986; Lewis *et al.*, 1988; Underwood and Moore, 1995; **Barbados** - Mascle *et al.*, 1990; Underwood and Moore, 1995; Huyghe *et al.*, 1996; **Cascadia** - Davis and Hyndman, 1989; Underwood and Moore, 1995; McAdoo *et al.*, 1997; **Makran** - White and Loudon, 1982; **Nankai and Japan** - Moore and Karig, 1976; Von Huene and Arthur, 1982; Okada, 1989; Underwood and Moore, 1995; Underwood *et al.*, 2003; **Sunda** - Moore and Karig, 1976; Karig *et al.*, 1979, 1980; Stevens and Moore, 1985; Underwood and Moore, 1995).

B) *The upper part of the lower trench-slope*

Offshore Wairarapa, the upper part of the lower trench-slope (inner subduction wedge) consists in a smooth shelf, 20 - 40 km wide, which gently deepens from shore to *c.* 200 - 500 m of water depth (Fig. V-2). The Wairarapa shelf develops from the coast to the first major structural feature affecting the seafloor, suggesting that the shelf geometry is mainly controlled by tectonic activity. The Wairarapa offshore area is covered by a 2D marine seismic survey (IAE1, Amoco New Zealand Exploration Company, 1990) and benefits from drillhole data (well Titihaoa-1, Amoco NZ Exploration Company, 1994) (Fig. V-2). The geophysical survey consists in 1574 line kms (67 seismic lines) recorded, from Cape Turnagain to Flat Point, using conventional multichannel seismic reflexion. The Titihaoa-1 petroleum exploration well was drilled 13 km offshore Akitio, at the junction between seismic lines IAE1-28 and IAE1-17 (40° 48' 5.20" S, 176° 25' 40.65" E) (Fig. V-2). All these data are now open file at the New Zealand Ministry of Commerce, Wellington (Adams and Sullivan, 1990; Biros *et al.*, 1995). Correlation between seismic profile IAE1-28 and well Titihaoa-1, using a time to depth model provided by the analysis of the sonic log, permits to tie seismic units and well logs. This allows to date seismic horizons from the well foraminifera and nannofossils data (Morgans *et al.*, 1995). Biostratigraphic determinations are based on the standard New Zealand Cenozoic stage classification of Edwards *et al.* (1988). Absolute ages used in this study refer to the recent New Zealand Cretaceous-Cenozoic Timescale (Cooper *et al.*, 2004).

For this study, we expose the interpretation of three transverse seismic lines. The line IAE1-28 is located on the Akitio transect (Fig. V-2) and is representative of the main structural pattern of the offshore inner subduction wedge. Seismic lines IAE1-39 and IAE1-41, located further south (Fig. V-2), present the lateral variations of basin deformation and of structural ridges development.

1) **Structure of the Wairarapa shelf offshore Akitio**

The structural development of the shelf offshore Akitio can be illustrated by the seismic line IAE1-288, which is precisely constrained in age and lithology with the results from well Titihaoa-1 (Biros *et al.*, 1995; Morgans *et al.*, 1995). The distribution of structures and sedimentary units has been analysed in detail and three major seismic units have to be distinguished (SI to SIII; Fig. V-4). From base to top, SI is characterized by highly disorganised internal seismic reflectors, SII by irregular and discontinuous internal reflections, and SIII by relatively continuous parallel to sub-parallel internal reflections. The adopted ages for the unit boundaries are: SB1 *c.* 14.2 Ma and SB2 *c.* 6.2 Ma.

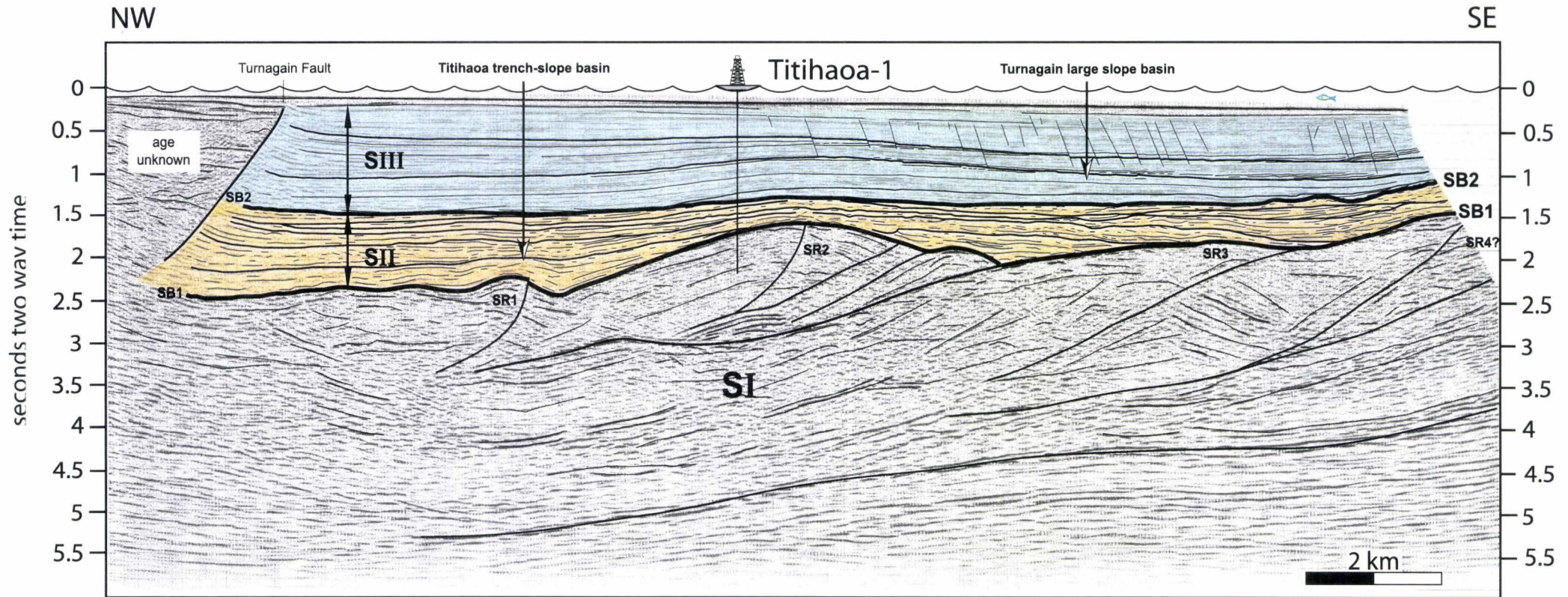


Fig.V- 4. Interpretation of IAE1-28 seismic line. SI - Highly disorganised seismic unit (deformed acoustic basement), SII - Irregular and discontinuous seismic unit (trench-slope basin infill), SIII - Well organised and continuous seismic unit (infill of the Turnagain large slope basin). U1 and U2 - main seismic units boundaries. See figure V-2 for location.

a) The acoustic basement (SI)

The basal unit SI is composed of chaotic internal reflections that traduced relative deformation of the unit compared to the overlying seismic units (Fig. V-4). Within SI, some strong west-dipping reflectors has been interpreted by Field, Uruski *et al.* (1997) as major thrust zones. Above these west-dipping reflectors the seismic unit SI forms structural ridges (SR1 to SR4). The relationships between structural ridges and the west-dipping reflectors suggest that deformation of this unit results from hanging wall anticline development over landward-dipping thrust faults (Field, Uruski *et al.*, 1997). Such a seaward-directed thrusts sheets imbrication is typical of accretionary wedges. This unit constitutes the acoustic basement of the overlying sedimentary units (Fig. V-4). To the west of the profile, a major reverse fault (Turnagain Fault, new name) is responsible for the seaward thrusting of an undetermined (age unknown) acoustic basement over basin strata of SII and SIII (Fig. V-4).

The acoustic basement incorporates middle Miocene (*c.* 15.5 – *c.* 14.2 Ma) and maybe older syn-subduction (early Miocene) and even pre-subduction (Cretaceous to Oligocene) sediments (Field, Uruski *et al.*, 1997). As on seismic data the acoustic basement depends on the degree of deformation and tilting of sedimentary series, this basement may present lateral changes in age related to lateral variations in intensity of tectonism.

b) The middle-late Miocene ponded basins (SII)

The basal boundary of the second unit SII is a highly undulating major angular unconformity (SB1, *c.* 14.2 Ma) that marks the onset of middle-late Miocene sedimentation over a deformed acoustic basement (SI). Seismic unit SII is composed of low amplitude, irregular and laterally discontinuous seismic reflectors (Fig. V-4) with a particularly well expressed divergent organisation. The lower part of SII is confined between acoustic basement structural ridges (SR2 and SR3) and its upper part shows the drowning of these ridges (Fig. V-4). Therefore, the unit presents a more continuous lateral extent in its upper part. The divergent arrangements of seismic reflectors characterize a progressive thickening of the unit away from major acoustic basement ridges. This unit geometry results from landward tilt of internal depositional surfaces that therefore correspond to angular unconformities (Fig. V-4). The internal angular unconformities are mainly localized on the western sides of major structural ridges suggesting that the landward tilted surfaces are related to the structural development of the eastern edges of structural depressions. Local intra-unit

folding (syncline), as well as seaward tilting, are also observed and traduce the growth of the western structural boundaries of the ponded depositional areas.

Seismic unit SII is clearly a syntectonic sedimentary unit deposited in ponded basins that we interpret as middle – late Miocene (*c.* 14.2 – *c.* 6.2 Ma) trench-slope basins that have developed above an acoustic basement in relation with the growth of structural ridges.

The westernmost offshore basin, the Titihaoa basin (Fig. V-4), is located at about 10 km from the coast line. Within this basin, angular unconformities near structural ridge SR2 are associated to landward tilting of depositional surfaces (Fig. V-4). This clearly illustrates syn-tectonic deposition during the development of SR2 which has formed the eastern edge of the Titihaoa basin during the middle-late Miocene (*c.* 13.7 – *c.* 6.2 Ma). The western border of the Miocene Titihaoa basin is more difficult to identify clearly, because of recent (post-Pliocene) tectonic activity along the Turnagain Fault (Fig. V-4). However, angular unconformities within seismic unit SII suggests that the Turnagain Fault zone is responsible for folding of SII sedimentary series before *c.* 6.2 Ma. Therefore, during middle and late Miocene, the Cape Turnagain Structural High (now emerged, Fig. V-2) has formed the eastern edge of the offshore Titihaoa basin. Early deformation of the Titihaoa basin also includes the development of structural ridge SR1 which is responsible for the division of the early Titihaoa basin onto two sub-basins (Fig. V-4). Considering that the Titihaoa basin hasn't undergone much shortening and that SR2 and the Cape Turnagain Structural High have constituted its borders during its sedimentary evolution, we show that the middle-late Miocene Titihaoa basin was about 5 km wide. The Titihaoa basin total thickness is at least 460 m deposited in 7.5 Ma, from *c.* 13.7 to *c.* 6.2 Ma.

c) The Plio-Quaternary Turnagain slope basin (SIII)

The third unit SIII is bounded at its base by a major angular unconformity (SB2, *c.* 6.2 Ma). In the eastern part of seismic line IAE1-28, SB2 is slightly undulated and shows small incised geometries (Fig. V-4). This erosive surface is overlaid by downlaps of SIII seismic unit (Fig. V-4). The surface SB2 also marks a rapid shallowing of depositional environment from lower bathyal to middle bathyal depths (Morgans *et al.*, 1995). The top of seismic unit SIII is the seafloor reflector. This unit is the most laterally continuous of the studied transect (Fig. V-4). It mainly consists of high amplitude and laterally continuous parallel to sub-

parallel seismic reflectors (Fig. V-4). These seismic reflectors are sub-horizontals or form low angle sigmoidal prograding clinoforms. This last seismic unit is affected by some post-depositional deformation illustrated by the development of large wavelength folds, notably on the west side of line IAE1-28 (Fig. V-4). The development of a syncline on the west side of line IAE1-28 can be related to recent motion along the Turnagain Fault, which affects the whole unit SIII (Fig. V-4). As for seismic unit SII, local internal angular unconformities are identified, notably above structural ridge SR2. Considering the location of these intra-unit erosional surfaces and the absence of contemporaneous global eustatic event, these geometries may be attributed to a late stage of SR2 development. This deformation affects the sedimentary series of seismic unit SIII and is therefore responsible for slight folding of its sedimentary series (Fig. V-4). The growth of this recent anticline above SR2 could be responsible for the development of normal faults on the eastern limb of SR2. Accordingly, these normal faults can be due to gravitational collapse of recently deposited poorly indurated sediments in response to anticline growth.

The sedimentation of SIII over SB2 (*c.* 6.2 Ma) reveals an important enlargement of the sedimentary domain that has led to the development of a large slope basin, the Plio-Quaternary Turnagain basin (*c.* 6.2 – 0 Ma). This basin is filled by the westward progradation of thick sedimentary series (1400 – 1600 m) deposited in the last 6.2 Ma. We could observe a significant change in amplitude of synclinal folding between seismic units SII and SIII close to the Turnagain Fault. This suggests that the Cape Turnagain Structural High has constituted the western edge of the Turnagain slope basin, at least in early stages of SIII deposition. To the East, the eastern border of the Turnagain basin is not visible on profile IAE1-28 but corresponds to the shelf edge area as exposed in the next section.

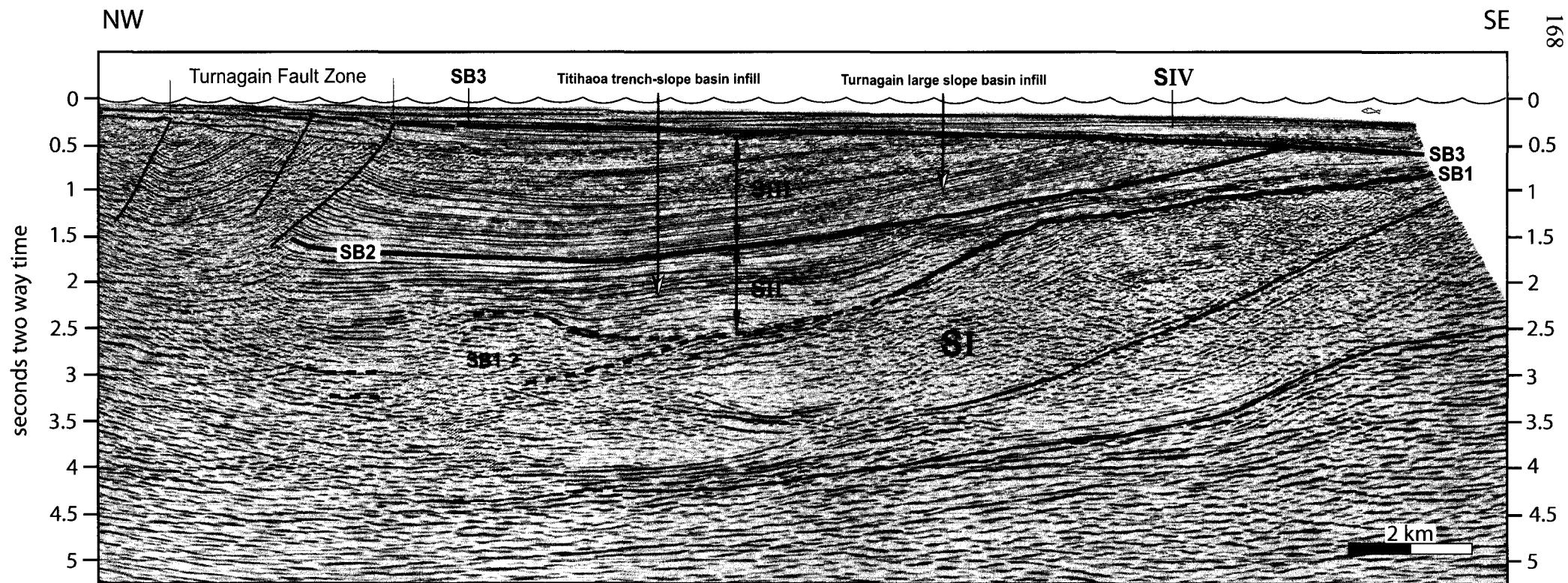


Fig.V- 5. Interpretation of IAE1-39 seismic line. SI - Highly disorganised seismic unit (deformed acoustic basement), SII - Irregular and discontinuous seismic unit (trench-slope basin infill), SIII - Well organised and continuous seismic unit (infill of the Turnagain large slope basin), SIV - Quaternary slope basin. U1 to U3 - main seismic units boundaries. See figure V-2 for location.

2) Structure of the Wairarapa shelf offshore Castlepoint

Further south from Akitio transect, offshore Castlepoint (Fig. V-2), the IAE1 seismic survey provides additional information on the structural development of the Wairarapa shelf. These information, mainly on recent deformation of this domain, are here exposed through the description of seismic lines IAE1-39 and IAE1-41. We could tie seismic units SI, SII and SIII to line IAE1-28 and Titihaoa-1 drillhole. These units, SI to SIII, are slightly more deformed and we notice the development of a fourth unit SIV on top of SIII (Figs V-5 and V-6). The basal boundary of SIV (SB3) cannot be tied on well Titihaoa-1 and its precise age is therefore unknown. However, its stratigraphic position suggests that SB3 is Quaternary in age.

Seismic unit boundaries SB1 and SB2 are clearly tilted landward on line IAE1-39 (Fig. V-5), unlike further north on line IAE1-28 (Fig. V-4). This tilting reveals a second phase of deformation affecting middle-late Miocene trench-slope basins, which are therefore more difficult to recognise on seismic lines. Because of this recent (post-SIII) tilting episode of basin strata, the most deformed basal part of trench-slope basin infilling (SII *p.p.* from line IAE1-28) could be incorporated within the acoustic basement (SI) on lines IAE1-39 and IAE1-41. Such uncertainties in correlation with line IAE1-28 concerns only the oldest sedimentary and seismic units (SI and base of SII). This section considers only the recent units and deformation that are precisely tied on seismic line IAE1-28 and Titihaoa-1 drillhole. The recent tilting also reveals synclinal folding of the Pliocene (to early Quaternary ?) series of the Turnagain slope basin (Fig. V-5). Considering the age of tilted strata, the folding is at least post-Pliocene in age.

Such recent deformation is also observed from seismic line IAE1-41 (Fig. V-6). On this profile, landward tilt of seismic units SI to SIII is only observed west of the shelf edge. On its eastern side, seismic reflectors are mainly seaward tilted (Fig. V-6). These geometries are related to post-Pliocene deformation of the shelf edge. The presence of a major strong west-dipping oblique reflector immediately to the west of the shelf edge suggests that it has been controlled by recent activity along a major landward-dipping thrust fault, the "Shelf Edge Fault" (Fig. V-6; new name). This thrust fault could have controlled the growth of the Shelf Edge Structural High which corresponds to the eastern edge of the Turnagain basin. Accordingly, the Turnagain basin was about 40 km wide during the Plio-Quaternary. The shelf edge is still active because it offsets the seafloor.

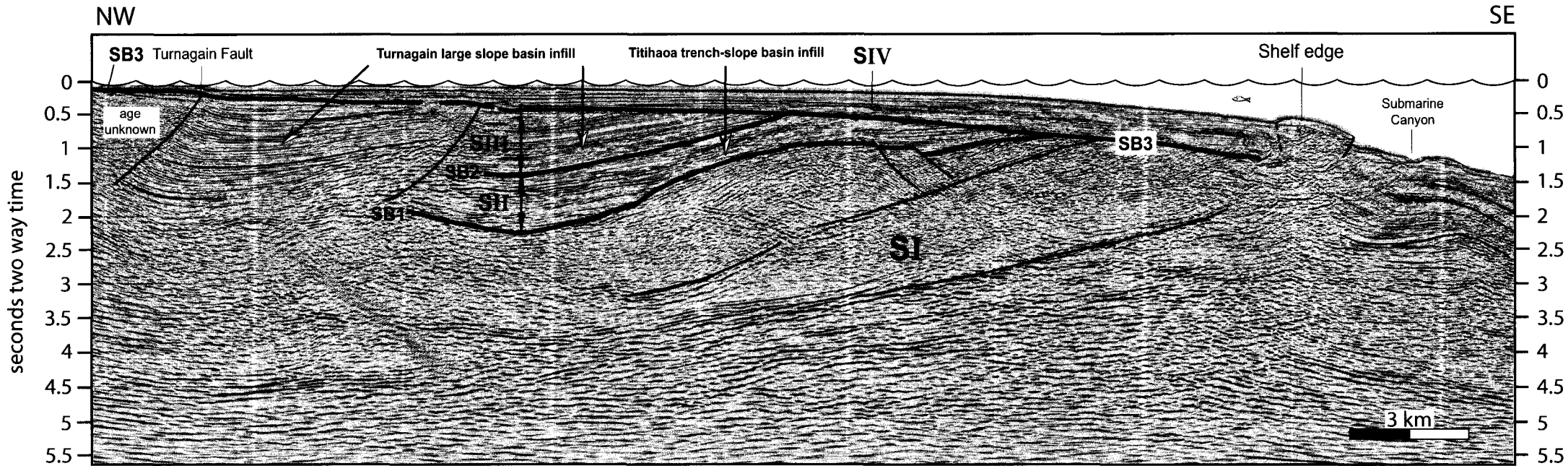


Fig.V- 6. Interpretation of IAE1-41 seismic line. SI - Highly disorganised seismic unit (deformed acoustic basement), SII - Irregular and discontinuous seismic unit (trench-slope basin infill), SIII - Well organised and continuous seismic unit (infill of the Turnagain large slope basin). U1 and U2 - main seismic units boundaries. See figure V-2 for location.

The high angle active faults and seismic disruptions below the shelf edge zone could be interpreted as a vertical fault zone with a possible strike-slip component. However, the Shelf Edge deformation zone always appears at the emerging front of the low angle Shelf Edge Fault (lines IAE1-22, IAE1-25, IAE1-41; Fig. V-2).

In the offshore Castlepoint area, the post-Pliocene deformation is also illustrated by the reverse motion along the Turnagain Fault (Figs V-5 and V-6). A second major post-Pliocene reverse fault divides the large Turnagain basin into two synclines (Fig. V-6). Similar subdivisions of large slope basins in two synclines by the growth of an axial seaward thrusting anticline has been documented onshore (Van der Lingen and Pettinga, 1980; Pettinga, 1982; Lewis and Pettinga, 1993), offshore (Davey *et al.*, 1986), as well as in other subduction margins (*e.g.* Huygues *et al.*, 1996).

The upper unit (SIV), observed offshore Castlepoint (Figs V-5 and V-6) is bounded at its base by a major angular unconformity (SB3, inferred to be Quaternary in age). This unconformity corresponds to a sharp erosional surface above the seismic units SI, SII and SIII, and marks therefore the end of post-Pliocene tilting. This event characterizes a stop in the Shelf Edge Structural High development. The following period of erosion is considered as a result of the Shelf Edge Structural High uplift rather than a consequence of a sea-level fall that could not explain the angular unconformity. Quaternary sediments of seismic unit SIV are deposited unconformably over the underlying deformed strata and thicken laterally from the shore line to the shelf edge suggesting a seaward paleoslope (Fig. V-6). The Shelf Edge Fault is still active as shown by the offset of sedimentary series of SIV and of the seafloor (Fig. V-6) and determines the wideness of the Wairarapa shelf.

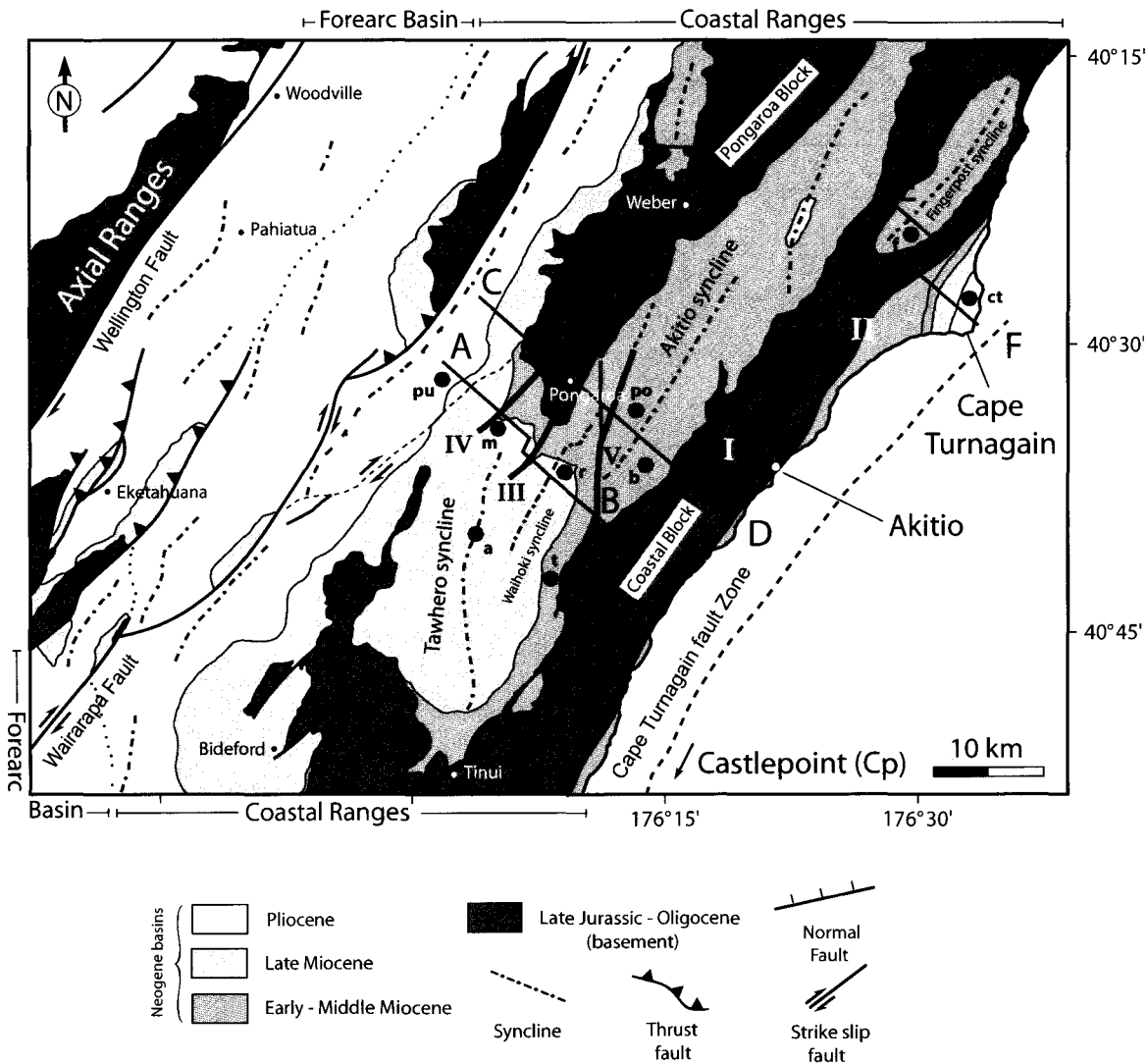


Fig.V- 7. Structural map of the Pongaroa area, northeastern Wairarapa. Location of sedimentological vertical sections and of cross sections: pu - Puketoi vertical section, m - Mangatiti vertical section, a - Annedale vertical section, r - Razorback vertical section, t - Takiritini vertical section, po - Pongaroa vertical section, b - Branscombe vertical section, f - Fingerpost vertical section, ct - Cape Turnagain vertical section, Cp - Castlepoint vertical section; A-B Tawhero cross section, C-D Pongaroa cross section, E-F Turnagain cross-section. I - Tinui Fault complex, II - Whakataki Fault, III - Waihoki Fault, IV - Mangatiti Fault, V - Breakdown Fault. Modified from Lee and Begg (2002).

V) THE ONSHORE LOWER TRENCH-SLOPE

Onshore, the Wairarapa area belongs to the Coastal Ranges (Fig. V-7). These Ranges correspond to a 260 km long by 30 km wide northeast – southwest deformed belt which bound seaward the forearc basin (Fig. V-1). The Coastal Ranges constitute, from Cape Palliser to Hawke Bay, the emerged part of the Hikurangi subduction wedge and may therefore be considered as the present-day trench-slope break of the Hikurangi margin (Fig. V-1; *i.e.* highest ridges and basins of the subduction wedge; Pettinga, 1982; Lewis and Pettinga, 1993). Because of the rapid uplift of the inner part of the Hikurangi margin during the Quaternary (Ghani, 1978; Cape *et al.*, 1990), Mio-Pliocene marine sediments, deposited on a lower trench-slope, are now well-exposed in the Pongaroa area, north-eastern Wairarapa (Fig. V-7). Although this area is structurally and stratigraphically complex, detailed mapping, structural analysis (*e.g.* mapping and brittle deformation analysis) and correlations of sedimentological vertical sections have allowed understanding of the geometry, the repartition and the vertical stacking of onshore Neogene basins and their bounding structural highs.

A) Structural analysis

Mio-Pliocene marine deposits are exposed within elongated wide synclines, which lie between two highly deformed basement structural highs, the Coastal Block and the Pongaroa Block (Fig. V-7). The basement is composed of early Cretaceous to Oligocene pre-subduction sedimentary rocks. The main structures are sub-parallel to the subduction front with northeast – southwest axis.

Two main faults, the Tinui Fault and the Whakataki Fault, affect the basement of the Coastal Block and represent major northeast – southwest structural lineament. The Tinui Fault is responsible for seaward thrusting of early Cretaceous basement rocks over late Cretaceous strata (*Wanghai formation*) (Fig. V-8). The Whakataki Fault, dipping landward 60°-70° W, marks the eastern boundary of the Coastal Block. It corresponds to seaward thrusting of late Cretaceous sedimentary rocks (*Wanghai formation*) over the basal Miocene flysch deposits (*Whakataki Formation*) (Fig. V-8). These two major thrust faults are related to a phase of nappes emplacement associated to the onset of subduction, 25 Myr ago (Chanier and Ferrière, 1989, 1991; Chanier, 1991; Rait *et al.*, 1991).

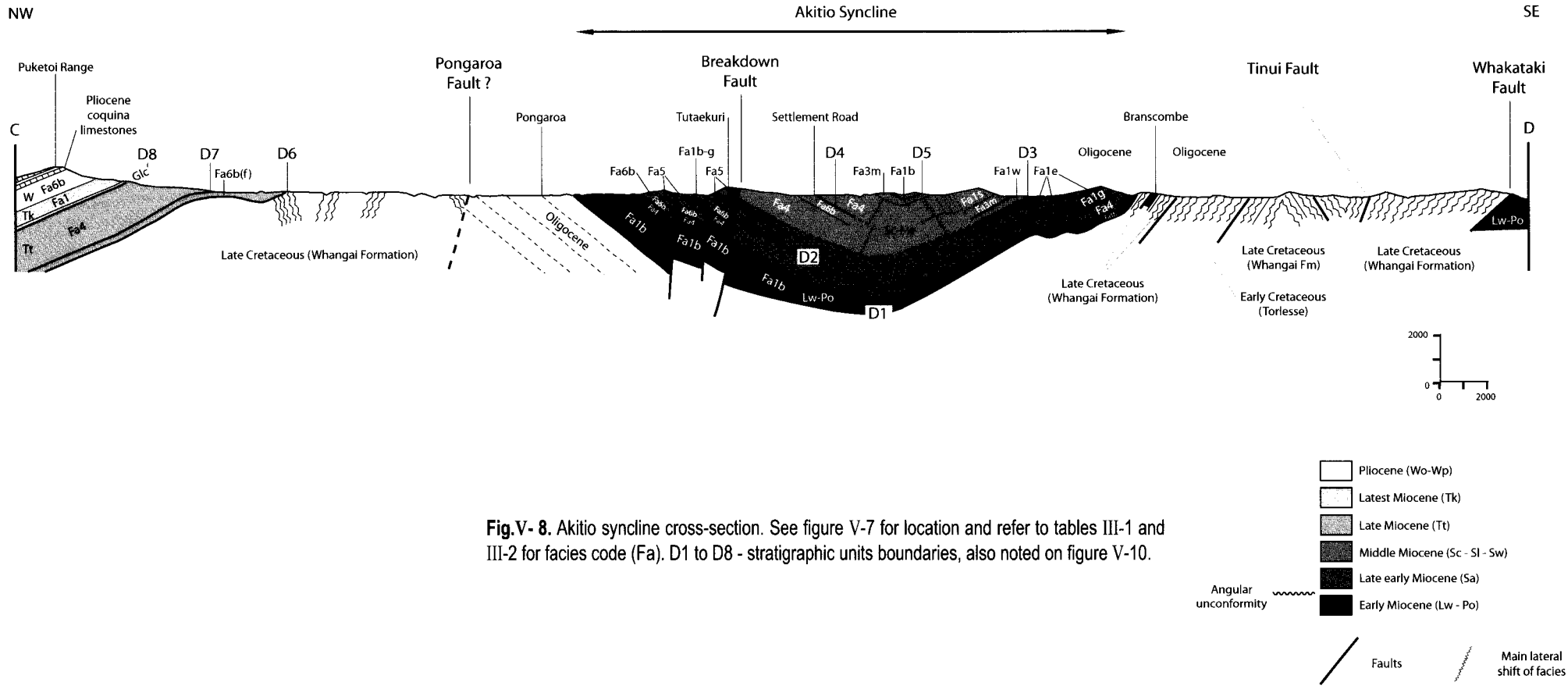


Fig.V- 8. Akitio syncline cross-section. See figure V-7 for location and refer to tables III-1 and III-2 for facies code (Fa). D1 to D8 - stratigraphic units boundaries, also noted on figure V-10.

Along the coast, about 10 kms north of Castlepoint, the Whakataki Fault affects Quaternary terrace deposits. This recent motion shows that the thrust fault have been, at least locally, reactivated during the Quaternary. The Tinui Fault and the Whakataki Fault present dip-slip motions which reflect SE-NW shortening (Fig. V-9, stereoplots b and c). This axis of compressive deformation is consistent with principal directions of post-Pliocene shortening. Similar post-Pliocene compressive directions are deduced from brittle deformation analysis of the Castlepoint Fault (Fig. V-9, stereoplot d), which is responsible for seaward thrusting of basal Miocene turbidites (*Whakataki Formation*) over Pliocene coquina limestones (Fig. V-9, stereoplots e). In addition, to the west of the Puketoi Range, progressive angular unconformities within late Pliocene coquina limestones show that tilting of strata follows NE-SW fold axis that are also related to NW-SE compressive deformation (Fig. V-9, stereoplot a).

On the coastal platform, north of Castlepoint, the Whakataki flysch Formation (basal Miocene) has undergone several episodes of brittle deformation. The most recent set of faults, post-dating the tilting of the whole formation, have a clear reverse motion with NW-SE direction of shortening (Fig. V-9, stereoplot f). This last shortening event can thus be considered contemporaneous with the late Pliocene to Quaternary shortening episode. All these results are in agreement with the important shortening of the emerged part of the subduction wedge described elsewhere within the Coastal Ranges (Beanland *et al.*, 1998; Nicol *et al.*, 2002). These authors distinguished pulses of contractional deformation over short period of time, notably in the late Pliocene and in the late Quaternary to present-day.

Because of the Plio-Quaternary reactivation of the main thrust faults of the Coastal Block, it is sometimes difficult to determine earlier motions along these faults. Some deformation patterns at the base of major nappes in the coastal ranges has shown a N-S direction of nappes emplacement in the Akitio area (Delteil *et al.*, 1996) and NNW-SSE to N-S directions further south, in the Flat point area (Chanier, 1991; Fig. V-2). Within the study area, the Whakataki Fault notably show some criteria for E-W shortening (Fig. V-9, stereoplot c). Such E-W directions of shortening can also be deduced from the deformation of Miocene sedimentary series that cover the nappes (Figs V-7 and V-8). Within these Miocene series, E-W compressive deformation is responsible for reverse faulting (*e.g.* Breakdown Fault; Figs V-7 and V-8) and small scale sets of conjugate strike-slip faults (Fig. V-9, stereoplot g). Moreover, these sites of E-W compression are located in areas where the trend of fold axis turns significantly to a N-S direction (*e.g.* Tawhero syncline, Te Wharau syncline; Figs V-2 and V-7), unlike the main present-day structural pattern of the study area (*i.e.* mainly NE-SW syncline axis). This N-S direction of fold axis appears only within pre-Pliocene series, up to the late Miocene.







These observations suggest that late Miocene E-W compressive deformation has occurred in the Wairarapa area, after the basal Miocene southward nappes emplacement, and before the late Pliocene to present-day SE-NW shortening episode. Alternatively, Delteil *et al.* (1996) have proposed large scale dextral strike-slip faulting, affecting the whole Coastal Ranges during the Miocene. In this hypothesis, the Tinui Fault zone is inferred to be a Miocene strike-slip fault with about 300 km of dextral offset. However, our brittle deformation analysis on the Tinui Fault Zone shows only dip-slip motions on all planes trending parallel to the fault plane (Fig. V-9, stereoplot b).

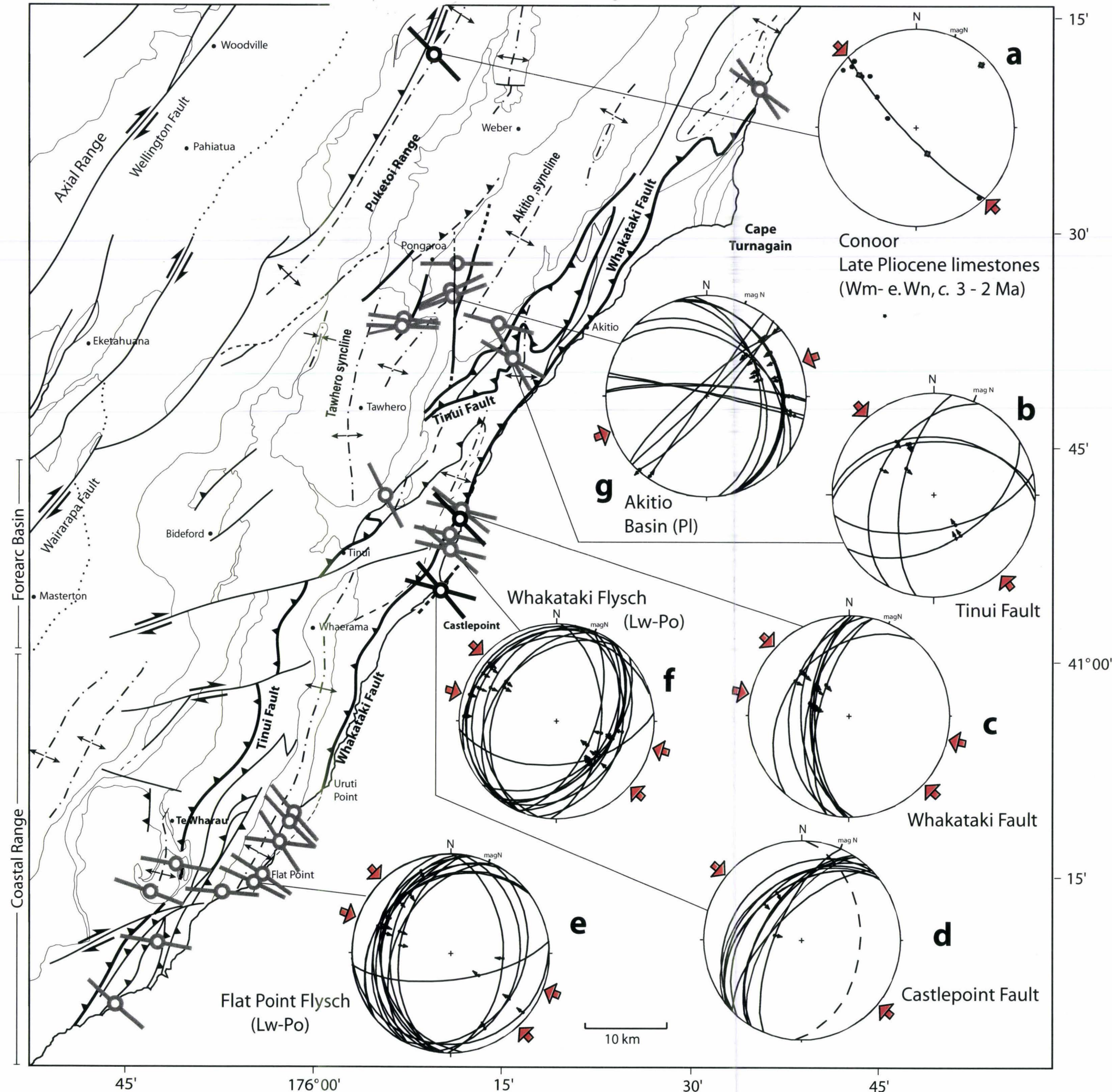
Apart from mapping and brittle deformation analysis, the development of structural highs is here also constrained by detailed analysis of Miocene series that led to reconstitute the evolution of basin geometries and of their boundaries.

B) Basin analysis

For this study, ten vertical sections were correlated (Fig. V-10), from the Puketoi Range to the Pacific coast, covering a complete transect of the Coastal Ranges: the 30 km long onshore Akitio transect (Fig. V-7). All together, the ten sedimentological vertical sections (Appendix 1) range in age from basal Miocene to early Pliocene (*c.* 24 – *c.* 3 Ma, Fig. V-10). Correlations between the sedimentological sections were first established using New Zealand stage boundaries, based on foraminiferal assemblages (Appendix 2). Vertical successions of facies in each section were then used to identify major sedimentary discontinuities (characterized by sharp facies changes). The characterization of facies and their interpretations in terms of depositional environments is based on the nomenclature proposed for the Akitio basin (Bailleul *et al.*, submitted). This paper also presents an overview of Miocene very fine grained gravitary deposits and shelf sediments of the Wairarapa area (Tables III-1 and III-2). The sedimentary discontinuities that bound the main stratigraphic units within the basins fill, are correlated with attention to the biostratigraphic framework. These correlations based on stratigraphic architecture and biostratigraphy permitted a good age constrain of unit boundaries for each section. Facies changes at each discontinuity, as well as the distal/proximal trend of sedimentary systems within each unit, were also considered in order to improve the precision of our correlations. Finally, our stratigraphic framework also take into account our mapping and structural analysis of the north-eastern Wairarapa area. This work led us to precise the lateral extent of some sedimentary units and permitted better constrains on their geometries and their boundaries (*i.e.* onlaps on basin edges *vs* angular unconformities).

Fig.V- 9. Simplified structural map of the Wairarapa region and stress tensor analysis (Schmidt, lower hemisphere) showing the main directions of compressional deformation. See text for explanations.

-  Strike-slip Fault
-  Thrust Fault
-  Anticline Axis
-  Syncline Axis
- Axis of horizontal shortening
-  Recent (3-0 Ma)
-  post-tilt of bedding planes



The result of these correlations between all measured sections of the onshore Akitio transect is exposed on Fig. V-10, which exposes a late Pliocene (youngest sediments in the study area) stage of the stratigraphic framework and structural development of the transect. These correlations led us to identify two slope basins which have developed after the basal Miocene phase of nappes emplacement: the Akitio basin (*c.* 17.5 – *c.* 13.2 Ma), and the Tawhero basin (*c.* 13.2 – *c.* 5.3 Ma). The Akitio basin is unconformable (angular unconformity D2) over basal –early Miocene (early Altonian) strata of sedimentary unit U1 (Fig. V-10).

1) basal Miocene flysch deposition: syn-nappes sedimentation (U1 - Lw-Po/Pl <, *c.* 25 – 17.5 Ma)

On the study area, basal Miocene series (*c.* 25 – 17.5 Ma) are mainly encountered on the east of the Coastal Block. They constitute impressive coastal exposures on the shore platform along the Wairarapa Coast (from Castlepoint to Cape Turnagain, Fig. V-2). To the west of the Coastal Block, the unit gets gradually thinner and is missing west of the Pongaroa Block. The present study is based on measured sections of these series in the Castlepoint, Fingerpost, Branscombe, Pongaroa, and Takiritini areas (Fig. V-10).

This sedimentary unit U1 corresponds to the eastward progradation of a mixed outer shelf/ramp system (Pongaroa and Branscombe sections). The onset of this phase of terrigenous sedimentation, at *c.* 25 Ma, is outlined by olistostromal deposition (Fa3a) at base of sedimentary unit U1 (Branscombe and Castlepoint sections). Then, the deposition of the basal Miocene distal turbidites (Fa1b) of the *Whakataki Formation* (Johnston, 1975, 1980) occurred. This sharp facies change, from Eocene – Oligocene pelagic sedimentation (marls and pelagic limestones) to thick basal Miocene turbidite series, occurred synchronously at the margin scale. The onset of turbidite deposition at *c.* 25 Ma corresponds to a brutal increase of the terrigenous flux and marks the inception of compressive deformation, coeval with the beginning of subduction in the earliest Miocene (Chanier and Ferrière, 1991; Rait *et al.*, 1991). These deposits (U1) are pinched under the Whakataki Fault and highly folded (Fig. V-11), suggesting their deformation during the late stages of nappes emplacement. Similar flysch deposits, of same age, have been described in detail further south and are also associated to this major thrusting event during the beginning of subduction beneath North Island (Chanier and Ferrière, 1991).

The sharp angular unconformity of younger sedimentary units (U2, *c.* 17.5 – 16.5 Ma) on top of the deformed U1 unit as well as on the nappes marks the end of this major thrusting event and the settlement of post-nappe sedimentation. On the western side of the Coastal Block, the basal Miocene series (U1) are less deformed and post-nappe series (U2 to U4) are almost conformable on top of them (Fig. V-8). These basal Miocene sediments, finer-grained and thinner than further east, were probably deposited on top of nappes rather than on front of them as inferred further east.

2) Development of the early-middle Miocene confined Akitio trench-slope basin (U2 to U4)

The late early and middle Miocene (*c.* 17.5 – 13.2 Ma) turbidite sediments of the Akitio basin (Bailleul *et al.*, submitted) are mainly exposed within the Akitio syncline (Fig. V-7). The sedimentary infill of the Akitio basin, mainly bathyal, is illustrated by two vertical sections, the Branscombe and the Pongaroa sections (Fig. V-10). They have been measured respectively on the eastern and western flanks of the Akitio syncline. Most of the measured sections also present these units and they permitted to identify and characterize the edges of the Akitio basin (Fig. V-10). The Akitio basin comprises 3 sedimentary units (U2 to U4) deposited from *c.* 17.5 to *c.* 13.2 Ma.

U2: late Altonian (PI >, *c.* 17.5 – *c.* 16.5 Ma)

The base of the Akitio basin corresponds to an angular unconformity (D2, *c.* 17.5 Ma) which is associated to inversions of paleocurrent directions, from eastward paleoflows within U1 to northwestward paleoflows within sedimentary unit U2, and shows subsequent settlement of depositional sandy lobes (Fa1g). In the Fingerpost section, D2 corresponds to unconformable deposition of late Altonian outer shelf facies (Fa5 + Fa6b/c) over basal Miocene distal turbidites (Fa1b) of the *Whakataki Formation* (U1). Further east, this late Altonian shelf onlaps over the Coastal Block. The location and geometry of the shelf, as well as inversions of paleocurrents within the Akitio basin suggest that the angular unconformity D2 results from the uplift of the eastern edge of the basin at 17.5 Ma. This uplift may have been controlled by major faults of the Coastal Block (Tinui and Whakataki Faults) and/or by the offshore Turnagain Fault leading to the development of the Cape Turnagain Structural High. In response to that uplift, sedimentary unit U2 develops a westward progradation of depositional lobes traducing the settlement of a well-organised long lived turbidite system within the Akitio basin.

Coastal ranges (Wairarapa onshore)

Wairarapa offshore area

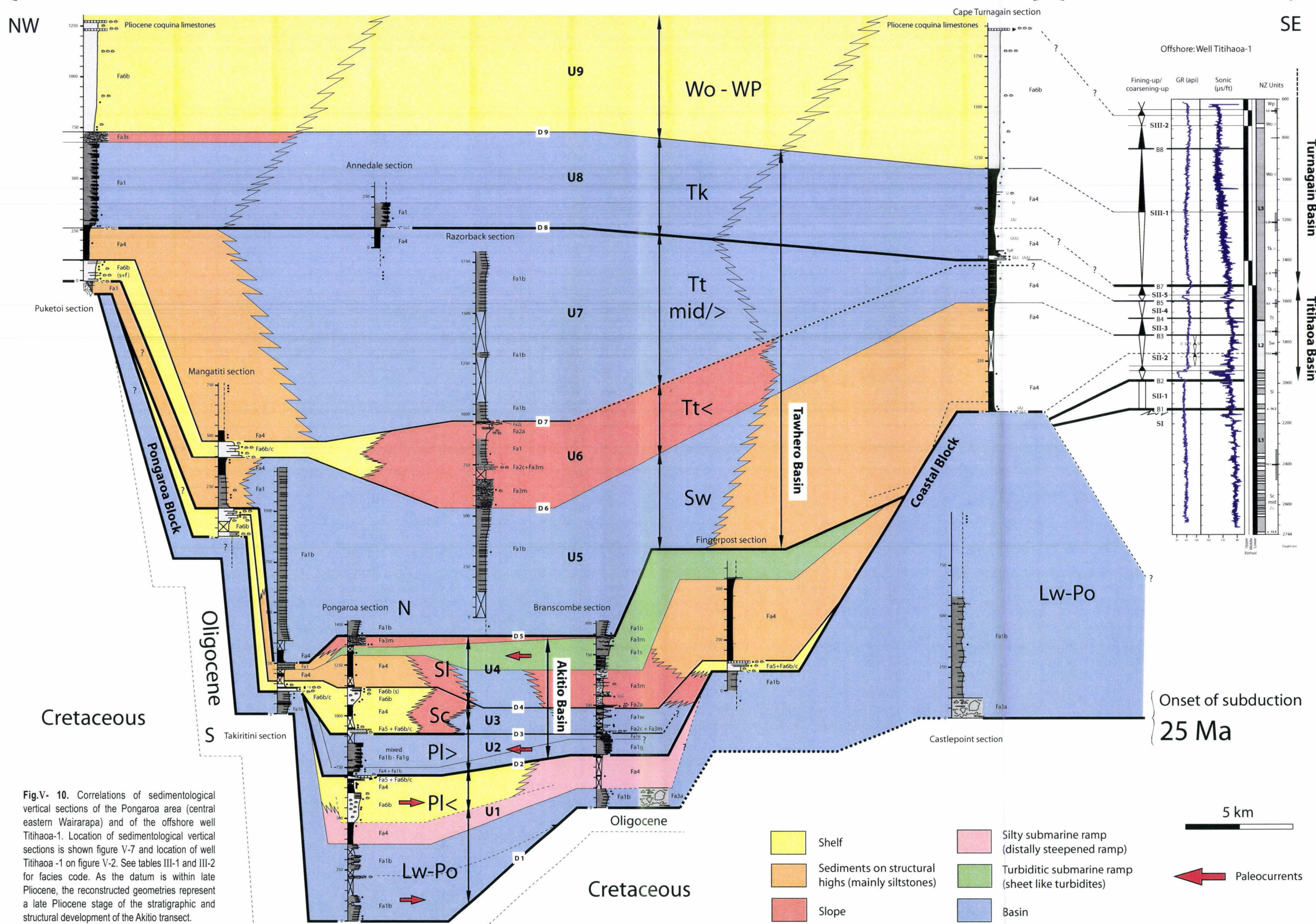


Fig.V- 10. Correlations of sedimentological vertical sections of the Pongaroa area (central eastern Wairarapa) and of the offshore well Titihaoa-1. Location of sedimentological vertical sections is shown figure V-7 and location of well Titihaoa -1 on figure V-2. See tables III-1 and III-2 for facies code. As the datum is within late Pliocene, the reconstructed geometries represent a late Pliocene stage of the stratigraphic and structural development of the Akitio transect.

100

1

U3: latest Altonian – Clifdenian (Sc, *c.* 16.5 – *c.* 15 Ma)

The basal boundary of sedimentary unit U3 is an angular unconformity (D3, *c.* 16.5 Ma) that affects the western part of the Akitio basin. In the Pongaroa section, it is marked by the brutal settlement of a latest Altonian - Clifdenian outer shelf (sedimentary unit U3, Fa5 + Fa6b/c + Fa4) over late Altonian distal sandy lobes (sedimentary unit U2, mixed Fa1b-Fa1g). Further south, correlations with the Takiritini section shows that this shelf overlies locally the basal Miocene sedimentary unit U1. The basal contact of U3 shelf is often characterized by a thin indurated sandy layer composed of exotic clasts, including fragments of pre-subduction basement rocks, broken shells and organic matter. All these observations suggest that D3 records the uplift of the Akitio basin western structural edge. As the latest Altonian – Clifdenian shelf is absent from the Puketoi section, the Puketoi area may have constituted the top of the structural high. It corresponds then to the source of basement exotic clasts.

At D3 (*c.* 16.5 Ma), the Akitio basin becomes therefore a very narrow, 5 km wide, trench-slope basin ponded between early – middle Miocene structural ridges: the Cape Turnagain and the Puketoi Structural Highs bounded by the Fingerpost shelf and the Pongaroa shelf respectively. These ridges may have been controlled by activity of the main faults identified in the study area: the Tinui, Whakataki and Turnagain Faults to the east, and the Waihoki, Mangatiti, Pongaroa and Breakdown Faults to the West (Figs. V-8, 11 and 12). The Breakdown Fault, striking N-S and dipping 70°-80° W, marks the eastern boundary of the Pongaroa shelf. Reconstructed paleogeography of the Akitio basin at the end of late Altonian (*c.* 16 Ma, Fig. V-13) shows that the repartition of shelf facies (late Altonian turitellidae carbonates, Fa5 and Fa6c) is consistent with a shelf edge oriented north-south. This suggests that the Puketoi Structural High have also developed with a north-south orientation during this stage.

U4: Lillburnian (Sl, *c.* 15 – *c.* 13.2 Ma)

U4 is bounded at base by a sedimentary discontinuity (D4, *c.* 15 Ma) that shows the drowning of the latest Altonian – Clifdenian shelves by massive silty facies (Fa4, Pongaroa, Takiritini and Fingerpost sections). Such silty facies were deposited during a period of high terrigenous flux within the axis of the Akitio basin (continuation of westward progradation of a turbidite system in the Branscombe section). The repartition of these silty formations on top of older shelf deposits suggests that the former structural highs, probably not any more active, were still constituting the borders of the Akitio basin.

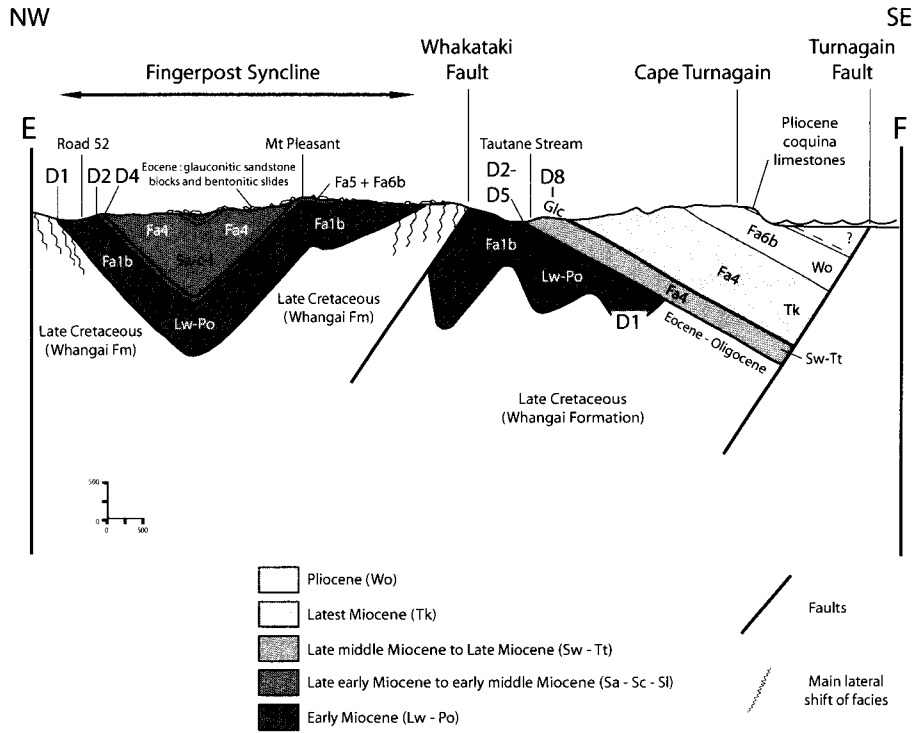


Fig.V- 11. Cape Turnagain cross-section. See figure V-7 for location and refer to tables III-1 and III-2 for facies code (Fa). D1, D2, D4, D5 and D8 - stratigraphic units boundaries, also noted on figure V-10.

On the western side of the Akitio basin, this is also confirmed by synchronous deposition of shelf facies (Fa6b) in the Mangatiti section. D4 represents a rapid deepening over the whole Akitio basin (*e.g.* from outer shelf to upper bathyal depths in the Pongaroa section) that is consistent with the facies changes described above. This sedimentary discontinuity therefore traduces the onset of subsidence of the Akitio basin and of its bounding Puketoi and Cape Turnagain Structural Highs. Despite the subsident regime, the continuation of the Akitio basin filling up is favoured by high sedimentary flux. Filling-up processes stopped at D5 (*c.* 13.2 Ma), which also characterized the base of the larger middle-late Miocene (*c.* 13.2 – *c.* 5.3 Ma) Tawhero slope basin.

3) Development of the late Miocene Tawhero slope basin (U5 to U8)

The Tawhero and the Waihoki synclines (Fig. V-12) include the late middle Miocene and late Miocene (*c.* 13.2 – *c.* 5 Ma) turbidite deposits of the Tawhero basin. At Cape Turnagain (Fig. V-11) and within the Puketoi monocline (Fig. V-12), the late Miocene sediments were deposited closer to the edges of the basin. The early Pliocene geometry of the Tawhero basin was therefore reconstructed on the basis of the Puketoi, Mangatiti, Takiritini, Annedale, Pongaroa, Razorback, Branscombe and Cape Turnagain sections (Fig. V-10). The Tawhero basin comprises 4 sedimentary units (U5 to U8) deposited from *c.* 13.2 to *c.* 5.3 Ma.

U5: Waiauan (Sw, *c.* 13.2 – *c.* 11 Ma)

The base of the Tawhero basin (D5, *c.* 13.2 Ma) is characterized by a rapid change in facies traducing an abrupt deepening of depositional environments confirmed by paleobathymetric estimations on foraminifera (*e.g.* Pongaroa and Branscombe sections; U5 mid-lower bathyal distal turbidites, Fa1b, over U4 middle bathyal slope facies, Fa3m). To the west of the Akitio transect, D5 is an erosional angular unconformity. To the east, a renewal of marine sedimentation is observed in the Cape Turnagain section with deposition of a decimetric basal glauconitic and highly bioturbated sandstone beds overlain by thick massive siltstone facies (fa4). This Waiauan (late middle Miocene) sedimentation occurred unconformably over basal Miocene series or, laterally, over pre-subduction basement rocks (Fig. 11) of the Cape Turnagain Structural High. D5 therefore marks an acceleration of subsidence at *c.* 13.2 Ma. This major subsidence has led to the drowning of the early-middle Miocene Akitio confined trench-slope basin. As subsidence also concerns bounding structural ridges, it results an important enlargement of the depositional domain: the large Tawhero slope basin.

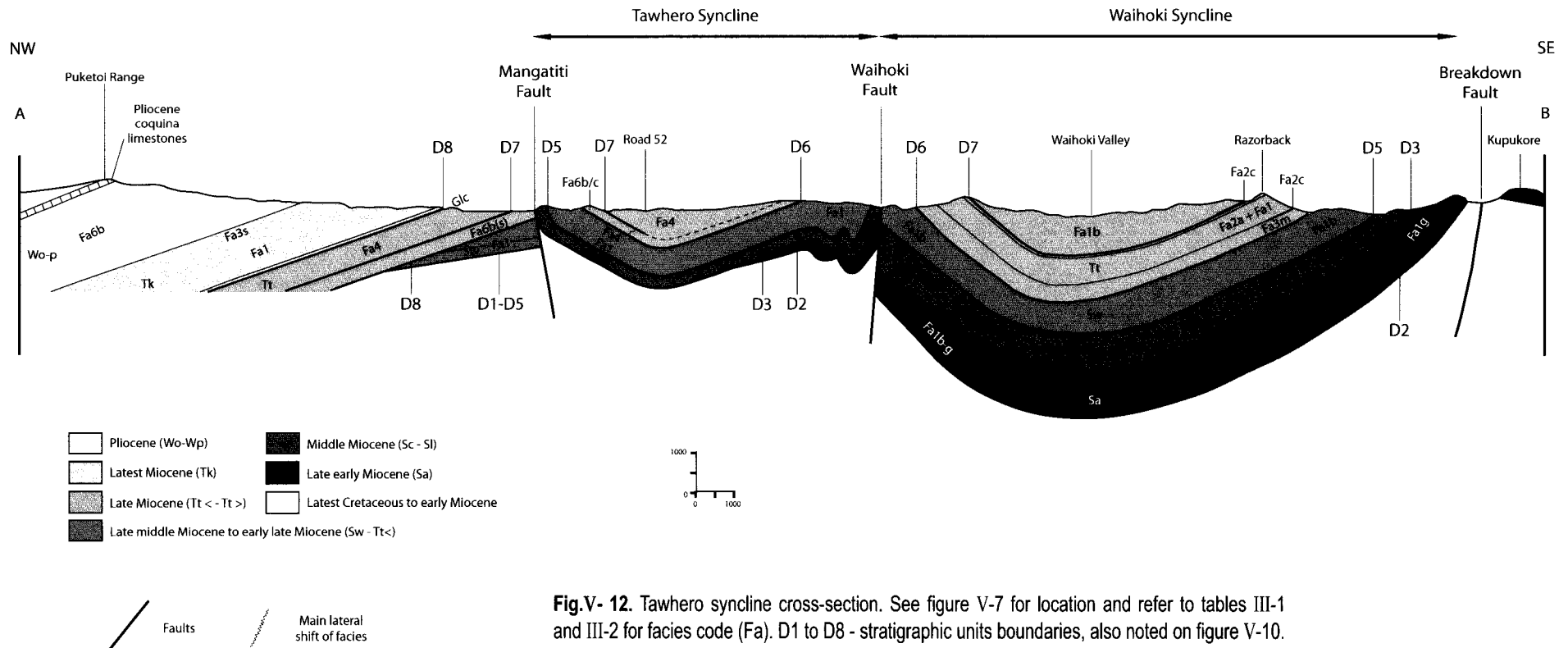


Fig.V- 12. Tawhero syncline cross-section. See figure V-7 for location and refer to tables III-1 and III-2 for facies code (Fa). D1 to D8 - stratigraphic units boundaries, also noted on figure V-10.

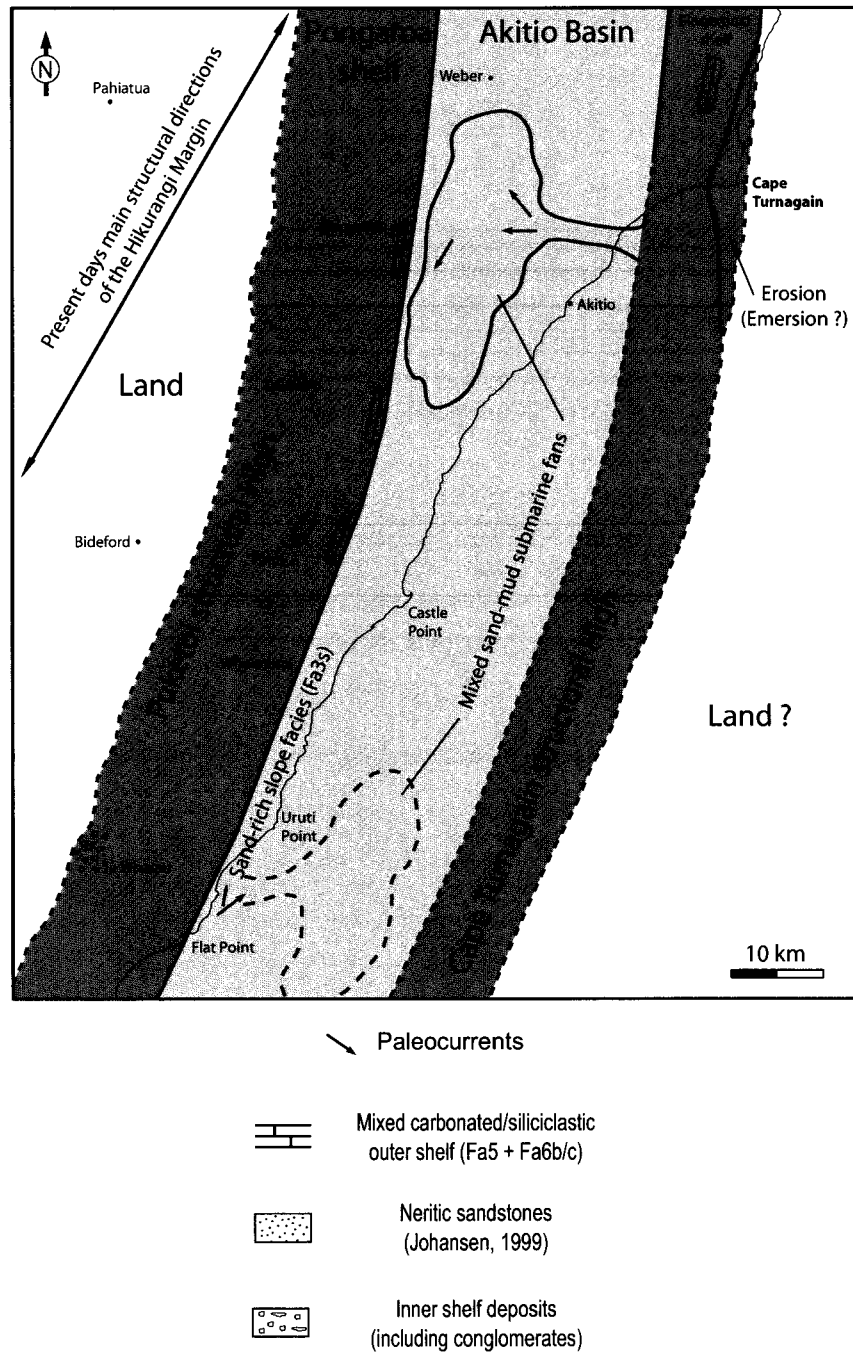


Fig.V- 13. Paleogeographic map of the Akitio basin at the end of early Miocene (c. 16 Ma). See tables III-1 and III-2 for facies code (Fa).

U6: Lower Tongaporutuan (Tt <, c. 11 – c. 9 Ma)

U6 basal boundary consists in a low angle angular unconformity (D6, c. 11 Ma) that affects the western part of the Tawhero basin. There, in the Puketoi section, sedimentary unit U6 is characterized by the development of an early Tongaporutuan (earliest late Miocene) shelf (Fa6b/s+f) which unconformably overlies either sedimentary series of U5 or the late Cretaceous (*Whangai Formation*) pre-subduction basement (Figs V-8 and V-12). This shelf extends as far east as the Mangatiti section (Fa6b/c) passing laterally through slope facies and channelized formations (Fa3m, Fa2c, Fa2a) in the Razorback section. This traduces the existence of a second deformational episode of the Puketoi area, responsible for tilting of U5 strata, at c. 11 Ma. This deformation may be attributed to a re-activation of the Puketoi Structural High.

U7: Middle-late Tongaporutuan (Tt mid/>, c. 9 – c. 6.5 Ma)

U7 is bounded at base by a sedimentary discontinuity (D7, c. 9 Ma) that corresponds to a rapid change in facies, associated with a brutal deepening of depositional environments (e.g. Puketoi section; U7 massive silty facies, Fa4, over U6 shelf facies, Fa6b/s+f). This deepening has continued through the whole unit as outlined by the westward retrogradation of U7 sedimentary systems. This retrogradation is also pointed out by the unconformable westward overlapping of Tongaporutuan proximal (inner shelf) deposits, above pre-subduction basement rocks, in the present-day emerged forearc basin (Fig. V-7).

U8: Kapitean (Tk, c. 6.5 – c. 5.3 Ma)

U8 basal boundary (D8, c. 6.5 Ma) is characterized by deposition of a glauconitic sand interval over the whole onshore Akitio transect. In the Cape Turnagain section, this glauconitic interval is plurimetric in thickness and is composed of beds of well sorted highly bioturbated glauconitic sands. In the Puketoi and Annedale sections, U8 basal interval is restricted to a 5 to 20 cm poorly sorted glauconitic bed that comprises exotic clasts derived from the pre-subduction basement. During deposition of unit U8, from 6.5 Ma, the Tawhero basin presents its maximum wideness. At that time, its western boundary lies to the west of the study area. To the east, the Cape Turnagain Structural High was probably sealed. In this hypothesis, the Tawhero and the offshore Turnagain slope basins may have been connected by the end of Miocene times. Seaward progradation of U8 sedimentary series led to the Tawhero basin filling-up with subsequent development of a Pliocene shelf (U9, Fig. V-10).

4) The Pliocene shelf (U9 – Wo/Wp, c. 5.3 Ma – c. 3 Ma)

Sedimentary unit U9 corresponds to the progressive installation of a sandy shelf (Fa6b) over the whole studied area. The unit thickens-up to coquina limestones that have been described in detail by Beu (1995). To the east, the first limestone occurrence is late Opoitian in age (Wo, c. 4 Ma) in the Turnagain section (Kairakau limestones, pectinid rich sandy barnacle grainstone) while it is basal Waipipian (Wp, c. 3.5 Ma) to the west, in the Puketoi section (Rongomai limestones, hard cemented sandy barnacle-bivalve grainstone with oysters). The progressive development of the Pliocene shelf marks a significant shallowing of all the depositional environments in the Coastal Ranges and forearc basin. It precedes the quaternary emersion of this whole area (Ghani, 1978; Cape *et al.*, 1990, Buret *et al.*, 1996).

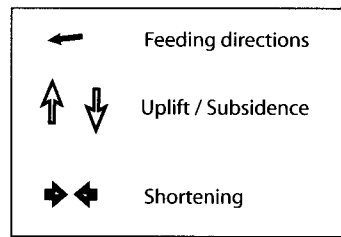
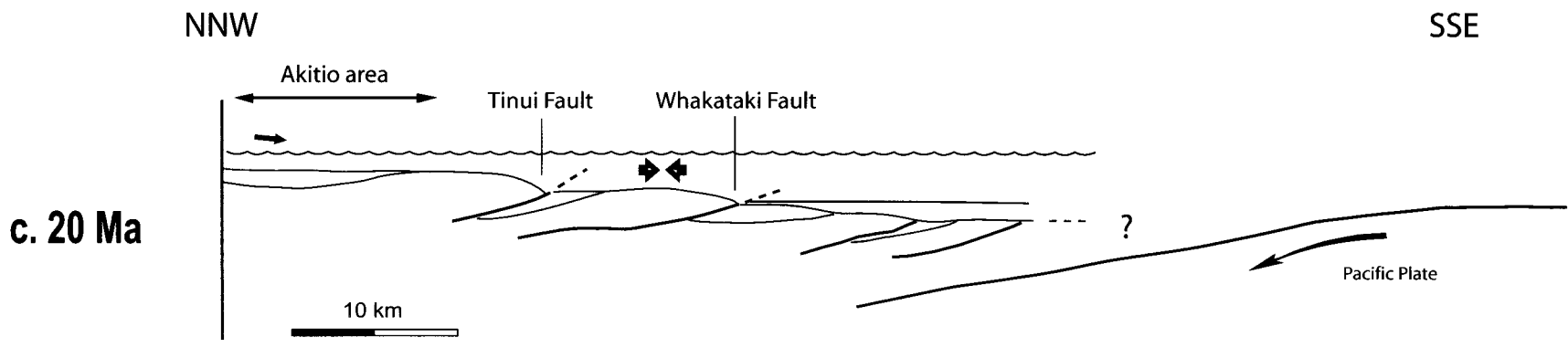
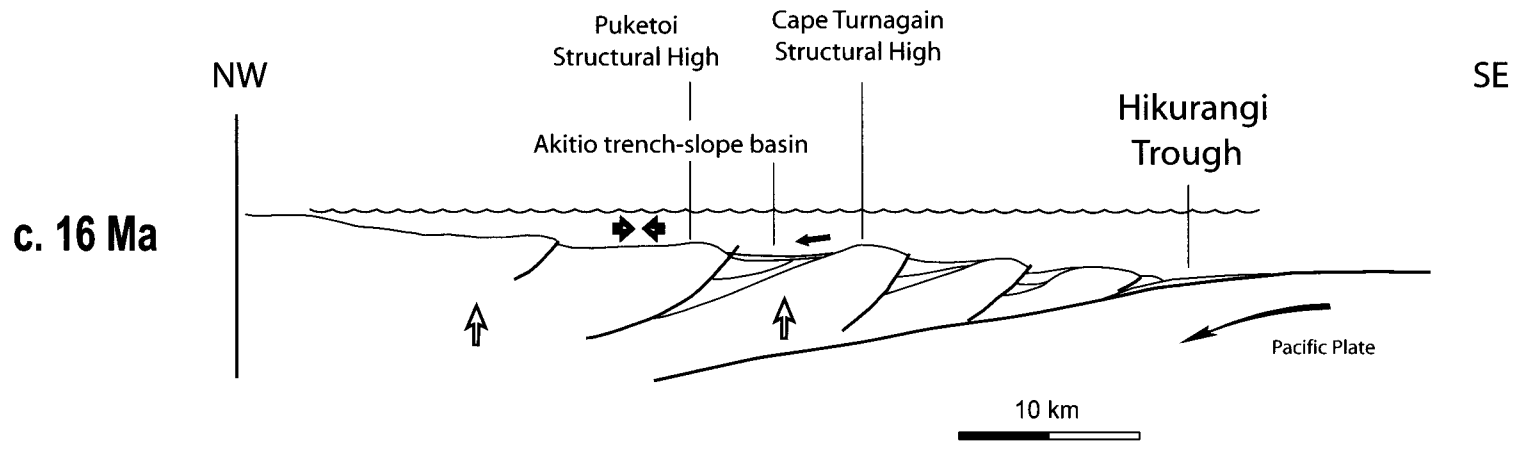


Fig.V- 14a. Tectonic evolution of the Hikurangi margin since the onset of subduction, 25 Myr ago.

VI) EVOLUTION OF THE HIKURANGI SUBDUCTION WEDGE ALONG THE AKITIO TRANSECT

The detailed study of the three morpho-structural domains across the Akitio transect of the Hikurangi subduction wedge shows an upslope increase in structural and stratigraphic complexity. Our analysis of syn-subduction depositional areas and of their structural boundaries allows a reconstitution through times of the structure and geometry of this subduction wedge (Fig. V-14). Four main tectonic periods are identified from the onset of subduction, 25 Myr ago, to present-day.

A) basal Miocene: phase of nappes emplacement (c. 25 – c. 18 Ma)

This tectonic episode (c. 25 – c. 18 Ma, Fig. V-14) is responsible for important deformation of the previous inactive margin that marks the onset of the inner subduction wedge development (Chanier and Ferrière, 1989, 1991; Chanier, 1991; Rait *et al.*, 1991).

Along the onshore Akitio transect (Coastal Ranges), this corresponds to the emplacement of seaward-directed thrust sheets that were controlled by major faults affecting the Coastal Block (*e.g.* Tinui and Whakataki Faults, Figs V-8 and V-11). The onset of deformation is associated with a sharp facies change from Eocene – Oligocene pelagic sedimentation (marls and pelagic limestones) to basal Miocene massive turbidite deposits of the *Whakataki Formation* (sedimentary unit U1, Fig. V-10). This discontinuity over the pre-Miocene basement is observed all along the East Coast and is contemporaneous with the onset of subduction (c. 25 Ma; Chanier and Ferrière, 1989, 1991; Chanier, 1991). The brutal increase of the terrigenous flux over the Hikurangi margin is characterized by olistostromal deposition at base of the *Whakataki Formation* (sedimentary unit U1, Fig. V-10). These facies are inferred to result from important sub-marine reworking related to active thrust faulting.

Thrust sheets emplacement continued during deposition of basal Miocene sedimentary series as suggested by interbedded slumps and debris-flows, which traduce slope rejuvenation (Pongaroa and Castlepoint sections - sedimentary unit U1, Fig. V-10). To the east of the Coastal Block, thick flysch deposition (Castlepoint section – sedimentary unit U1, Fig. V-10) occurred at the front of a nappe controlled by the Tinui and Whakataki Faults (Figs V-11 and V-14). To the west of the Coastal Block, syn-nappe sediments are fine-grained and much thinner (Figs V-8 and V-10 – sedimentary unit U1). These deposits were probably deposited on top of basal Miocene nappes rather than at the front of thrust sheets.

There, the significant change in the sedimentary system on top of syn-nappes series (Fig. V-10 - decrease in siliciclastic input within the distal basin plain associated to an increase in accommodation and carbonate production on the shelf as in the Pongaroa and Branscombe sections) suggests a decrease in tectonic activity during earliest Altonian (c. 19 – c. 17.5 Ma).

B) Late Altonian - Lillburnian: N-S compressional deformation (c. 17.5 – c. 15 Ma)

Some of the main thrusts related to nappes emplacement are clearly covered by Altonian sedimentary formations (19 –16 Ma; e.g. Tinui Fault, Figs V-2 and V-7). This post-nappe period is characterized by the development of highly confined trench-slope basins (e.g. the Akitio basin, Figs V-10 and V-14) associated with the rise of structural ridges. Our sedimentological analysis demonstrated that these ridges were trending NNE – SSW and developed mainly during mid-late Altonian (c. 17.5 – c. 15 Ma, Fig. V-14). The structural ridges (e.g. Cape Turnagain and Puketoi Structural Highs, Figs V-13 and V-14) were therefore likely controlled by approximately WNW-ESE compressional deformation. The Cape Turnagain bathymetric ridge was probably partially controlled by the reactivation of some previous thrust faults (e.g. Whakataki Fault, Turnagain Fault; Figs V-2, V-4 and V-8). The development of basin structural edges (slope creations or modifications traducing paleogeographic changes) had a strong influence on the basin stratigraphic architecture. These paleoenvironmental modifications are associated with rapid shifts of facies within the basin while they are often associated with local angular unconformities near the basin edges (Fig. V-10).

Offshore, the upper part of the acoustic basement (SI, Fig. V-4) is middle-late Clifdenian to early Lillburnian in age. Therefore, in the offshore Wairarapa area, the depositional environments that have existed before c. 14.2 Ma can not be constrained. However, as the acoustic basement reached by the well contains distal turbidites deposited at lower bathyal depth (Biros *et al.*, 1995), sedimentation may have occurred as well in trench-slope basins as in the trench.

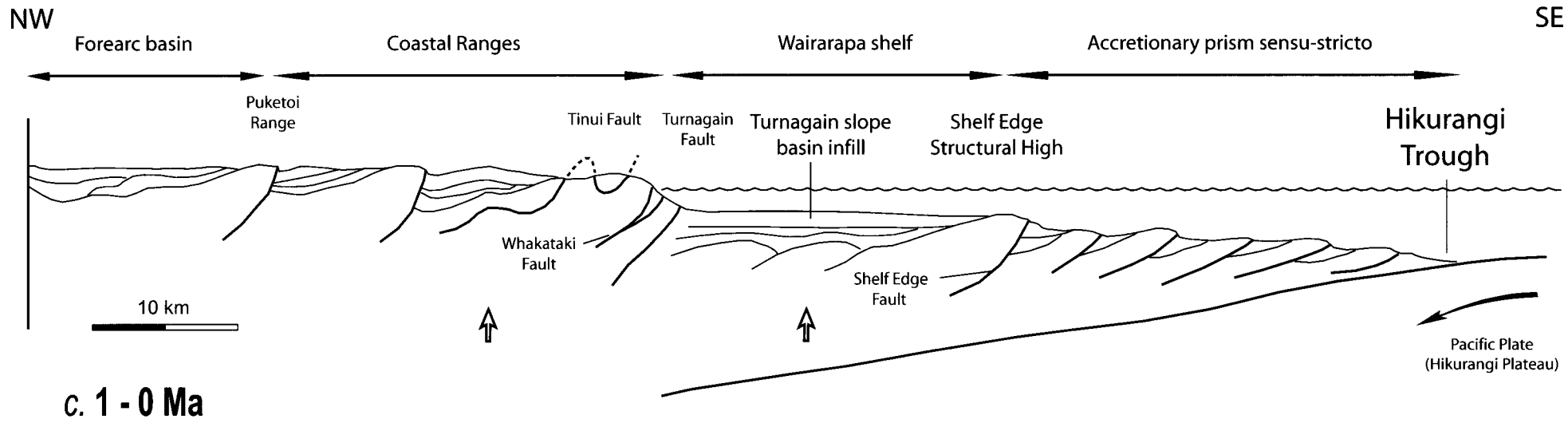
This early - middle Miocene contractional episode corresponds apparently to approximately N 110°E shortening according to the orientation of slope basins (Fig. V-13).

C) *Waiauan – Tongaporutuan: subsidence and extensional deformation (c. 15 Ma – 6.5 Ma)*

This period shows the contemporaneous development of two different structural domains separated by the Cape Turnagain Structural High area (Fig. V-14).

In the Coastal Ranges, a major subsidence event is observed and affects as well early-middle Miocene trench-slope basins as their borders (Fig. V-10). This subsident regime marks the stop of early-middle Miocene structural ridges development in the Wairarapa onshore area. Despite the subsidence, sedimentary flux can be high enough to fill-up some confined basins as observed for the Akitio basin (Fig. V-10). Moreover, the structural ridges are progressively drowned by sediments. An acceleration of subsidence is recorded trough facies changes at *c.* 13.2 Ma and favoured the development of the unconformable Tawhero slope basin (Figs V-10 and V-14). This basin is characterized by an important enlargement of the depositional area compared to the underlying confined trench-slope basins (Figs. V-10 and V-14). The widespread subsidence and associated normal faults, that affects the whole Coastal Ranges, is interpreted as the result of tectonic erosion of the Hikurangi margin by Chanier *et al.* (1999). During this episode, a local uplift pulse can be envisaged from the sedimentary record of the western edge of the Tawhero basin (Fig. V-10, D6 – *c.* 11 Ma). This shallowing event occurred after an important eustatic minima, the highest recorded for the Neogene (Hardenbol *et al.*, 1998), that is therefore not be responsible for the development of the lower Tongaporutuan shelf.

Contemporaneously, east of the Cape Turnagain Structural High, the structure of the Wairarapa shelf area shows the development of a succession of acoustic basement ridges (rising between *c.* 14.2 and *c.* 6.2 Ma) which bound middle-late Miocene (*c.* 13.7 – *c.* 6.2 Ma) highly confined basins (*e.g.* the Titihaoa basin, Figs V-4 and V-14). The geometry and stratigraphic architecture of these basins (Fig. V-4) present the same characteristics than trench slope basins described on accretionary margins (*i.e.* seaward tilted surfaces related to the growth of structural ridges, local angular unconformities in the vicinity of the structural ridges ...; *e.g.* Moore and Karig, 1976; Lewis, 1980; Stevens and Moore, 1985; Davey *et al.*, 1986; Lewis *et al.*, 1988).



- ↑ ↓ Uplift / Subsidence
- ↔ ↔ Shortening
- ↔ ↔ Extension

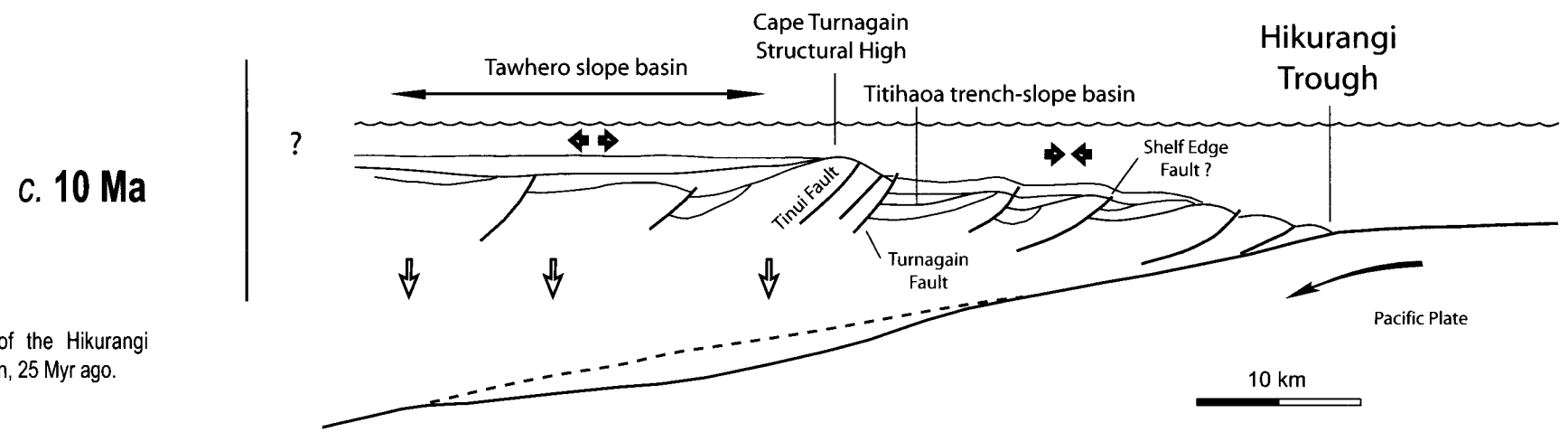


Fig.V- 14b. Tectonic evolution of the Hikurangi margin since the onset of subduction, 25 Myr ago.

According to both offshore and onshore analysis of this Waiauuan – Tongaporutuan period (*c.* 15 – *c.* 6.5 Ma), we propose that 1) the Hikurangi margin was probably mainly controlled by tectonic erosion, responsible for subsidence and extensional deformation within the upper part of the subduction wedge (present-day Coastal ranges, Fig. V-14); and 2) Closer to the subduction front (present day Wairarapa shelf), the presence of contemporaneous trench-slope basins suggests the continuation, at least locally, of accretionary processes leading to the development of a small frontal subduction wedge (Fig. V-14). This late Miocene model for the Hikurangi active margin can be for example similar to the present-day tectonic setting of the Peru Trench (Von Huene *et al.*, 1986), where a small accretionary prism develops in the lower slope of a margin dominated by tectonic erosion.

D) Kapitean – Present-day: contraction and global uplift of the margin (c. 6.5 Ma – c. 0 Ma)

From the latest Miocene times (*c.* 7 – 6 Ma) to present-day, the Coastal Ranges are characterized by the return to dominating contractional deformation. During this period, at least three main shortening episodes have been recognised widespread within the Coastal Ranges: *c.* 8 – *c.* 6 Ma, *c.* 3.4 – *c.* 2.4 Ma, and *c.* 1.8 – 0 Ma (Nicol *et al.*, 2002). Within the study area, onshore, the first episode corresponds to the folding of late Miocene strata. Many folds axis are striking N-S (*e.g.* Tawhero syncline, Te Wharau syncline; Fig. V-2). This N-S direction never appears in Pliocene and younger deposits. We thus consider that this first episode was driven by E-W compression. The second paroxysmal shortening event can be notably identified from progressive tilting during folding of late Pliocene coquina limestones, as observed NW of Pongaroa where it can be associated to NW-SE shortening (Fig. V-9, stereoplot a). The third event, still active, corresponds also to NW-SE shortening and is outlined by recent motions along some major faults within the Coastal Block (*e.g.* Whakataki Fault, Castlpoint Fault, Fig. V-2).

As regards sedimentological evolution, this period is characterized by deposition of a prograding parasequence, from basin turbidites to shelf facies, within the Tawhero basin (Fig. V-10). The base of this parasequence corresponds to a glauconitic interval, basal Kapitean in age (*c.* 6.3 Ma), that probably characterizes a maximum of water depth. This is consistent with the contemporaneous change from retrogradational to progradational sedimentary systems within the Tawhero basin, and with the subsequent shallowing of depositional environments pointed out by paleontological data. All these observations suggest that post-6.5 Ma shortening episodes are accompanied by global uplift of the margin (Fig. V-14) that has started at base of Kapitean (*c.* 6.5 Ma).

Offshore, in the Wairarapa shelf area, deformation features attributed to the post- 6.5 Ma period are mainly associated with large faults. Some corresponds to major reverse faults that affect the whole Pliocene series (*i.e.* Turnagain Fault, Fig. V-4), or to more complex deformation zones as along the Shelf Edge Fault (Fig. V-6). Latest Miocene compressive deformation is also identified and is pointed out by the slight folding of the Turnagain basin sedimentary series and local angular unconformities related to the reactivation of old structural ridges (*i.e.* structural ridge SR2) (Fig. V-4). At base of the Turnagain basin, a major angular unconformity (SB2, *c.* 6.2 Ma; Fig. V-4) seals the middle-late Miocene narrow trench-slope basins, as well as their borders. This unconformity marks the end of confined basin filling-up before important enlargement of the depositional domain as shown by the development of the Turnagain slope basin. This event is accompanied by an abrupt shallowing suggesting the rapid uplift of the whole Hikurangi margin (Fig. V-14). At that time, most of the compressive deformation occurs probably in the lower part of the subduction wedge and early-middle Miocene structural ridges located in the Wairarapa shelf area are blocked.

From offshore and onshore data, we can observe that the whole margin has been uplifted by approximately 6.5 Ma, leading to a rapid shallowing of depositional environments. This event is also outlined by a brief episode of shortening. This 6.5 Ma event can be related to the possible onset of subduction of the Hikurangi Plateau carried by the Pacific Plate. This has been proposed to account for similar events (general event and compression at *c.* 5 Ma further North (Buret *et al.*, 1997). Alternatively, if we consider that the Hikurangi plateau is subducted since the onset of subduction, the arrival into the trench of a thicker part of the plateau may explain the uplift event. At this stage, accretion and Pliocene trench-slope basins development may have began to the east of the shelf edge.

After the Pliocene, NW-SE contractional deformation has continued over the whole Hikurangi subduction wedge leading to the recent emersion of the Coastal Ranges (Ghani, 1978; Cape *et al.*, 1990). In the Akitio transect, it is expressed by the continuation of NE-SW folding onshore (initiated during late Pliocene) and by the reactivation of old thrust faults such the Whakataki, Castlepoint, and Turnagain faults. Offshore, the Quaternary compression is mainly expressed further south, in the Castlepoint transect, by recent activity on the shelf edge and the subdivision of the Turnagain basin into two synclines (Fig. V-6). We also notice that the Turnagain Fault zone, which includes the Castlepoint Fault and the Whakataki Fault, presents a very recent Quaternary reverse motion. The motion along this major fault zone probably controls most of the uplift and subsequent emersion of the Coastal Ranges.

VII) CONCLUSIONS

The main tectonic episodes identified along the Akitio transect of the Hikurangi subduction wedge are (Fig. V-14): **1)** Basal Miocene phase of nappe emplacement (*c.* 25 – *c.* 18 Ma), **2)** Early-middle Miocene E-W compressive deformation (*c.* 17.5 – *c.* 15 Ma), **3)** Major subsidence and extensional deformation probably related to tectonic erosion (*c.* 15 – *c.* 6.5 Ma), and **4)** Latest Miocene-Quaternary N-S to NW-SE compressional deformation and general uplift of the margin (*c.* 6.5 – *c.* 0 Ma). Tectonic episodes may have been induced by modifications of the sedimentary influx within the trench or by variations in thickness and coupling of the downgoing Hikurangi Plateau.

Nowadays, three morphostructural domains may be distinguished along the Akitio transect (Fig. V-2):

The first Domain, the Coastal Ranges (present-day emerged trench-slope break of the Hikurangi margin), has developed since 25 Myr and has therefore registered the four tectonic episodes with **1)** emplacement of seaward directed thrust sheets responsible for intense deformation of the pre-subduction passive margin during the basal Miocene shortening, **2)** Folding and faulting of the basal Miocene nappes with development of early-middle Miocene trench-slope basins confined between active structural ridges during E-W compressional deformation, **3)** subsidence, enlargement of the depositional domain and normal faulting during the period of tectonic erosion, and **4)** uplift, folding, reverse faulting and emersion during the Plio-Quaternary contractional episodes. During the Pliocene, the Coastal Ranges domain was forming a shelf bounded by active structural highs, the Cape Turnagain Structural High constituting the Pliocene shelf edge. At that time, this domain was very similar to the present-day Wairarapa shelf.

The second domain, the Wairarapa shelf, shows signs of ancient nappes that may have developed over large flat strong seismic reflectors. However, this domain mainly illustrates the two last tectonic episodes: **1)** trench-slope basin development associated to the growth of a frontal subduction wedge during the period of tectonic erosion, and **2)** uplift, enlargement of the depositional domain (related to an upslope stop of structural ridges development) and slight compressive deformations leading finally to the settlement of the Wairarapa shelf with the Shelf Edge Structural High area constituting the present-day shelf edge.

The third domain, the accretionary prism *sensu-stricto*, has only undergone the most recent tectonic episode with development of an accretionary wedge, typical imbricated thrust geometry and development of Plio-Quaternary trench-slope basins.

These domains are separated by major ancient thrust faults, now reactivated, such as the Whakataki, Turnagain and Shelf Edge Faults. These Faults had controlled the growth of structural ridges (the Cape Turnagain Structural High and the Shelf Edge Structural High) that have bounded Mio-Pliocene slope basins: the highly confined Akitio and Titihaoa trench-slope basins, and the large Tawhero and Turnagain slope basins. The Turnagain fault zone and the Shelf Edge fault zone have been reactivated during the most recent contractional episode. The location of this major fault zones coincides with present-day geographic boundaries: the Wairarapa coast-line and the Wairarapa shelf edge.

This stratigraphic and structural study, onshore and offshore, therefore shows that the complex structural pattern of the Hikurangi margin results **1)** from a complex tectonic history which comprises several phases of deformation since the onset of subduction, 25 Myr ago, and **2)** from transversal variations in the distribution of the deformation during this tectonic evolution. The present-day juxtaposition of three morpho-structural domains along the Akitio transect is therefore explained by their difference in age and their relative position in the subduction wedge trough times. Finally, we also notice latitudinal variations in the amplitude of deformation as illustrated, during the Plio-Quaternary tectonic episode, by the southward increase of basin strata tilting within the large Turnagain basin.

Chapitre VI

Synthèse et Conclusions



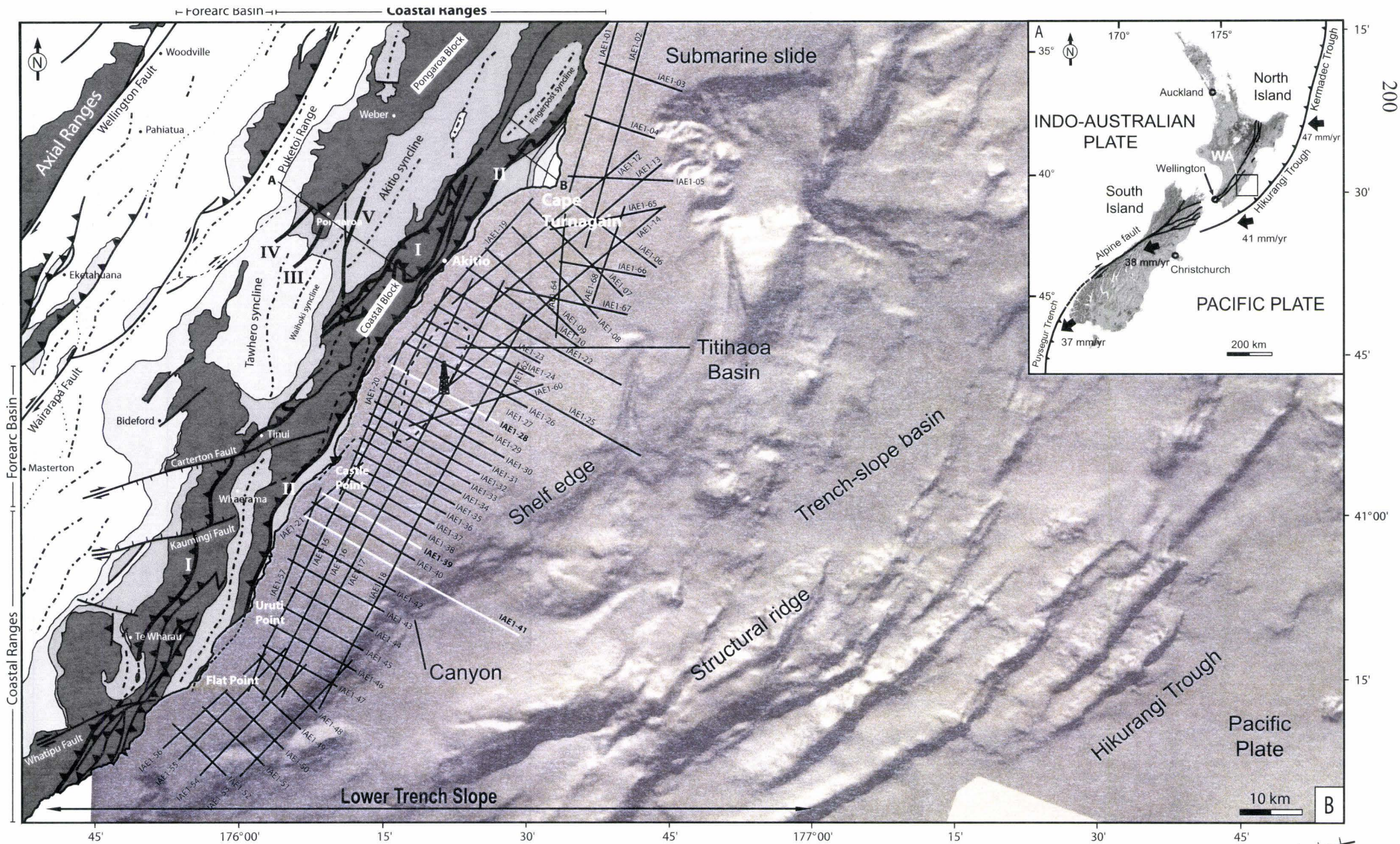
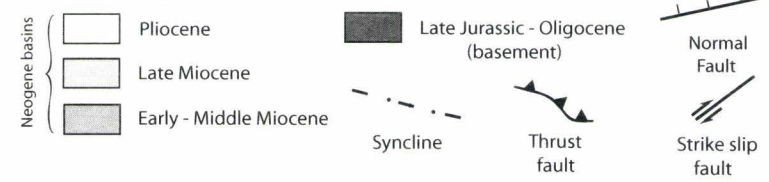


Fig.VI- 1. A - Plate tectonic setting of New Zealand, black arrows show present-day relative plate motion between Pacific and Australian plates (WA - Wairarapa Area). **B** - Bathymetric map (Lewis *et al.*, 1999) and onshore structural map (modified from Lee and Begg, 2002) of the Wairarapa area. The offshore Wairarapa area includes location of the Amoco IAE1 seismic survey and well Titihaoa-1. I - Tinui Fault Complex, II - Whakataki Fault, III - Waihoki Fault, IV - Mangatiti Fault, V - Breakdown Fault, A-B location of cross-section shown figure VI-7.



Chapitre VI

Synthèse et Conclusions

Les principaux résultats obtenus au cours de ce travail de thèse ont été exposés et synthétisés dans les publications intégrées au manuscrit. Je ne présenterais donc ici qu'une vue d'ensemble, en essayant de dégager les résultats majeurs et/ou nouveaux qui permettent de mieux appréhender l'évolution stratigraphique et structurale des bassins perchés et de la marge active qui les porte. De plus, je propose ici une discussion sur l'évolution des mouvements verticaux à partir de courbes de subsidence.

Le prisme de subduction Hikurangi, objet de cette étude, est particulier pour deux raisons majeures. Tout d'abord, sa partie interne (côté arc) est en grande partie émergée et forme une chaîne côtière déformée où affleurent d'épaisses séries sédimentaires syn-subduction (Fig. VI-1). De plus, la partie interne de ce prisme déformé comprend un soubassement qui ne résulte pas d'accrétion *sensu-stricto* mais de la déformation (grandes nappes chevauchantes) de l'ancienne marge passive qui existait à ce niveau avant le démarrage de la subduction, il y a 25 Ma. Ceci nous a conduit à définir l'ensemble du prisme déformé compris entre la fosse Hikurangi et le bassin avant-arc comme un *prisme de subduction* qui comprend **1**) un prisme de subduction externe (à proximité de la fosse de subduction) qui correspond à un prisme d'accrétion *sensu-stricto*, et **2**) un prisme de subduction interne qui comprend un soubassement plus ancien, plus déformé et résultant de la déstructuration de la marge passive anté-subduction. Il est probable que cette terminologie puisse s'appliquer à la plupart des prismes dit *d'accrétion* ceux-ci pouvant également inclure dans leur partie interne un tel soubassement (probablement difficile à différencier en sismique d'un soubassement lié à de l'accrétion pure).

L'analyse stratigraphique et structurale, à terre et en mer, du prisme de subduction Hikurangi a montré : **1**) une grande variabilité des environnements sédimentaires comprenant des bassins perchés confinés (5 à 10 km de large) qui se développent entre des rides structurales (*trench-slope basins* ; Moore et Karig, 1976 ; Stevens et Moore, 1985 ; Underwood et Moore, 1995 ; cf. Figs I-3 et I-5), des bassins de pente beaucoup plus larges (30 à 40 km de large), et des plate-formes mixtes carbonatées-silicoclastiques ; et **2**) une histoire tectonique polyphasée qui, associée à des variations transversales de la déformation aux différentes époques, est à l'origine de la juxtaposition actuelle de trois domaines morphostructuraux différents : la Chaîne Côtière, la plate-forme du Wairarapa et le prisme d'accrétion *sensu-stricto* (Fig. VI-1)

Cette étude a tout d'abord été axée sur la dynamique sédimentaire et structurale des bassins perchés confinés qui constituent l'environnement de dépôt le plus caractéristique et le plus complexe des prismes de subduction.

I) LES BASSINS PERCHÉS CONFINÉS

L'étude combinée des bassins miocènes d'Akitio, situé à terre (analyse de faciès, stratigraphie, cartographie et analyse structurale), et de Titihaoa, situé en mer (stratigraphie sismique et données de forage) a permis de caractériser le fonctionnement en contexte compressif des bassins perchés confinés du prisme de subduction Hikurangi, du point de vue sédimentaire, de la déformation, et de leurs interactions (Fig. VI-2). Dans les deux cas, il s'agit de bassins matures (Underwood et Bachman, 1982) c'est à dire directement connectés à des zones d'alimentation, ce qui permet de forts flux sédimentaires à l'origine de leur comblement et du caractère très progradant des séries sédimentaires. Le bassin d'Akitio est daté du Miocène inférieur au Miocène moyen (*c.* 17.5 – *c.* 13.2 Ma) et contient 900 à 1000 m de sédiments turbiditiques déposés en 4.3 Ma. Le bassin de Titihaoa se développe du Miocène moyen au Miocène supérieur (*c.* 13.7 – *c.* 6.2 Ma) et son épaisseur sédimentaire est de l'ordre de 600 m pour une durée de 7.5 Ma.

A) Faciès et systèmes de dépôt

Afin de mener à bien l'étude stratigraphique détaillée des bassins perchés sur le prisme de subduction Hikurangi, il était nécessaire d'effectuer une analyse préalable des faciès rencontrés afin de typer les systèmes de dépôts et d'en comprendre le fonctionnement. Cette étude de faciès a été menée sur l'ensemble du domaine émergé Est-Wairarapa (Fig. VI-1) qui présente à l'affleurement d'épaisses séries sédimentaires miocènes, en apparence homogènes, représentatives de la sédimentation au sein des bassins perchés néo-zélandais ainsi que sur leurs bordures. Ces faciès ont été partiellement décrits auparavant (*e.g.* Vella and Briggs, 1971 ; Moore, 1980 ; Crundwell, 1997 ; Chanier et Ferrière, 1991 ; Neef, 1992a) mais ces études étaient soit trop anciennes pour prendre en compte les avancées récentes concernant les systèmes gravitaires, soit relativement localisées. De plus, la plupart de ces études n'incluaient pas de levés stratigraphiques détaillés ni l'analyse de faciès pouvant y être associée.

Coastal ranges (Wairarapa onshore area)

Wairarapa offshore area

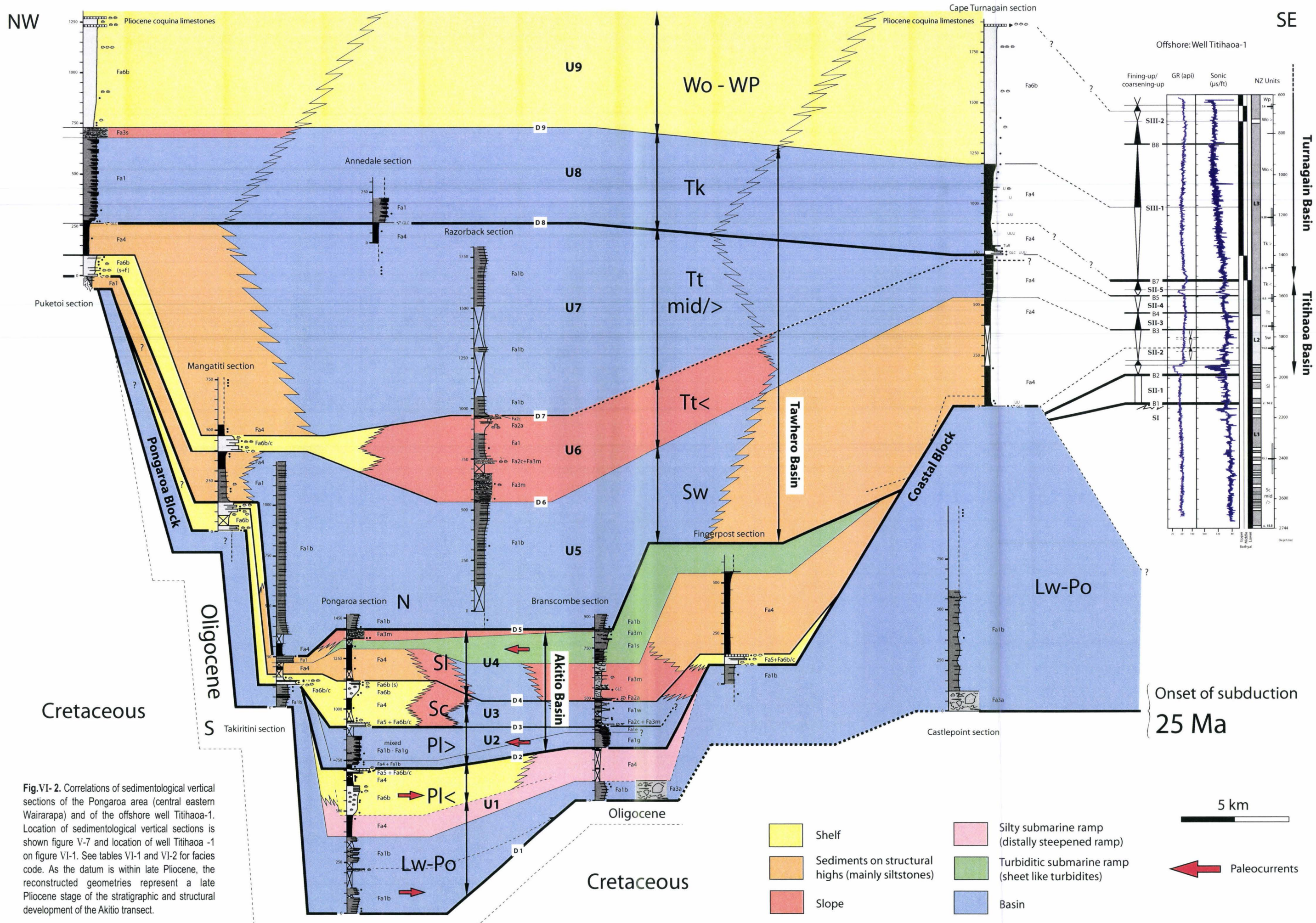


Fig.VI- 2. Correlations of sedimentological vertical sections of the Pongaroa area (central eastern Wairarapa) and of the offshore well Titihaoa-1. Location of sedimentological vertical sections is shown figure V-7 and location of well Titihaoa -1 on figure VI-1. See tables VI-1 and VI-2 for facies code. As the datum is within late Pliocene, the reconstructed geometries represent a late Pliocene stage of the stratigraphic and structural development of the Akito transect.

1) Faciès

La principale particularité des faciès étudiés est leur très faible granulométrie qui affecte jusqu'aux faciès les plus proximaux (*e.g.* les faciès de crue identifiés en domaine de plate-forme interne présentent une granulométrie proche de celle des sables moyens). Ceci peut s'expliquer par la nature des roches du soubassement dont l'érosion est à l'origine des apports terrigènes dans les bassins. Dans le secteur d'étude, il s'agit essentiellement de turbidites distales et silts massifs du Crétacé supérieur (*Whanghai Formation*), d'argiles riches en smectites et de grès glauconieux de l'Eocène, et de marnes blanches et de turbidites distales de l'Oligocène (*Weber Formation*). La faible granulométrie des séries sédimentaires miocènes a nécessité l'établissement d'un nouveau modèle de faciès (Tableaux VI-1 et VI-2) plutôt que l'utilisation du modèle de lithofaciès de Mutti et Ricci Lucchi (1978) utilisé dans la plupart des études sédimentologiques concernant le remplissage des bassins perchés (*e.g.* Underwood and Bachman, 1982 ; Underwood and Moore, 1995). Deux types principaux d'environnements sédimentaires ont été différenciés dans ce modèle : les dépôts gravitaires et les sédiments de plate-forme.

Les dépôts marins profonds (Tableaux VI-1 et VI-2) comprennent des alternances turbiditiques (Fa1), des faciès chenalisés (Fa2), des faciès chaotiques (Fa3) ainsi que des argiles et silts massifs (Fa4). Les dépôts de plate-forme incluent des calcaires alguaires (Fa5) ainsi que des silts et grès bioclastiques (Fa6). Nous nous sommes particulièrement intéressés aux faciès gravitaires qui ont été interprétés en termes d'environnements de dépôt (prenant en compte les processus d'écoulement gravitaire) et intégrés au sein d'un modèle de dépôt basé sur les caractéristiques des systèmes turbiditiques. Pour cela, nous nous sommes basés sur les travaux de Mutti et Normark (1987, 1991) qui décrivent les différents éléments morphologiques constitutifs de ces systèmes gravitaires. Ceci nous a permis d'établir une zonation distal/proximal des faciès de la zone d'étude par rapport à la source des apports sédimentaires (Tableaux VI-1 et VI-2 : Fa1b et Fa4 distal – plaine sous-marine, Fa1g – lobe de dépôt, Fa1e – transition chenal-lobe, Fa1w – levées de chenaux, Fa2a et Fa2c – remplissage de petits chenaux, Fa3s et Fa3m – associations de faciès de pente. Comme déjà signalé auparavant cette zonation reflète une distance relative par rapport à la source des apports sédimentaires et les faciès gravitaires n'ont donc pas été utilisés comme marqueurs paléobathymétriques (si ce n'est relativement, par rapport aux faciès de plate-forme).

Table VI-1. Characteristics and interpretation of the sedimentary facies for the turbidites and the related deep-sea deposits identified in this study

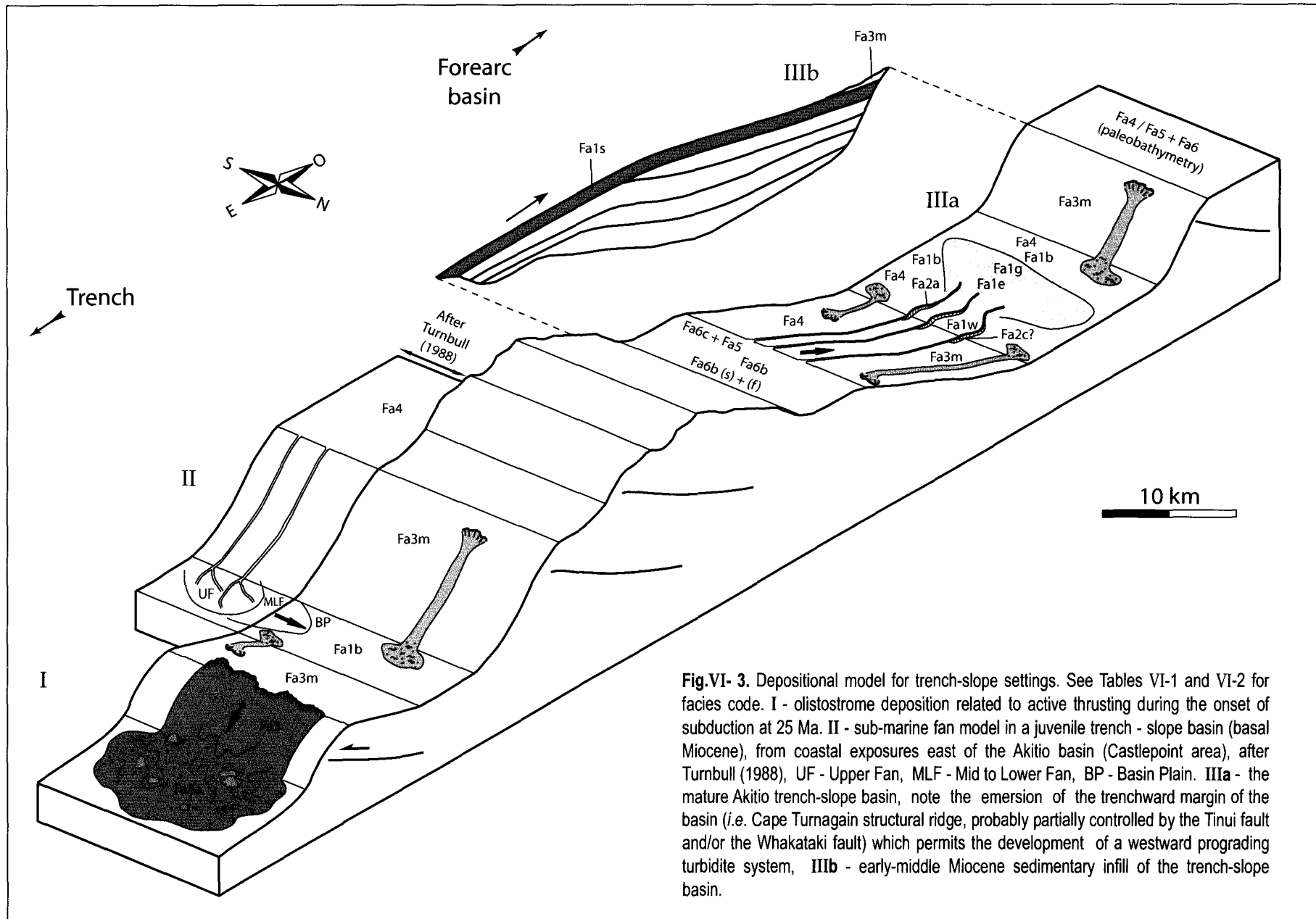
Facies code	Lithology	Stratification	Internal bedding	Gravity processes	Interpretation
<i>Alternation of fine grained sandstones with siltstones, Fa1</i>					
1b	Alternation of 1 to 50 cm thick siltstones with 1 to 50 cm thick fine grained sandstones, well sorted	Tabular, good lateral continuity of beds, sharp bases (rare flute casts) and gradational tops	Well developed Bouma sequences, Ta-e to Tc-e, most common Tb-e, systematic climbing ripples, common convolutions, local escape and load structures, sometimes non-erosive amalgamation surfaces	Low density turbidity currents (unsteady turbulent flows)	Deep sea plain like turbidites (Bouma type turbidites), distal basin plain
1g	Alternation of 5 mm to 5 cm thick siltstones with 0.5 to 2 m thick dirty fine grained sandstones, well sorted	Tabular, sharp bases and tops	Commonly massive, restricted intervals with plane laminations (traction) and well developed intervals with growing up hummocks (aggradation), sometimes non erosive amalgamation surfaces	Low density turbidity currents (unsteady turbulent flows)	Depositional lobe
1e	Alternation of 1 to 50 cm thick siltstones with 1 to 30 cm thick dirty fine grained sandstones, well sorted	Laterally discontinuous beds, numerous erosive features at bed boundaries	Commonly massive, climbing ripples (Tc), rare plane laminations (Tb), systematic intra-beds erosive amalgamation surfaces and/or "reprises granulo"??	high density turbidity currents (unsteady turbulent flows), mostly erosive (low degree of sediment preservation)	Bypass (channel – lobe transition)
1w	Alternation of 10 cm to plurimetric thick siltstones with 1 to 20 cm thick bioturbated fine grained sandstones, well sorted, bioturbated	Wedge geometry (plurimetric scale), laterally discontinuous beds, local low angle unconformities, erosive bases and gradational tops	Massive (due to the bioturbation ?), sometimes climbing ripples, rare basal coarser intervals	Lateral spreading from a high density confined turbidity current (unsteady turbulent flows)	Channel levee (overbank deposits)
1s	Alternation of 5 to 50 cm thick siltstones with 5 cm to 2 m thick fine grained sandstones, well sorted, bioturbated	Tabular (sheets), good lateral continuity of beds, sharp erosive bases and gradational to sharp tops, local low displacement slumps and slump scours	Commonly massive, sometimes plane laminations, rare ripples and convolutions, intra-beds erosive to non-erosive amalgamation surfaces	Unconfined turbidity currents (unsteady turbulent flows)	Sheet like turbidites
<i>Channelized facies association, Fa2</i>					
2a	Alternation of 5 to 10 cm thick fine grained sandstones and 5 to 30 cm thick siltstones with scattered extraformational centimetric to decimetric clasts and broken bioclasts (bivalvia, gastropoda)	Lenticular (metric scale and poorly erosive) - laterally discontinuous beds		Mud-flows (cohesive flows) and turbidity currents (unsteady turbulent flows)	Small channel
2c	Conglomerates made up of broken bioclasts (bivalvia, rare gastropoda) and minor centimetric extraformational clasts	Lenticular ?		Debris-flows (cohesive flows)	Small channel ?
<i>Disorganized facies association, Fa3</i>					
3s	Disorganized facies, syn-sedimentary deformation of alternating 20 cm to 1 m thick sandstones and 10 cm to 2 m thick conglomerates	Large displacement slumps, low displacement slumps, slump scours	Shear and load structures	Slumping and debris-flows (cohesive flows)	"Sandrich" slope facies association
3m	Disorganized facies, syn-sedimentary deformation of alternating 1 to 20 cm thick sandstones and 10 cm to plurimetric thick siltstones with scattered centimetric to decimetric extraformational clasts and broken bioclasts (bivalvia, gastropoda and rare scleractinia)	Large displacement slumps, low displacement slumps, in situ slumps, slump scours		Slumping and mud-flows (cohesive flows)	"Mudrich" slope facies association
3a	Disorganized facies, syn-sedimentary deformation of conglomerates made up of centimetric to plurimetric extraformational clasts, sometimes punctuated by mudstones or siltstones with scattered extraformational centimetric clasts	Good lateral continuity of huge sedimentary volumes, large displacement slumps	Shear and load structures	Slumping, debris-flows and sometimes mud-flows (cohesive flows)	Olistostromes

Table VI-1. (Contd.) Characteristics and interpretation of the sedimentary facies for the turbidites and the related deep-sea deposits identified in this study

Facies code	Lithology	Stratification	Internal bedding	Gravity processes	Interpretation
<i>Massive mudstones to siltstones facies association, Fa4</i>					
4	Blue grey mudstones to siltstones, more or less carbonaceous and bioturbated, scattered foraminifera, sometimes wood, common indurated diagenetic concretions and pipes	Massive, no clear stratification		Pelagic to hemipelagic deposition	Slope to distal basin plain deposition (may be precised by palaeo-ecology on foraminifers)

Table VI-2. Characteristics and interpretation of the sedimentary facies for the shelf deposits identified in this study

Facies code	Lithology	Stratification	Internal bedding	Interpretation
<i>Limestones facies association, Fa5</i>				
5	Alternation of 1 to 20 cm thick siltstones (scattered centimetric extraformational clasts and broken bivalvia bioclasts, common layers of red algae bowls) with 5 to 50 cm thick more or less clastic algal limestones. Less clastic limestones made up of abundant broken or encrusting red algae, amphisteginid foraminifers and broken bryozoa; common broken bivalvia, gastropoda; echinoderms, echinoid spines, benthic and planktonic foraminifers; rare encrusting foraminifers, oyster fragments and scaphopod molluscs; glauconite, rare quartz	Crudely stratified, lenticular, laterally discontinuous beds (lateral disappearance or shift to Fa6c or to a centimetric layer of algal layer bowls), erosive surfaces and scours	Red algal encrusting, sometimes polyphase, of reworked shelf bioclasts or aggregates (matrix and bioclasts): floatstone; micritic matrix or sometimes sparitic cement, bio-erosion	Bryozoa and amphisteginid red algal encrusted floatstone; high energy Outermost shelf
<i>Bioclastics siltstones to fine grained sandstones facies association, Fa6</i>				
6c	Well cemented 10 to 50 cm thick bioclastic fine grained sandstones (abundant broken and unbroken bivalvia, gastropoda), well sorted	Laterally discontinuous beds, generally associated at base or laterally to Fa5	Macrofauna scattered within the micritic cemented sandy component	High energy Outermost shelf
6b	Extensively bioturbated bioclastic siltstones to fine grained sandstones (bivalvia, gastropoda, scaphopoda), well sorted	Massive, may presents interstratified sub-facies: 6bs - HCS (well cemented and well sorted decimetric "en dôme" sandstone beds, erosive bases, scattered disarticulated fossils), 6bf - high flooding deposits (plurimetric beds of poorly sorted fine to medium grained sandstones, sharp bases, plane laminated, no bioclasts)	Fossils in live position, or highly concentrated within bioturbated pockets, or concentrated by storm waves within centimetric thick layers, or scattered and disarticulated.	No gravitary deposit Outer shelf (confirmed by palaeo-ecology on foraminifers) to Middle shelf (locally influenced by storm waves and high flood currents)



En effet, nous avons montré que dans ce contexte tectonique particulier, caractérisé par des sources multiples et par de très faibles granulométries, un faciès donné pouvait se rencontrer à diverses profondeurs (Fa1b - bathyal inférieur à bathyal supérieur), et inversement, des faciès différents pouvaient avoir été déposés à une bathymétrie donnée (e.g. Fa1b, Fa3m et Fa4 - bathyal moyen). Les paléobathymétries ont donc été estimées d'après les données paléontologiques (foraminifères et macrofaunes, Annexe 2), indépendamment de l'analyse de faciès. Etant donné que la zonation distal/proximal proposée représente bien une position relative des faciès (pour la plupart génétiquement liés) au sein d'un système turbiditique, deux faciès n'ont pas été intégrés dans cette zonation car ils caractérisent des systèmes gravitaires particuliers. Il s'agit des olistostromes (Fa3a) et des turbidites de type « *sheet-like* » (Fa1s).

2) les systèmes gravitaires

La plupart des études antérieures concernant des analogues anciens de bassins perchés matures montraient le développement de cônes sous-marins profonds au débouché de canyons (e.g. Smith *et al.*, 1979, Moore *et al.*, 1980, Turnbull, 1988). Ces résultats contrastaient généralement avec les études de sismique marine qui montraient rarement le développement de systèmes turbiditiques bien organisés, mais plutôt l'installation de systèmes non-chenalisés de type « *sheet-like* » (e.g. Underwood and Moore, 1995) tels que définis par Mutti and Normark (1987). Dans le bassin d'Akitio, trois systèmes gravitaires différents ont été identifiés et apparaissent successivement, à différents stades d'évolution du bassin (Fig. VI-3) :

- Le premier système gravitaire correspond à d'importants glissements sous-marins conduisant au dépôt d'olistostromes à la base des pentes. Ces dépôts se rencontrent généralement au cours des phases très précoces de développement des bassins confinés. Ils se déposent au front de nappes et sont considérés comme des marqueurs de chevauchement actif.

- Le second système gravitaire constitue l'essentiel du remplissage des bassins perchés confinés matures et marque l'installation d'une sédimentation mieux organisée au sein des bassins. Ceci traduit une diminution de l'intensité de l'activité tectonique et une certaine stabilisation des rides structurales qui continuent à se déformer mais fonctionnent alors en tant que bordures de bassin bien définies. Ce système gravitaire correspond à des cônes sous-marins de type riches en sable fin (*fine grained sand-rich submarine fans* ; Reading et Richards, 1994 ; Richards *et al.*, 1998).

Branscombe section

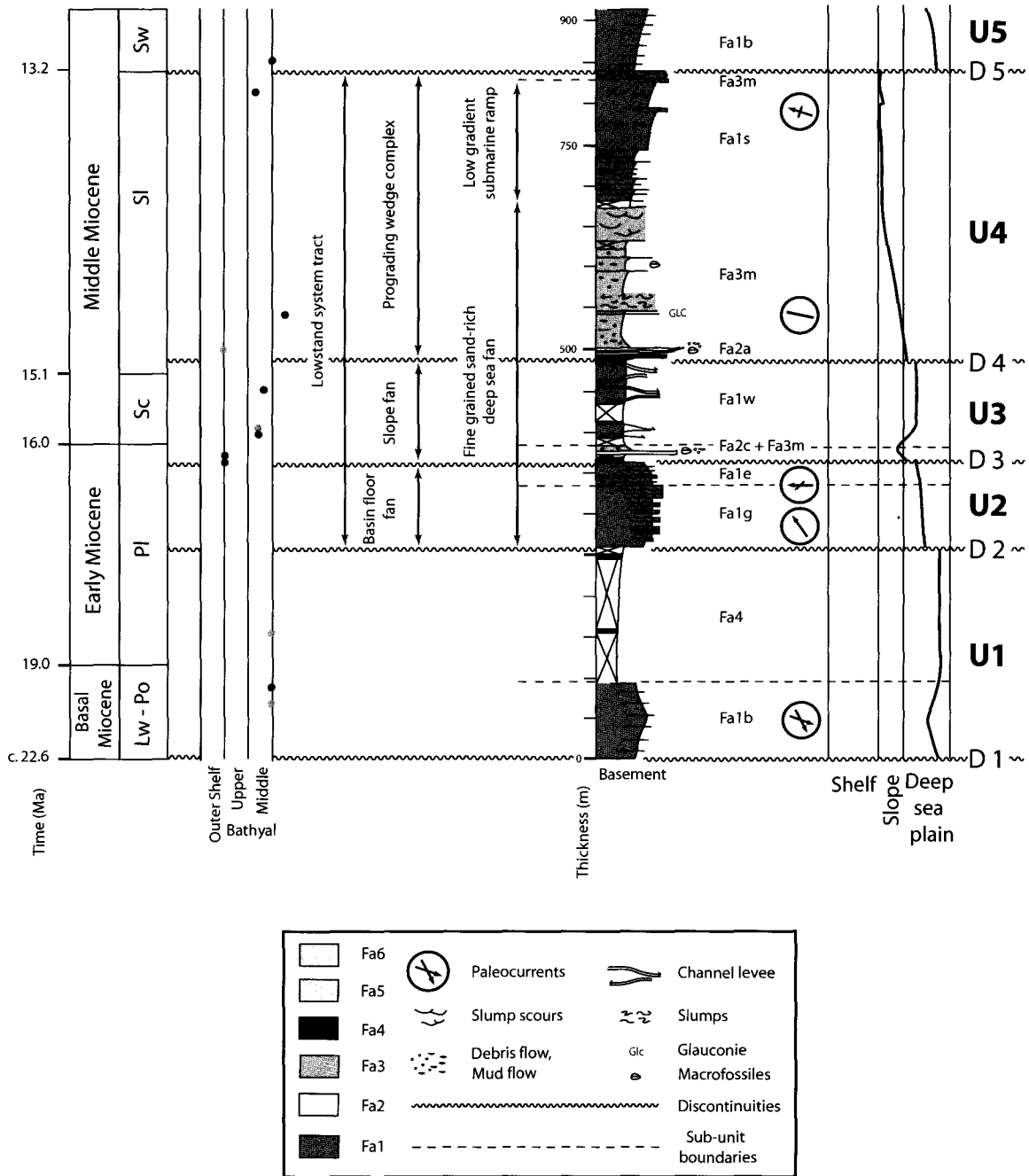


Fig.VI- 4. A - Depositional model for trench-slope settings. I - olistostrome deposition related to active thrusting during the onset of subduction at 25 Ma. II - sub-marine fan model in a juvenile trench - slope basin (basal Miocene), from coastal exposures east of the Akitio basin (Castlepoint area), after Turnbull (1988), UF - Upper Fan, MLF - Mid to Lower Fan, BP - Basin Plain. IIIa - the Akitio mature trench-slope basin (Bailleul *et al.*, submitted; see chapter III of this manuscript), note the emersion of the trenchward margin of the basin (*i.e.* Cape Turnagain structural ridge, probably controlled by the main thrust faults: the Tinui Fault, the Whakataki Fault and the Turnagain Fault) which permits the development of a westward prograding turbidite system, IIIb - early-middle Miocene sedimentary infill of the trench-slope basin. **B** - Major discontinuities and correlations of the Branscombe sedimentological section (see text for abbreviations and explanations). Refer to figure VI-1 for location, and table VI-1 for facies code.

Ces cônes sous-marins incluent des associations de faciès de plaine sous-marine (basin plain ; Fa1b + Fa4 distal), des lobes dépositionnels (Fa1g), des zones de transition chenal-lobe (Fa1e), des levées de chenaux (Fa1w) et de rares petits chenaux (Fa2a + Fa2c). Ces systèmes sont canalisés dans l'axe des bassins avec des lobes allongés pouvant atteindre plusieurs dizaines de kilomètres latéralement et seulement moins de 10 km (dépendant de la largeur du bassin) transversalement dans le bassin.

- Le troisième système sédimentaire gravitaire est représenté par une rampe sous-marine à faible gradient de pente permettant la mise en place de courants turbiditiques non-confinés. Ces courants sont à l'origine du dépôt de drapages turbiditiques (Fa1s). Ce système caractérise les derniers stades de comblement des bassins perchés, lorsque la paléotopographie du bassin est pratiquement comblée et les pentes beaucoup plus faibles.

Finalement, outre les faibles granulométries, une autre des caractéristiques de ces environnements de dépôt est la présence très fréquente de faciès de pente, silteux (Fa3m) ou sableux (Fa3s), qui montrent l'importante contribution des processus de pente au budget sédimentaire des bassins perchés. Ceci s'explique par le confinement des bassins et par le contexte de tectonique active qui favorise les déstabilisations de pente.

B) Architecture stratigraphique et déformation

1) Les méga-séquences de comblement

Le remplissage caractéristique des bassins perchés confinés matures a longtemps été considéré comme une méga-séquence de comblement strato- et grano- croissante reflétant la surrection progressive des bassins au cours de la croissance du prisme (Moore *et al.*, 1980 ; Underwood et Moore, 1995 ; *cf.* Fig. I-16). Cependant, Underwood *et al.* (2003) ont montré que certains bassins pouvaient également présenter des méga-séquences strato- et grano-décroissantes qui marqueraient l'influence des variations eustatiques ou des processus de déformation sur l'architecture sédimentaires des bassins perchés (*cf.* Fig. I-17). Sur le prisme d'accrétion Hikurangi, l'étude du remplissage du bassin d'Akitio (Fig. VI-4) montre également que les méga-séquences turbiditiques strato et grano-croissantes ne sont pas symptomatiques des bassins perchés sur les prismes de subduction. En effet, le développement de telles séquences dépend également des interactions complexes entre la granulométrie du matériel d'origine, la nature du système gravitaire, la position du bassin sur la pente du prisme de subduction et la localisation des sources.

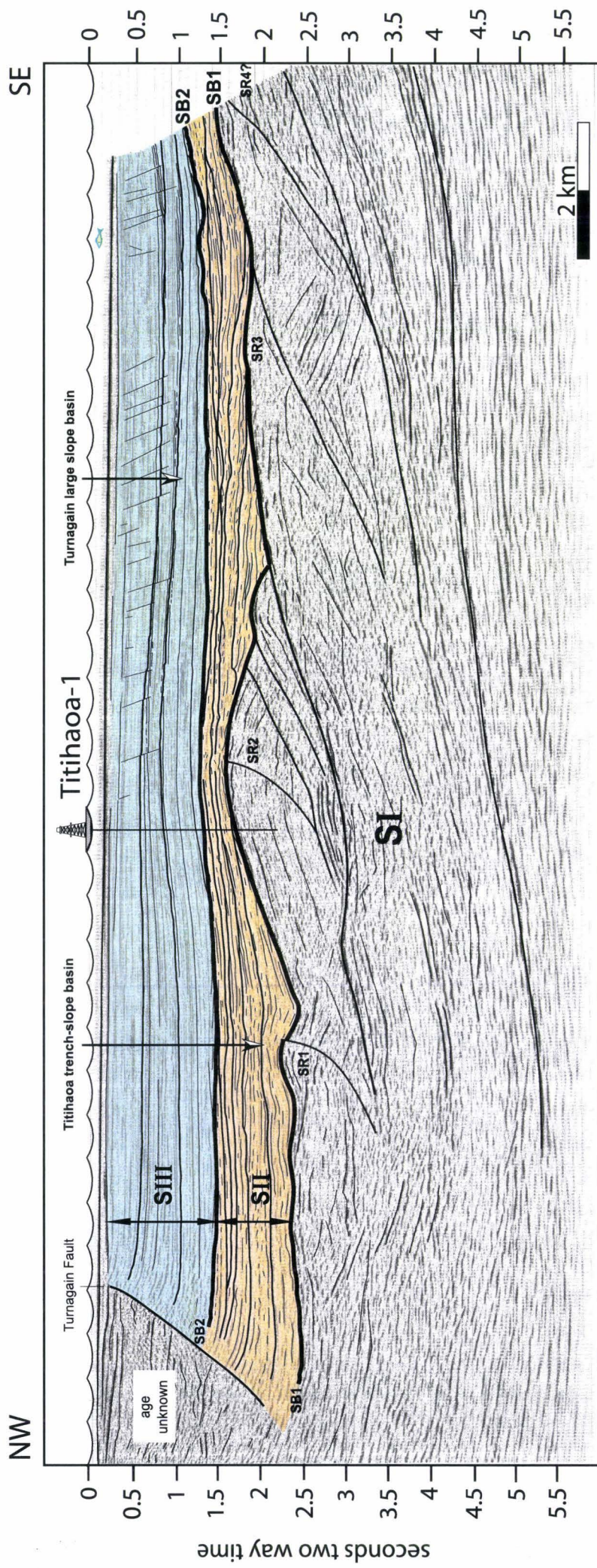


Fig. VI-5. Interpretation of IAE1-28 seismic line. SI - Irregular and discontinuous seismic unit (deformed acoustic basement), SII - Highly disorganised seismic unit (deformed acoustic basement), SIII - Well organised and continuous seismic unit (infill of the Turnagain large slope basin). U1 and U2 - main seismic units boundaries. See figure VI-1 for location.

Il faut noter qu'un bassin perché peut-être mature sans pour autant être connecté directement au pôle continental, source du matériel grossier. Les rides structurales, y compris celles situées du côté océanique par rapport au bassin, peuvent également constituer d'importantes zones d'alimentation comme dans le cas du bassin d'Akitio (Fig. VI-3). Le bassin d'Akitio présente une unique méga-séquence de comblement en bas niveau (Posamentier *et al.*, 1988) semblable à celles décrites pour les bassins d'avant-pays (Fig. VI-4) avec une succession verticale *basin-floor fan*, *slope fan* et *prograding wedge complex*.

2) Les discontinuités d'origine tectonique

A terre et en mer, le remplissage des bassins perchés confinés est caractérisé par la succession verticale d'unités sédimentaires séparées par des surfaces de discontinuité dont nous avons démontré l'origine tectonique. Ces discontinuités marquent les étapes de développement des rides structurales bordant les bassins (Fig. VI-2). Dans le bassin d'Akitio, ces surfaces, dont celle qui marque la base du bassin, sont caractérisées par des changements brutaux de faciès pouvant aller jusqu'à l'inversion des pôles distaux et proximaux. Ces modifications brutales dans la sédimentation peuvent également s'accompagner par des inversions de paléocourants. A proximité des bordures, les surfaces de discontinuité correspondent généralement à des discordances angulaires (Fig. VI-2). A l'échelle du bassin, l'étude d'après les données de sismique marine, notamment du bassin de Titihaoa, montre que ces surfaces, lorsqu'elles sont associées à la surrection des bordures du bassin, peuvent être basculées soit vers le continent, soit vers l'océan (Fig. VI-5). Ces basculements contrôlent en grande partie la localisation de l'accommodation au sein des bassins et donc la répartition de leurs dépôt-centres. De plus, tant que les rides structurales se développent, les pentes existantes sont régulièrement rajeunies (déstabilisations et basculements des surfaces de dépôt) et d'autres sont créées, ce qui favorise la progradation des systèmes sédimentaires en association avec les forts flux sédimentaires.

Dans le cas de bassins confinés très matures, et en l'absence d'événements eustatiques ou tectoniques majeurs, l'arrêt du fonctionnement des rides structurales (en théorie signalé par la dernière surface basculée) est rapidement suivi du comblement des bassins. La fin de ce comblement est caractérisée par une surface de discontinuité majeure qui annonce un élargissement du domaine de sédimentation. Des bassins perchés plus larges (30 à 40 km) se développent alors en discordance.

NW

Onshore: Akitio basin (c. 17.5 - 13.2 Ma)

Offshore: Titihaoa basin (c. 13.7 - 6.2 Ma)

SE

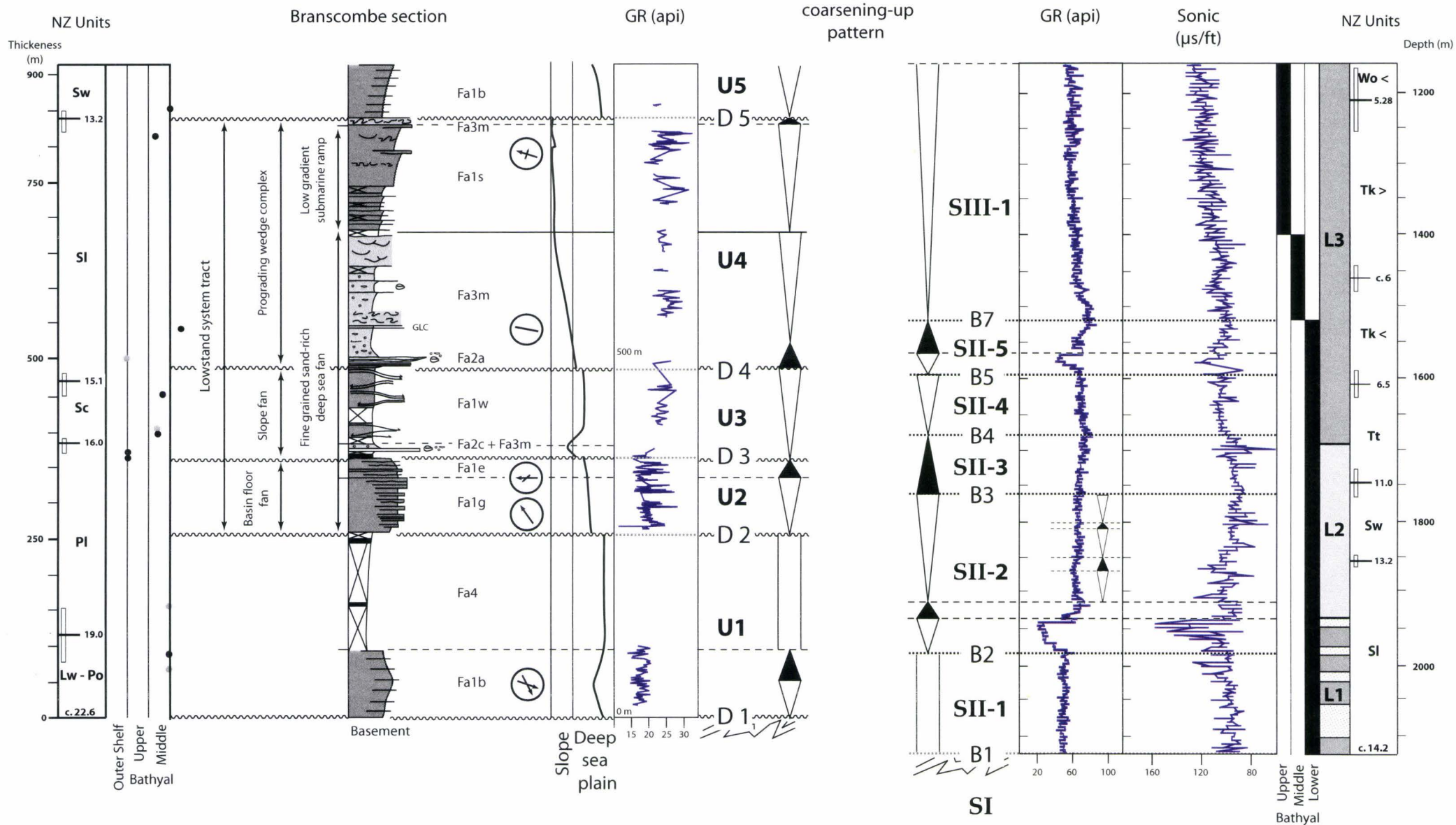


Fig.VI- 6. Comparison between the Akitio onshore trench-slope basin and the younger Titihaoa offshore trench-slope basin. See figure VI-4 for legend of the Branscombe section and table VI-1 for facies code.

A terre comme en mer, la datation des surfaces de discontinuité liées à la déformation, et donc l'estimation de la durée des unités sédimentaires qu'elles délimitent, montre que les pulsations tectoniques liées au jeu des bordures ont une fréquence de l'ordre de 1 à 2 Ma (Fig. VI-6). Certaines de ces pulsations précèdent le développement des éléments constituant la méga-séquence de comblement identifiée à terre (Fig. VI-4 ; *i.e.* D2 – installation du *basin-floor fan*, D3 – installation du *slope fan* et D4 – installation du *prograding wedge complex*). Il apparaît donc que la tectonique exerce un contrôle peut-être partiel mais majeur sur la chronologie du développement de la méga-séquence de bas niveau du bassin d'Akitio.

3) les séquences de quatrième ordre

Entre chaque discontinuité d'origine tectonique, les unités sédimentaires sont composées de séquences grano- et/ou strato-croissantes (*coarsening-up*) et de séquences grano- et/ou strato-décroissantes (*fining-up*) que l'on peut rattacher de par leur durée (de l'ordre de 1 à 2 Ma) à des séquences de quatrième ordre (Fig. VI-6). Les séquences dominantes (les plus nombreuses) sont les séquences de type *coarsening-up* qui soulignent l'importance des processus de remplissage dans ces bassins matures caractérisés par des apports terrigènes très importants. Dans cette étude, notamment pour la partie marine, nous n'avons pas traduit directement ces séquences en termes de progradation/rétrogradation car la faible granulométrie des séries sédimentaires, associée à la géométrie et à la dynamique particulière des systèmes gravitaires, pouvaient être source d'erreur. Ainsi dans le bassin d'Akitio (Fig. VI-4), la succession verticale de lobe dépositionnel (bancs métriques, granulométrie dans les sables fin-moyen) à des faciès de transit (bancs centimétriques, granulométrie dominante dans les sables fins) correspond à une séquence de *fining-up* pouvant être interprétée en diagraphie comme une rétrogradation. Le déplacement de la zone de transit (située en amont du lobe turbiditique qu'elle alimente) vers le pôle distal du bassin montre qu'il s'agit en fait d'une progradation.

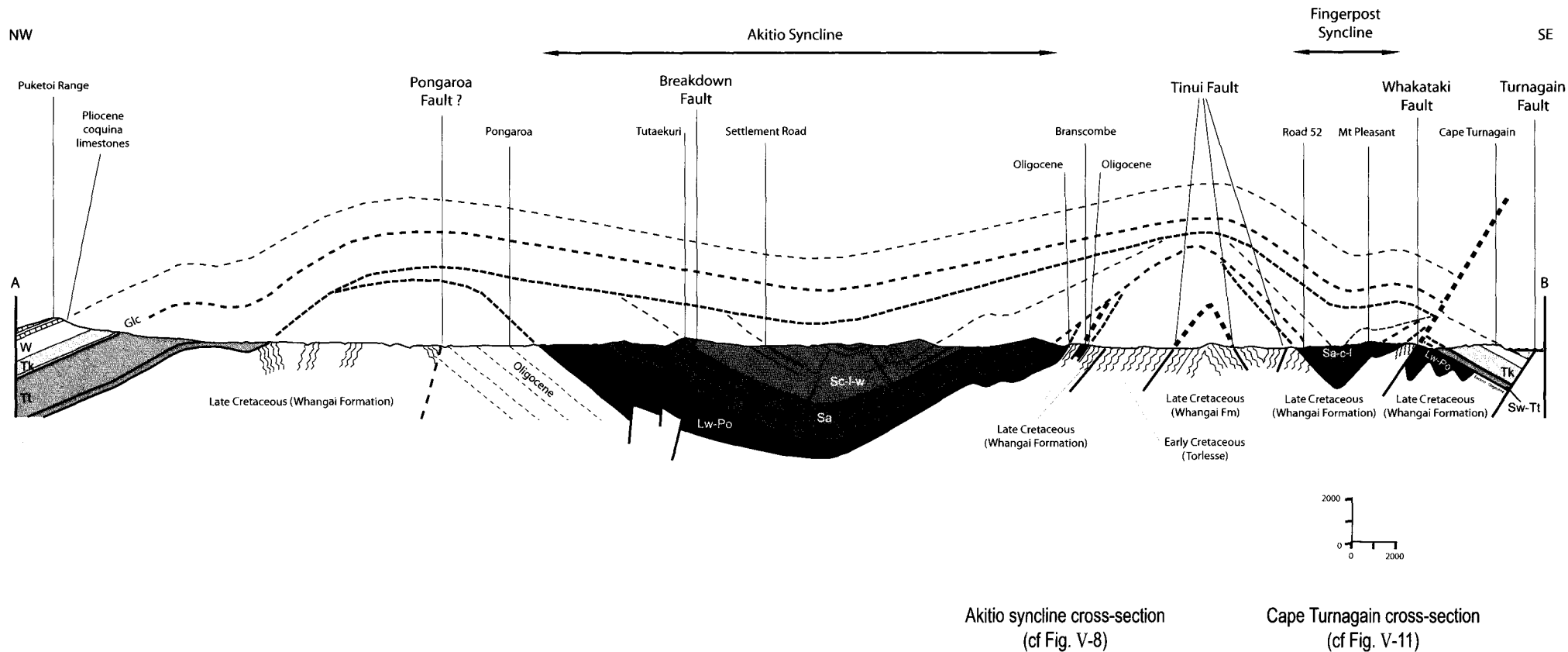
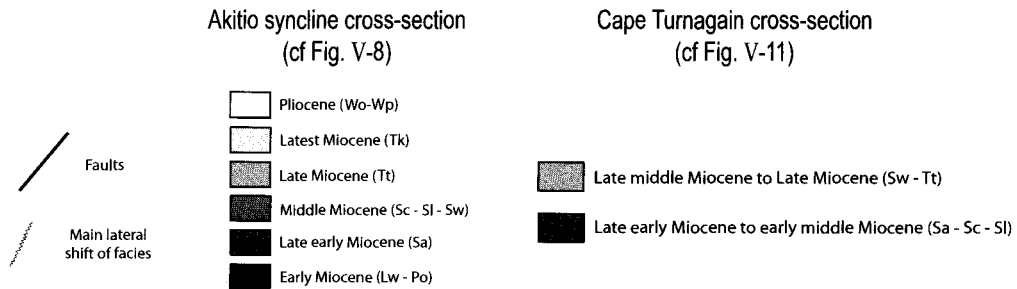


Fig.VI-7 . Coupe synthétique de la chaîne côtière au niveau de la transversale d'Akitio (région du Wairarapa). Localisation Figure VI-1.



II) Les phases de déformation du prisme Hikurangi et l'évolution des bassins de pente et de leurs bordures (hauts structuraux)

L'analyse stratigraphique et structurale, à terre (Figs VI-2 et VI-7) et en mer (Fig. VI-5 et VI-10), de la transversale d'Akitio (Fig. VI-1) a permis de contraindre l'histoire tectonique du prisme de subduction depuis le démarrage de la subduction, il y a 25 Ma. L'évolution tectonique et morphologique de la marge peut-être résumée en quatre phases de déformation majeures (Fig. VI-8). Ces phases sont à l'origine de la structuration des trois domaines morfo-structuraux majeurs que comprend l'actuel prisme de subduction (Fig. VI-1) : la Chaîne Côtière (qui correspond à la plus haute ride du prisme Hikurangi, actuellement émergée), la plate-forme du Wairarapa et le prisme d'accrétion Plio-Quaternaire, encore actif. Le domaine de la Chaîne Côtière se développe depuis la première phase et a donc enregistré l'ensemble des phases reconnues. Seuls les troisième et quatrième épisodes de déformation sont clairement documentés dans le secteur de la plate-forme du Wairarapa. On note en outre dans ce secteur, des réflecteurs sub-horizontaux profonds qui évoquent des bases de nappes pouvant correspondre à la première phase de déformation (celle liée au démarrage de la subduction) (Fig. VI-5). Le prisme d'accrétion Plio-Quaternaire se développe quand à lui uniquement au cours de la dernière phase.

A) Evolution structurale du prisme de subduction Hikurangi

- La première phase, d'âge Miocène basal (c. 25 – c. 19 Ma), est liée au démarrage de la subduction et correspond à la déformation de l'ancienne marge passive paléogène (Fig. VI-8a). Cette première phase de compression se traduit par la mise en place de nappes qui chevauchent vers la mer. Ces nappes sont contrôlées par des chevauchements majeurs qui sont identifiés dans le Wairarapa au niveau de la lanière de soubassement déformé du Bloc Côtier (Fig. VI-1). Il s'agit principalement des failles de Tinui et de Whakataki (Figs VI-1 et VI-7). Du point de vue sédimentaire, cette phase est associée à la mise en place d'olistostromes et d'épaisses séries turbiditiques à la base des séries miocènes (Fig. VI-2 - Lw-Po). Elle se traduit donc par une augmentation brutale des apports terrigènes sur l'ensemble de la marge.

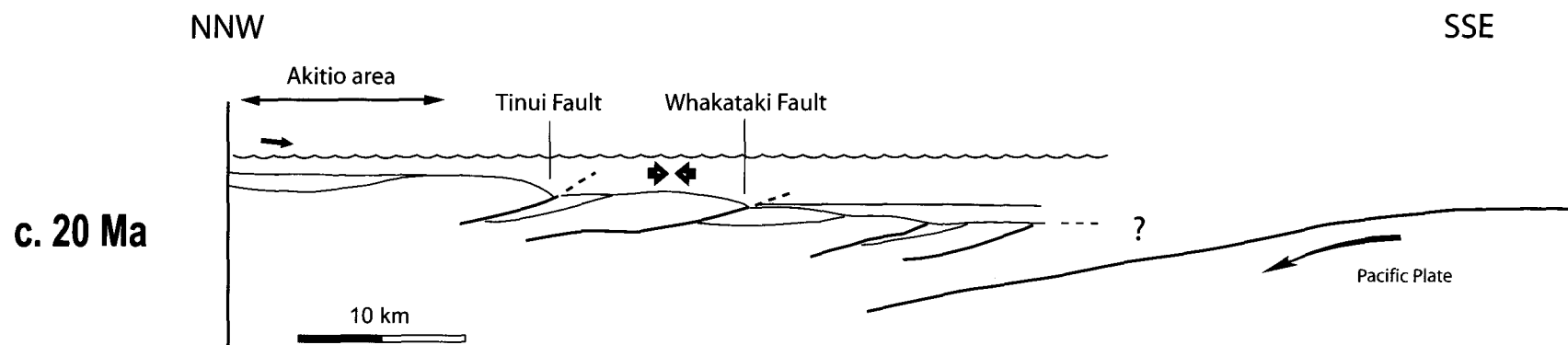
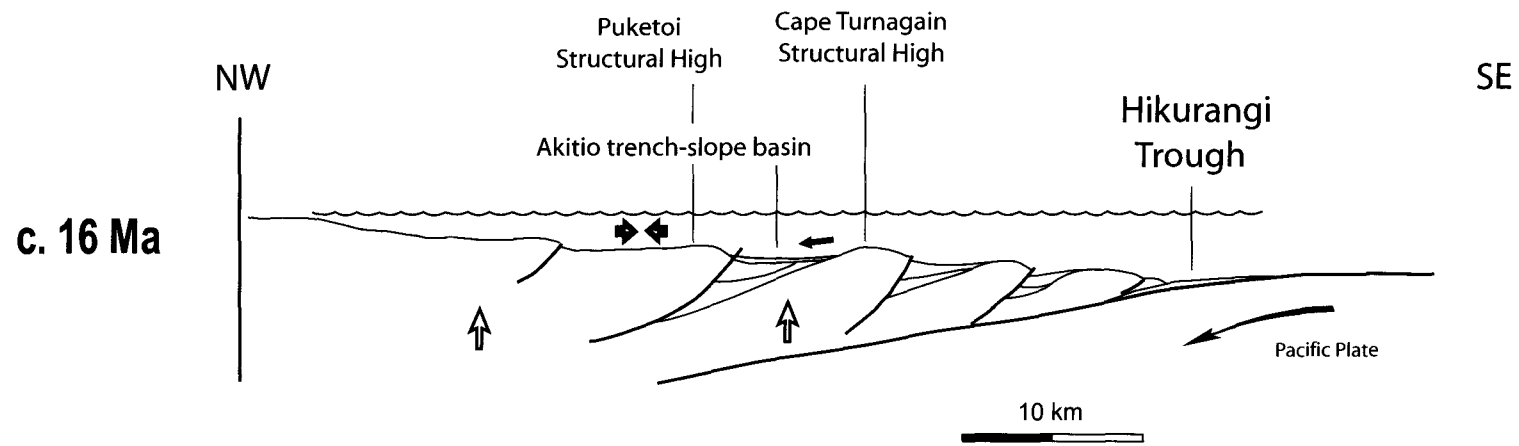
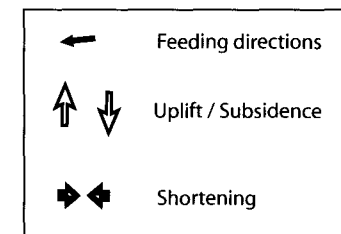


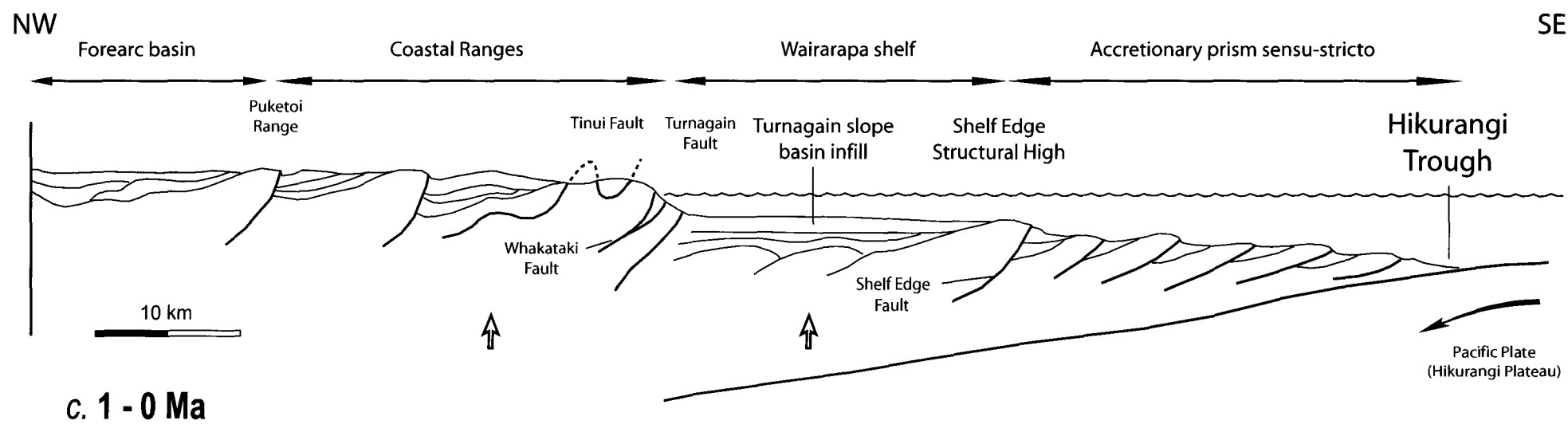
Fig.VI- 8a. Tectonic evolution of the Hikurangi margin since the onset of subduction, 25 Myr ago.



- La seconde phase, d'âge Miocène inférieur à moyen (*c.* 17.5 – *c.* 15 Ma) se caractérise par des déformations compressives présentant une direction principale de raccourcissement approximativement N110°E. Au cours de cette phase, les nappes du Miocène basal sont déformées (plissement et failles inverses) et des bassins perchés confinés (*e.g.* bassin d'Akitio, Fig. VI-2) se développent entre des rides structurales actives d'axe NNE-SSW (*e.g.* rides structurales de Puketoi, à l'Ouest, et de Cape Turnagain, à l'Est) (Fig. VI-8). Le haut structural de Cape Turnagain était alors certainement contrôlé par le jeu inverse de certaines failles majeures mises en place lors de la première phase : les failles de Whakataki (Fig. VI-7) et de Turnagain (Fig. VI-5).

- Le troisième épisode de déformation, d'âge Miocène moyen à supérieur (*c.* 15 – *c.* 6.5 Ma), est marqué sur la partie haute du prisme de subduction (*i.e.* Chaîne Côtière, Fig. VI-1) par une subsidence importante, un élargissement du domaine de sédimentation (*e.g.* passage du bassin confiné d'Akitio au large bassin de Tawehro, Fig. VI-2) et la mise en place de déformations en extension. Cet épisode tectonique a été attribué à de l'érosion tectonique ayant affecté le prisme Hikurangi au cours du Miocène supérieur (Chanier *et al.*, 1999) (Fig. VI-8). Plus bas sur le prisme (*i.e.* plate-forme actuelle de la région du Wairarapa, Fig. VI-1), à l'Est du haut structural de Cape Turnagain, des bassins perchés confinés (*e.g.* bassin de Titihaoa, Fig. VI-5) se développent ce qui suggère l'existence de processus compressifs et la croissance d'un prisme d'accrétion au front de la marge au cours de cette même période surtout marquée par de l'extension (plus à l'Ouest) attribuée à de l'érosion tectonique (Fig. VI-8). Ce modèle pour la marge active Hikurangi au Miocène supérieur est par exemple très similaire au cadre tectonique actuel de la marge active du Pérou (Von Huene, 1986) où un prisme d'accrétion réduit se développe dans la partie basse d'une marge dominée par des processus d'extension et d'érosion tectonique.

- La quatrième et dernière phase, d'âge Miocène terminal à actuel (*c.* 6.5 – 0 Ma) correspond à un soulèvement généralisé de l'ensemble de la marge contemporain d'une reprise de la déformation compressive (Fig. VI-8). Dans la Chaîne Côtière (Fig. VI-1), trois épisodes principaux de raccourcissement ont été identifiés auparavant au cours de cette période (Nicol *et al.*, 2002) : *c.* 8 – 6 Ma, *c.* 3.4 – 2.4 Ma, et *c.* 1.8 – 0 Ma. Dans notre zone d'étude, le premier épisode correspond au plissement des séries sédimentaires du Miocène supérieur. Beaucoup de ces plis montrent un axe N-S (*e.g.* Tawhero syncline, Te Wharau syncline ; Fig. VI-1). Cette direction structurale N-S n'est jamais observée dans les séries sédimentaires Plio-Quaternaires. Nous considérons donc que le premier épisode de raccourcissement est lié à une compression E-W.



- ↑ ↓ Uplift / Subsidence
- ↔ Shortening
- ↔ Extension

c. 10 Ma

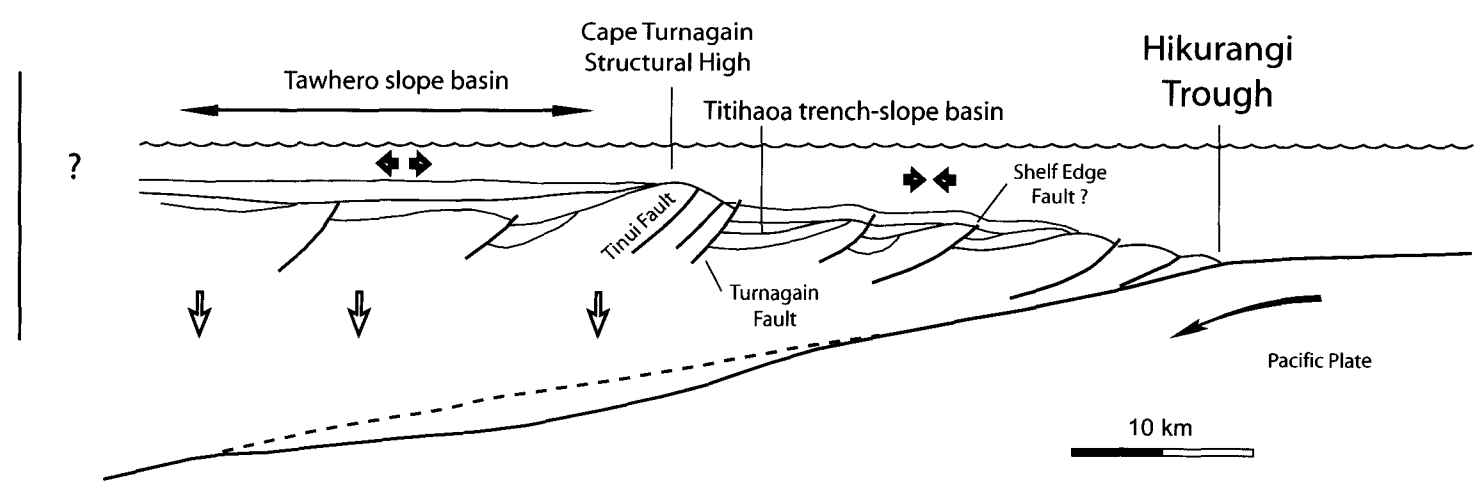


Fig.VI- 8b. Tectonic evolution of the Hikurangi margin since the onset of subduction, 25 Myr ago.

Le second épisode de raccourcissement est notamment mis en évidence par le basculement progressif des couches de calcaire Pliocène au cours d'une compression NW-SE (*cf.* Fig. V-9, stéréogramme a). Cette deuxième période de raccourcissement (Pliocène) est également contemporaine de la mise en place d'une plate-forme mixte carbonatée/silico-clastique qui recouvre progressivement l'ensemble du secteur de la Chaîne Côtière (Fig. VI-2 – Wo/Wp). Après le Pliocène, le raccourcissement se poursuit et aboutit finalement à l'émersion de la Chaîne Côtière (Ghani, 1978 ; Cape *et al.*, 1990). Cette phase notamment est marquée par la réactivation des failles anciennes de Whakataki et de Castlepoint (Fig. VI-1).

En mer, dans le secteur de la plate-forme actuelle du Wairarapa (Fig. VI-1), le développement d'un bassin de pente très large (environ 40 km de large), le bassin Plio-Quaternaire de Turnagain, fait suite à l'arrêt du fonctionnement vers 6.2 Ma des rides structurales du miocène supérieur (Fig. VI-5). Cet arrêt accompagne la surrection rapide de ce secteur de la marge au Miocène terminal. Les déformations compressives post-6.5 Ma s'expriment ensuite essentiellement par la réactivation des zones de failles majeures anté-Miocène terminal. Cette réactivation récente s'effectue soit avec un jeu inverse qui affecte l'ensemble des séries Pliocènes (*i.e.* zone de faille de Turnagain, Fig. VI-5), soit par l'intermédiaire de zones de déformation plus complexes le long de la zone faillée du Shelf Edge (*cf.* Fig. V-6). Au sud de la transversale d'Akitio, le raccourcissement post-6.5 Ma aboutit également à la subdivision du bassin de Turnagain en deux synclinaux séparés par une faille inverse majeure (*cf.* Fig. V-6). Du côté océanique, à l'Est de la bordure de plate-forme, l'initiation du prisme d'accrétion actuellement actif s'effectue probablement dès le Pliocène (Lewis et Pettinga, 1993).

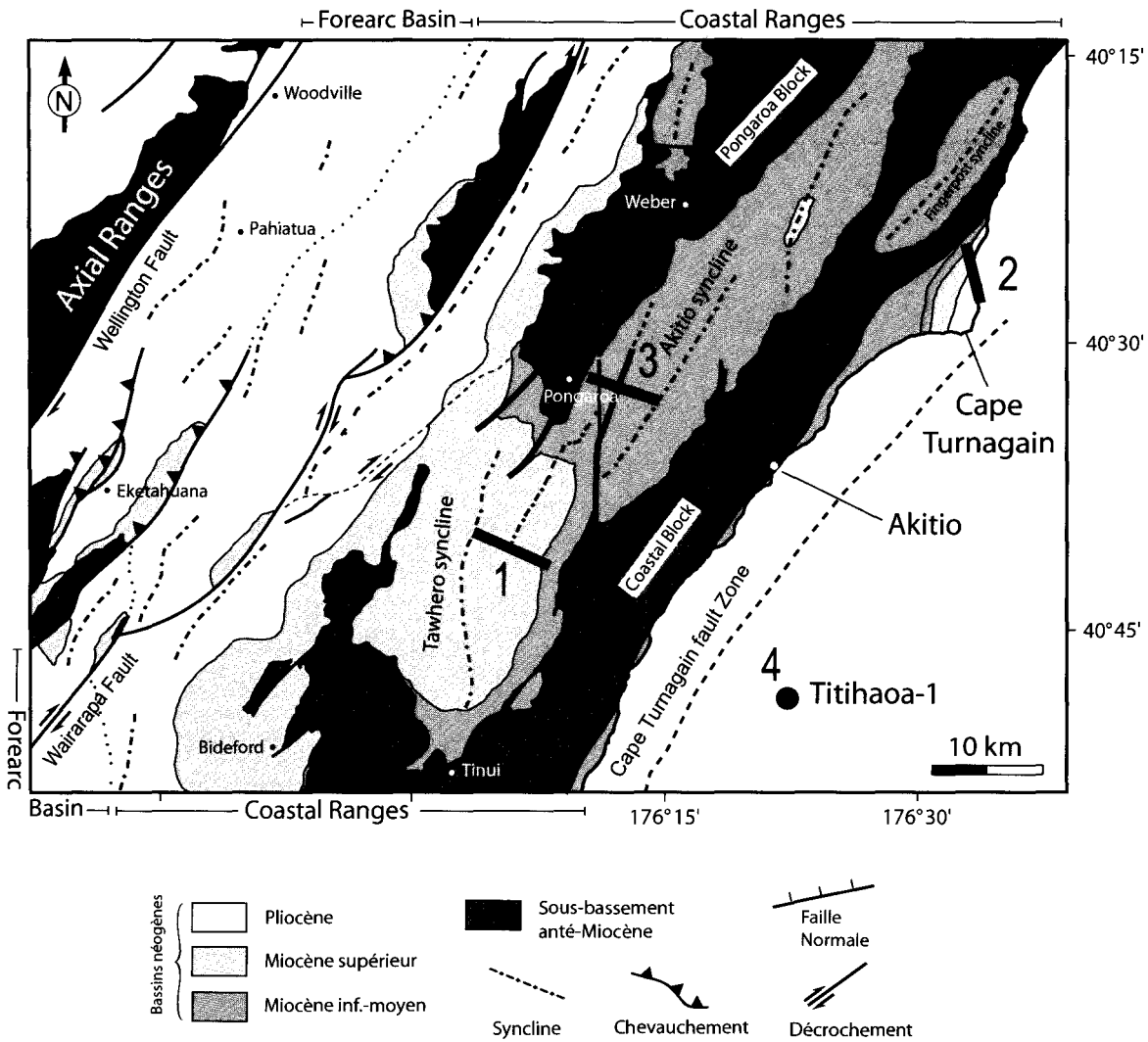


Fig. VI- 9. Cadre structural du secteur de Pongaroa, NE Wairarapa, et localisation des coupes analysées en termes de mouvements verticaux par le biais de courbes de subsidence :

- 1 - Coupe du synclinal de Tawhero (Fig. VI-10)
- 2 - Coupe de Cape Turnagain (Fig. VI-11)
- 3 - Coupe de Pongaroa, synclinal d'Akitio (Fig. VI-12)
- 4 - Forage Titihaoa-1 (Fig. VI-13)

B) Evolution de la subsidence des bassins perchés

Les données sédimentologiques recueillies et analysées sur la transversale d'Akitio nous permettent de proposer des courbes illustrant l'évolution de la subsidence des bassins de pente.

1) Méthode

Ces courbes sont basées sur les épaisseurs des unités sédimentaires, sur les âges obtenus à partir des données paléontologiques, ainsi que sur les paléo-tranches d'eau déduites pour l'essentiel des biofaciès. Les séries considérées ont été décompactées par tranches de 50 à 150 m. Les unités sédimentaires épaisses et homogènes ont été subdivisées selon un modèle d'âge linéaire afin d'optimiser la décompaction de ces séries. Par exemple, une section donnée de dépôts homogènes de silts de plate-forme épaisse de 300 m et représentant une durée de *c.* 1.5 Ma, a été subdivisée en trois tranches de 100 m d'épaisseur, avec une durée estimée à 0.5 Ma chacune.

Les calculs de décompaction, de subsidence totale, et de subsidence tectonique ont été effectués par l'utilisation du programme SUBSILOG développé à Lille (Dubois *et al.*, 2000). Les paramètres utilisés notamment pour la décompaction sont ceux proposés par Sclater et Christie (1980) pour les sédiments de la mer du Nord. Les caractéristiques des sédiments de la Chaîne côtière de Nouvelle-Zélande sont très comparables et ces paramètres (Sclater et Christie, 1980) ont été utilisés pour les analyses de subsidence effectuées antérieurement dans d'autres secteurs de la Chaîne Côtière et du bassin avant-arc (*e.g.*, Wells, 1989 ; Buret 1996). La courbe de subsidence totale montre les mouvements verticaux du soubassement des bassins sur une verticale donnée, incluant naturellement l'effet de la charge sédimentaire. La subsidence tectonique a été calculée en considérant un réajustement isostatique local, de type Airy, comme cela est généralement utilisé y compris dans ces contextes de marge active.

Des courbes de subsidence sont ainsi proposées pour le forage de Titihaoa-1, ainsi que pour un certain nombre de successions stratigraphiques levées à terre (Fig. VI-9). Classiquement, la principale source d'incertitude sur de telles courbes est liée aux estimations des paléo-tranches d'eau. Les marges d'incertitudes sont donc particulièrement importantes lorsque l'on considère les ensembles sédimentaires déposés sous de fortes tranches d'eau. Cela est notamment le cas pour les dépôts miocènes traversés par le forage Titihaoa. Les séries levées à terre sont généralement de plus faible tranche d'eau, donc mieux contraintes en paléo-bathymétries. Cependant, le levé de coupe sur une transversale, et non pas sur un puits vertical, engendre une distorsion des épaisseurs adoptées pour les unités sédimentaires superposées.

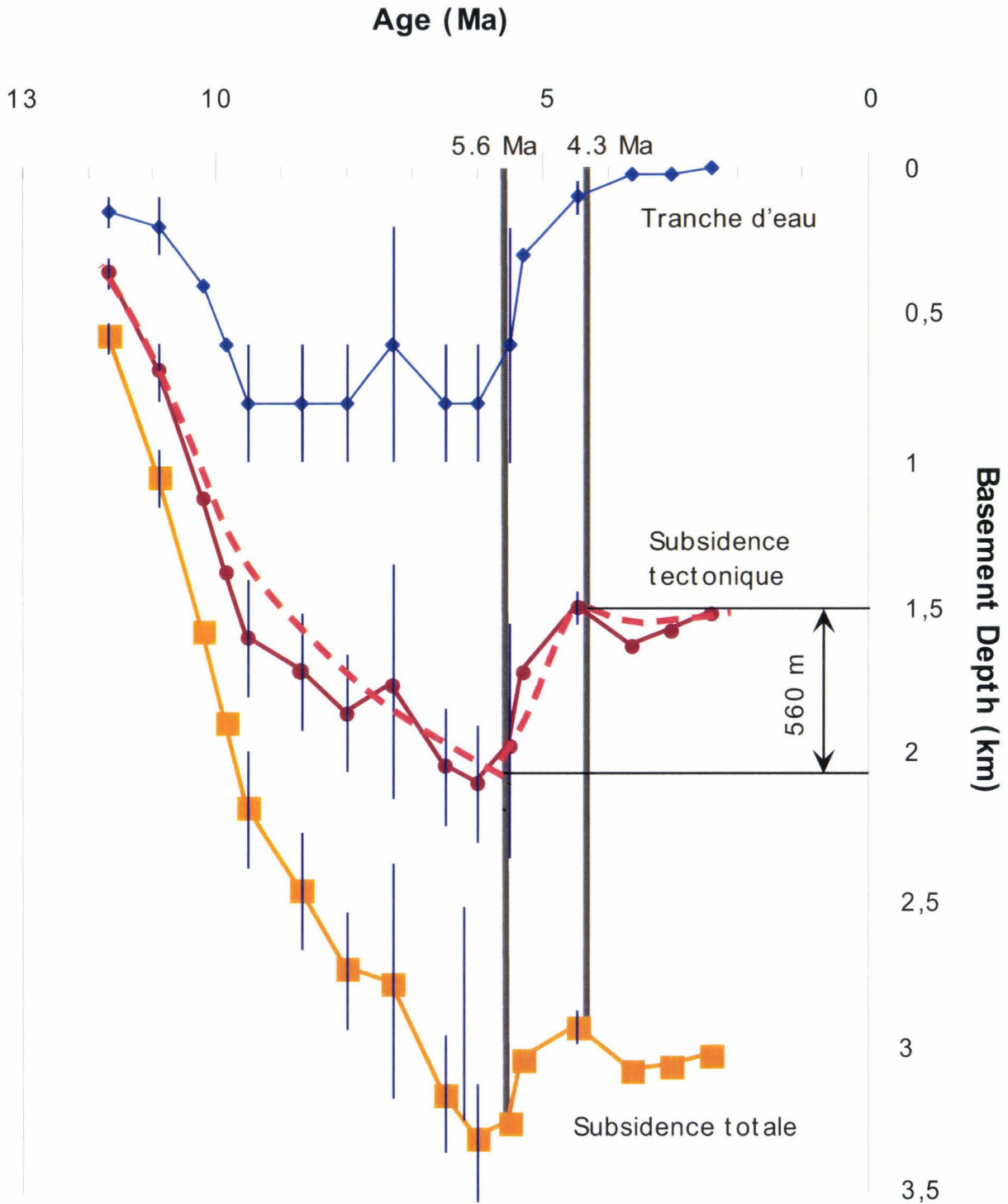


Fig.VI-10. Courbe de subsidence établie à partir des séries d'âge Miocène moyen à Pliocène, levées sur le flanc Est du Synclinal de Tawhero (localisation Fig.VI-9). Les marges d'incertitudes sur la détermination des paléo-tranches d'eau sont reportées sur l'ensemble des 3 courbes figurées ci-dessus.

Quoiqu'il en soit, et étant donné les amplitudes importantes des mouvements observés, ces courbes de subsidence permettent de mettre en évidence les principales tendances des mouvements verticaux sur la marge, notamment les phases majeures d'inversion de ces mouvements verticaux. Il reste que les mouvements de trop faible amplitude ne peuvent pas apparaître, ou être interprétés, si ils sont trop proches des domaines d'incertitudes (notamment sur les paléo-tranches d'eau).

2) Résultats

a) Domaine émergé : Bassin d'Akitio – Bassin de Tawhero – Cape Turnagain

Le bassin de Tawhero correspond à un large domaine de sédimentation qui se développe à partir du Miocène moyen. La série levée sur les flancs du synclinal de Tawhero au Sud de Pongaroa (Fig. VI-9) montre tout d'abord une nette période de subsidence avec un affaissement total du soubassement anté – Miocène moyen de l'ordre de 2.5 km (Fig. VI-10). Cette subsidence se développe entre 12.5 et 6 Ma et semble relativement régulière. Les faibles variations de subsidence observés sur la courbe au sein de cette période ne sont pas significatives étant donné les marges d'erreur sur les tranches d'eau. Par contre, la surrection rapide de ce domaine de sédimentation vers 6 Ma apparaît très clairement. Selon les valeurs adoptées pour les paléo-tranches d'eau, il s'agit d'un épisode qui conduit à un soulèvement de l'ordre de 400 à 1000 m. Un second épisode de surrection apparaît vers 3.5 Ma ; il est beaucoup plus faible en amplitude mais est probablement significatif dans la mesure où les paléo-tranches d'eau semblent bien contraintes et précises.

La série levée au nord de Cape Turnagain (Fig. VI-9) présente des ensembles sédimentaires de même âge que ceux du synclinal de Tawhero. On note aussi une subsidence nette au cours du Miocène moyen et supérieur, au moins entre 13 et 9 Ma, voire jusque 7 Ma (Fig. VI-11). On retrouve la remontée brutale du substratum entre 7 et 6 Ma (amplitude de l'ordre de 300 à 600 m). D'après cette courbe, la surrection pourrait débuter dès 9 Ma mais cette période (9-7 Ma) est mal contrainte en termes de paléo-tranches d'eau. Au regard des résultats obtenus sur l'ensemble des courbes, il apparaît que la surrection se développe probablement à partir de 7 Ma. Quoiqu'il en soit, l'incertitude « paléo-bathymétrique » est ici trop importante pour permettre de préciser l'âge du début de la surrection. Cet épisode de soulèvement, cependant bien réel, est suivi d'une reprise de la subsidence à partir de *c.* 5 Ma. Une seconde période d'inversion de la courbe de subsidence, et donc un retour à la surrection, semble débuter à partir de *c.* 3.5 Ma

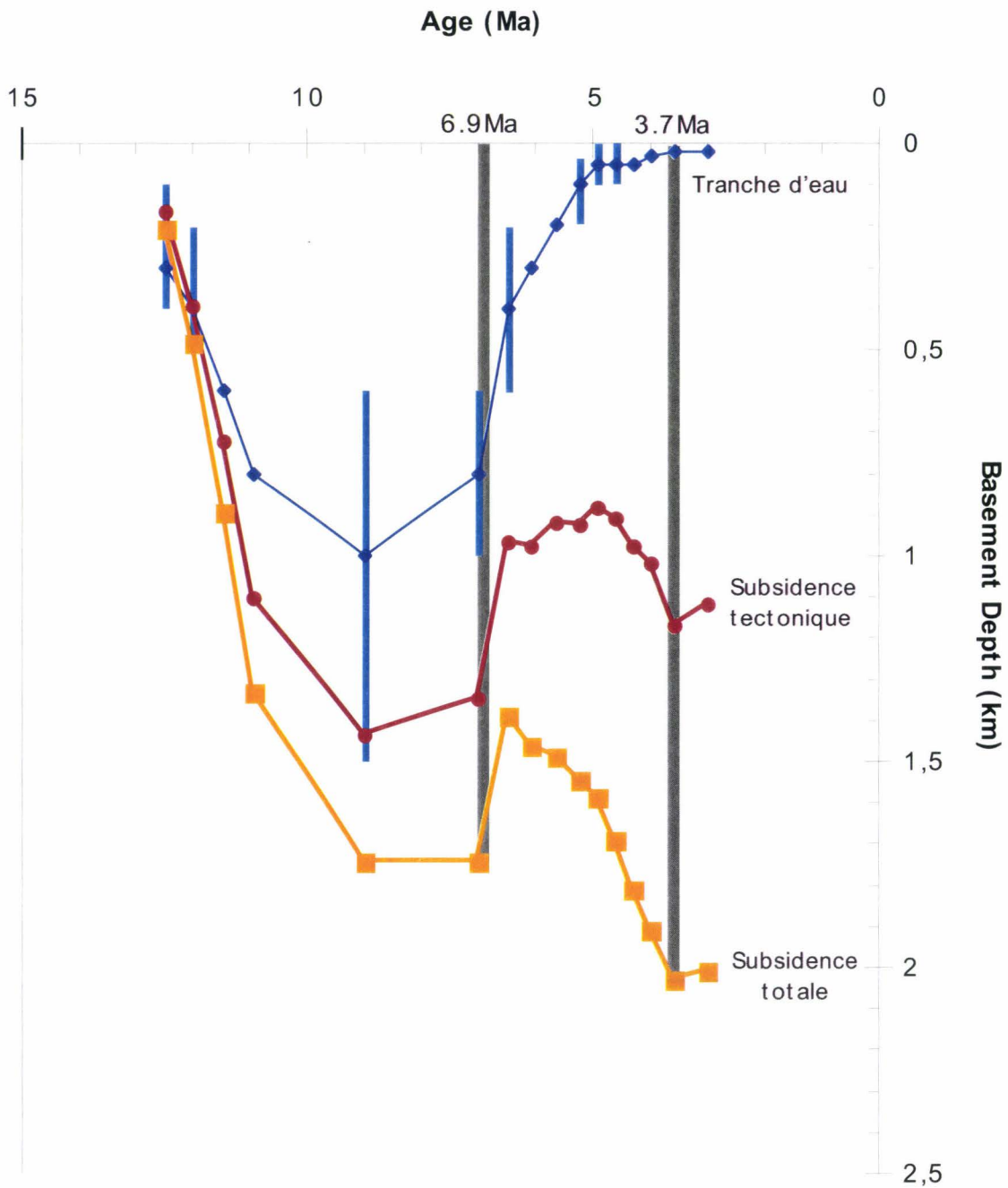


Fig.VI-11. Courbe de subsidence établie à partir des séries d'âge Miocène moyen à Pliocène, levées au Nord de Cape Turnagain (localisation Fig.VI-9). Pour des raisons de clarté, les marges d'incertitudes sur la détermination des paléo-bathymétries sont figurées uniquement sur la courbe d'évolution des tranches d'eau.

Nous avons par ailleurs établi une courbe de subsidence pour le bassin de pente d'Akitio, d'âge Miocène inférieur (Fig. VI-12). La série ici analysée correspond à la coupe dite de « Pongaroa » (*cf.* Fig. III-7) levée sur le flanc Ouest et au cœur du synclinal d'Akitio (Fig. VI-9). Afin de décompacter correctement cette série, nous devons considérer la charge des sédiments sus-jacents, supposés exister au dessus du bassin d'Akitio avant leur érosion récente suite à l'émersion de la Chaîne Côtière. En tenant compte de notre reconstitution du domaine de sédimentation, avec un large bassin de Tawhero se développant au dessus des bassins confinés plus anciens, la série sédimentaire levée latéralement dans le synclinal de Tawhero a été superposée aux séries levées dans le synclinal d'Akitio. L'évolution générale de ce domaine au cours du Miocène inférieur et moyen montre une subsidence relativement modérée entre 20 et 15 Ma. Deux épisodes marquants ressortent de l'analyse de cette courbe. Tout d'abord, on note un épisode de surrection assez marqué vers 16.5 Ma. Il coïncide avec la principale phase de surrection de la bordure Ouest du bassin confiné d'Akitio. Ensuite, nous observons une nette accélération de la subsidence à partir de *c.* 15 Ma. Il s'agit ici de la période de fin de confinement du bassin d'Akitio et du début d'une période tectonique qui est dominée par de l'extension et qui est considérée comme une phase d'érosion tectonique majeure sur la marge (Chanier *et al.*, 1999).

b) Domaine immergé : Bassin de Titihaoa – Bassin de Turnagain

Comme mentionné dans le paragraphe précédent, ce domaine s'est développé au cours du Miocène sous des tranches d'eau relativement importante, ce qui augmente de manière très significative les incertitudes sur l'établissement des courbes de subsidence. Deux courbes de subsidence sont proposées (Fig. VI-13) présentant respectivement des estimations maximales (courbe A) ou minimale des tranches d'eau (courbe B).

La subsidence semble relativement régulière dans ce domaine de sédimentation au cours du Miocène. Cependant elle n'est pas démonstrative dans la mesure où les tranches d'eau sont alors très élevées (*cf.* incertitudes). Le fait marquant qui peut être déduit de ces courbes est la surrection brutale qui affecte ce domaine vers 6.5 à 7 Ma. Aux incertitudes près, l'amplitude de cette surrection est de l'ordre de 500 à 1000 m. Cet épisode est à ce titre comparable aux surrections observées à terre au cours de la même période. Il correspond aussi à un changement majeur du régime tectonique de la marge, déduit par ailleurs de l'analyse sédimentologique et structurale.

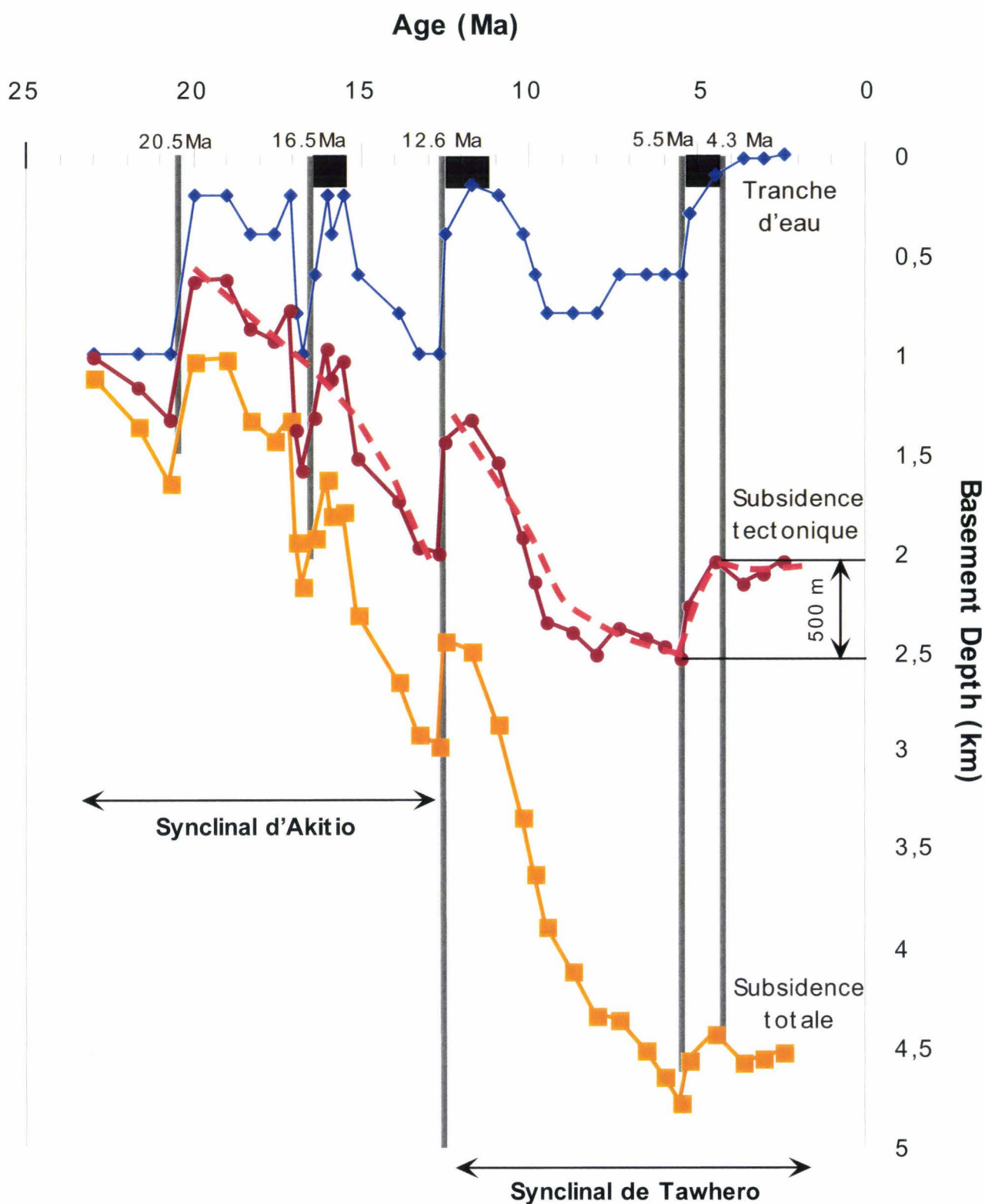
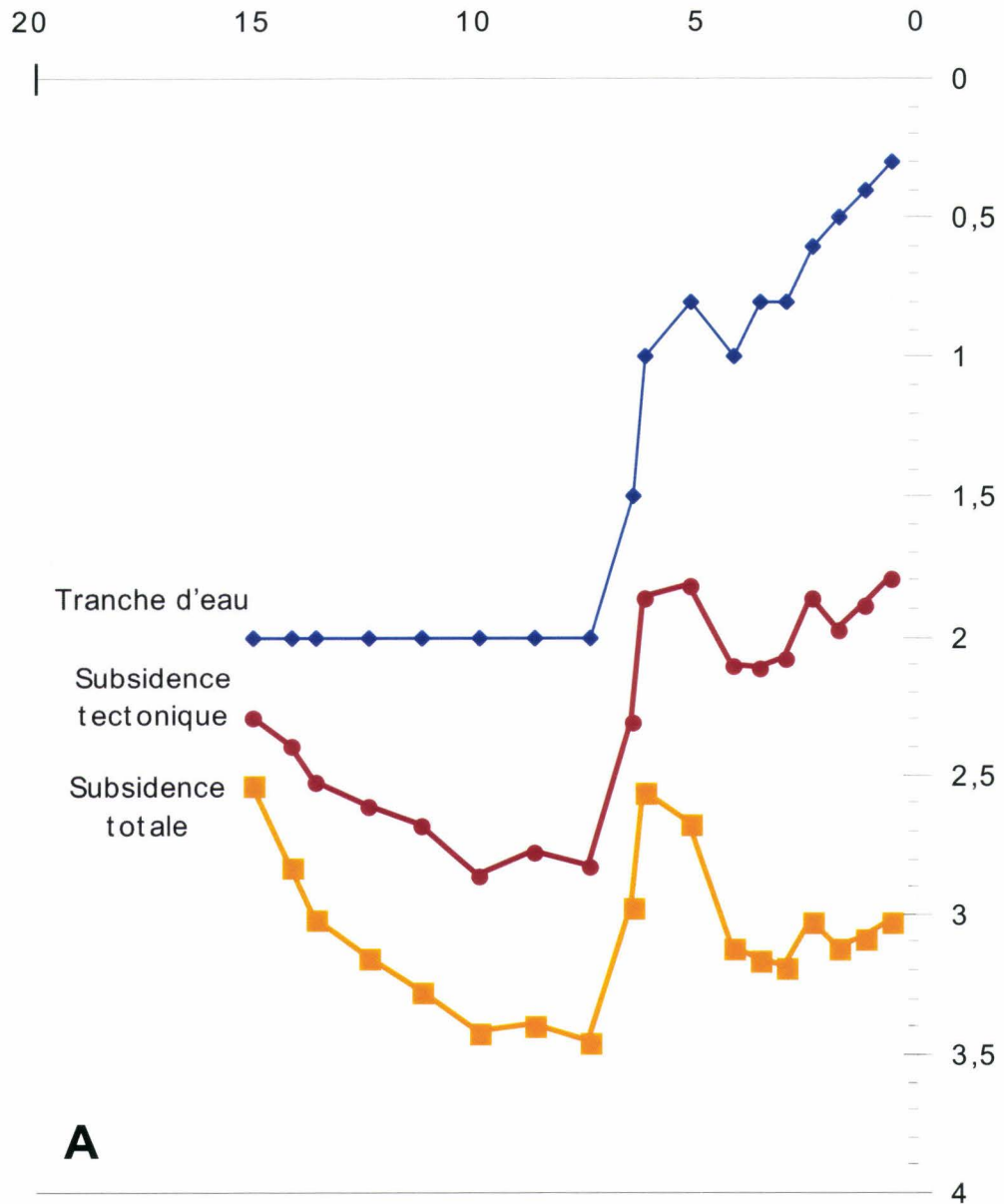


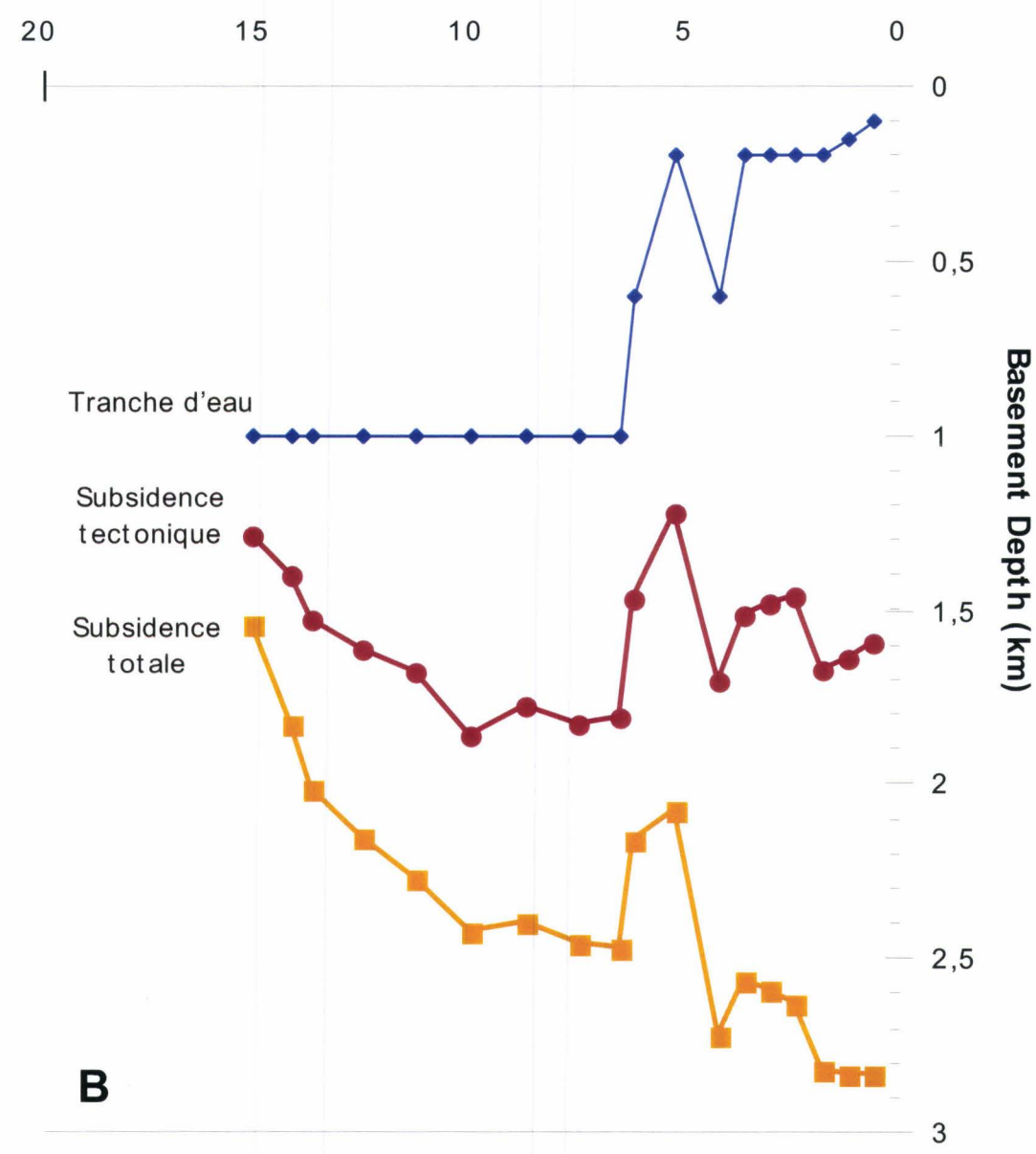
Fig.VI-12. Courbe de subsidence établie à partir des séries d'âge Miocène inférieur et moyen du synclinal d'Akitio (coupe de Pongaroa, localisation Fig.VI-9). La série sédimentaire du synclinal de Tawhero (fin Miocène moyen à Pliocène), présentée figure VI-10, a été superposée au bassin d'Akitio pour les calculs de décompaction.

Age (Ma)



A

Age (Ma)



B

Fig.VI-13. Courbes de subsidence établies à partir des séries traversées par le forage Titihaoa-1 (localisation Fig.VI-9). Ces courbes ont été réalisées en considérant des valeurs maximales (A) ou minimales (B) des estimations des paléo-tranches d' eau.

Au cours du Pliocène, les tranches d'eau sont plus réduites, et donc mieux contraintes. On note aussi au cours de cette période un épisode de surrection, de plus faible en amplitude, qui apparaît vers 3 à 4 Ma. Cet épisode serait alors à mettre en relation avec un autre épisode de déformation compressive rapide qui affecte aussi le domaine émergé. Cet épisode a été notamment mis en évidence à terre par le plissement progressif des calcaires coquilliers du Pliocène supérieur au NW de Pongaroa (*cf.* Fig. V-9, stéréogramme a). Plus généralement, il correspond à la « pulsation » de déformation compressive qui affecte l'ensemble du domaine avant-arc émergé entre 3.4 et 2.4 Ma (Nicol *et al.*, 2002).

En conclusion, cette analyse des mouvements verticaux sur la marge montre clairement une phase de subsidence générale sur cette transversale au cours du Miocène moyen et supérieur (c. 15 à 6.5 Ma). L'un des résultats marquants est aussi la mise en évidence d'un épisode brutal de surrection importante de la marge, de l'ordre de 500 à 1000 m, à la fin du Miocène supérieur débutant probablement vers 6.5 Ma.. Cet événement est identifié sur toutes les coupes analysées dans le secteur d'étude. Même si elle est toutefois moins nette, une autre phase de surrection apparaît sur toutes les courbes vers 3.5 Ma. Nous pouvons noter que ces différentes phases d'évolution des mouvements verticaux sont tout à fait compatibles avec l'analyse structurale et sédimentaire détaillée précédemment dans ce chapitre.

C) Les domaines morpho-structuraux du prisme de subduction Hikurangi

Au niveau de la zone d'étude, trois domaines morpho-structuraux peuvent donc être distingués sur une transversale donnée (transversale d'Akitio, Fig. VI-1). Il s'agit de la Chaîne Côtière (qui correspond à la plus haute ride du prisme Hikurangi, actuellement émergée), de la plate-forme du Wairarapa et du prisme d'accrétion Plio-Quaternaire, encore actif (Fig. VI-1). Les différences entre ces domaines résultent de leur différence en âge et de leur position relative au sein du prisme au cours du temps. En effet, comme nous l'avons montré dans le paragraphe précédent, la différence de complexité structurale entre ces domaines est en partie liée à l'histoire tectonique qu'ils ont subie et donc à leur différence d'âge. Nous avons également observé des variations transverses dans le style et l'amplitude de la déformation à une époque donnée. Par exemple, au cours de la troisième phase tectonique (c. 15 – c. 6.5 Ma), le domaine morpho-structural de la chaîne Côtière est en subsidence et affecté principalement de déformations en extension, alors que le secteur de la plate-forme du Wairarapa est en accrétion (Fig. VI-8).

Les limites entre ces domaines correspondent à d'anciennes zones de failles majeures, actives depuis les premiers épisodes compressifs liés à la subduction : la zone de faille de Turnagain (qui comprend notamment les failles de Whakataki, de Castlepoint et de Turnagain, Figs VI-1 et VI-5) et la zone de faille du Shelf Edge (*cf.* Fig. V-6). Au cours de l'évolution de la marge, ces zones de failles ont toujours constitué les limites entre les différents secteurs morphostructuraux (Fig. VI-8). Aux différentes époques chacun de ces secteurs a pu être caractérisé par une paléogéographie propre et donc des environnements de dépôt particuliers :

- Au cours du Miocène inférieur à moyen, la zone de faille de Turnagain a contrôlé la surrection de la ride structurale de Cape Turnagain qui constituait la bordure Est du bassin perché confiné d'Akitio.
- Au cours du Miocène moyen à supérieur, le haut structural de Turnagain sépare le large bassin de pente de Tawhero des bassins perchés confinés (dont le bassin de Titihaoa) qui se développent plus à l'Est. Par ailleurs, la zone de faille du Shelf Edge contrôle alors la surrection du haut structural du Shelf Edge.

- Au cours du Pliocène, le haut structural de Turnagain marque la limite, probablement en tant que bordure de plate-forme, entre, à l'Ouest, une plate-forme Pliocène, et à l'Est, le large bassin de pente de Turnagain. A la même période, le haut structural du Shelf Edge marque la limite entre le large bassin de Turnagain et, plus à l'Est, les bassins de pente confinés du prisme d'accrétion récent.
- Actuellement, le secteur du haut structural de Turnagain sépare le domaine continental émergé (probablement au cours du dernier million d'années ; Ghani, 1978 ; Cape et al., 1990) de la plate-forme du Wairarapa. Le secteur du haut structural du Shelf Edge délimite la plate-forme des bassins perchés confinés situés plus à l'Est. Les deux zones de failles majeures, les zones de Turnagain et du Shelf Edge, ont été réactivées au cours de l'épisode de raccourcissement le plus récent et coïncident désormais avec des limites géographiques bien définies : la ligne de côte du Wairarapa et la bordure de la plate-forme (Fig. VI-1).

L'ensemble de ces observations illustre ainsi les fortes interactions en contexte de marge active entre déformation, morphologie/paléogéographie et environnements sédimentaires. Le fort contrôle qu'exerce la tectonique sur l'enregistrement sédimentaire, notamment aux ordres supérieurs (durées de 1 à 10 Ma), reste prépondérant par rapport aux forçages eustatiques, mieux exprimés, surtout dans les faciès proximaux, aux ordres inférieurs.

III) CONCLUSION ET PERSPECTIVES

La plupart des études antérieures concernant les bassins portés par les prismes d'accrétion concernaient essentiellement des bassins situés en mer et à proximité du front de subduction. A ce niveau, les processus d'accrétion sont assez bien connus et l'évolution structurale du prisme d'accrétion *sensu-stricto* peut-être considérée comme continue. Dans ce contexte, dominé par la compression, se développent des bassins perchés confinés séparés par des rides structurales sub-parallèles au front de subduction (*trench-slope basins* ; Moore et Karig, 1976 ; Stevens et Moore, 1985 ; Underwood et Moore, 1995 ; cf. Figs I-3 et I-5).

Notre étude a montré que l'architecture stratigraphique des bassins de pente confinés est fortement contrôlée par la surrection des rides qui les bordent. Ils présentent donc une logique d'évolution tectono-sédimentaire qui nous renseigne sur la croissance du prisme de subduction qui les porte (cf. *supra*, paragraphe I de ce chapitre). Sur le prisme Hikurangi, cette évolution est caractérisée par des pulsations de quatrième ordre (durée de 1 à 2 Ma) dont nous avons démontré qu'elles n'étaient pas d'origine eustatique mais tectonique et liées au développement des bordures structurales des bassins. Cette cyclicité, observée sur une assez longue durée, semble être une des caractéristiques du prisme de subduction, et des bassins associés, en régime compressif.

L'évolution du prisme de subduction Hikurangi depuis le démarrage de la subduction, il y a 25 Ma, nous montre de plus une succession de plus longues périodes de déformation qui se traduit notamment par des modifications majeures des environnements de dépôt sur une verticale donnée (cf. *supra*, paragraphe II de ce chapitre). On note ainsi essentiellement trois grands domaines sédimentaires : des bassins perchés confinés de 5 à 10 km de large, des bassins de pente de 30 à 40 km de large, et des environnements de plate-forme. Les changements majeurs de régime tectonique (démarrage de la subduction vers 25 Ma, érosion tectonique vers 15 Ma et retour à la compression vers 6.5 Ma) ont lieu environ tous les 10 Ma dans le cas étudié. Hormis le démarrage de la subduction, ces phénomènes de troisième ordre peuvent être attribués à des variations *aléatoires* des paramètres de la subduction, pouvant notamment inclure des variations dans l'alimentation de la fosse en matériel détritique (et croissance corrélative du prisme) ou des variations de l'épaisseur et de la rugosité de la plaque plongeante.

Notre étude montre et confirme que la répartition dans l'espace et dans le temps des différents environnements de dépôts reconnus sur marge active reflète la déformation du prisme de subduction. Ceci nous renseigne donc sur l'évolution structurale de ces marges actives et sur les mouvements verticaux associés. La compréhension de ces interactions peut ainsi permettre d'accéder indirectement aux paramètres géodynamiques qui contrôlent les processus de subduction océanique.

Afin de déterminer si les résultats obtenus, concernant les paramètres qui contrôlent l'évolution des bassins perchés, ont une valeur régionale ou une valeur générale, il serait souhaitable dans l'avenir de pouvoir comparer l'exemple du prisme de subduction Hikurangi avec d'autres marges actives analysées en détail avec des objectifs et des méthodes similaires.

Références bibliographiques

Références Bibliographiques

- ADAMS, D., AND SULLIVAN, D., 1990, Amoco New Zealand Petroleum Company 2D seismic survey acquisition report PPL 38318/38323, East Coast Basin 1989-90 (IAE1): New Zealand unpublished openfile petroleum report 1665: Wellington, Ministry of Commerce.
- AUZENDE, J.-M., PELLETIER, B. AND EISSEN, J.-P., 1995, The North Fiji Basin, geology, structure and geodynamic evolution, *in* Brian Taylor, ed., *Backarc Basins: Tectonics and Magmatism*: New York, Plenum Press, p. 139-175.
- AUZENDE, J.-M., VAN DE BEUQUE, S., REGNIER, M., LAFOY, Y., AND SYMONDS, P., 2000, ORIGIN OF THE NEW CALEDONIAN OPHIOLITES BASED ON A FRENCH-AUSTRALIAN SEISMIC TRANSECT: MARINE GEOLOGY, V. 162, P. 225-236.
- BAILLEUL, J., 2001, Etude morphostructurale d'un bassin en contexte de subduction: origine et evolution du bassin de Norfolk, Sud-Ouest Pacifique [unpublished Master of Science with Honour thesis] : Université Pierre et Marie Curie, Paris VI, France, 28 p.
- BAILLEUL, J., MAUFFRET, A., VAN DE BEUQUE, S., GORINI, C., AND CHANIER, F., 2002, Etude morphostructurale d'un bassin en contexte de subduction: origine et evolution du bassin de Norfolk, Sud-Ouest Pacifique : Résumés de la 19^{ème} Réunion des Sciences de la Terre, Nantes, April 9-10-11-12, p. 54.
- BAILLEUL, J., ROBIN, C., CHANIER, F., GUILLOCHEAU, F., FIELD, B., AND FERRIÈRE, J., accepted, Turbidite systems in the inner forearc domain of the Hikurangi convergent margin (New Zealand): new constraints on the development of trench-slope basins: *Journal of Sedimentary Research*.
- BALLANCE, P.F., 1976, Evolution of the upper Cenozoic magmatic arc and plate boundary in Northland, New Zealand: *Earth and Planetary Science Letters*, v. 28, p. 356-370.
- BALLANCE, P. F., 1988, Late Cenozoic time-lines and calc-alkaline volcanic arcs in northern New Zealand - further discussion: *Journal of the Royal Society of New Zealand*, v. 18, p. 347-358.
- BALLANCE, P.F., 1993, The New Zealand Neogene forearc basins, *in* Hsü, K.J., ed., *South Pacific Sedimentary Basins, Sedimentary Basins of the World*: Amsterdam, Elsevier Science Publishers B.V., p. 177-193.
- BALLANCE, P.F., 1999, Simplification of the Southwest Pacific Neogene arcs: inherited complexity and control by a retreating pole of rotation, *in* Mac Niocaill, C. & Ryan, P.D., eds, *Continental Tectonics*, Geological Society of London Special Publication: London, Blackwell Scientific Publications, v. 164, p. 7-19.
- BALLANCE, P.F., AND SPORLI, K.B., 1979, Northland Allochthon: *Journal of the Royal Society of New Zealand*, v. 9, p. 259-275.
- BALLANCE, P. F., HAYWARD, B. W., AND BROOK, F. J., 1985, Subduction regression of volcanism in New Zealand: *Nature*, v. 313, p. 820.
- BARNES, P. M., AND MERCIER DE LEPINAY, B., 1997, Rates and mechanics of rapid frontal accretion along the very obliquely convergent southern Hikurangi margin, New Zealand: *Journal of Geophysical Research*, v. 102, B11, p. 24931-24952.
- BARNES, P.M., MERCIER DE LÉPINAY, B., COLLOT, J-Y., DELTEIL, J., AND AUDRU, J-C., 1998, Strain partitioning in the transition area between oblique subduction and continental collision, Hikurangi margin, New Zealand: *Tectonics*, v. 17, p. 534-557.
- BEANLAND, S., MELHUIH, A., NICOL, A., AND RAVENS, J., 1998, Structure and deformational history of the inner forearc region, Hikurangi subduction margin, New Zealand: *New Zealand Journal of Geology and Geophysics*, v. 41, p. 325-342.
- BEU, A.G., 1995, Pliocene limestones and their scallops: lithostratigraphy, pectinid biostratigraphy and paleogeography of eastern North Island late Neogene limestone: *Institute of Geological and Nuclear Sciences Monograph 10*, 243 p.
- BIROS, D., CUEVAS, R., AND MOEHL, B., 1995, Amoco New Zealand Petroleum Company well completion report Titihaoa-1 PPL38318: New Zealand unpublished openfile petroleum report 2081: Wellington, Ministry of Commerce.
- BISHOP, D.G., BRADSHAW, J.D., AND LANDIS, C.A., 1985, Provisional terrane map of South Island, New Zealand, *in* Howell, D.G., ed., *Tectonostratigraphic Terranes of the Circum-Pacific Region*: Council for Energy and Mineral Resources, Earth Science series, v. 1, p. 515-521.

BRADSHAW, J.D., 1989, Cretaceous geotectonic patterns in the New Zealand region: *Tectonics*, v. 8, n° 4, p. 803-820.

BRADSHAW, J.D., ADAMS, C.J., AND ANDREWS, P.B., 1980, Carboniferous to Cretaceous on the Pacific margin of Gondwana: the Rangitata phase of New Zealand: Fifth International Gondwana Symposium, Wellington, New Zealand, p. 218-219.

BROTHERS, R.N., 1974, Kaikoura orogeny in Northland, New Zealand: *New Zealand Journal of Geology and Geophysics*, v. 18, p. 1-18.

BURET, C., 1996, Les bassins sédimentaires d'un domaine avant-arc: la marge active de Nouvelle-Zélande [unpublished PhD thesis] : Université des Sciences et Technologies de Lille-Flandres, Villeneuve d'Ascq, France, 353 p.

BURET, C., CHANIER, F., FERRIERE, J., AND PROUST, J.-N., 1997, Individualisation d'un bassin d'avant-arc au cours du fonctionnement d'une marge active : la marge Hikurangi, Nouvelle-Zélande : *Comptes Rendus de l'Académie des Sciences (Paris)*, v. 325, p. 615-621.

CAPE, C.D., LAMB, S.H., VELLA, P., WELLS, P.E., AND WOODWARD, D.J., 1990, Geological structure of Wairarapa valley, New Zealand, from seismic reflection profiling: *Journal of the Royal Society of New Zealand*, v. 20, p. 85-105.

CASHMAN, S.M., KELSEY, H.M., ERDMAN, C.F., CUTTEN, H.N.C., AND BERRYMAN, K.R., 1992, Strain partitioning between structural domains in the forearc of the Hikurangi subduction zone, New Zealand: *Tectonics*, v. 11, No. 2, p. 242-257.

CASSIDY, J., AND LOCKE, C.A., 1987, Thin ophiolites of North Island, New Zealand: *Tectonophysics*, v. 137, p. 315-319.

CHANIER, F., AND FERRIERE, J., 1990, Mud volcanoes on the emerged ridge of the Hikurangi accretionary prism, New Zealand: tectonic setting and structural significance, *in* International conference on fluids in subduction zones and related processes, Paris, November 5-6, 1990.

CHANIER, F., 1991, Le prisme d'accrétion Hikurangi: un témoin de l'évolution géodynamique d'une marge active péripacifique (Nouvelle-Zélande) [unpublished PhD thesis]: Université des Sciences et Techniques de Lille-Flandres-Artois, Villeneuve d'Ascq, France, 357 p.

CHANIER, F., AND FERRIÈRE, J., 1989, Sur l'existence de mouvements tangentiels majeurs dans la chaîne côtière orientale de Nouvelle Zélande; signification dans le cadre de la subduction de la plaque Pacifique: *Comptes Rendus de l'Académie des Sciences (Paris)*, v. 308, série II, p. 1645-1650.

CHANIER, F., AND FERRIÈRE, J., 1991, From a passive to an active margin: tectonic and sedimentary processes linked to the birth of an accretionary prism (Hikurangi Margin, New Zealand): *Bulletin de la Société Géologique de France*, v. 162, p. 649-660.

CHANIER, F., BURET, C., FERRIERE, J., AND LARROQUE, C., 1994, Le bassin avant-arc de la marge néo-zélandaise, *in* Les bassins d'avant-chaînes, Scéance de la Société Géologique de France, Grenoble : *Géologie Alpine, Série Spéciale Résumés de Colloques*, v. 4, p.20-21.

CHANIER, F., FERRIÈRE, J., AND ANGELIER, J., 1999, Extensional deformation across an active margin, relations with subsidence, uplift and rotations: the Hikurangi subduction, New Zealand: *Tectonics*, v. 18, p. 862-876.

CLARK, R.H., AND WELLMAN, H.W., 1959, The Alpine Fault from lake McKerrow to Milford Sound: *New Zealand Journal of Geology and Geophysics*, v. 2, p. 590-601.

CLIFT, P.D., BEDNARZ, U., BOE, R., ROTHWELL, R.G., HODKINSON, R.A., LEDBETTER, J.K., PRATT, C.E., AND SOAKAI, S., 1994, Sedimentation on the Tonga forearc related to arc rifting, subduction erosion, and ridge collision: a synthesis of results from Sites 840 and 841: *Proceedings of the Ocean Drilling Program, Scientific Results*, v. 135, p. 843-855.

CLUZEL, D., AITCHISON, J., CLARKE, G., MEFFRE, S., AND PICARD, C., 1994, Point de vue sur l'évolution tectonique et géodynamique de la Nouvelle-Calédonie (Pacifique, France) : *Comptes Rendus de l'Académie des Sciences (Paris)*, v. 319, série IIa, p. 683-690.

COLE, J.W., 1979, Structure, petrology and genesis of Cenozoic volcanism, Taupo volcanic zone, New Zealand – a review: *New Zealand Journal of Geology and Geophysics*, v. 22, p. 631-657.

COLE, J. W., 1984, Taupo-Rotorua Depression : an ensialic marginal basin of North Island, New Zealand, *in* Kokelaar, B.P. and Howells, M.F., eds, *Marginal basin geology: Geological Society of London Special Publication*, v. 16, pp. 109-120.

COLE, J.W., 1986, Distribution and tectonic setting of late Cenozoic volcanism in New Zealand, *in* Smith, I.E.M., ed., *Late Cenozoic volcanism in New Zealand: Bulletin of the Royal Society of New Zealand*, v. 23, p. 7-20.

- COLLOT, J.Y., MISSEGUE, F., AND MALAHOFF, A., 1982, Anomalies gravimétriques et structure de la croûte dans la région de la Nouvelle-Calédonie : enracinement des péridotites, *In* Equipe de Géologie-Géophysique ORSTOM Nouméa, ed., Contribution à l'étude Géodynamique du Sud-Ouest Pacifique : Trav. Doc. ORSTOM, v. 147, p. 549-564.
- COLLOT, J.Y., MALAHOFF, A., RECY, J., LATHAM, G., AND MISSEGUE, F., 1987, Overthrust emplacement of New Caledonia ophiolites: geophysical evidence: *Tectonics*, v. 16, p. 215-232.
- COLLOT, J.-Y., DELTEIL, J., LEWIS, K.B., DAVY, B., LAMARCHE, G., AUDRU, J.-C., BARNES, P., CHANIER, F., CHAUMILLON, E., LALLEMAND, S., MERCIER DE LÉPINAY, B., ORPIN, A., PELLETIER, B., SOSSON, M., TOUSSAINT, B., AND URUSKI, C., 1996, From oblique subduction to intra-continental transpression: structures of the southern Kermadec-Hikurangi margin from multibeam bathymetry, side-scan sonar and seismic reflection: *Marine Geophysical Researches*, v. 18, p. 357-381.
- COOPER, R.A., 1979, Lower Paleozoic rocks of New Zealand: *Journal of the Royal Society of New Zealand*, v. 9, p. 29-84.
- COOPER, R.A., ed., 2004, The New Zealand Geological Timescale: Geological and Nuclear Sciences Monograph, v. 22: Lower Hutt, Geological and Nuclear Sciences, 284 p. <http://www.gns.cri.nz/what/earthhist/dating/index.html>.
- CROOK, K.A.W., AND FEARY, D.A., 1982, Development of New Zealand according to the forearc model of crustal evolution, *in* Packham, G.H., ed., The evolution of the India-Pacific plate boundaries: *Tectonophysics*, v. 87, p. 65-107.
- CROSS, T.A., BAKER, M.R., CHAPIN, M.A., CLARK, M.S., GARDNER, M.H., HANSON, M.S., LESSENGER, M.A., LITTLE, L.D., MCDONOUGH, K.J., SONNEFELD, M.D., VALASAK, D.W., WILLIAMS, M.R., AND WRITTER, D.N., 1993, Application of high resolution sequence stratigraphy to reservoir analysis, *in* Eschard, R., and Doligez, B., ed., Subsurface Reservoir Characterization from Outcrop Observations: Paris, Technip, p. 11-33.
- CROTTY, K.J., 1995, Special paleontological summary, Amoco New Zealand Petroleum Company Titihaoa-1 Exploratory Well, Wairarapa Coast offshore North Island, New Zealand, *in* Biro, D., Cuevas, R., and Moehl, B., ed., Amoco New Zealand Petroleum Company well completion report Titihaoa-1 PPL38318: Wellington, Ministry of Commerce.
- CRUNDWELL, M.P., 1987, Neogene stratigraphy and geological history of the Wainuioru valley, eastern Wairarapa, New Zealand [unpublished Master of Science with Honour thesis]: Victoria University, Wellington, 126 p.
- CRUNDWELL, M.P., 1997, Neogene lithostratigraphy of southern Wairarapa: Institute of Geological and Nuclear Sciences science report 97/36. 57 p.
- CRUNDWELL, M.P., SCOTT, G.H., AND THRASHER, G.P., 1994, Calibration of paleobathymetry indicators by integrated seismic and paleontological analysis of foreset sequences, Taranaki basin, New Zealand, 1994 New Zealand Petroleum Conference Proceedings: Wellington, Ministry of commerce, p. 169-178.
- DAVEY, F.J., 1982, The structure of the South Fiji Basin: *Tectonophysics*, v. 87, p. 185-241.
- DAVEY, F.J., HAMPTON, M., CHILDS, J., FISHER, M.A., LEWIS, K.B., AND PETTINGA, J.R., 1986, Structure of a growing accretionary prism, Hikurangi margin, New Zealand: *Geology*, v. 14, p. 663-666.
- DAVIS, E.E., AND HYNDMAN, R.D., 1989, Accretion and recent deformation of sediments along the northern Cascadia subduction zone: *Geological Society of America Bulletin*, v. 101, p. 1465-1480.
- DAVY, B., 1993, The influence of subducting plate buoyancy on subduction of the Hikurangi-Chatham Plateau beneath the North Island, New Zealand, *in* Watkins, J., Zhigiang, F., and McMillen, K., eds, Advances in the Geology and Geophysics of the Continental Margin: American Association of Petroleum Geologists Memoir, v. 53, p. 75-91.
- DAVY, B., AND WOOD, R., 1994, Gravity and magnetic modelling of the Hikurangi Plateau: *Marine Geology*, v. 118, p. 139-151.
- DELTEIL, J., MORGANS, H.E.G., RAINE, J.I., FIELD, B.D., AND CUTTEN, H.N.C., 1996, Early Miocene thin-skinned tectonics and wrench faulting in the Pongaroa district, Hikurangi margin, North Island, New Zealand: *New Zealand Journal of Geology and Geophysics*, v. 39, p. 271-282.
- DEMETS, C., GORDON, R.G., ARGUS, D.F., AND STEIN, S., 1994, Effect of recent revisions to the geomagnetic time scale on estimates of current plate motions: *Geophysical Research Letters*, v. 21, p. 2191-2194.
- DICKINSON, W.R., AND SEELY, D.R., 1979, Structure and stratigraphy of forearc regions: *American Association of Petroleum Geologists bulletin*, v. 63, p. 2-31.
- DUBOIS, J., RAVENNE, C., AUBERTIN, A., LOUIS, J., GUILLAUME, R., LAUNAY, J. AND MONTADERT, L., 1974, Continental margin near New Caledonia, *in* Burck, C.A., and Drake, C.L., eds, The geology of Continental margins: New York, Springer-Verlag, p. 521-535.

- DUBOIS, M., BURET, C., AND CHANIER, F., 2000, SUBSILOG, a "C" program for decompaction and subsidence computation. Application to the New Zealand forearc basin: *Annales de la Société Géologique du Nord*, v. 8, p. 19-24.
- DUPONT, J., 1982, Le cadre general et les traits essentiels de l'arc insulaire des Tonga-Kermadecs, *in* Equipe de Géologie-Géophysique ORSTOM Nouméa, ed., Contribution à l'étude Géodynamique du Sud-Ouest Pacifique : Trav. Doc. ORSTOM, v. 147, p. 249-261.
- EADE, J.V., 1988, The Norfolk Ridge system and its margins, *in* Nairn, A.E.M., Stehli, F.G., and Uyeda, S., eds, *The Ocean Basins and Margins v. 7B, The Pacific Ocean: New York and London*, Plenum Press, p. 303-322.
- EDBROOKE, S.W., AND BROWNE, G.H., 1996, An outcrop study of bed thickness and continuity in thin-bedded facies of the Whakataki formation at Whakataki Beach, east Wairarapa: Institute of Geological and Nuclear Sciences science report 96/34, 18 p.
- EDWARDS, A.R., HORNIBROOK, N. DE B., RAINE, J.I., SCOTT, G.H., STEVENS, G.R., STRONG, C.P., AND WILSON, G.J., 1988, A New Zealand Cretaceous-Cenozoic geological time scale: *New Zealand geological survey Record*, v. 35, p. 135-149.
- FERRIÈRE, J., 1987, Nouvelle-Zélande: quelques aspects de la "tectonique alpine", post-carbonifère, d'une chaîne péripacifique: *Comptes Rendus de l'Académie des Sciences (Paris)*, v. 305, série II, p. 615-618.
- FERRIERE, J., AND CHANIER, F., 1993, La tectonique des plaques à l'épreuve de la réalité: SW Pacifique et Nouvelle-Zélande: *Géochronique*, v. 45, p. 14-20.
- FIELD, B.D., 2005, Cyclicality in turbidites of the Miocene Whakataki Formation, Castlepoint, North Island, and implications for hydrocarbon reservoir modeling: *New Zealand Journal of Geology and Geophysics*.
- FIELD, B.D., URUSKI, C.I., BEU, A.G., BROWNE, G.H., CRAMPTON, J.S., FUNNELL, R., KILLOPS, S., LAIRD, M.G., MAZENGARB, C., MORGANS, H.E.G., RAIT, G.J., SMALE, D., AND STRONG, C.P., 1997, Cretaceous - Cenozoic geology and petroleum systems of the East Coast region: *New Zealand: Institute of Geological and Nuclear Sciences Monograph 19*, 301 p.
- FRANCIS, D.A., 1990, Report on the geology of coastal Wairarapa, between Riversdale and Porangahau, adjacent to offshore prospecting leases 38318 and 38323, *New Zealand open-file petroleum report 2138 for Amoco New Zealand Exploration Company: Wellington, Ministry of Economic Development*.
- GALLOWAY, W.E., 1989, Genetic stratigraphic sequences in basin analysis I: Architecture and genesis of flooding-surface bounded depositional units: *American Association of Petroleum Geologists bulletin*, v. 73, p. 125-142.
- GEORGE, A.D., 1992, Deposition and deformation of an Early Cretaceous trench-slope basin deposit, Torlesse terrane, *New Zealand: Geological Society of America Bulletin*, v. 104, p. 570-580.
- GHANI, M.A., 1978, Late Cenozoic vertical crustal movements in the southern North Island, *New Zealand: New Zealand Journal of Geology and Geophysics*, v. 21, p. 117-125.
- GNS, Fossil Record Electronic Database (FRED). <http://data.gns.cri.nz/fred/index.jsp>
- HARDENBOL, J., THIERRY, J., FARLEY, M.B., JACQUIN, T., DE GRACIANSKI, P.-C., AND VAIL, P.R., 1998, Mesozoic - Cenozoic sequence chronostratigraphic framework, *in* De Gracianski, P.-C., Hardenbol, J., Jacquin, T., Vail, P.R., and Farley, M.B., ed., *Sequence Stratigraphy of European Basins*, SEPM Special Publication, p. 3-13.
- HAWKINS, J.W., AND PARSON, L.M., 1994, Scientific results of Leg 135: Lau Basin-Tonga Ridge drilling transect, *in* Proceedings of the Ocean Drilling Program, Scientific Results, v. 135, 816 p.
- HAYES, D.E., AND RINGIS, J., 1973, Seafloor spreading in the Tasman Sea: *Nature*, v. 243, p. 454-58.
- HAYWARD, B.W., 1986, A guide to paleoenvironmental assesment using New Zealand Cenozoic foraminiferal faunas: *New Zealand Survey paleontology report*, v. 109.
- HAYWARD, B.W., 1987, Paleobathymetry and structural and tectonic history of Cenozoic drillhole sequences in Taranaki basin: *New Zealand geological survey Report PAL122*.
- HELLER, P.L., AND DICKINSON, W.R., 1985, Submarine ramp facies model for delta-fed, sand-rich turbidite systems: *American Association of Petroleum Geologists bulletin*, v. 69, No. 6, p. 960-976.
- HERZER, R. H., 1995, Seismic stratigraphy of a buried volcanic arc, Northland, New Zealand, and implications for Neogene subduction: *Marine and Petroleum Geology*, v. 12, p. 511-531.
- HERZER, R. H., AND MASCLE, J., 1996, Anatomy of a continent-backarc transform- the Vening Meinesz Fracture Zone northwest of New Zealand: *Marine Geophysical Research*, 1B, p. 401-407.

- HERZER, R.H., CHAPRONIERE, G.C.H., EDWARDS, A.R., HOLLIS, C.J., PELLETIER, B., RAINE, J.I., SCOTT, G.H., STAGPOOLE, V., STRONG, C.P., SYMONDS, P., WILSON, G.J., AND ZHU, H., 1997, Seismic stratigraphy and structural history of the Reinga Basin and its margins, southern Norfolk Ridge system: *New Zealand Journal of Geology and Geophysics*, v 40, p 425-451.
- HOMEWOOD, P., GUILLOCHEAU, F., ESCHARD, R., AND CROSS, T.A., 1992, High resolution correlations and genetic stratigraphy: an integrated approach: *Bulletin Centre Exploration-Production Elf Aquitaine*, v. 16, p. 357-381.
- HOWELL, D.G., 1980, Mesozoic accretion of exotics terranes along the New Zealand segment of Gondwanaland: *Geology*, v. 8, p. 487-491.
- HUYGHE, P., GRIBOULARD, R., FAUGERES, J.-C., GONTHIER, E., AND BOBIER, C., 1996, Geometry of supra-prism basins of southern Barbados wedge: *Bulletin de la société géologique de France*, v. 167, n° 3, p. 345-359.
- JOHANSEN, A., 1999, The geology of the upper Tinui Valley, Wairarapa, New Zealand [unpublished Master of Science with Honour thesis]: Victoria University, Wellington.
- JOHNSTON, M.R., 1975, Sheet N159 and part sheet N158, Tinui - Awatoitoti: Geological map of New Zealand 1:63 360. Wellington, New Zealand, Department of Scientific and Industrial Research.
- JOHNSTON, M.R., 1980, Geology of the Tinui - Awatoitoti district, New Zealand: *New Zealand geological survey Bulletin*, v. 94, 60 p.
- KARIG, D.E., 1970, Ridges and basins of the Tonga-Kermadec island-arc system: *Journal of Geophysical Research*, v. 75, p. 239-254.
- KARIG, D.E., 1971, Origin and development of marginal basins in the western Pacific: *Journal of Geophysical Research*, v. 76, p. 2542-2561.
- KARIG, D.E., 1982, Initiation of subduction zones: implications for arc evolution and ophiolite development, *in* Leggett, J.K., ed., *Trench-forearc Geology*, Geological Society of London Special Publication: London, Blackwell Scientific publications, v. 10, p. 563-576.
- KARIG, D.E., AND SHARMAN, G.F., 1975, Subduction and accretion in trenches: *Geological Society of America Bulletin*, v. 86, p. 377-389.
- KARIG, D.E., SUPARKA, S., MOORE, G.F, AND HEHANUSSA, P.E., 1979, Structure and Cenozoic evolution of the Sunda arc in the central Sumatra region, *in* Watkins, J.S., Montadert, L., and Dickerson, P.W., ed., *Geological and Geophysical Investigations of Continental Margins*, American Association of Petroleum Geologists, memoir 29, p. 223-237.
- KARIG, D.E., MOORE, G.F, CURRAY, J.R., AND LAWRENCE, M.B., 1980, Morphology and shallow structure of the lower trench slope off Nias Island, Sunda arc, *in* Hayes, D.E., ed., *The tectonic and Geologic Evolution of Southeast Asian Seas and Islands*, American Geophysical Union, Monograph 23, p. 179-208.
- KELSEY, H.M., CASHMAN, S.M., BEANLAND, S., AND BERRYMAN, K.R., 1995, Structural evolution along the inner forearc of the obliquely convergent Hikurangi margin, New Zealand: *Tectonics*, v. 14, p. 1-18.
- KING, P.R., 2000, Tectonic reconstruction of New Zealand: 40 Ma to the present: *New Zealand Journal of Geology and Geophysics*, v. 43, p. 611-638.
- KING, P.R., SCOTT, G.H., AND ROBINSON, P.H., 1993, Description, correlation and depositional history of Miocene sediments outcropping along North Taranaki coast: *Institute of Geological and Nuclear Sciences Monograph* 13.
- KINGMA, J.T., 1967, Sheet 12, Wellington: Geological map of New Zealand 1:250 000. Wellington, New Zealand, Department of Scientific and Industrial Research.
- KROENKE, L.W., 1984, Cenozoic tectonic development of the Southwest Pacific, *in* Kroenke, L.W., ed., *Committee for coordination of joint prospecting for mineral resources in South Pacific offshore areas (CCOP/SOPAC)*, *Tech. Bull.*: New Zealand, 122 p.
- KROENKE, L.W., AND EADE, J.V., 1982, Three Kings Ridge: a west-facing arc: *Geo-Marine Letters*, v.2, p. 5-10.
- KROENKE, L.W., AND DUPONT, J., 1982, Subduction: a possible North-South transition along the West flank of the Three Kings Ridge: *Geo-Marine Letters*, v. 2, p. 11-16.
- LAMARCHE, G., BEANLAND, S. AND RAVENS, J., 1995, Deformation style and history of the Eketahuna region, Hikurangi forearc, New Zealand, from shallow seismic reflection data: *New Zealand Journal of Geology and Geophysics*, v. 38, p. 105-115.

LAMB, S.H., AND VELLA, P., 1987, The last million years of deformation in part of New Zealand plate boundary zone: *Journal of Structural Geology*, v. 11, No. 4, p. 473-492.

LAPOUILLE, A., 1982, Etude des bassins marginaux fossiles du Sud-Ouest Pacifique : Bassin Nord-d'Entrecasteaux, Bassin Nord-Loyauté, Bassin Sud-Fidjien, *in* Equipe de Géologie-Géophysique ORSTOM Nouméa, ed., Contribution à l'étude Géodynamique du Sud-Ouest Pacifique : Trav. Doc. ORSTOM, v. 147, p. 409-438.

LAUNEY, J., DUPONT, J., AND LAPOUILLE, A., 1982, THE THREE KINGS RIDGE AND THE NORFOLK BASIN (SOUTHWEST PACIFIC): AN ATTEMPT AT STRUCTURAL INTERPRETATION: SOUTH PACIFIC MARINE GEOLOGY NOTES, V. 2, P. 121-130.

LEE, J.M., AND BEGG, J.G., (COMPILERS), 2002, Geology of the Wairarapa area: Institute of Geological and Nuclear Sciences 1:250 000 geological map 11. 1 sheet + 66 p. Lower Hutt, New Zealand. Institute of Geological and Nuclear Sciences Limited.

LEITCH, E.C., 1984, Marginal basins of the SW Pacific and the preservation and recognition of their ancient analogues : a review, *in* Kokelaar, B.P., and Howells, M.F., eds., Geological Society of London Special Publication: London, Blackwell Scientific Publications, v. 16, p. 97-108.

LENSEN, G.J., 1969, Sheet N153, Eketahuna: Late Quaternary tectonic map of New Zealand 1:63 360. Wellington, Department of Scientific and Industrial Research.

LEVERENZ, A., 2000, Trench sedimentation versus accreted submarine fan – an approach to regional-scale facies analysis in a Mesozoic accretionary complex: "Torlesse" terrane, northeastern North Island, New Zealand: *Sedimentary Geology*, v. 132, p. 125-160.

LEWIS, K.B., 1980, Quaternary sedimentation of the Hikurangi oblique subduction and transform margin, *in* Ballance, P.F., and Reading, H.G., ed., Sedimentation in Oblique-slip Mobile Zones, Special Publication of the International Association of Sedimentologists: Oxford, Blackwell Scientific Publications, p. 171-189.

LEWIS, K.B., AND PETTINGA, J.R., 1993, The emerging, imbricate frontal wedge of the Hikurangi margin, *in* Ballance, P.F., (Series Editor: Hsu, K.J.), ed., South Pacific Sedimentary Basins, *Sedimentary Basins of the World 2*: Amsterdam, Elsevier Science Publishers B.V.

LEWIS, K.B., AND BARNES, P.M., 1999, Kaikoura canyon, New Zealand: active conduit from near-shore sediment zones to trench-axis channel: *Marine Geology*, v. 162, p. 39-69.

LEWIS, K.B., AND PANTIN, H.M., 2002, Channel-axis, overbank and drift sediment waves in the southern Hikurangi Trough, New Zealand: *Marine Geology*, v. 192, p. 123-151.

LEWIS, K.B., BARNES, P.M., COLLOT, J.-Y., MERCIER DE LÉPINAY, B., DELTEIL, J., AND GEODYNZ TEAM, 1999, Central Hikurangi GeodyNZ swath maps: depths, texture and geological interpretation., NIWA chart, Miscellaneous Series N°. 77: Wellington, National Institute of Water and Atmospheric Research.

LEWIS, S.D., LADD, J.W., AND BRUNS, T.R., 1988, Structural development of an accretionary prism by thrust and strike-slip faulting: Shumagin region, Aleutian Trench: *Geological Society of America Bulletin*, v. 100, p. 767-782.

LILLIE, A.R., 1953, The Geology of the Dannevirke subdivision: *New Zealand Geological Survey Bulletin*, v. 46, 10 sheets + 156 p.

LUYENDYK, B.P., 1995, Hypothesis for Cretaceous rifting of east Gondwana caused by subducted slab capture: *Geology*, v. 23, p. 373-376.

MACKINNON, T.C., 1983, Origin of the Torlesse terrane and coeval rocks, South Island, New Zealand: *Geological Society of America Bulletin*, v. 94, p. 967-985.

MACKINNON, T.C., AND HOWELL, D.G., 1985, Torlesse turbidite system, New Zealand, *in* Bouma, A.H., Normark, W.R., and Barnes, N.E., eds, *Submarine Fans and Related Turbidite Systems*: New York, Springer-Verlag, p. 223-228.

MALAHOFF, A., FEDEN, R.H., AND FLEMING, H.F., 1982, Magnetic anomalies and tectonic fabric of marginal basins north of New Zealand: *Journal of Geophysical Research*, v. 87, p. 4109-4125.

MALPAS, J., SPÖRLI, K.B., BLACK, P.M., AND SMITH, I.E.M., 1992, Northland ophiolites, New Zealand, and implications for plate tectonic evolution of the South-West Pacific: *Geology*, v. 20, p. 149-152.

MASCLE, A., ENDIGNOUX, L., AND CHENNOUF, T., 1990, Frontal accretion and piggyback basin development at the southern edge of the Barbados Ridge accretionary complex: *Proceedings of the Ocean Drilling Program, Scientific Results*, v. 110.

- McADOO, B.G., ORANGE, D.L., SCREATON, E., LEE, H.E., AND KAYEN, R., 1997, Slope basins, headless canyons, and submarine palaeoseismology of the Cascadia accretionary complex: *Basin Research*, v. 9, p. 313-324.
- MIGNOT, A., 1984, SISMO-STRATIGRAPHIE DE LA TERMINAISON NORD DE LA RIDE DE NORFOLK [UNPUBLISHED PHD THESIS] : UNIVERSITE PIERRE ET MARIE CURIE, PARIS VI, 203 P.
- MITCHUM, R.M.J., VAIL, P.R., AND SANGREE, J.B., 1977a, Seismic stratigraphy and global changes of sea levels VI: stratigraphic interpretation of seismic reflexion patterns in depositional sequences, *in* Payton, C.E., ed., *Seismic stratigraphy: Application to hydrocarbon exploration*: Tulsa, Society of Economic Paleontologists and Mineralogists Special Publication, p. 117-133.
- MITCHUM, R.M.J., VAIL, P.R., AND THOMPSON, S., 1977b, Seismic stratigraphy and global changes of sea levels II: The depositional sequence as a basic unit for stratigraphic analysis, *in* Payton, C.E., ed., *Seismic stratigraphy: Application to hydrocarbon exploration*: Tulsa, Society of Economic Paleontologists and Mineralogists Special Publication, p. 53-62.
- MONZIER, M., 1993, Un modèle de collision arc insulaire-ride océanique : Evolution sismo-tectonique et pétrologie des volcanites de la zone d'affrontement arc des Nouvelles-Hébrides - ride des Loyauté [unpublished PhD thesis] : ORSTOM, Université Française du Pacifique, Nouméa, 322 p.
- MONZIER, M., DANIEL, J. AND MAILLET, P., 1990, La collision ride des Loyauté/arc des Nouvelles Hébrides (Pacifique Sud-Ouest) : *Oceanologica Acta*, v. 10, p. 43-56.
- MOORE, G.F., AND KARIG, D.E., 1976, Development of sedimentary basins on the lower trench slope: *Geology*, v. 4, p. 693-697.
- MOORE, G.F., AND KARIG, D.E., 1980, Structural geology of Nias Island, Indonesia: implications for subduction zone tectonics: *American Journal of Science*, v. 280, p. 193-223.
- MOORE, G.F., BILLMAN, H.G., HEHANUSSA, P.E., AND KARIG, D.E., 1980, Sedimentology and paleobathymetry of Neogene trench-slope deposits, Nias Island, Indonesia: *Journal of Geology*, v. 88, p. 161-180.
- MOORE, J.C., AND ALLWARDT, A., 1980, Progressive deformation of a tertiary trench slope, Kodaik Island, Alaska: *Journal of Geophysical Research*, v. 85, p.4741-4756.
- MOORE, P.R., 1980, Late Cretaceous - early Tertiary stratigraphy, structure and tectonic history of the area between Whareama and Ngahape, eastern Wairarapa, New Zealand: *New Zealand Journal of Geology and Geophysics*, v. 23, p. 167-177.
- MOORE, P.R., 1988, Structural divisions of eastern North Island, New Zealand: *New Zealand Geological Survey Record*, v. 30, 24 p.
- MORGANS, H.E.G., CRUNDWELL, M.P., SCOTT, G.H., AND EDWARDS, A.R., 1995, Biostratigraphy of Titihaoa-1 offshore petroleum exploration well, Wairarapa coast, New Zealand, *in* Biros, D., Cuevas, R., and Moehl, B., ed., *Amoco New Zealand Petroleum Company well completion report Titihaoa-1 PPL38318*: New Zealand unpublished openfile petroleum report 2081: Wellington, Ministry of Commerce.
- MORTIMER, N., AND PARKINSON, D., 1996, Hikurangi Plateau: a Cretaceous large igneous province in the southwest Pacific Ocean: *Journal of Geophysical Research*, v. 101, p. 687-696.
- MORTIMER, N., HERZER, R.H., GANS, P.B., PARKINSON, D.L., AND SEWARD, D., 1998, Basement geology from the Three Kings ridge to West Norfolk ridge, Southwest Pacific ocean: evidence from petrology, geochemistry and isotopic dating of dredge samples: *Marine Geology*, v. 148, p. 135-162.
- MUTTI, E., AND NORMARK, W.R., 1987, Comparing examples of modern and ancient turbidite systems: problems and concepts, *in* Leggett, J.K., and Zuffa, G.G., ed., *Marine Clastic Sedimentology: concepts and cases studies*: London, Graham and Trotman, p. 1-37.
- MUTTI, E., AND NORMARK, W.R., 1991, An Integrated Approach to the study of turbidite systems, *in* Weimer, P., and Link, M.H., ed., *Seismic facies and sedimentary processes of submarine fans and turbidite systems*: New-York, Springer - Verlag, p. 75-106.
- MUTTI, E., AND RICCI LUCCHI, F., 1978, Turbidites of the northern Apennines: introduction to facies analysis (English translation): *International Geology Review*, v. 20, p. 125-166.
- NEEF, G., 1992a, Turbidite deposition in five Miocene, bathyal formations along an active plate margin, North Island, New Zealand: with notes on styles of deposition at the margins of east coast bathyal basins: *Sedimentary Geology*, v. 78, p. 111-136.
- NEEF, G., 1992b, Geology of the Akitio area (1:50 000 metric sheet U25BD, east), northeastern Wairarapa, New Zealand: *New Zealand Journal of Geology and Geophysics*, v. 35, p. 533-548.

- NEEF, G., 1995, Cretaceous and Cenozoic geology east of the Tinui Fault Complex in northeastern Wairarapa, New Zealand: *New Zealand Journal of Geology and Geophysics*, v. 38, p. 375-394.
- NEEF, G., 1997a, Stratigraphy, structural evolution, and tectonics of the northern part of the Tawhero Basin and adjacent areas, northern Wairarapa, North Island, New Zealand: *New Zealand Journal of Geology and Geophysics*, v. 40, p. 335-358.
- NEEF, G., 1997b, Stratigraphy and structure of an outboard part of the forearc of the Hikurangi Margin, North Wairarapa, New Zealand: *Journal and Proceedings of the Royal Society of NSW*, v. 130, parts 1-2, p. 1-24.
- NEEF, G., 1999, Neogene development of the onland part of the forearc in the northern Wairarapa, North Island, New Zealand: a synthesis: *New Zealand Journal of Geology and Geophysics*, v. 42, p. 113-115.
- NICOL, A., VAN DISSEN, R., VELLA, P., ALLOWAY, B., AND MELHUISE, A., 2002, Growth of contractional structures during the last 10 m.y. at the southern end of the emergent Hikurangi forearc basin, New Zealand: *New Zealand Journal of Geology and Geophysics*, v. 45, p. 365-385.
- NORMARK, W.R., 1970, Growth patterns of deep-sea fans: *American Association of Petroleum Geologists bulletin*, v. 54, p. 2170-2195.
- OKADA, H., 1989, Anatomy of trench-slope basins: examples from the Nankai Trough: *Palaeogeography, Palaeoclimatology, Palaeoecology*, v. 71, p. 3-13.
- PACKHAM, G.H., AND FALVEY, D.A., 1971, A hypothesis for the formation of marginal seas in the western Pacific: *Tectonophysics*, v. 11, p. 79-109.
- PARIS, J.P., 1981, *Géologie de la Nouvelle-Calédonie* [unpublished PhD thesis]: *Mémoire du Bureau de Recherche géologique et minier*, 278 p.
- PARIS, J.P., AND LILLIE, R., 1977, New Caledonia – evolution from Permian to Miocene, Mapping data and hypothesis about geotectonics, *in* *International Symposium on Geodynamics in South-West Pacific*, Nouméa, New Caledonia: Paris, Technip, p. 195-208.
- PARIS, J.P., ANDREIEFF, P., AND COUDRAY, J., 1979, Sur l'âge Eocène supérieur de la mise en place de la nappe ophiolitique de Nouvelle-Calédonie, unité de charriage océanique périaustralien, déduit d'observations nouvelles sur la série de Népoui : *Comptes Rendus de l'Académie des Sciences (Paris)*, v. 307, série II, p. 179-184.
- PELLETIER, B., AND DUPONT, J., 1990, Erosion, accretion, extension arrière-arc et longueur du plan de subduction le long de la marge active des Kermadecs, Pacifique Sud-Ouest: *Comptes Rendus de l'Académie des Sciences (Paris)*, v. 310, série II, p. 1657-1664.
- PELLETIER, B., CALMANT, S. AND PILLET, R., 1998, Current tectonics of the Tonga - New Hebrides region: *Earth and Planetary Science Letters*, v. 164, 1-2, p. 263-276.
- PETTINGA, J.R., 1982, Upper Cenozoic structural history, coastal Hawke's Bay, New Zealand: *New Zealand Journal of Geology and Geophysics*, v. 25, p. 149-191.
- PICKERING, K.T., HISCOTT, R.N. AND HEIN, F.J., 1989, *Deep Marine Environments, clastic sedimentation and tectonics*: London, Unwin Hyman.
- PILLANS, B., 1986, A Late Quaternary uplift map for North Island, New Zealand, *in* Reilly, W.I., and Harford, B.E., eds, *Recent Crustal Movements of the Pacific Region*: *Royal Society of New Zealand Bulletin*, v. 24, p. 409-417.
- POSAMENTIER, H.W., AND VAIL, P.R., 1988, Eustatic controls on clastic deposition II: Sequence and systems tract models, *in* Wilgus, C.K., Hastings, B.S., Posamentier, H.W., and Van Wagoner, J., ed., *Sea Level Changes: an Integrated Approach*: Tulsa, Society of Economic Paleontologists and Mineralogists Special Publication.
- POSAMENTIER, H.W., JERVEY, M.T., AND VAIL, P.R., 1988, Eustatic controls on clastic deposition I - conceptual framework, *in* Wilgus, C.K., Hastings, B.S., Posamentier, H.W., and Van Wagoner, J., ed., *Sea Level Changes: an Integrated Approach*: Tulsa, Society of Economic Paleontologists and Mineralogists Special Publication, p. 109-124.
- RAIT, G.J., CHANIER, F., AND WATERS, D.W., 1991, Landward and seaward directed thrusting accompanying the onset of subduction beneath New Zealand: *Geology*, v. 19, p. 230-233.
- READING, H.G., 1991, The classification of deep-sea depositional systems by sediment calibre and feeder system: *Journal of the Geological Society of London*, v. 148, p. 427-430.
- READING, H.G., AND RICHARDS, M., 1994, Turbidite systems in deep-water basin margins classified by grain size and feeder system: *American Association of Petroleum Geologists bulletin*, v. 78, No. 5, p. 792-822.

- REID, C.M., 1998, Stratigraphy, paleontology, and tectonics of lower Miocene rocks in the Waipatiki/Mangatuna area, southern Hawke's Bay, New Zealand: *New Zealand Journal of Geology and Geophysics*, v. 41, p. 115-131.
- RICHARDS, M., BOWMAN, M., READING, H., 1998, Submarine fan I: characterisation and stratigraphic prediction: *Marine and Petroleum Geology*, v. 15, p. 689-717.
- RIGOLOTT, P., 1989, Origine et évolution du "système" ride de Nouvelle-Calédonie / Norfolk (Sud-Ouest Pacifique) : synthèse des données de géologie et de géophysique marine, étude des marges et bassins associés [unpublished PhD thesis] : Université de Bretagne Occidentale, 319 p.
- ROBINSON, R., 1986, Seismicity, structure and tectonics of the Wellington region, New Zealand: *Geophysical Journal of the Royal astronomical Society*, v. 87, p. 379-409.
- SCHOLL, D.W., MARLOW, M.S., AND COOPER, A.K., 1977, Sediment subduction and offscraping at Pacific margins, *in* Talwani, M., and Pitman, W.C., eds, *Island Arcs, Deep Sea Trenches, and Back-arc Basins: M. Ewing Series 1, A.G.U.*, p. 199-210.
- SDROLIAS, M., 2000, Tectonic history of the Southwest Pacific back-arc basins, [unpublished Honours Thesis in Geology and Geophysics]: University of Sydney, 108 p.
- SEELY, D.R., 1979, The evolution of structural highs bordering major forearc basins: *American Association of Petroleum Geology*, memoir 29, p. 245-261.
- SEELY, D.R., VAIL, P.R., AND WALTON, G.G., 1974, Trench slope model, *in* Burk, C.A., and Drake, C.L., eds, *The Geology of Continental Margins*, p. 249-260.
- SHANMUGAM, G., DAMUTH, J.E., AND MOIOLA, R.J., 1985, Is the turbidite facies association scheme valid for interpreting ancient submarine fan environments?: *Geology*, v. 13, p. 234-237.
- SHOR, G.G., KIRK, H.K., AND MENARD, G.L., 1971, Crustal structure of the Melaneasian arc: *Journal of Geophysical Research*, v. 76, p. 2562-2586.
- SING, L.J., 1971, Uplift and tilting of the Oterei Coast, Wairarapa, New Zealand, during the last ten thousand years: *Royal Society of New Zealand Bulletin*, v. 9, p. 217-219.
- SMITH, G.W., HOWELL, D.G., AND INGERSOLL, R.V., 1979, Late Cretaceous trench-slope basins of central California: *Geology*, v. 7, p. 303-306.
- SPÖRLI, K.B., 1978, Mesozoic tectonics, North Island, New Zealand: *Geological Society of America Bulletin*, v. 89, p. 415-425.
- SPÖRLI, K.B., 1980, New Zealand and oblique-slip margins: tectonic development up to and during the Cainozoic: *Special Publication International Association of Sedimentologists*, v. 4, p. 147-170.
- SPÖRLI, K.B., 1987, Development of the New Zealand micro-continent, *in* Monger, J.W.H., and Francheteau, J., eds, *Circum Pacific Orogenic Belts and Evolution of the Pacific Ocean Basin: A.G.U. Geodynamics Series*, v. 18, p. 115-132.
- SPÖRLI, K.B., AND KEAR, D., 1989, Geology of Northland: accretion, allochthons and arcs at the edge of the New Zealand micro-continent: *The Royal Society of New Zealand Bulletin*, v. 26, 235 p.
- STEVENS, S.H., AND MOORE, G.F., 1985, Deformational and sedimentary processes in trench slope basins of the western Sunda Arc, Indonesia: *Marine Geology*, v. 69, p. 93-112.
- SUGGATE, R.P., STEVENS, G.R., AND TE PUNGA, M.T., 1978, *The Geology of New Zealand*: Wellington, Government printer, v. 2, 820 p.
- SUTHERLAND, R., 1999a, Cenozoic bending of New Zealand basement terranes and Alpine Fault displacement: a brief review: *New Zealand Journal of Geology and Geophysics*, v. 42, p. 295-301.
- SUTHERLAND, R., 1999b, Basement geology and tectonic development of the greater New Zealand region: an interpretation from regional magnetic data: *Tectonophysics*, v. 308, p. 341-362.
- SUTHERLAND, F., DAVEY, F., AND BEAVAN, J., 2000, Plate boundary deformation in South Island, New Zealand, is related to inherited lithospheric structure: *Earth and Planetary Science Letters*, v. 177, n°3-4, p.141-151.
- TAYLOR, Z.B., ZELLMER, M.K., AND GOODLIFE, A., 1996, Seafloor spreading in the Lau backarc basin: *Earth and Planetary Science Letters*, v. 144, p. 35-40.
- TURNBULL, R.J., 1988, The geology of the lower Miocene Whakataki formation, eastern Wairarapa [unpublished Master of Science with Honour thesis]: Victoria University, Wellington, 101 p.

- UNDERWOOD, M.B., 1985, Sedimentology and hydrocarbon potential of Yager Structural Complex – possible Paleogene source rocks in Eel River Basin, Northern California: the American Association of Petroleum Geologists Bulletin, v. 69, No.7, p. 1088-1100.
- UNDERWOOD, M.B., AND KARIG, D.E., 1980, Role of submarine canyons in trench and trench-slope sedimentation: *Geology*, v. 8, p. 432-436.
- UNDERWOOD, M.B., AND BACHMAN, S.B., 1982, Sedimentary facies associations within subduction complexes, *in* Leggett, J.K., ed., *Trench-forearc Geology*, Geological Society of London Special Publication: London, Blackwell Scientific publications, v. 10, p. 537-550.
- UNDERWOOD, M.B., AND NORVILLE, C.R., 1986, Deposition of sand in a trench-slope basin by unconfined turbidity currents: *Marine Geology*, v. 71, p. 383-392.
- UNDERWOOD, M.B., AND MOORE, G.F., 1995, Trenches and trench-slope basins, *in* Busby, C.J., and Ingersoll, R.V., ed., *Tectonic of Sedimentary Basins*: Cambridge, Blackwell Science, p. 179-219.
- UNDERWOOD, M.B., MOORE, G.F., TAIRA, A., KLAUS, A., WILSON, M.E.J., FERGUSSON, C.L., HIRANO, S., STEURER, J., AND THE LEG 190 SHIPBOARD SCIENTIFIC PARTY, 2003, Sedimentary and tectonic evolution of a trench-slope basin in the Nankai subduction zone of southwest Japan: *Journal of Sedimentary Research*, v. 73, N° 4, p. 589-602.
- URUSKI, C., AND WOOD, R., 1991, A new look at the New Caledonia Basin, an extension of the Taranaki Basin, offshore North Island, N. Z: *Marine and Petroleum Geology*, v. 8, p. 379-391.
- VAIL, P.R., MITCHUM, R.M. JR., TODD, R.G., WIDMERI, J.W., THOMPSON, S., SANGREE, J.B., BUBB, J.N., AND HATELID, W.G., 1977, Seismic stratigraphy and global changes of sea level, *in* Payton, C.E., ed., *Seismic stratigraphy: Application to hydrocarbon exploration*: Tulsa, Society of Economic Paleontologists and Mineralogists Special Publication, p. 49-212.
- VAN DE BEUQUE, S., 1999, Evolution géologique du domaine péri-Calédonien (Sud-Ouest Pacifique) [unpublished PhD thesis]: Université de Bretagne Occidentale, 270 p.
- VAN De BEUQUE, S., AUZENDE, J.-M., LAFOY, Y. AND MISSEGUE, F., 1998, Tectonique et volcanisme tertiaire sur la ride de Lord Howe (Sud-Ouest Pacifique): *Comptes Rendus de l'Académie des Sciences (Paris)*, v. 326, série II, p. 663-669.
- VAN DER LINGEN, G.J., 1982, Development of the North Island subduction system, New Zealand, *in* Leggett, J.K., ed., *Trench-forearc Geology*, Geological Society of London Special Publication: London, Blackwell Scientific publications, v. 10, p. 259-274.
- VAN DER LINGEN, G.J., 1988, Textural characteristics of Flysch sediments in the upper-Miocene Makara basin, Hawkes Bay, New Zealand: *New Zealand Geological Survey Record*, v. 35, p. 14-20.
- VAN DER LINGEN, G.J., AND PETTINGA, J.G., 1980, The Makara basin: a Miocene slope-basin along the New Zealand sector of the Australian-Pacific obliquely convergent plate boundary: *International Association of Sedimentologists Special Publication*, v. 4, p. 191-215.
- VAN DER LINGEN, G.J., ANDREWS, J.E., BURNS, R.E., CHURKIN, M.Jr., DAVIES, T.A., DUMITRICA, P., EDWARDS, A.R., GALEHOUSE, J.S., KENNET, J.P., AND PACKHAM, G.H., 1973, Lithostratigraphy of eight drill sites in the Sout-West Pacific – Preliminary results of Leg 21 of the Deep Sea Drilling Project, *in* Fraser, R., comp., *Oceanography of the South Pacific*: Wellington, New Zealand National Commission for UNESCO, p. 299-318.
- VELLA, P., AND BRIGGS, W.M., 1971, Lithostratigraphic names, Upper Miocene to lower Pleistocene, northern Aorangi Range, Wairarapa: *New Zealand Journal of Geology and Geophysics*, v. 14, p. 253-274.
- VON HUENE, R., AND ARTHUR, M.S., 1982, Sedimentation across the Japan Trench off northern Honshu Island, *in* Leggett, J.K., ed., *Trench-forearc Geology*, Geological Society of London Special Publication: London, Blackwell Scientific publications, v. 10, p. 27-48.
- VON HUENE, R., AND SCHOLL, D.W., 1991, Observations at convergent margins concerning sediment subduction, subduction erosion, and the growth of continental crust: *Reviews of Geophysics*, v. 29, Issue 3, p. 279-316.
- VON HUENE, R., 1986, To accrete or not to accrete: that is the question: *Geol. Rdsch*, v. 75, N° 1, p. 1-15.
- WALCOTT, R.I., 1978, Present tectonics and late Cenozoic evolution of New Zealand: *Geophys. J. R. astr. Soc.*, v. 52, p. 137-164.
- WALCOTT, R.I., 1984, Reconstructions of the New Zealand region for the Neogene: *Palaeogeography, Palaeoclimatology, Palaeoecology*, v. 46, p. 217-231.

- WALCOTT, R.I., 1987, Geodetic strain and the deformational history of the North Island of New Zealand during the late Cainozoic: *Philosophical Transactions of the Royal Society of London*, v. A 321, p. 163-181.
- WALCOTT, R.I., 1998, Modes of oblique compression: late Cenozoic tectonics of the South Island of New Zealand: *Rev. Geophys*, v. 36, p. 1-26.
- WALKER, R.G., 1978, Deep-water sandstone facies and ancient submarine fans: models for exploration for stratigraphic traps: *American Association of Petroleum Geologists bulletin*, v. 62, No.6, p. 932-966.
- WATTS, A.B., WEISSEL, J.K., AND DAVEY, F.J., 1977, Tectonic evolution of the South Fiji marginal basin, *in* Talwani, M., and Pitman, W.C., eds, *Island arcs, deep sea trenches and back arc basins*, American Geophysical Union, v. 1, p. 419-427.
- WEISSEL, J.K., 1977, Evolution of the Lau Basin by the growth of small plates, *in* Talwani, M., and Pitman, W.C., eds, *Island Arcs, Deep Sea Trenches, and Back-arc Basins: M. Ewing Series 1*, A.G.U., p. 429-436.
- WEISSEL, J.K., AND WATTS, A.B., 1975, Tectonic complexities in the South Fiji Basin: *Tectonophysics*, v. 87, p. 185-241.
- WEISSEL, J.K. AND HAYES, D.E., 1977, Evolution of the Tasman Sea reappraised: *Earth and Planetary Science Letters*, v. 36, p. 77-84.
- WEISSEL, J.K., HAYES, D.E., AND HERON, E.M., 1977, Plate tectonic synthesis: the displacements between Australia, New Zealand and Antarctica since the late Cretaceous: *Marine Geology*, v. 25, p. 231-277.
- WELLMAN, H.W., 1971, Holocene tilting and uplift on the White Rocks Coast, Wairarapa, New Zealand: *The Royal Society of New Zealand Bulletin*, v. 9, p. 211-215.
- WELLS, P.E., 1989, Burial history of late Neogene sedimentary basins on part of the New Zealand convergent plate margin: *Basin Research*, v. 2, p. 145-160.
- WHITE, R.S., AND LOUDEN, K.E., 1982, The Makran continental margin: structure of a thickly sedimented convergent plate boundary, *in* Watkins, J.S., and Drake, C.L., ed., *Studies in Continental Margin Geology*, American Association of Petroleum Geologists, memoir 34, p. 499-518.
- WILLCOX, J.B., SYMONDS, P.A., HINZ, K., AND BENNETT, D., 1980, Lord Howe Rise, Tasman Sea – preliminary geophysical results and petroleum prospects: *BMR Journal of Australian Geology and Geophysics*, v. 5, p. 225-236.
- WILLCOX, J.B. AND STAGG, H.M.J., 1990, Australia's Southern margin: a product of oblique extension: *Tectonophysics*, v. 173, p. 269-281.
- WOOD, R., AND DAVY, B., 1994, The Hikurangi Plateau: *Marine Geology*, v. 118, p. 153-173.
- WOODWARD, D.J., AND HUNT, T.M., 1971, Crustal structure across the Tasman Sea: *New Zealand Journal of Geology and Geophysics*, v. 14, p. 39-45.
- YAN, C.Y., AND KROENKE, L.W., 1993, A plate tectonic reconstruction of the South-West Pacific, 0-100 Ma: *Proceedings of the Ocean Drilling Program, Scientific Results*, v. 30, p. 697-709.
- ZHU, H. AND SYMONDS, P.A., 1994, Seismic interpretation, gravity modelling and petroleum potential of the southern Lord Howe Rise region, *in* 1994 New Zealand Petroleum Conference Proceedings: the Post Maui Challenge-investment and development opportunities: Wellington, New Zealand, Ministry of Commerce, Energy and Resources Division, p 223-230.

Table des figures

TABLE DES FIGURES

INTRODUCTION GENERALE

Fig. I-1. Echelle chronostratigraphique utilisée en Nouvelle-Zélande, et équivalences internationales, du Néogène à l'actuel. Etages néo-zélandais d'après Cooper *et al.* (2004). . p. 9

CHAPITRE I

Les bassins de pente associés aux prismes de subduction

Fig. I-2. Carte bathymétrique et du relief mondial, localisation de la sismicité et du volcanisme aux limites de plaques (<http://www.solarviews.com>). Localisation des marges actives dont les bassins perchés ont fait l'objet d'études antérieures. Position géographique de la région du Sud-Ouest Pacifique, incluant la Nouvelle-Zélande. p. 12

Fig. I-3. Bloc diagramme synthétique du complexe de subduction de Sumatra (Indonésie). Localisation des bassins perchés (*trench-slope basins*) et des rides structurales sur le prisme d'accrétion. Cette succession de hauts bathymétriques rectilignes et de dépressions structurales étroites caractérise le grain structural de la pente vers la fosse (*lower trench slope*). Cette structuration s'effectue parallèlement à la limite de plaque. D'après Moore *et al.* (1980). p. 14

Fig. I-4. Schéma structural du prisme d'accrétion de Sumatra (Indonésie) au niveau de la transversale de Nias Island. Notons la bonne corrélation entre les rides structurales, les chevauchements inclinés vers le Nord-Est (vers l'arc) et les bassins perchés. Toutes ces structures sont sub-parallèles à la fosse de Sunda. Stevens et Moore (1985). p. 14

Fig. I-5. Coupe schématique du prisme d'accrétion de Sumatra (Indonésie) montrant la répartition, la géométrie et la structure des bassins perchés. Cette coupe interprétative est issue de données de sismique marine. D'après Moore et Karig (1976), Karig *et al.* (1978). p. 14

Fig. I-6. Vue 3D de la pente du prisme d'accrétion des Cascades (Amérique du Nord). Les rides structurales constituent les bordures de bassins perchés étroits et allongés parallèlement à la fosse. L'espacement de la grille est de 135 m et l'exageration verticale d'environ 5 x. McAdoo (1997). p. 15

Fig. I-7. Coupe schématique du complexe de subduction de Sumatra (Indonésie) dans la région de Nias Island. Cette île correspond à l'émersion de la plus haute ride du prisme d'accrétion (*trench slope break*) et présente à l'affleurement les séries sédimentaires de bassins perchés néogènes. Ces bassins se développent sur la pente du prisme d'accrétion, depuis la fosse jusqu'au *trench slope break*. Karig *et al.* (1979). p. 15

Fig. I-8. Profil de sismique réflexion et interprétation d'un bassin perché récent situé à proximité du front de subduction de Sumatra (Indonésie). Stevens et Moore (1995). Noter l'asymétrie du bassin et le chevauchement qui contrôle la surrection d'une bordure. p. 16

Fig. I-9. Profil de sismique réflexion et interprétation d'un bassin perché récent situé à proximité du front de subduction de la Barbade (Caraïbes). Huyghe *et al.* (1996). Noter le développement de rides anticlinales constituant les bordures du bassin, la migration rétrograde des dépôts-centres et les onlaps sur la bordure externe. p. 16

Fig. I-10. Modèle synthétique d'évolution stratigraphique et structurale de bassins perchés sur un prisme d'accrétion. La surrection progressive des bassins et leur éloignement du front de subduction au cours du temps (i.e. rapprochement des zones d'alimentation) conduisent à la formation de séquences strato- et grano-croissantes caractéristiques de leur remplissage. Pickering *et al.* (1989). Noter que, contrairement à ce modèle, le développement de ce type de séquences au sein des bassins perchés peut s'effectuer en relation avec la surrection de hauts structuraux contrôlés par des chevauchements, sans intervention des phénomènes d'extension ici invoqués. p. 18

Fig. I-11. Profil de sismique réflexion et interprétation d'un bassin perché récent situé à proximité du front de subduction de Sumatra (Indonésie), Stevens et Moore (1995). Noter l'asymétrie du bassin, les onlaps sur sa bordure externe, les discontinuités à l'Est, et la présence d'importantes instabilités gravitaires affectant la bordure Est du bassin. p. 18

Fig. I-12. Modèle synthétique montrant une localisation prédictive des faciès marins profonds, dont les turbidites, et leurs relations sur la pente du prisme d'accrétion. Le code de lithofaciès (lettres) réfère au modèle de faciès marins profonds de Mutti et Ricci Lucchi (1978). D'après Underwood et Bachman (1982). p. 20

Fig. I-13. Modèle de faciès de Mutti et Ricci Lucchi (1978) - Caractéristiques et interprétations des lithofaciès correspondant aux turbidites et aux dépôts marins profonds qui leur sont associés. Underwood et Moore (1995). p. 20

Fig. I-14. Carte bathymétrique simplifiée et structure du prisme d'accrétion des Cascades (Amérique du Nord). La pente du prisme est entaillée de nombreux canyons sous-marins (marqués par des flèches) qui alimentent la fosse et les bassins perchés (marqués en traits gras sub-parallèles à la fosse). Underwood et Moore (1995), d'après l'équipe scientifique EEZ SCAN 84 (1986). p. 22

Fig. I-15. Modèle sédimentaire et morphostructural d'une zone de subduction. Pickering *et al.* (1989). p. 22

Fig. I-16. Modèle conceptuel d'évolution stratigraphique d'un bassin perché. La séquence strato- et grano-croissante reflète ici la surrection progressive du bassin qui est associée à une augmentation des apports terrigènes. Log sédimentologique d'après Underwood and Moore (1995), et Underwood *et al.* (2003). Synthèse basée sur les observations de Moore *et al.* (1980), Nias Island (Indonesia). p. 23

Fig. I-17. Alternative au modèle précédent (Fig.I-Q) - Lithostratigraphie des sites ODP 1175 et 1176 montrant l'existence de séquences strato- et grano-décroissantes au sein des bassins perchés du prisme d'accrétion de Nankai (Japon). Ces séquences peuvent résulter soit d'un blocage des systèmes d'alimentation (déformation du prisme), soit d'une déconnection des systèmes par rapport aux sources (i.e. augmentation du niveau eustatique). Underwood *et al.* (2003). p. 23

CHAPITRE II

Cadre géodynamique et bassins de la marge Hikurangi

Fig. II-1. Carte bathymétrique du Sud-Ouest Pacifique et localisation des structures majeures (la bathymétrie est issue du site internet du groupe de géodésie de l'université de Curtin, Australie; <http://www.cage.curtin.edu.au/~geogrp/links.html>). BL - bassin des Loyauté, RL - ride des Loyauté, RE - ride d'entrecasteaux, RTR - ride des Trois-Rois, RON - Ride Ouest-Norfolk. p. 26

Fig. II-2. A - La Nouvelle-Zélande dans son cadre géodynamique. 1 - zones émergées ; 2 - croûte continentale immergée; 3 - arcs volcaniques inactifs probables; 4 - arcs volcaniques actifs. An - anomalies magnétiques. L'âge des différents bassins océaniques est indiqué entre parenthèses; 3 K.R. - ride des Trois-Rois; N.C. - bassin de Nouvelle-Calédonie; S.F.B. - bassin Sud-Fidjien; V.M.F.Z. - zone de fracture de Vening-Meinesz; C.F.Z. - zone de fracture de Cook. Ferrière et Chanier (1993). **B** - Localisation du pôle de rotation Pacifique/Australie au Sud-Est du plateau de Campbell. NZsi – Ile Sud de Nouvelle-Zélande. King, 2000. p. 28

Fig. II-3. Bloc diagramme montrant le plongement de la plaque Pacifique sous l'Ile Nord de Nouvelle-Zélande (dont la projection en surface des lignes d'isoprotecteurs 20 km et 60 km) et la localisation en coupe de la sismicité superficielle sur la transversale de Wellington. Ansell et Bannister (1996). p. 34

Fig. II-4. Le plateau Hikurangi dans son cadre géodynamique. Porté par la plaque Pacifique, il correspond à une croûte océanique épaissie (10 à 15 km d'épaisseur) qui passe en subduction sous l'Ile Nord de Nouvelle-Zélande au niveau de la fosse Hikurangi. Wood et Davy (1994). p. 34

Fig. II-5. Carte (A) et coupe (B) des grands éléments morphostructuraux constituant le complexe de subduction Hikurangi, Ile Nord de Nouvelle-Zélande. N.I. - North Island, S.I. - South Island, WA - Wairarapa Area, TSB - Trench Slope Break. Modifié d'après Chanier *et al.* (1999). p. 36

Fig. II-6. A - Localisation du chenal Hikurangi et du canyon de Kaikoura. La fosse Hikurangi est essentiellement alimentée par un flux sédimentaire issu de l'érosion de la Chaîne Alpine dans L'Ile Sud de Nouvelle-Zélande. Les sédiments transitent par le canyon de Kaikoura. Lewis et Barnes (1999). **B** - morphologie du système d'alimentation canyon de Kaikoura/chenal Hikurangi. Lewis et Pantin (2002). p. 36

Fig. II-7. Bloc diagramme d'une marge active en convergence oblique. Appliqué à la subduction Hikurangi (Nouvelle-Zélande): trench - fosse Hikurangi, accretionary slope (lower trench slope) - pente du prisme d'accrétion Hikurangi, highest accretionary ridge (trench slope break) - Chaîne Côtière, highest accretionary basin - bassin avant-arc, frontal ridge - Chaîne Axiale (Taranua Range), Volcanic basin - zone volcanique de Taupo. Lewis (1980), adapté de Walcott (1978), Karig et Sharman (1975). p. 38

Fig. II-8. Synthèse de l'histoire géodynamique de la Nouvelle-Zélande depuis 700 Ma. Ferrière et Chanier (1993). p. 38

Fig. II-9. Orogenèse Kaikoura (25-0 Ma). a- volcans actifs, b- volcans néogènes éteints, c- fossés récents, d- bassins cénozoïques, e- arc volcanique actif des Kermadec, f- arc volcanique inactif (ride de Colville), g et h- sédiments et ophiolites de l'allochtone du Northland (obduction du Miocène basal), F.A.B.- bassin avant-arc, Pr.A- prisme d'accrétion Hikurangi, Taupo V.Z.- Taupo Volcanic Zone. Ferrière et Chanier (1993). p. 38

Fig. II-10. Episodes de déformation enregistrés dans la Chaîne Côtière (marge Hikurangi - côte Est de l'Île Nord de Nouvelle-Zélande) depuis le démarrage de la subduction il y a 25 Ma. Chanier (1991). p. 40

Fig. II-11. Schéma structural et coupes au sein du domaine Sud-Wairarapa (marge Hikurangi - côte Est de l'Île Nord de Nouvelle-Zélande). Mise en évidence d'une tectonique de nappe au Miocène inférieur (*cf.* carte et coupe A). Les nappes ont ensuite été plissées au cours d'épisodes de déformation plus récents. Chanier (1991); dans Field, Uruski *et al.* (1997). p. 42

Fig. II-12. Coupes au sein du domaine Nord-Wairarapa (marge Hikurangi - côte Est de l'Île Nord de Nouvelle-Zélande). Hypothèse d'une tectonique dominée par du décrochement dextre au Miocène inférieur. Delteil *et al.* (1996); dans Field, Uruski *et al.* (1997). p. 42

Fig. II-13. Coupes schématiques montrant l'évolution du prisme d'accrétion Hikurangi du Miocène basal à l'actuel. Echelles approximatives: *cf.* croûte océanique (6 à 8 km). Chanier (1991). p. 43

Fig. II-14. a - Failles normales conjuguées, antérieures à la compression la plus récente (*c.* 5-0 Ma), affectant des calcaires paléocènes dans la région du Wairarapa (marge Hikurangi - côte Est de l'Île Nord de Nouvelle-Zélande). Ces failles décalent de plus des plans inverses d'angle faible (compression du Miocène basal). **b** - analyse stéréographique associée. Chanier *et al.* (1999). p. 44

Fig. II-15. Résumé des déformations en extension miocènes le long de la marge Est de l'Île Nord de Nouvelle-Zélande. **a** - Axes d'extension majeurs déduits des calculs de paléocontraintes. **b** - Orientation des axes d'extension il y a 10 Ma en considérant une rotation générale de 45° de l'ensemble de la marge. Chanier *et al.* (1999). p. 44

Fig. II-16. Raccourcissement enregistré au Sud de la chaîne Côtière (marge Hikurangi - côte Est de l'Île Nord de Nouvelle-Zélande) au cours de la phase compressive récente. Nicol *et al.* (2002). p. 44

Fig. II-17. A - Lithostratigraphie détaillée de la région du Wairarapa (marge Hikurangi - côte Est de l'Île Nord de Nouvelle-Zélande). Field, Uruski *et al.* (1997); et **B** - Principales unités stratigraphiques de la Chaîne Côtière. Lee et Begg (2002). p. 46

Fig. II-18. A - Cadre géodynamique de la Nouvelle-Zélande, les flèches noires indiquent les taux de convergence actuels entre les plaques Pacifique et Australienne (WA - Wairarapa Area). **B** - Carte bathymétrique (Lewis *et al.*, 1999) et schéma structural (d'après Lee et Begg, 2002) du secteur du Wairarapa. En mer, localisation des bassins perchés récents et des rides structurales majeures de la marge Hikurangi. A terre, localisation des synclinaux où affleurent les épaisses séries turbiditiques constituant le remplissage de bassins perchés néogènes. PA - Pongaroa Area, I - Tinui Fault Complex, II - Whakataki fault, III - Waioki fault. p. 48

- Fig. II-19.** Coupes sériées au travers du prisme d'accrétion Hikurangi (Nouvelle-Zélande). Géométrie, structure et localisation de bassins perchés quaternaires. Lewis (1980).
..... p. 50
- Fig. II-20.** Coupe au travers de la fosse (ligne sismique 201) et du prisme d'accrétion (ligne sismique 203) Hikurangi (Nouvelle-Zélande). Géométrie, structure et localisation des bassins perchés. TSB - bassins perchés (Trench Slope Basins), SR - rides structurales associées à des chevauchements inclinés vers l'arc (Structural Ridges), D - niveau de décollement. Davey *et al.* (1986). p. 50
- Fig. II-21.** Localisation dans la Chaîne Côtière (Côte Est de l'Ile Nord de Nouvelle-Zélande) des affleurements de séries sédimentaires miocènes correspondant aux remplissages des bassins perchés de Makara, de Tawhero, de Whakataki et de Waipatiki. Fond cartographique d'après Field, Uruski *et al.* (1997). p. 52
- Fig. II-22.** Coupe montrant la déformation du bassin perché miocène de Makara (Chaîne côtière, secteur Sud d'Hawke Bay - localisation Fig.II-21). Lewis et Pettinga (1993), d'après Van der Lingen et Pettinga (1980). p. 52
- Fig. II-23.** Principales étapes du développement du bassin de Makara, de l'Oligocène au Miocène supérieur (Chaîne côtière, secteur Sud d'Hawke Bay - localisation Fig.II-21). Lewis et Pettinga (1993), d'après Van der Lingen et Pettinga (1980). p. 54
- Fig. II-24.** Cartes paléogéographiques du secteur Sud d'Hawke bay (Chaîne côtière - localisation Fig.II-21). Développement du bassin de Makara au cours du Miocène Moyen et du Miocène Supérieur. WMCH - Waimarama-Mangakuri Coastal High, OAC - Otane Anticlinal Complex, E - Elsthorpe. Van der Lingen et Pettinga (1980). p. 56
- Fig. II-25.** Reconstitution paléoenvironnementale du bassin de Whakataki (Chaîne côtière - localisation Fig.II-21). Ce bassin présente une sédimentation contrôlée par un système turbiditique de type deep sea fan. A l'exception du débouché des canyons, les directions de courant dominantes sont parallèles à l'axe du bassin. Turnbull (1988). p. 56
- Fig. II-26.** Cartes paléogéographiques du secteur de Pongaroa (Chaîne côtière - localisation Fig.II-21). Développement du bassin de Tawhero du Miocène basal au Miocène supérieur. D'après Neef (1992a). Dans notre étude nous différencierons d'une part, les séries du Miocène inférieur et du Miocène moyen qui appartiennent à un bassin confiné, le bassin que nous nommerons d'Akitio, et d'autre part, les séries du Miocène supérieur qui appartiennent à un bassin plus large et plus récent, le bassin de Tawhero proprement dit. p. 57
- Fig. II-27.** Représentation schématique des environnements de dépôt du secteur du synclinal de Waipatiki (Chaîne Côtière - localisation Fig.II-21) au Miocène inférieur. Le bassin de Waipatiki y est interprété comme un bassin perché (slope basin) daté du Miocène basal. Reid (1998). p. 58
- Fig. II-28.** Lithostratigraphie et paléobathymétries du bassin de Waipatiki, Miocène inférieur (Chaîne Côtière - localisation Fig.II-21). Divisions bathymétriques d'après Hayward (1986). Reid (1998). p. 58
- Fig. II-29.** Reconstitution des environnements de dépôt de la Whatarangi Formation suggérant l'existence de bassins perchés au Crétacé inférieur sur le prisme d'accrétion du Torlesse (Sud-Est de l'Ile Nord de Nouvelle-Zélande - localisation Fig.II-21). George (1992).
..... p. 58

CHAPITRE III

Les systèmes turbiditiques du domaine avant-arc interne de la marge convergente Hikurangi (Nouvelle-Zélande): de nouvelles contraintes sur le développement des bassins perchés sur le prisme de subduction

Fig. III-1. Plate tectonic setting of New Zealand (A) and major subduction related morphostructural features of the Hikurangi active margin (B). Black arrows show present-day relative plate motion between Pacific and Australian plates. See fig.2 for the a - b cross-section. N.I. – North Island, S.I. - South Island, N.W. - Northeastern Wairarapa. Modified after Chanier *et al.* (1999). p. 66

Fig. III-2. A - General cross-section of the Hikurangi subduction complex (TSB - Trench Slope Break). B - Seismic line Lee 203 (detail), location and geometry of offshore Quaternary trench-slope basins near the subduction front. Modified after Lewis and Pettinga (1993). C - Panorama of the Te Wharau syncline which presents Miocene trench-slope basin sediments cropping out onshore in the Coastal Ranges (southeastern Wairarapa). p. 66

Fig. III-3. Synthetic model showing a predictive location for deep sea facies, included turbidites, and their relationships within trench-slope settings. The lithofacies code (letters) refers to the deep sea sedimentary facies model defined by Mutti and Ricci Lucchi (1978). After Underwood and Bachman (1982). p. 68

Fig. III-4. Main stratigraphic units of the Wairarapa area correlated to major deformation episodes recorded since the onset of subduction (basal Miocene, 25 Myr). Deformation episodes along the Hikurangi active margin after Chanier (1991). See the chronostratigraphic chart for equivalence between New Zealand stages (Cooper *et al.*, 2004), used in this paper, and standard international stages. p. 70

Fig. III-5. Structural map of the Pongaroa area, central eastern Wairarapa. Location of the sedimentological vertical sections within the Akitio syncline: I - Pongaroa section, II - Branscomb section. P - Pongaroa, CH - Cross Hills, B - Branscombe. After Lee and Begg (2002). p. 72

Table III-1. Characteristics and interpretation of the sedimentary facies for the turbidites and the related deep-sea deposits identified in this study. p. 78

Table III-2. Characteristics and interpretation of the sedimentary facies for the shelf deposits identified in this study. p. 79

Plate III-1. Turbidites and related deep-sea sediments encountered within trench-slope basin environments (Fa1b to Fa2a). See table III-1 and III-2 for description and interpretation of the facies. p. 80

Plate III-2. Turbidites and related deep-sea sediments encountered within trench-slope basin environments (Fa3s to Fa3m), and outer shelf to middle shelf deposits (Fa5 to Fa6c). See table III-1 and III-2 for description and interpretation of the facies. p. 81

Fig. III-6. Time lines correlations of the Pongaroa and Branscombe sedimentological sections. B1-5, P1-5, U1-5 and U'1-5: see text. Refer to Figure III-5 for location, Table III-1 and III-2 for facies code and Appendix 2 for datations. p. 82

Fig. III-7. Major discontinuities and correlations of the Pongaroa and Branscombe sedimentological sections (see text for abbreviations and explanations). Refer to Fig.III-5 for location, Table III-1 and III-2 for facies code and Appendix 2 for paleobathymetries / datations. p. 86

Fig. III-8. Early and middle Miocene paleoenvironments and paleocurrents of the Akitio basin. Note the inversion of facies proximal - distal signature between steps 1 and 2, and between steps 2 and 3. The paleocurrents are in opposition with the paleoenvironments locations at step 3. See Table III-1 and III-2 for facies code. A.S. - Akitio Syncline, P.B. - Pongaroa Block, C.B. - Coastal Block, P - Pongaroa, B - Branscombe. p. 88

Fig. III-9. Depositional model for trench-slope settings. See Tables III-1 and III-2 for facies code. I - olistostrome deposition related to active thrusting during the onset of subduction at 25 Ma. II - sub-marine fan model in a juvenile trench - slope basin (basal Miocene), from coastal exposures east of the Akitio basin (Castlepoint area), after Turnbull (1988), UF - Upper Fan, MLF - Mid to Lower Fan, BP - Basin Plain. IIIa - mature trench-slope basin in the studied area (this paper), note the emersion of the trenchward margin of the basin (*i.e.* Cape Turnagain structural ridge, probably partially controlled by the Tinui fault and/or the Whakataki fault) which permits the development of a westward prograding turbidite system, IIIb - early-middle Miocene sedimentary infill of the trench-slope basin. p. 92

Fig. III-10. Stages of development of the Akitio trench-slope basin. Stage numbers also correspond to the five stratigraphic units identified in this study (comments in text). P - Pongaroa vertical section, B - Branscombe vertical section. p. 98

CHAPITRE IV

Structure et stratigraphie sismique d'un bassin perché immergé, comparaison avec un analogue de terrain (marge active Hikurangi, Nouvelle-Zélande)

Fig. IV-1. **A** - Tectonic setting of the Hikurangi subduction zone, North Island of New Zealand (N.I. - North Island, S.I. - South Island, WA - Wairarapa Area). Black arrow shows present-day relative plate motion between Pacific and Australian plates. Modified after Chanier *et al.* (1999). **B** - General cross-section a - b of the Hikurangi subduction complex showing major subduction related morphostructural features of the Hikurangi active margin (TSB - Trench Slope Break). p. 106

Fig. IV-2. Conceptual model showing morphology, structure and sedimentology of trench-slope basins. **A** - Bloc 3D after Underwood (1985), reflector within the basin after Stevens & Moore (1985), turbidites and depositional system after Underwood & Bachman (1982) (Letters refers to the deep sea lithofacies nomenclature defined by Mutti & Ricci Lucchi (1978), (IF - Inner Fan, MF - Middle Fan, OF - Outer Fan, BP - Basin Plain). **B** - Stratigraphic model for the evolution of a trench-slope basin. The upward coarsening and thickening trend reflects the progressive uplift of the basin which is associated to an increase in siliciclastic input. Sedimentological vertical section after Underwood *et al.* (2003), and Underwood & Moore (1995). Synthesis based on observations of Moore *et al.* (1980) on Nias Island, Indonesia. p. 108

Fig. IV-3. **A** - Plate tectonic setting of New Zealand, black arrows show present-day relative plate motion between Pacific and Australian plates (WA - Wairarapa Area). **B** - Structural map of the onshore Wairarapa area (after Lee & Begg, 2002) and location of the offshore Wairarapa area including the Amoco IAE1 seismic survey and well Titihaoa-1 (PA - Pongaroa Area, I - Tinui Fault Complex, II - Whakataki fault). p. 114

Fig. IV-4. Correlation between IAE1-28 seismic profile and Titihaoa-1 sonic logs (twtt (s) and m). See text for explanations. p. 116

Fig. IV-5. IAE1-28 seismic line (A) and line drawing (B). SI - Highly disorganised seismic unit (deformed acoustic basement), SII - Irregular and discontinuous seismic unit (trench-slope basin infill), SIII - Well organised and continuous seismic unit. "a", "b", "c" and "d" - trench-slope basins. B1 to B9 - seismic units/sub-units boundaries. See figure IV-6 for enlargements. p. 121

Fig. IV-6. Parts of the IAE1-28 seismic line and interpretations. Location of the enlargements is shown figure IV-5. Their numerotation also refers to figure IV-5. SI - Highly disorganised seismic unit (deformed acoustic basement), SII - Irregular and discontinuous seismic unit (trench-slope basin infill), SIII - Well organised and continuous seismic unit. "a", "b", "c" and "d" - trench-slope basins. B1 to B9 - seismic units/sub-units boundaries. p. 124

Fig. IV-7. Data compilation from well Titihaoa-1: lithologic log, paleobathymetry and wireline logs (GR, sonic). Lithologic log after Biroš *et al.* (1995), Biostratigraphy and paleobathymetry estimations (from foraminiferal assemblages) after Morgans *et al.* (1995). p. 126

Fig. IV-8. Correlation between IAE1-28 seismic profile and Titihaoa-1 well data. p. 130

Fig. IV-9. A - Depositional model for trench-slope settings. I - olistostrome deposition related to active thrusting during the onset of subduction at 25 Ma. II - sub-marine fan model in a juvenile trench - slope basin (basal Miocene), from coastal exposures east of the Akitio basin (Castlepoint area), after Turnbull (1988), UF - Upper Fan, MLF - Mid to Lower Fan, BP - Basin Plain. IIIa - the Akitio mature trench-slope basin (Bailleul *et al.*, submitted; see chapter III of this manuscript), note the emersion of the trenchward margin of the basin (*i.e.* Cape Turnagain structural ridge, probably controlled by the main thrust faults: the Tinui Fault, the Whakataki Fault and the Turnagain Fault) which permits the development of a westward prograding turbidite system, IIIb - early-middle Miocene sedimentary infill of the trench-slope basin. **B** - Major discontinuities and stratigraphic architecture of the Branscombe sedimentological section (see text for abbreviations and explanations). Refer to figure IV-1 for location, and table III-1 for facies code. p. 138

Fig. IV-10. Comparison between the Akitio onshore trench-slope basin and the younger Titihaoa offshore trench-slope basin. See figure IV-9B for legend of the Branscombe section and table III-1 for facies code. p. 140

Fig. IV-11. Location and ages of trench-slope basins on the lower trench slope of the Hikurangi active margin. **A** - general cross section of the Hikurangi margin (TSB - trench-slope break), **B** - Middle and late Miocene cross-sections of the onshore Akitio basin (B - Branscombe vertical section, U2 to U5 - sedimentary units identified in the Branscombe vertical section, see figure IV-9B), **C** - Late Miocene and Plio-Quaternary line drawings (from IAE1-28 seismic profile) of the offshore Titihaoa basin (B1 to B9 - seismic units and sub-units boundaries, SR1 to SR4 - structural ridges). p. 142

CHAPITRE V

Déformation discontinue d'un prisme de subduction: Evolution de la marge Hikurangi (Nouvelle-Zélande) au cours des derniers 25 Ma

Fig. V-1. **A** - Tectonic setting of the Hikurangi subduction zone (modified from Chanier *et al.*, 1999), North Island of New Zealand (N.I. - North Island, S.I. - South Island, WA - Wairarapa Area). Black arrow shows present-day relative plate motion between Pacific and Australian plates. **B** - General cross-section a - b of the Hikurangi subduction complex showing major subduction related morphostructural features of the Hikurangi active margin (TSB - Trench Slope Break). p. 154

Fig. V-2. **A** - Plate tectonic setting of New Zealand, black arrows show present-day relative plate motion between Pacific and Australian plates (WA - Wairarapa Area). **B** - bathymetric map (Lewis *et al.*, 1999) and onshore structural map (modified from Lee and Begg, 2002) of the Wairarapa area. The offshore Wairarapa area includes location of the Amoco IAE1 seismic survey and well Titihaoa-1 (I - Tinui Fault Complex, II - Whakataki Fault, III - Waihoki Fault, IV - Mangatiti Fault, V - Breakdown Fault). p. 158

Fig. V-3. **A** - Line drawing of seismic lines Lee 201 and 203, and **B** - Enlargement of seismic line Lee 203 : location and geometry of offshore Quaternary trench-slope basins near the Hikurangi subduction front. SR - Structural Ridges, M - Multiple. **C** - Location of seismic line Lee 203. C.T - Cape Turnagain, A - Akitio, Cstp - Castlepoint, FP - Flat Point. Modified from Davey *et al.* (1986) and Lewis and Pettinga (1993). p. 160

Fig. V-4. Interpretation of IAE1-28 seismic line. SI - Highly disorganised seismic unit (deformed acoustic basement), SII - Irregular and discontinuous seismic unit (trench-slope basin infill), SIII - Well organised and continuous seismic unit (infill of the Turnagain large slope basin). U1 and U2 - main seismic units boundaries. See figure V-2 for location. p. 164

Fig. V-5. Interpretation of IAE1-39 seismic line. SI - Highly disorganised seismic unit (deformed acoustic basement), SII - Irregular and discontinuous seismic unit (trench-slope basin infill), SIII - Well organised and continuous seismic unit (infill of the Turnagain large slope basin), SIV - Quaternary slope basin. U1 to U3 - main seismic units boundaries. See figure V-2 for location. p. 168

Fig. V-6. Interpretation of IAE1-41 seismic line. SI - Highly disorganised seismic unit (deformed acoustic basement), SII - Irregular and discontinuous seismic unit (trench-slope basin infill), SIII - Well organised and continuous seismic unit (infill of the Turnagain large slope basin). U1 and U2 - main seismic units boundaries. See figure V-2 for location. p. 170

Fig. V-7. Structural map of the Pongaroa area, northeastern Wairarapa. Location of sedimentological vertical sections and of cross sections: pu - Puketoi vertical section, m - Mangatiti vertical section, a - Annedale vertical section, r - Razorback vertical section, t - Takiritini vertical section, po - Pongaroa vertical section, b - Branscombe vertical section, f - Fingerpost vertical section, ct - Cape Turnagain vertical section, Cp - Castlepoint vertical section; A-B Tawhero cross section, C-D Pongaroa cross section, E-F Turnagain cross-section. I - Tinui Fault complex, II - Whakataki Fault, III - Waihoki Fault, IV - Mangatiti Fault, V - Breakdown Fault. Modified from Lee and Begg (2002). p. 172

Fig. V-8. Akitio syncline cross-section. See figure V-7 for location and refer to tables III-1 and III-2 for facies code (Fa). D1 to D8 - stratigraphic units boundaries, also noted on figure V-10. p. 174

Fig. V-9. Simplified structural map of the Wairarapa region and stress tensor analysis (Schmidt, lower hemisphere) showing the main directions of compressional deformation. See text for explanations. p. 177

Fig. V-10. Correlations of sedimentological vertical sections of the Pongaroa area (northeastern Wairarapa) and of the offshore well Titihaoa-1. Location of sedimentological vertical sections is shown figure V-7 and location of well Titihaoa -1 on figure V-2. See tables III-1 and III-2 for facies code. As the datum is within late Pliocene, the reconstructed geometries represent a late Pliocene stage of the stratigraphic and structural development of the Akitio transect. p. 181

Fig. V-11. Cape Turnagain cross-section. See figure V-7 for location and refer to tables III-1 and III-2 for facies code (Fa). D1, D2, D4, D5 and D8 - stratigraphic units boundaries, also noted on figure V-10. p. 184

Fig. V-12. Tawhero syncline cross-section. See figure V-7 for location and refer to tables III-1 and III-2 for facies code (Fa). D1 to D8 - stratigraphic units boundaries, also noted on figure V-10. p. 186

Fig. V-13. Paleogeographic map of the Akitio basin at the end of early Miocene (*c.* 16 Ma). See tables III-1 and III-2 for facies code. p. 187

Fig. V-14. Tectonic evolution of the Hikurangi margin since the onset of subduction, 25 Myr ago. p. 190 et 194

CHAPITRE VI

Synthèse et Conclusions

Fig. VI-1. A - Plate tectonic setting of New Zealand, black arrows show present-day relative plate motion between Pacific and Australian plates (WA - Wairarapa Area). **B** - bathymetric map (Lewis *et al.*, 1999) and onshore structural map (modified from Lee and Begg, 2002) of the Wairarapa area. The offshore Wairarapa area includes location of the Amoco IAE1 seismic survey and well Titihaoa-1. I - Tinui Fault Complex, II - Whakataki Fault, III - Waihoki Fault, IV - Mangatiti Fault, V - Breakdown Fault, A-B location of cross-section shown figure VI-7. p. 200

Fig. VI-2. Correlations of sedimentological vertical sections of the Pongaroa area (northeastern Wairarapa) and of the offshore well Titihaoa-1. Location of sedimentological vertical sections is shown figure V-7 and location of well Titihaoa -1 on figure VI-1. See tables VI-1 and VI-2 for facies code. As the datum is within late Pliocene, the reconstructed geometries represent a late Pliocene stage of the stratigraphic and structural development of the Akitio transect. p. 203

Fig. VI-3. Depositional model for trench-slope settings. See Tables VI-1 and VI-2 for facies code. **I** - olistostrome deposition related to active thrusting during the onset of subduction at 25 Ma. **II** - sub-marine fan model in a juvenile trench - slope basin (basal Miocene), from coastal exposures east of the Akitio basin (Castlepoint area), after Turnbull (1988), UF - Upper Fan, MLF - Mid to Lower Fan, BP - Basin Plain. **IIIa** - the mature Akitio trench-slope basin, note the emersion of the trenchward margin of the basin (*i.e.* Cape Turnagain structural ridge, probably partially controlled by the Tinui fault and/or the Whakataki fault) which permits the development of a westward prograding turbidite system, **IIIb** - early-middle Miocene sedimentary infill of the trench-slope basin. p. 208

Fig. VI-4. Major discontinuities and stratigraphic architecture of the Akitio basin as illustrate in the Branscombe sedimentological section (see text for abbreviations and explanations). Refer to figures VI-1 and V-7 for location, and table VI-1 for facies code. p. 210

Fig. VI-5. Interpretation of IAE1-28 seismic line. SI - Highly disorganised seismic unit (deformed acoustic basement), SII - Irregular and discontinuous seismic unit (trench-slope basin infill), SIII - Well organised and continuous seismic unit (infill of the Turnagain large slope basin). U1 and U2 - main seismic units boundaries. See figure VI-1 for location. . p. 212

Fig. VI-6. Comparison between the Akitio onshore trench-slope basin and the younger Titihaoa offshore trench-slope basin. See figure VI-4 for legend of the Branscombe section and table VI-1 for facies code. p. 214

Fig. VI-7. Coupe synthétique de la chaîne côtière au niveau de la transversale d'Akitio (région du Wairarapa). Localisation Figure VI-1. p. 216

Fig. VI-8. Tectonic evolution of the Hikurangi margin since the onset of subduction, 25 Myr ago. p. 218 et 220

Fig. VI-9. Cadre structural du secteur de Pongaroa, NE Wairarapa, et localisation des coupes analysées en termes de mouvements verticaux par le biais de courbes de subsidence : 1 - Coupe du synclinal de Tawhero (Fig. VI-10), 2 - Coupe de Cape Turnagain (Fig. VI-11), 3 - Coupe de Pongaroa, synclinal d'Akitio (Fig. VI-12), 4 - Forage Titihaoa-1 (Fig. VI-13). p. 222

Fig. VI-10. Courbe de subsidence établie à partir des séries d'âge Miocène moyen à Pliocène, levées sur le flanc Est du Synclinal de Tawhero (localisation Fig. VI-9). Les marges d'incertitudes sur la détermination des paléo-tranches d'eau sont reportées sur l'ensemble des 3 courbes figurées ci-dessus. p. 224

Fig. VI-11. Courbe de subsidence établie à partir des séries d'âge Miocène moyen à Pliocène, levées au Nord de Cape Turnagain (localisation Fig. VI-9). Pour des raisons de clarté, les marges d'incertitudes sur la détermination des paléo-bathymétries sont figurées uniquement sur la courbe d'évolution des tranches d'eau. p. 226

Fig. VI-12. Courbe de subsidence établie à partir des séries d'âge Miocène inférieur et Moyen du synclinal d'Akitio (coupe de Pongaroa, localisation Fig. VI-9). La série sédimentaire du synclinal de Tawhero (fin Miocène moyen à Pliocène), présentée figure VI-10, a été superposée au bassin d'Akitio pour les calculs de décompaction. p. 228

Fig. VI-13. Courbes de subsidence établies à partir des séries traversées par le forage Titihaoa-1 (localisation Fig. VI-9). Ces courbes ont été réalisées en considérant des valeurs maximales (A) ou minimales (B) des estimations des paléo-tranches d'eau. p. 229

Table VI-1. Characteristics and interpretation of the sedimentary facies for the turbidites and the related deep-sea deposits identified in this study. p. 206

Table VI-2. Characteristics and interpretation of the sedimentary facies for the shelf deposits identified in this study. p. 207

ANNEXES

Appendix 1. Vertical sedimentological sections used in this study p. 265

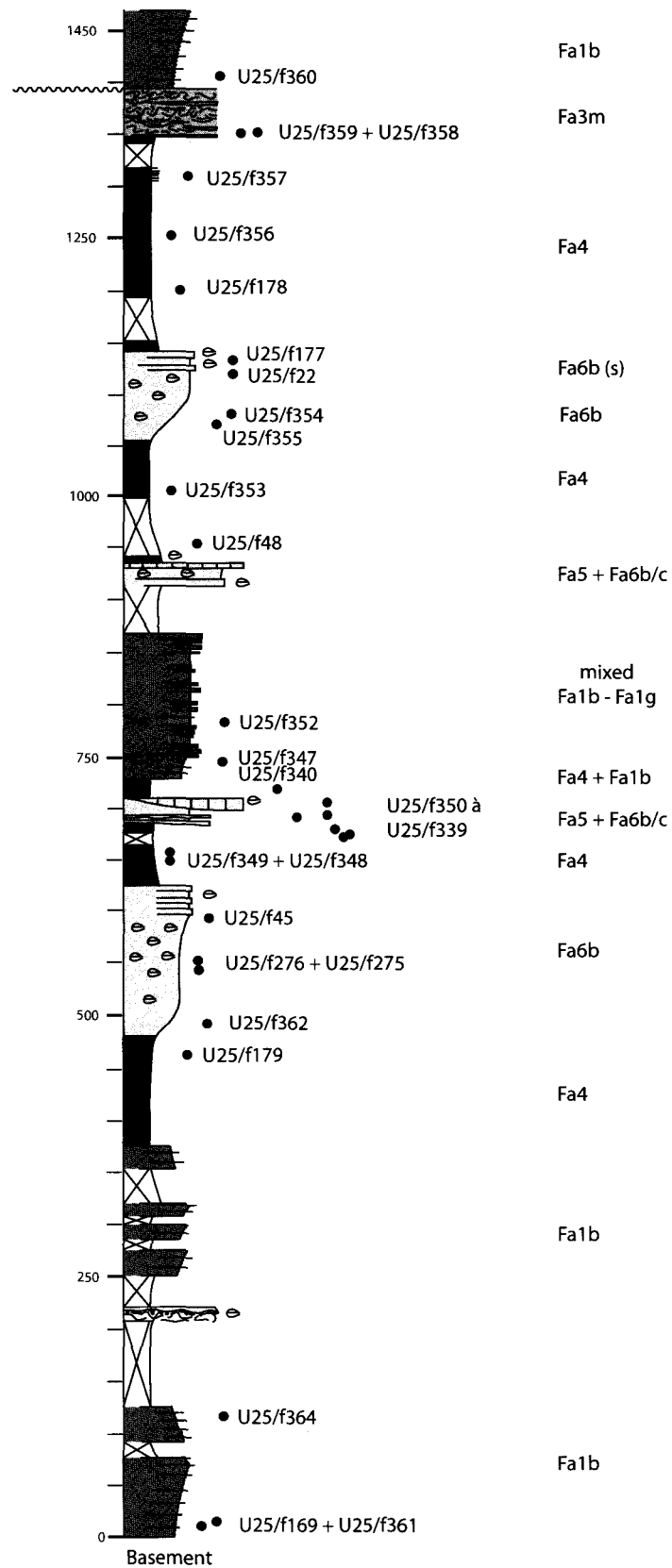
Appendix 2. Sample list and Datations/paleobathymetrics used for sedimentological vertical sections. Data are given from top to base for each section (see Appendix 1). Fossil Record numbers relate to NZMS 1:50 000 series U25 – Pongaroa. See Table III-1 and III-2 for facies code. All data available at the IGNS Paleontological Data Open File. p. 277

Appendix 3. Correlations of both onshore and offshore discontinuities on eustatic curves. p. 287

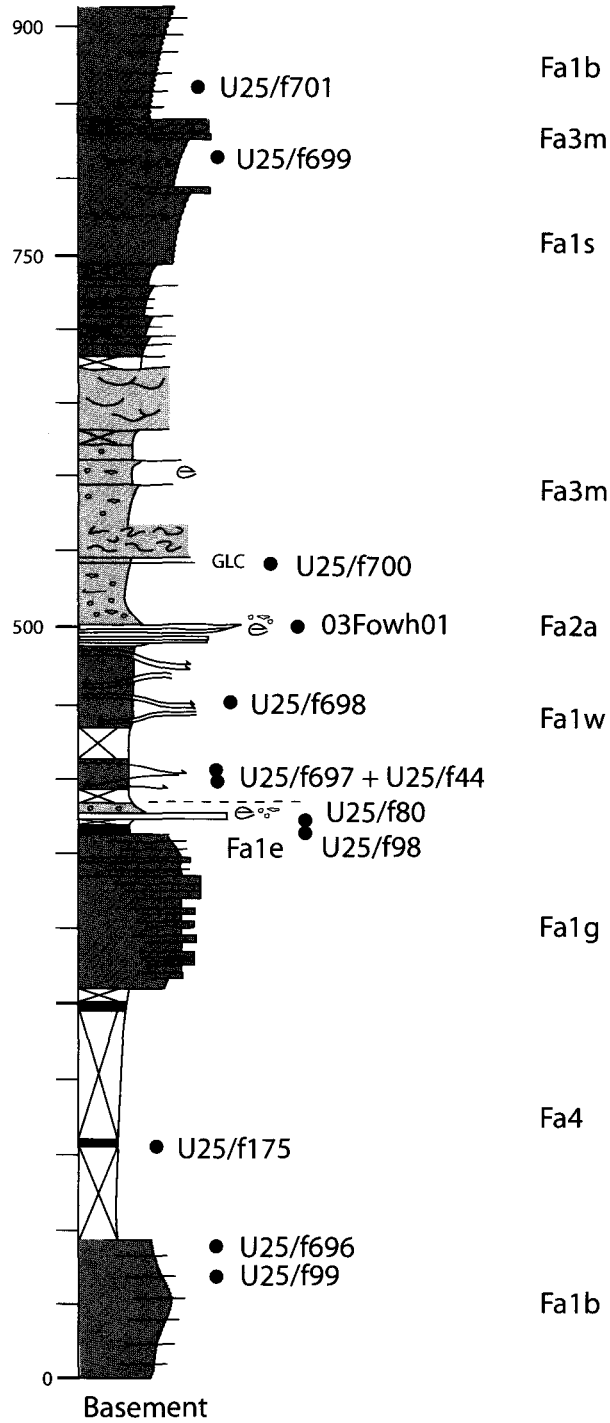
ANNEXE I

Colonnes lithostratigraphiques

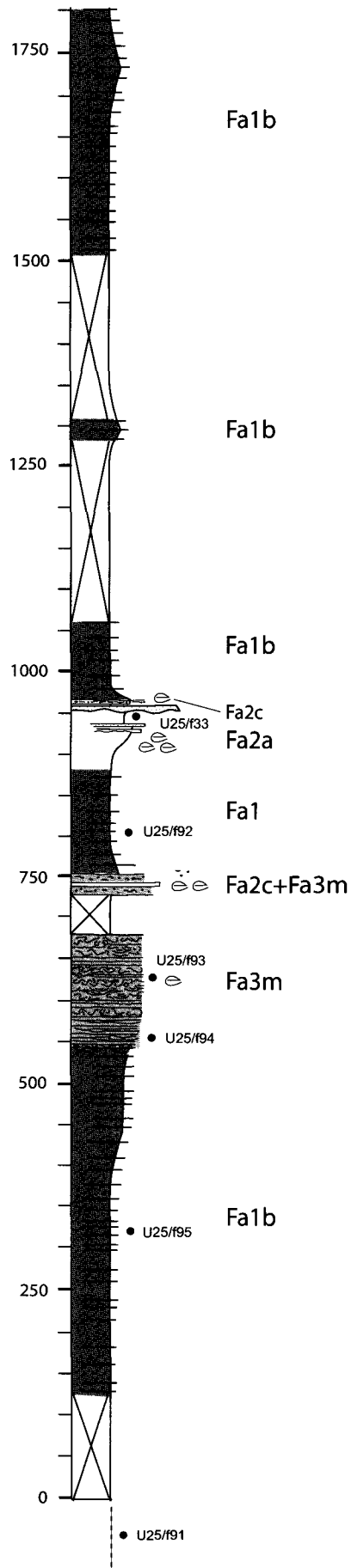
Pongaroa section



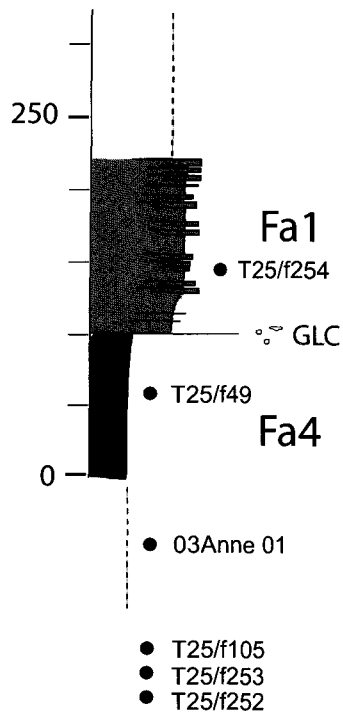
Branscombe section



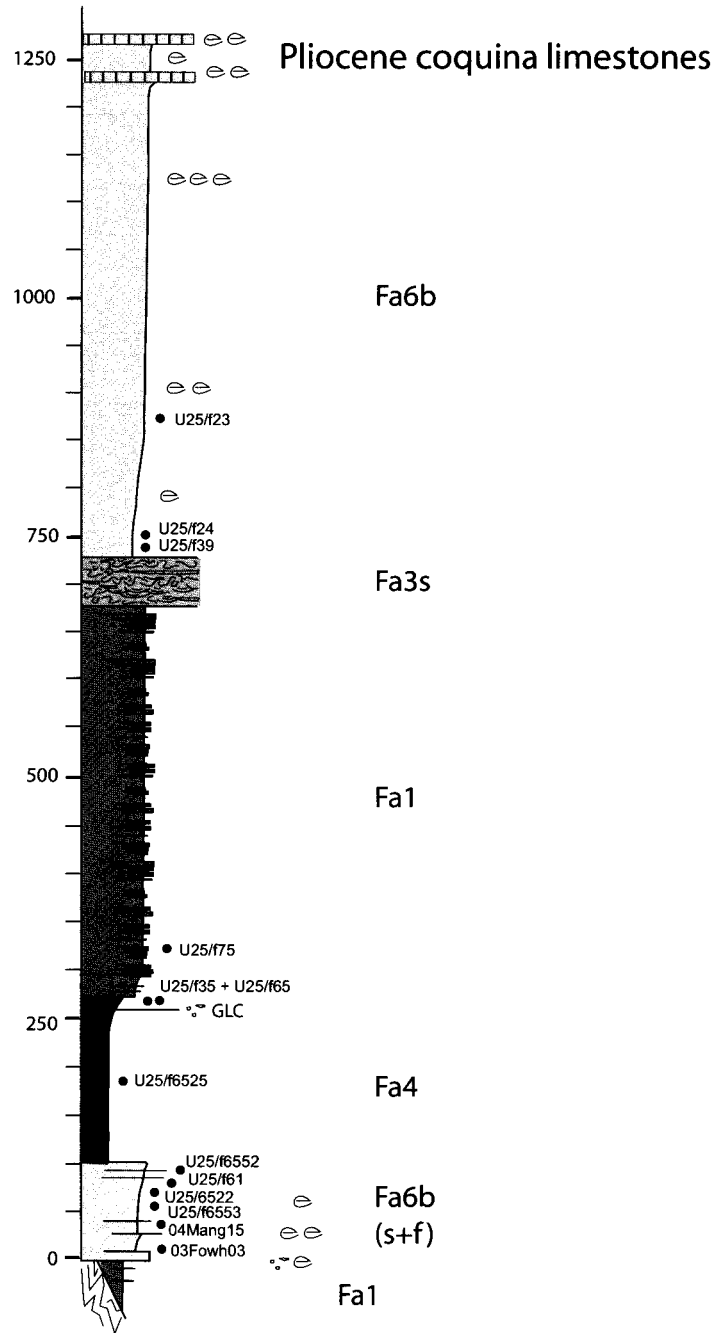
Razorback section



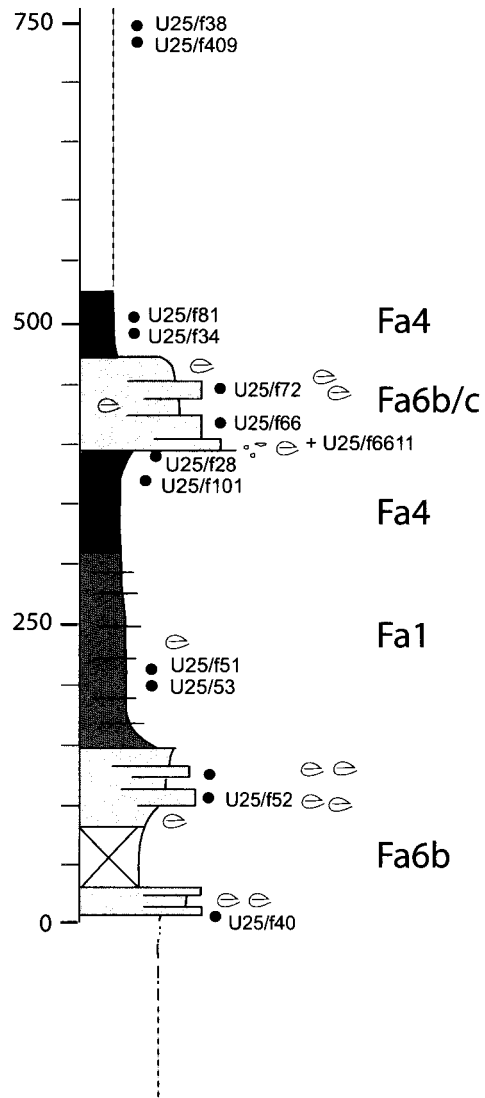
Annedale section



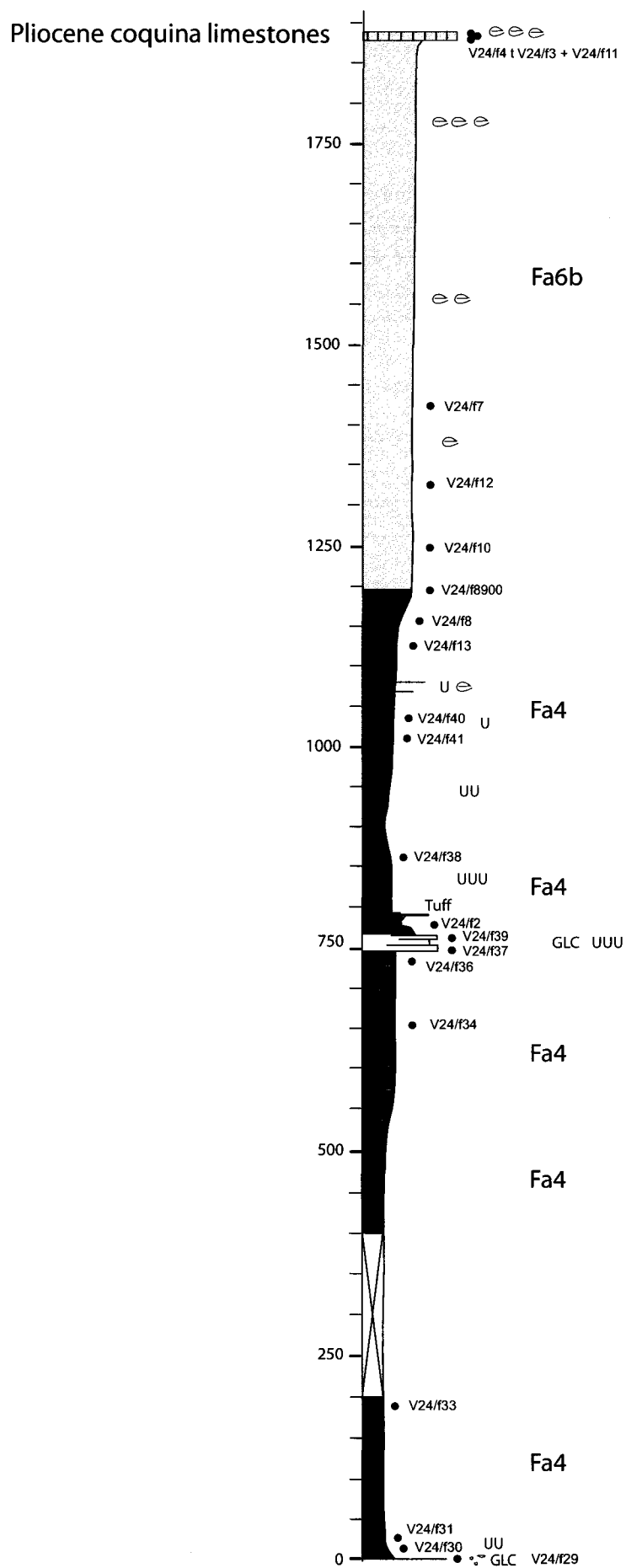
Puketoi section



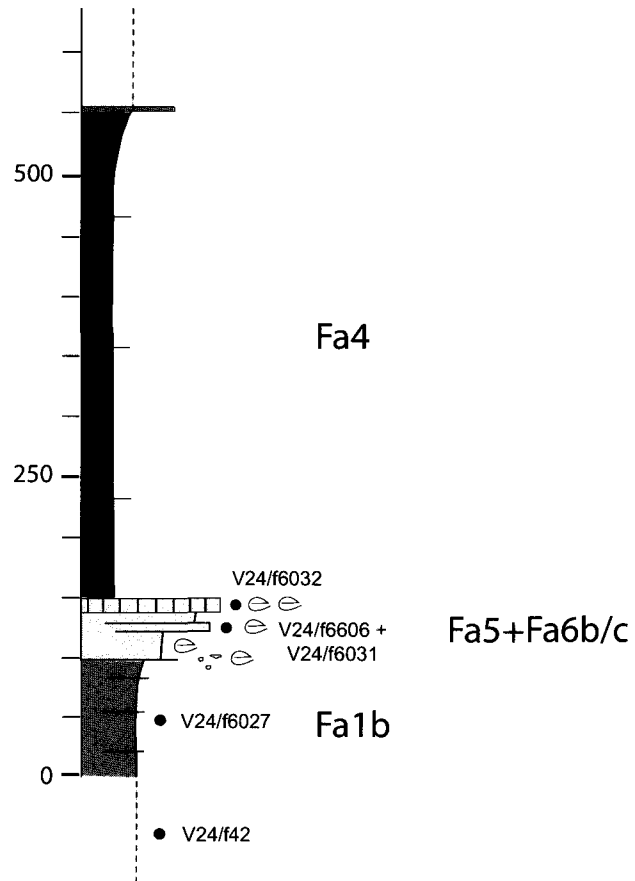
Mangatiti section



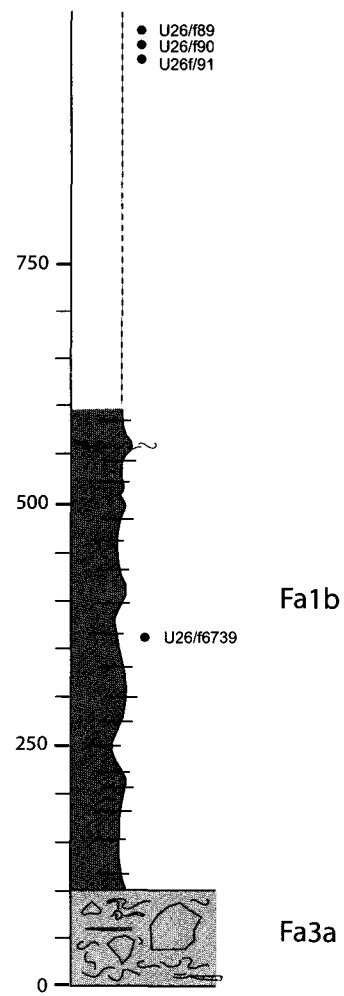
Cape Turnagain section



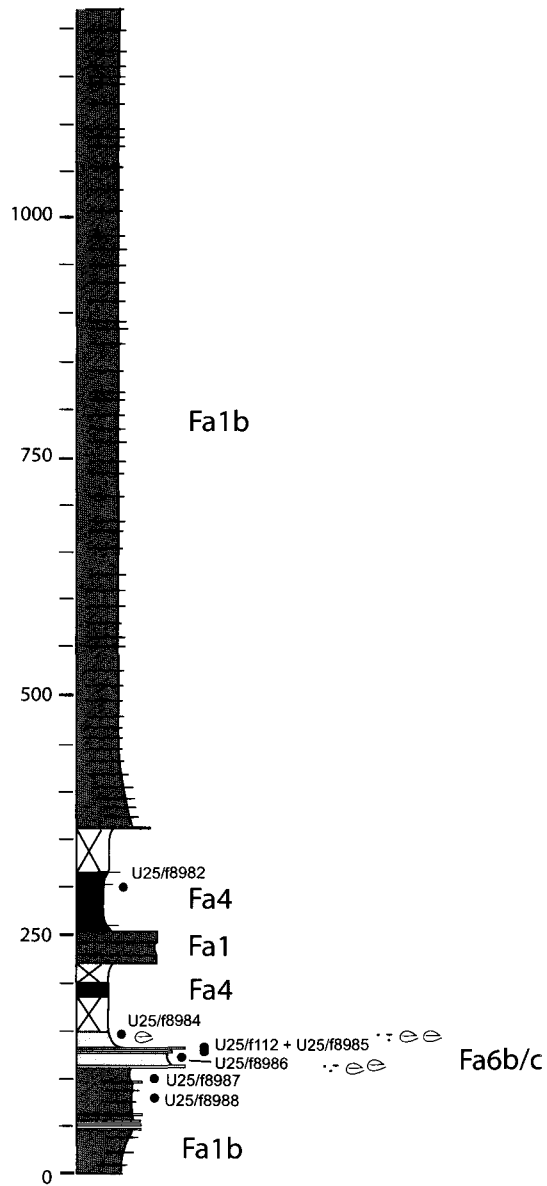
Fingerpost section



Castlepoint section



Takiritini section



ANNEXE II

Datations et données paléobathymétriques (foraminifères)

Branscombe section

Fossil record No.	Facies No.	Identifier	Date	Age	Age Comment	Paleobathymetries
U25/f701	Fa1b	H.E.G. MORGANS	06/05/2004	Sw	Waiauan	Middle - lower bathyal (600 - 1000 m ? +), fully open oceanic watermass
U25/f699	Fa1s	H.E.G. MORGANS	06/05/2004	SI <	Lower Lillburnian	Middle bathyal (or deeper) paleodepth (600 m +++), open oceanic watermass
U25/f700	Fa3m	H.E.G. MORGANS	06/05/2004	SI <	Lower Lillburnian	Lower bathyal (1250 m +), near full oceanic watermass
03 Fowh 01	Fa2a + Fa3m	A.G. BEU	06/03/2003	Sc-SI	Clifdenian-Tongaporutuan, almost certainly Clifdenian-Lillburnian	This is an inner to middle shelf fauna (NB : fauna reworked downslope by mud-flows)
U25/f698	Fa1w	H.E.G. MORGANS	06/05/2004	SI <	Lower Lillburnian	Middle - lower bathyal (600 - 1000 m +), open oceanic watermass
U25/f44	Fa1w	H.E.G. MORGANS	06/08/1982	Sc <	Early Clifdenian	Lower - upper bathyal
U25/f697	Fa1w	H.E.G. MORGANS	06/05/2004	PI >>-Sc <<	Latest Altonian or basal Clifdenian	Middle bathyal (600 - 1000 m), open oceanic watermass
U25/f80	Fa4	H.E.G. MORGANS	30/05/1983	PI >	Upper Altonian	Outer shelf - upper bathyal
U25/f98	Fa4	H.E.G. MORGANS	24/06/1983	PI >	Upper Altonian	Outer shelf - upper bathyal
U25/f175	Fa4	H.E.G. MORGANS	04/08/1986	PI mid/>	Mid - upper Altonian	Open water bathyal deposition
U25/f696	Fa1b	H.E.G. MORGANS	06/05/2004	Po >>-PI <	Uppermost Otaian to lower Altonian	Lower bathyal (1000 m +), near fully oceanic watermass
U25/f99	Fa1b	H.E.G. MORGANS	24/06/1983	Lw mid	Mid Waitakian	Bathyal

Pongaroa section

Fossil record No.	Facies No.	Identifier	Date	Age	Age Comment	Paleobathymetries
U25/f360	Fa1b	H.E.G. MORGANS	19/08/1994	Sw	The age is most likely to be restricted to the Waiauan	The depth of deposition was probably at mid (or even lower) bathyal depths (1000 m +), the overlying watermass is considered to be slightly oceanic in character
U25/f359	Fa3m	H.E.G. MORGANS	19/08/1994	SI	The age is Lillburnian	Mid bathyal (1000 m) depth of deposition, the overlying watermass was slightly oceanic in character
U25/f358	Fa3m	H.E.G. MORGANS	12/08/1994	SI	The age is Lillburnian	Paleodepth of mid-upper bathyal (400-1000 m), oceanic watermass
U25/f357	Fa4	H.E.G. MORGANS	12/08/1994	SI >	The age is upper Lillburnian	The depth of deposition was at mid bathyal depths (600-1000 m), the watermass was mainly oceanic
U25/f356	Fa4	H.E.G. MORGANS	11/08/1994	SI	No evidence for an age younger than Lillburnian, it is suggested that the age is restricted to the Lillburnian, the general stratigraphic position agrees with this age	Suggests shelf depths perhaps outer shelf - uppermost bathyal, the overlying watermass was neritic
U25/f178	Fa4	H.E.G. MORGANS	05/08/1986	SI <	Lower Lillburnian	Upper bathyal
U25/f177	Fa6b (s)	H.E.G. MORGANS	05/08/1986	SI <	Lower Lillburnian	Plenty of communiated shell material, shelly deposition
U25/f22	Fa6b (s)	H.E.G. MORGANS	31/03/1982	Sc-SI	More likely Clifdenian	
		A.G. BEU	05/03/1982	Sc-SI	More likely Clifdenian	
U25/f354	Fa6b	H.E.G. MORGANS	11/08/1994	Sc	The age is possibly restricted to the Clifdenian	The fauna indicates relatively shallower depths compared to lower in the sequence, perhaps mid-outer shelf, the overlying watermass was neritic, the taxa were small and generally thin-walled indicating that low oxygen condition may have prevailed
U25/f355	Fa6b	H.E.G. MORGANS	11/08/1994	S	There are no age diagnostic taxa in the fauna, the age is based on stratigraphic position	The depth of deposition was probably similar to f354 and somewhere on the shelf, although may indicate more outer shelf to uppermost bathyal depths, the overlying watermass was neritic

Pongaroa section (Contd.)

Fossil record No.	Facies No.	Identifier	Date	Age	Age Comment	Paleobathymetries
U25/f353	Fa4	H.E.G. MORGANS	28/07/1994	PI-S	This age is not well constrained, with the stratigraphic position the age may be still upper Altonian, but has broad age range of Sa-S	The paleodepth is possibly outermost shelf to upper bathyal, the watermass was neritic, many to most of the calcareous taxa are pyritised
U25/f48	Fa4	H.E.G. MORGANS	16/08/1982	PI >-Sc	Uppermost Altonian to Lillburnian, Cibicides Victoriensis is Altonian - Clifdenian	Upper bathyal - outer shelf
U25/f352	Fa1b	H.E.G. MORGANS	29/07/1994	PI >	The age is upper Altonian, may be fairly low in the upper Altonian	Perhaps mid to upper bathyal (downslope reworking may occurred), the overlying watermass was mainly oceanic
U25/f347	Fa4	H.E.G. MORGANS	28/07/1994	PI >	The age is restricted to upper Altonian	Significant change in fauna compared to the underlying f346, 348, 349 samples, this is similar to f345, the depth of deposition was probably at mid to upper bathyal perhaps around the 1000 m mark, the overlying watermass was mainly oceanic in character
U25/f340	Fa4	M.P. CRUNDWELL	06/04/1993	PI >	A late Altonian age	Mid bathyal, marginal neritic watermass, moderately well preserved
U25/f339	Fa6b	M.P. CRUNDWELL	06/04/1993	PI-SI	Specimens suggests Early Lillburnian, although this poses a problem with respect to the Altonian age of bracketing samples, contamination of the first wash is suspected	Outer shelf - upper bathyal, sheltered neritic watermass, suggests a stressed environment, moderately well to poorly preserved
U25/f339A	Fa6b	M.P. CRUNDWELL	23/04/1993	PI mid	Indicates mid Altonian	Outer shelf - upper bathyal, sheltered neritic watermass, moderately preserved
U25/f137	Fa6b	H.E.G. MORGANS	16/08/1985	PI-S?	Probably more like Southland (S) than Altonian	Shelf environment, poorly preserved fauna
U25/f170	Fa6b	H.E.G. MORGANS	20/07/1986	Po >	Probably upper Otaian	Mid - inner shelf, poorly preserved
U25/f346	Fa4	H.E.G. MORGANS	27/07/1994	Po	There are no age definitive taxa, the age is still considered to be Otaian (this sample is similar to the f349 and f348)	The depth of deposition was most likely at upper bathyal depths perhaps uppermost, the overlying watermass was neritic, the specimens are highly pyritic
U25/f345	Fa4	H.E.G. MORGANS	29/04/1994	PI >	Is assigned an upper Altonian age	Was deposited at mid-upper bathyal depths, perhaps at the shallower end (may be at ?400m), good open oceanic conditions
U25/f350	Fa4	H.E.G. MORGANS	28/07/1994	Po >-PI	There is very little evidence to base an age, a basal Altonian age could be the youngest age possible, specimens supports an uppermost Otaian to Altonian age	The depth is probably upper bathyal, although specimens suggest outermost shelf (downslope reworking?), the overlying watermass is neritic, the high pyrite content may indicate some anoxia?, similar fauna to f346, 348, 349
U25/f348	Fa4	H.E.G. MORGANS	28/07/1994	Po >	On the stratigraphy, the age of the previous sample and the general fauna compared to f349 & f346, the age is probably Otaian, an upper Otaian age may have been reached	The depth of deposition was probably about upper bathyal, downslope reworking may occurred, may be a bit shallower?, the overlying watermass was neritic, the fauna is still similar to f346, 349
U25/f349	Fa4	H.E.G. MORGANS	28/07/1994	Lw-Po	It may be possible to restrict the fauna to the Otaian, perhaps upper Otaian, but an broad age of upper Waitakian - Otaian is probably safest	The depth of deposition was possibly at upper bathyal depths perhaps 400-1000 m, the overlying watermass was neritic, contains a lot of pyritised biogenic material plus large fromboids of pyrite, may have been slightly anoxic?
U25/f45	Fa6b	H.E.G. MORGANS	09/08/1982	PI-Sc	Sample reworked, not lower than Altonian, probably not higher than Clifdenian	Quite shallow water
U25/f275	Fa6b	M.P. CRUNDWELL	21/10/1991	Lw-PI	Waitakian to Altonian, good age control difficult due to very poor planktic assemblage	Outer shelf to uppermost bathyal
U25/f276	Fa6b	M.P. CRUNDWELL	21/10/1991	Po >-PI	Late Otaian to Altonian	Outer shelf to uppermost bathyal
U25/f362	Fa6b	H.E.G. MORGANS	11/05/1994	PI	A very early Altonian age can be assigned to this sample	There is nothing to say this is very deep, although it is possibly just off the shelf, it is best to call it upper bathyal, the site was overlain by a fully neritic watermass
U25/f179	Fa4	H.E.G. MORGANS	05/08/1986	Po		Bathyal, low diversity fauna
U25/f364	Fa1b	H.E.G. MORGANS	04/10/1994	Lw-Po	The broad age range is Waitakian-Otaian, but the age may be restricted to Waitakian perhaps about mid Waitakian	The paleodepth is most probably at mid-upper bathyal depths but may have some down slope contamination
U25/f361	Fa1b	H.E.G. MORGANS	11/05/1994	Lw-Tt <	Waitakian to lower Tongaporutuan, a more precise age cannot be assigned	Most of the taxa recovered indicated a mid-upper bathyal depth of deposition with some shelf downslope reworking
U25/f169	Fa1b	H.E.G. MORGANS	20/07/1986	Lw	Lower Waitakian	Upper bathyal, open water

Razorback section

Fossil record No.	Facies No.	Identifier	Date	Age	Age Comment
U25/f33	Fa4	H.E.G. MORGANS	13/07/1982	Tt	Deep water. Heavily pyritized
U25/f92	Fa1	H.E.G. MORGANS	20/06/1983	Tt <	Lower Tongaporutuan Outer shelf - upper bathyal with poor oceanic circulation
U25/f93	Fa1/Fa3m	H.E.G. MORGANS	23/06/1983	Tt <	Lower Tongaporutuan Deep water benthics but poor open ocean circulation with low planktic percentage
U25/f94	Fa1/Fa3m	H.E.G. MORGANS	21/06/1983	Sw-Tt mid	No younger than middle Tongaporutuan Mid-outer shelf
U25/f95	Fa1b	H.E.G. MORGANS	22/06/1983	Sw	Mid shelf
U25/f91	Fa1b	H.E.G. MORGANS	15/06/1983	Sl >-Sw	Upper Lillburnian - Waiauan Outer shelf - upper bathyal

Annedale section

Fossil record No.	Facies No.	Identifier	Date	Age	Age Comment
T25/f254	Fa1	M.P. CRUNDWELL	11/12/1993	Tk <	Adopted age: early Kapitean Presence of mid bathyal markers which indicate water depths > 600 m, maybe > 700 m. Marginal neritic watermass
		M.P. CRUNDWELL	11/12/1993	Tk <	Adopted age: early Kapitean Presence of the mid bathyal markers which indicate water depths > 600 m, maybe > 700 m. Marginal neritic watermass
T25/f49	Fa4	H.E.G. MORGANS	26/05/1983	Tt	No evidence of being younger Mid-outer shelf. Poor circulation <i>i.e.</i> enclosed
03Anne01	Fa4	H.E.G. MORGANS	06/05/2004	Sl-Tt	Very sparse fauna, age from Lillburnian to Tongaporutuan
T25/f105	Fa4	H.E.G. MORGANS	30/04/1986	Tt (>?)-Wp	?upper Tongaporutuan - Kapitean Depth of deposition is probably mid-upper bathyal with restricted circulation
T25/f253	Fa4	M.P. CRUNDWELL	11/12/1993	Tt (>?)	Adopted age: ?late Tongaporutuan Common specimens of mid bathyal species, indicates water depths > 600 m, suggest depths > 700 m. Neritic watermass
		M.P. CRUNDWELL	11/12/1993	Tt (>?)	Adopted age: ?late Tongaporutuan Common specimens of mid bathyal species, indicates water depths > 600 m, suggest depths > 700 m. Neritic watermass
T25/f252	Fa4	M.P. CRUNDWELL	11/12/1993	Tt <	Adopted age: early Tongaporutuan Common specimens of mid bathyal species, indicates water depths > 600 m. No evidence for deeper. Inner Neritic
		M.P. CRUNDWELL	11/12/1993	Tt <	Adopted age: early Tongaporutuan Common specimens of mid bathyal species, indicates water depths > 600 m. No evidence for deeper. Inner Neritic

Castlepoint section

Fossil record No.	Facies No.	Identifier	Date	Age	Age Comment
U26/f89	Fa1b	H.E.G. MORGANS	15/09/1995	Lw >-Po	The age is upper Waitakian to Otaian (perhaps not upper Po) The paleodepth is considered to be about mid bathyal perhaps 1000-1500 m?. The fauna would appear to be stressed perhaps lowered oxygen levels.
U26/f90	Fa1b	H.E.G. MORGANS	15/09/1995	Lw >-Po	The age is upper Waitakian to Otaian
U26/f91	Fa1b	H.E.G. MORGANS	15/09/1995	Lw >-Po	Upper Waitakian on stratigraphy and the presence of possible <i>Globoquadrina dehiscens</i> and <i>Globigerina woodi</i> .
U26/f6739	Fa1b	N.de B. HORNIBROOK		?Lw-Po?	

Takiritini section

Fossil record No.	Facies No.	Identifier	Date	Age	Age Comment	Paleobathymetries
U25/f8982	Fa1	G.H. SCOTT	06/05/1968	SI		
U25/f8984	Fa4	G.H. SCOTT	09/05/1968	Sc >-SI <	About Clifdenian - Lillburnian boundary	
U25/f8985	Fa6b	G.H. SCOTT	09/05/1968	PI >	Upper Altonian	
U25/f112	Fa6b	H.E.G. MORGANS	01/02/1984	PI >	Upper Altonian	A shallow inshore environment
		A.G. BEU	24/02/1984	Po-Sw	Not much that's very diagnostic, see forams for age	
		I.W. KEYES	06/03/1991	PI	Foram sample	
		I.W. KEYES	06/05/1991	PI	Foram sample	
U25/f8986	Fa1b	G.H. SCOTT	10/05/1968	PI	Probably Altonian - i.e. above altonian limestone	
U25/f8987	Fa1b	G.H. SCOTT	10/05/1968	Lw >-Po	Probably upper Waitakian-Otaian	
U25/f8988	Fa1b	G.H. SCOTT	10/05/1968	Lw-Po		

Mangatiti section

Fossil record No.	Facies No.	Identifier	Date	Age	Age Comment	Paleobathymetries
U25/f38	Fa4	H.E.G. MORGANS	30/07/1982	Tt		Upper bathyal. Not in open water
U25/f409	Fa4/Fa1b ?	R. WALTERS	12/11/1963	Tt <-Tk	Lower Tongaporutuan - Kapitean on paleo	
U25/f81	Fa4	H.E.G. MORGANS	03/06/1983	Tt		Outer shelf
U25/f34	Fa4	H.E.G. MORGANS	14/07/1982	Sw-Tt </mid	No higher than lower - middle Tongaporutuan	
U25/f72	Fa6c	A.G. BEU	02/07/1982	S?-Tt		
U25/f66	Fa6b	A.G. BEU	02/07/1982	Tt		
U25/f6611	Fa6b	J. MARWICK		Tt		
U25/f28	Fa6b	H.E.G. MORGANS	30/06/1982	Sw?		Close inshore
U25/f101	Fa4	A.G. BEU	02/08/1983	Sw-Tt?	it seem more like Waiauan than Tongaporutuan	
U25/f51	Fa1b/Fa4	H.E.G. MORGANS	27/09/1982	SI?-Sw	not older than Clifdenian	Mid shelf
		D.C. MILDENHALL	16/11/1982	nd	Upper Southland Series with massive Mesozoic reworking	Preservation poor, palynomorphs broken and corroded. ?Water sorted . Spores all? reworked
U25/f53	Fa1b/Fa4	H.E.G. MORGANS	26/08/1982	PI >	Upper Altonian, unlikely to be higher than Altonian	Outer shelf
U25/f52	Fa6b	H.E.G. MORGANS	24/08/1982	Sc-Sw	Probably Clifdenian - Waiauan, not lower than upper Alonian	Mid-outer shelf
U25/f40	Fa6b	H.E.G. MORGANS	03/08/1982	Sc-SI	probably about Clifdenian - Lillburnian	Quite shallow, near shore
U25/f287	mixed Fa1b/Fa1g	H.E.G. MORGANS	07/01/1992	nd	Contains no age diagnostic taxa, may be restricted to Otaian - Waiauan. The most safest age estimate would be Neogene	The depth of deposition is most likely to be at mid to outer shelf, an outer shelf depth (100-200 m) most possible. The site of deposition was overlain by a neritic watermass

Puketoi section

Fossil record No.	Facies No.	Identifier	Date	Age	Age Comment	
U25/f23	Fa4/Fa6b	G.H. SCOTT	30/03/1982	Tk >-Wo	Upper Kapitean - Opoitian	
U25/f24	Fa4/Fa6b	G.H. SCOTT	31/03/1982	Tk >-Wo	Upper Kapitean - Opoitian, probably upper Kapitean	Bathyal. Marginal rather than oceanic locus, although deep. Otolith
U25/f39	Fa4	H.E.G. MORGANS	02/08/1982	Tk >	Upper Kapitean	Upper bathyal
U25/f75	Fa1 (mixed b-g ?)	H.E.G. MORGANS	23/09/1982	Tk >	Upper Kapitean	Outer shelf - upper bathyal
U25/f35	Fa4	H.E.G. MORGANS	27/07/1983	Tk?	Upper Kapitean ?, could be upper Kapitean - Opoitian	Mid-outer shelf
U25/f65	Fa4	H.E.G. MORGANS	30/08/1982	Tt >-Tk	Upper Tongaporutuan - Kapitean	Upper bathyal
U25/f6525	Fa4	G.H. SCOTT		Tt mid/>	No older than middle Tongaporutuan	
U25/f6552	Fa6b	G.H. SCOTT		Tt <	Probably lower	
U25/f61	Fa6b	A.G. BEU	05/03/1982	Tt		
U25/f6522	Fa6b	G.H. SCOTT		Tt <	Lower Tongaporutuan	Plant fragments
U25/f6553	Fa6b	G.H. SCOTT		Tt <	Lower Tongaporutuan	
04Mang15	Fa6b	A.G. BEU	19/04/2004	Tt </mid	Of early to mid Tongaporutuan age; early Late Miocene	
03Fowh03	Fa6b	A.G. BEU	06/03/2003	Tt?	Tongaporutuan. However, it is difficult to rule out Lillburnian - Waiauian	
		A.G. BEU	06/03/2003	Tt	Tongaporutuan age is more likely	

Fingerpost section

Fossil record No.	Facies No.	Identifier	Date	Age	Age Comment	
V24/f6032	Fa5	N.de B. HORNIBROOK		Sl		
V24/f6031	Fa6b	N.de B. HORNIBROOK	06/03/1987	Sl		
		N.de B. HORNIBROOK		Sl		
V24/f6606	Fa6b	J. MARWICK		Lw-P		
V24/f6027		I.W. KEYES		Lw-Po		
		UNKNOWN		nd		
		P.N. WEBB		Lw-Po		
V24/f42		H.E.G. MORGANS	27/02/1989	Lw <	Lower Waitakian	Depth of deposition at about mid to upper bathyal (400-1000 m). Oceanic watermass

Cape Turnagain s.

Fossil record No.	Facies No.	Identifier	Date	Age	Age Comment	Paleobathymetries
V24/f11	shelf coquina	A.G. BEU	24/10/1978	Wo-Wp	Age significance obscure	
V24/f3	shelf coquina	A.G. BEU	16/12/1976	Wo		
V24/f4	shelf coquina	A.G. BEU	25/11/1976	Wo		
V24/f7	Fa6c?	N.de B. HORNIBROOK	09/11/1976	Tk-Wo		Very shallow water fauna
V24/f12	Fa6b	N.de B. HORNIBROOK	21/02/1979	Tk-Wo		Shallow inner shelf
V24/f10	Fa6b	N.de B. HORNIBROOK	21/02/1979	Wo		
		G.H. SCOTT	21/08/1980	Wo <	Near or at base of Wo	Possibly <outer shelf> but either near shore or sheltered from full oceanic circulation
		A.G. BEU	24/10/1978	?	No use for age	One bivalve only
V24/f8900	Fa6b	G.H. SCOTT		Tk		
		G.H. SCOTT	25/08/1980	Tt >-Tk <	Upper Tongaporutuan to lower Kapitean	Outer shelf or somewhat deeper (deep, approximately 800 feet). Oceanic circulation probably better than in V24/f10 but low planktic abundance indicates shore proximity or barrier influence. Benthics much commoner than planktics. Latter are fullsized
V24/f8	Fa6b?	A.G. BEU	24/10/1978	Tk?		Good collection of about 5 pieces of crab carapaces and chelae
V24/f13	Fa6b/Fa4 ?	A.G. BEU	12/02/1982	Tk		
V24/f40	Fa4	A.G. BEU	30/06/1987	Tt-Tk	Estimated by collector	Apparently a deep-water assemblage, <i>i.e.</i> upper bathyal zone. Nothing very diagnostic
V24/f41	Fa4	G.H. SCOTT	03/07/1987	Tt >-Tk <	Upper Tongaporutuan to lower Kapitean	
V24/f38	Fa4	I.W. KEYES	25/07/1987	Sw-Tk	Inferred stage	
V24/f2	Fa4	N.de B. HORNIBROOK	08/11/1976	Tk		
V24/f39	greensand	G.H. SCOTT	03/07/1987	Tt >-Tk <	Probably in upper Tongaporutuan - lower Kapitean zone	Upper bathyal. Slightly weathered glauconite, sparse foraminifera, rare planktics, echinoid spines
		G.H. SCOTT	18/08/1993	Tt >-Tk <	Upper Tongaporutuan - lower Kapitean	Assessed as upper bathyal (?400 - 600 m). Possibly deeper than f37 but under similar sheltered neritic watermass. Update on material on 1987 slide
V24/f37	greensand	G.H. SCOTT	03/07/1987	Tt >-Tk	Upper Tongaporutuan - Kapitean	Outer shelf ?. Planktics rare
		G.H. SCOTT	18/08/1993	Tt >-Tk <	Upper Tongaporutuan - lower Kapitean	Assessed as outer shelf - upper bathyal, probably outer shelf or on uppermost slope. Sheltered neritic watermass. Significant depth, watermass change between f36 and f37. Update on material in 1987 slide

Cape Turmagain s. (contd.)

Fossil record No.	Facies No.	Identifier	Date	Age	Age Comment	Paleobathymetries
V24/f36	Fa4	G.H. SCOTT	19/05/1987	Tt >	Probably upper Tongaporutuan	Benthics indicate bathyal deposition, mid-upper, possibly shallower than f34. Suggests proximal oceanic position
		G.H. SCOTT	18/08/1993	Tt >-Tk <	Upper Tongaporutuan - lower Kapitean	Assessed as middle bathyal (?600 - 1000 m), deeper than 600 m, probably shallower than f34. Update on material on 1987 slide
V24/f34	Fa4	G.H. SCOTT	18/05/1987	Sw >-Tt <	Upper Waiauan - lower Tongaporutuan	About mid-bathyal. Good exposure to oceanic water
		G.H. SCOTT	18/08/1993	Sw >-Tt <	Upper Waiauan - lower Tongaporutuan. Closer sampling in this part of sequence might locate dextral coiling zone and base of Tt.	Assessed as lower middle bathyal to lower bathyal (?800 - 1500 m). Update on material on 1987 slide
V24/f33	Fa4	G.H. SCOTT	18/05/1987	Sw		Outer shelf to upper bathyal. Moderate exposure to oceanic circulation
		G.H. SCOTT	18/08/1993	Sw		Assessed as outer shelf - upper bathyal (> 100 - 400 m), probably below shelf, no clear evidence that horizon is significantly deeper than f29-31 but site was in more open water. Update on material on 1987 slide
V24/f31	Fa4	G.H. SCOTT	18/05/1987	Sw		Mid-outer shelf, possibly adjacent to bathyal zone. Neritic water
		G.H. SCOTT	18/08/1993	Sw		Assessed as outer shelf - upper bathyal (?100 - 400 m), suggest bathyal. Update on material on 1987 slide
V24/f30	Fa4	G.H. SCOTT	18/05/1987	Sw		Shelf. About 50% glauconite. Neritic water
		G.H. SCOTT	18/08/1993	Sl >-Sw	Upper Lillburnian - Waiauan, suggests Sw	Given as outer shelf - upper bathyal (?100 - 400 m), suggest bathyal rather than shelf. Update on material on 1987 slide
V24/f29	greensand	G.H. SCOTT	18/05/1987	Sl >?-Sw	Upper Lillburnian-Waiauan	Shelf assemblage, Fine glauconitic sand
		G.H. SCOTT	18/08/1993	Sl >-Sw	Upper Lillburnian-Waiauan	Outer shelf - upper bathyal bathymetry (?100 - 400 m). Update of material on 1987 slide

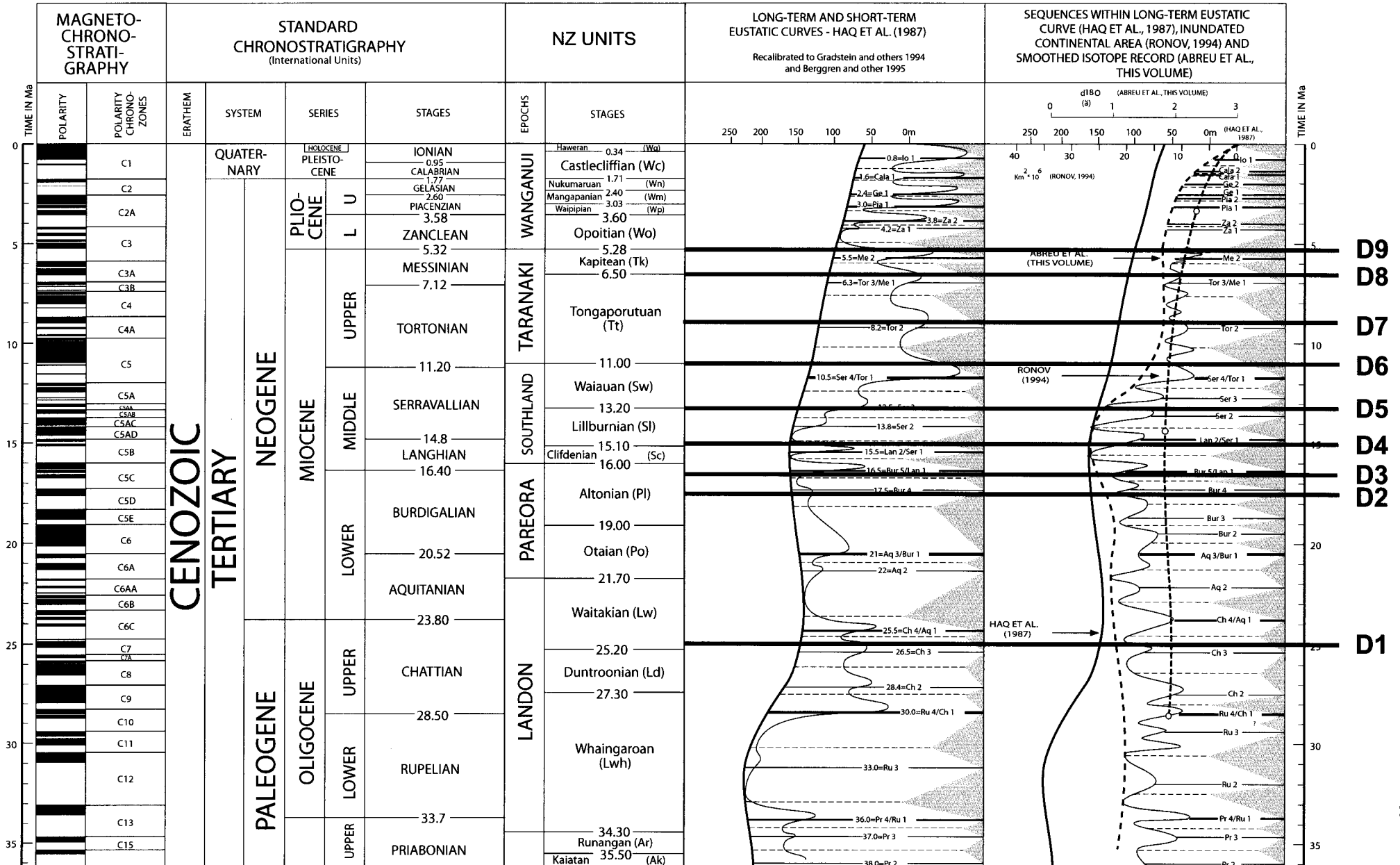
ANNEXE III

Courbes eustatiques

Part of the

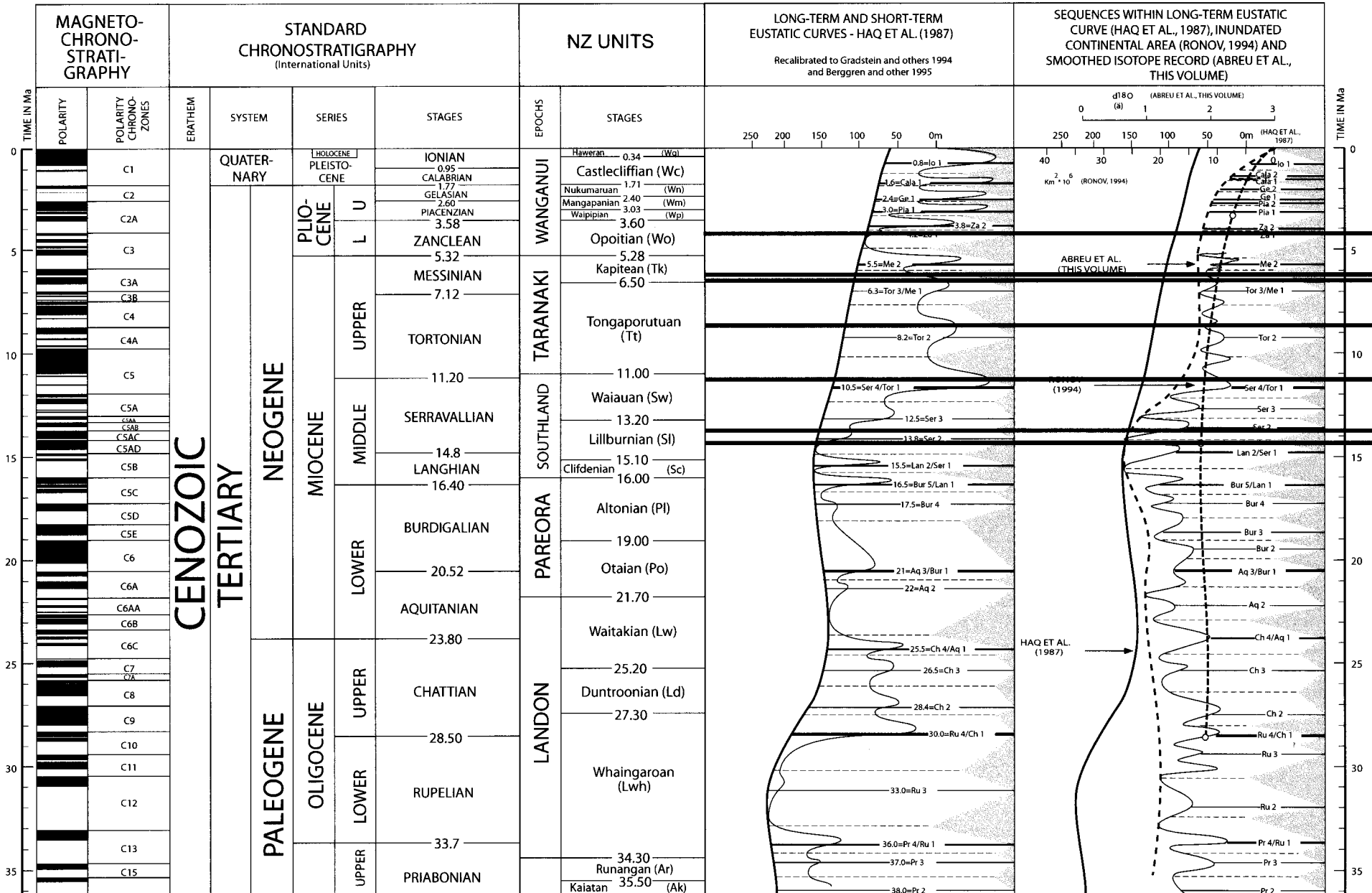
MESOZOIC-CENOZOIC SEQUENCE CHRONOSTRATIGRAPHIC CHART

HARDENBOL, J., THIERRY, J., FARLEY, M.B., JACQUIN, T., DE GRACIANSKY, P.-C., & VAIL, P.R., 1997,
Mesozoic-Cenozoic Sequence Chronostratigraphic Framework,
in De Graciansky, P.-C., Hardenbol, J., Jacquin, T., Vail, P.R., & Farley, M.B., eds.,
Sequence Stratigraphy of European Basins, SEPM Special Publication 59



Calage sur les courbes eustatiques des discontinuités majeures observées à terre sur la transversale d'Akitio (cf Fig.V- 10)

MESOZOIC-CENOZOIC SEQUENCE CHRONOSTRATIGRAPHIC CHART



B9?
B8
B7
B5
B4
B3
B2
B1

Calage sur les courbes eustatiques des discontinuités majeures observées en mer sur le profil sismique IAE1-28 (cf Fig.IV- 5; transversale d'Akitio)